School of Earth and Planetary Sciences

Title: Reconstructing Terrestrial Ecosystems in Tropical and Coastal Marine Environments using Sedimentary Ancient DNA (*sed*aDNA): Case Studies from Lake Towuti (Sulawesi) and the Black Sea.

Md. Akhtar-E-Ekram

ORCID iD: 0000-0002-0446-7789

This thesis is presented for the Degree of
Doctor of Philosophy
of
Curtin University

November 2023

Declaration

To the best of my knowledge and belief, this thesis contains no material previously published by any other person except where due acknowledgement has been made. This thesis contains no material which has been accepted for the award of any other degree or diploma in any university.

Md. Akhtar-E-Ekram

Perth (WA, Australia), 9th November 2023

Abstract

Microscopic analysis of fossil pollen continues to be one of the most used approach to reconstruct regional changes in paleo-floristic landscapes in the context of climatic or anthropogenic perturbations. However, spurious data interpretations can result from overlapping pollen morphologies, over-presentation of high-pollen-producing taxa, and unknown remote origins of wind-dispersed pollen. More recently, plant-derived chloroplast metabarcoding genes have been successfully recovered and sequenced from lake sedimentary records and used to complement pollen in reconstructing paleo-environmentally-relevant taxa that cannot be resolved otherwise, notably local- and low-pollen-producing taxa. These studies mainly targeted Holocene lakes in floristically less diverse, high-latitude environments, where cold conditions promoted long-term preservation of sedimentary ancient DNA (*sed*aDNA). This thesis investigates the potential of expanding the emerging field of *sed*aDNA research to include (a) sedimentary records from lakes located in floristically diverse, warm tropical environments (i.e., Pleistocene Lake Towuti, Sulawesi, Indonesia), and (b) marine basins with much more extensive and complicated catchment areas compared to inland lakes (i.e., the Black Sea), for reconstructing paleovegetation assemblages. These datasets were correlated with geochemical parameters to infer concomitant changes in the paleodepositional environment (both settings), pollen palynomorphs (Black Sea), and to infer paleo-biotic associations between tropical vegetation and symbiotic, pathogenic, and saprotrophic fungi (Lake Towuti).

Chapter 1 of the thesis is a general introduction, which compares the use of morphological remains (pollen palynomorphs vs macrofossils) and *sed*aDNA stratigraphy to reconstruct paleo-floristic landscapes and provides relevant background information about Lake Towuti and the Black Sea.

Chapter 2 describes sedimentary *trn*L-P6 amplicon sequencing to generate a record of Quaternary tropical catchment and aquatic vegetation changes associated with major transitions in limnological and hydrological changes throughout Lake Towuti's more than 1 Myr developmental history. Furthermore, the potential origins of the sedimentary chloroplast DNA were inferred from Pearson correlations between downcore relative changes in the *trn*L-P6-inferred paleovegetation assemblages and available (in) organic geochemical paleohydrological and paleo-environmental proxy data.

This chapter aims to address the following knowledge gaps:

- *What is the preservation potential of sedaDNA in tropical lake records, and how far back in time can plant-specific metabarcoding genes be recovered and sequenced?*

- *Can metabarcoding of sedimentary chloroplast marker genes accurately describe the paleovegetation assemblages in tropical biodiversity hotspots?*

- *To what extent does the terrestrial paleovegetation sedaDNA record in tropical lakes inform about concomitant climate-induced changes in the paleodepositional environment?*

Chapter 3 uses 18S rRNA amplicon sequencing to compare the paleovegetation community composition with those described in Chapter 2 and to identify additional palaeo-environmentally relevant members of the Domain Eukarya throughout Lake Towuti's history. Since this analysis revealed an overwhelming predominance of fungal communities, Pearson correlation analysis between the sedimentary *trn*L-P6 (Chapter 2) and 18S rRNA (this chapter) was used to study the potential symbiotic, parasitic, and saprotrophic associations that existed between fungi and the local paleovegetation community.

This chapter aims to address the following specific research questions:

- *What was the origin of the fungal taxa identified throughout Lake Towuti's record?*

- *Which fungal taxa represented symbiotic endophytes, ectomycorrhiza, plant pathogens, or lignin/cellulose degrading saprobes involved in wood, leaf, or soil organic matter degradation?*

- *Do saprobic fungi have the potential to continue decomposing sedimentary OM as anaerobic fermenters and form a symbiotic relationship with hydrogenotrophic methanogens?*

- *If so, can they still form an indirect genomic record of the role they played in the decomposition of dead wood or plant litter at the time of deposition?*

Chapter 4 describes a combined pollen and sedimentary *trn*L-P6 record of late-Glacial and Holocene vegetation changes in the Black Sea region at multi-decadal resolution. The Black Sea was chosen for this study due to the wealth of information that is available concerning its sensitivity to paleohydrological and paleo-environmental perturbations. The well-dated core used for this study was obtained from a water depth of 971 m, ~200 km offshore Varna (Bulgaria), and extensively studied previously for the reconstruction of plankton-climate interactions through paired stratigraphic analysis of *sed*aDNA and geochemical and isotopic paleo-environmental parameters. The record covers the cold and dry Younger Dryas, the deglacial, and the warmer and wetter Holocene.

This chapter aims to address the following knowledge gaps:

- *Do remote marine basins with much more extensive and complicated catchment areas compared to inland lakes represent suitable sedimentary archives of terrestrial and marine paleovegetation communities?*

- *To what extent does the composition, relative abundance, and geographic origin of the source vegetation overlap between sedaDNA and pollen datasets in marine sedimentary records?*

- *Can marine sedaDNA datasets complement, refine, or overturn pollen-inferred interpretations concerning the climatic or anthropogenic perturbations that may have contributed to changes in the regional paleo-floristic landscape?*

Chapter 5 comprises concluding remarks and an outlook for future studies.

Acknowledgements

Primary Publications

A 1Ma sedimentary ancient DNA (*sed*aDNA) record of catchment vegetation changes and the developmental history of tropical Lake Towuti (Sulawesi, Indonesia).

Ekram, M.-E., Campbell, M., Kose, S.H., Plet, C., Hamilton, R., Bijaksana, S., Grice, K., Russell, J., Stevenson, J., Vogel, H., & Coolen, M. J. L. (2024). A 1 Ma sedimentary ancient DNA (*sed*aDNA) record of catchment vegetation changes and the developmental history of tropical Lake Towuti (Sulawesi, Indonesia). *Geobiology*, 22, e12599.

Secondary Publications

Conference abstract

Ekram, A. E., Hamilton, R., Campbell, M., Plett, C., Kose, S., Russell, J., Stevenson, J., and Coolen, M. (2021). A 1 Ma record of climate-induced vegetation changes using *sed*aDNA and pollen in a biodiversity hotspot: Lake Towuti, Sulawesi, Indonesia. EGU General Assembly 2021, online, 19–30 Apr 2021, EGU21-4003, oral presentation.

Contribution of others

Under the principal supervision and guidance of A/Prof. Marco Coolen, the first author (Md. Akhtar-E-Ekram), primarily conducted all experiments, analysed the results, and wrote the individual manuscripts for this thesis. Contributions by co-authors are detailed below.

Chapter 2: A 1Ma sedimentary ancient DNA (*sed*aDNA) record of catchment vegetation changes and the developmental history of tropical Lake Towuti (Sulawesi, Indonesia).

Md Akhtar-E Ekram, Matthew Campbell, Chloe Plet, Rebecca Hamilton, Satria Bijaksana, Kliti Grice, James Russell, Janelle Stevenson, and Marco JL Coolen.

JR, JS, and RH organised and managed the field campaign and sampling. AE and MJLC designed the study and AE wrote the chapter with contributions from all co-authors; AE and CP performed experiments, and MC performed data analysis using ObiTools.

Chapter 3: A 1 Ma *sed*aDNA record of tropical paleovegetation assemblages and their associations with parasitic, endophytic, and saprophytic fungi.

Md Akhtar-E Ekram, Cornelia Wuchter, Kliti Grice, James Russell, and Marco JL Coolen.

AE and MJLC designed the study and AE wrote the chapter with contributions from all co-authors; AE performed the lab experiments and data analysis.

Chapter 4: A combined pollen and sedimentary ancient DNA (*sed*aDNA) record of vegetation changes in the Black Sea region since the Younger Dryas.

Md Akhtar-E Ekram, Cornelia Wuchter, Liviu Giosan, Kliti Grice, and Marco JL Coolen.

MJLC and LG secured funding for this project from the US National Science Foundation (NSF). MJLC and CW organised and managed the field campaign and sampling. AE and MJLC designed the study, and AE wrote the chapter with contributions from the other authors. AE performed all lab experiments and data analysis.

Signed statements of the co-authors are attached at the end of the thesis in the appendix section.

Table of Contents

List of Figures

Chapter 2: A 1Ma sedimentary ancient DNA (*sed*aDNA) record of catchment vegetation   changes and the developmental history of tropical Lake Towuti (Sulawesi, Indonesia).

Figure No.	Title	Page No.

Figure 2.2 Total environmental DNA (eDNA) concentration and general overview of the recovered Paleogenic sequence data: (A) Amount of extracted total eDNA (ng/g sediment). (B) The total number of reads from paleovegetation. Samples containing fewer than 200 *trn*L-P6 reads of paleovegetation, which were excluded from further analysis are indicated in red. (C) Total number of ASVs that could be assigned to paleovegetation at family, clade, subfamily, tribe, or genus levels. The number of taxa inferred from the sum of ASVs assigned to the same taxonomic ranks in the 82 remaining analysed sediment intervals. See Figs. S2.1-S2.3 for an overview of the contaminants and unassigned ASVs or sequencing artefacts removed from the dataset before processing. The lithology graph left of panel A shows the alternating deposition of silty clay and peat intervals during the pre-lake stage (Unit 2), followed by permanent lacustrine conditions above the U2/U1 transition at 98 mcd. See Russell et al. (2020) and results and discussion in the main text for a detailed description of the main lithologies (lacustrine green clays, red sideritic clays, and diatom ooze intervals vs pre-lake fluvial silts and peats) and for the paleohydrological/paleodepositional conditions that were used to define the major pre-lake U2 and lacustrine U1a-, U1b, and U1c stages and their transitions. The lithology graph further shows

Figure No.	Title	Page No.

Supplementary figures

Chapter 3: A 1 Ma *sed*aDNA record of tropical paleovegetation assemblages and their associations with parasitic, endophytic, and saprophytic fungi

Figure No.	Title	Page No.

Figure No.	Title	Page No.

Supplementary figures

Chapter 5: Conclusion and Future Prospective

List of Tables

Abbreviations

aDNA	:	Ancient DNA
AT	:	Atlantic
Sed aDNA	:	Sedimentary Ancient DNA
AGRF	:	Australian Genomic Research Facility
ANOSIM	:	Analysis of similarity
ASVs	:	Amplicon Sequence Variants
B/A	:	Bølling-Allerød interstadial
BLAST	:	Basic Local Alignment Search Tool
BP	:	Before Present
bp	:	Base pair
cal. BP	:	Calibrated years before the present
CAP	:	Canonical Analysis of Principal coordinates
cm	:	Centimetre
cpDNA	:	Chloroplast DNA
C3	:	C_3-carbon fixation pathway
C4	:	C_4-carbon fixation pathway
DLDS	:	Deep Lakes Drilling System
DNA	:	Deoxyribonucleic acid
eDNA	:	environmental DNA
e.g.	:	For example,
GC	:	Gravity Core
GGC	:	Giant Gravity Core
ICDP	:	International Continental Scientific Drilling Program
IPWP	:	Indo Pacific Warm Pool
IS	:	Interstadial

ISA	:	Indicator Species Analysis
HPC	:	Hydraulic piston corer
ka	:	Kilo-annum
km	:	kilometre
kyrs	:	Kilo-years
LacCORE	:	National Lacustrine Core Facility
LGM	:	Last Glacial Maximum
LPAZ	:	Local Pollen Assemblage Zones
m	:	Meter
Ma	:	Mega annum
m.a.s.l.	:	Meters above sea level
MC	:	MultiCore
mcd	:	Meters composite depth
MIS	:	Marine Isotope Stage
MiSeq	:	Illumina's integrated next generation sequencing instrument
NE	:	Northeastern
NGS	:	Next generation sequencing
NMDS	:	Nonmetric MultiDimensional Scaling
OIS	:	Oxygen isotope stage
OM	:	Organic Matter
ORF	:	Open Reading Frames
OTUs	:	Operational Taxonomic Units
PB	:	Preboreal
PCR	:	Polymerase Chain Reaction
qPCR	:	Quantitative PCR
rDNA	:	Ribosomal DNA
rRNA	:	Ribosomal RNA

S	:	Stadial
SA	:	Subatlantic
SB	:	Subboreal
SIMPER	:	Similarity of Percentage
SOM	:	Soil Organic Matter
SSS	:	Sea Surface Salinity
SST	:	Sea Surface Temperature
SW	:	Southwestern
TDP	:	Towuti Drilling Project
TLE	:	Total Lipid Extract
TRSH	:	Trees and/or Shrubs
TOC	:	Total Organic Carbon
vs.	:	Versus/ opposed to
WHOI	:	Woods Hole Oceanographic Institution
wt.	:	Weight
XRF	:	X-ray fluorescence
YD	:	Younger dryas

Chapter 1

Introduction

1.1 Paleoclimate and paleoecology

Vegetation plays a central role in global carbon fixation and mitigating global warming. As primary producers, they shape Earth's biosphere and biodiversity. While it would have been possible for plants to have evolved without animals, animals would not have existed in a world without plants (Fernando, 2012). The Anthropocene and its impact on landscape degradation, not limited to deforestation for agricultural activities, started as early as 10,000 years ago, coincident with the end of the last Glacial and the transition into the warmer and wetter Holocene (Steffen et al., 2011). However, the disastrous human impact on Earth's ecosystems and landscape deterioration only started to increase exponentially since the start of the Industrial Revolution and subsequent population growth (Doughty et al., 2013). The continuous tracking of ecosystem changes only started a few decades ago. However, long-term records of ecosystem responses to climatic and anthropogenic perturbations are required to properly understand the significance of events such as the current biodiversity crisis ("the sixth mass extinction") and to anticipate long-term potential outcomes (Rull, 2022; Melinda, 2018).

Marine and lake sediments provide decadal to millennial-scale geobiological archives of past ecosystem community compositions and diversity and their interactions with changes in the paleodepositional environment. Traditionally, the most used approaches involve the microscopic or macroscopic analysis of diagnostic morphological remains preserved in terrestrial and marine sedimentary records. In case of tracking changes in paleovegetation, these studies mainly rely on the microscopic determination of pollen, spores, and phytoliths and the macroscopic determination of plant parts such as leaves, seeds, and flowers (Horrocks, 2020; Lisztes-Szabó et al., 2019; Souto et al., 2019). DNA-barcoding approaches utilising a variety of variable regions of chloroplast DNA (cpDNA) are also widely used to identify plants (Dong et al., 2012; Palmer et al., 1988), often at unprecedented high taxonomic resolution. For example, cpDNA barcoding methods have been developed to study the evolution and phylogeny of the genus *Triticum*, which includes the bread

wheat species *T. aestivum* L., as well as other cultivated and wild-type species (Golovnina et al., 2007). Such detailed species-level taxonomic resolution for *Triticum* is not possible otherwise. Over the last two decades, various studies have shown that lacustrine and marine sedimentary records also represent important archives of ancient vegetation DNA (see Capo et al., 2021 and references therein for a relatively recent overview). Extraction of this ancient sedimentary DNA (*sed*aDNA) and subsequent sequencing analysis of preserved vegetation metabarcoding genes has the potential to complement fossil pollen in reconstructing past vegetation assemblages and their responses to paleoenvironmental and more recent anthropogenic perturbations (e.g., Alsos et al., 2021; Courtin et al., 2021; Epp et al., 2015; Li et al., 2021; Niemeyer et al., 2017; Parducci et al., 2013; 2015; Pederson et al., 2013; Zimmermann et al., 2017).

The following paragraphs provide a more detailed overview of these approaches and the pros and cons of using microscopic, macrofossils, and chloroplast metabarcoding genes to reconstruct Quaternary paleovegetation assemblages, the geological *era* targeted for this PhD thesis.

1.2 Reconstruction of paleovegetation assemblages and environmental changes using micro- and macroscopic sedimentary plant remains

1.2.1 Fossil pollen palynomorphs and spores provide a valuable record of the evolutionary history of vegetation and their response to past climate change (e.g., Anshari et al., 2004; Hamilton et al., 2019; Hope, 2001; Stevenson, 2018). However, overlapping morphological features can complicate the identification of various plant families at lower taxonomic levels, even for Quaternary paleovegetation assemblages, despite the relatively well-known relationship between pollen and source plants compared to records from this relatively recent chronozone (e.g., Giesecke et al., 2014). For example, identifying true grasses at the genus or species level is mainly restricted to cultivated grasses such as wheat and barley, whereas most native grasses can only be identified at the family level (Poaceae) due to overlapping pollen morphology. Identification at sub-family to species-level taxonomic ranks would be required to distinguish between wet climate C_3 and dry climate C_4 grasses and those that can switch between C_3 and C_4 carbon fixation pathways (Mander and Punyasena, 2014 and references therein). Although the parallel analysis of phytoliths (as detailed

below) could help to lower the taxonomic resolution of native grasses, pollen-based paleo-floristic studies almost exclusively interpret a relative increase in the abundance of graminoid- over arboreal pollen grains as evidence for the expansion of steppe vegetation during drier climate conditions. In contrast, an inversed pollen ratio suggests an expansion of forest vegetation during periods of increased precipitation (Filipova-Marinova et al., 2012). This generalised scenario implies that C_4 grasses dominated the landscape during drier conditions. Since grasses can occupy a wide range of habitats, an increase in graminoid palynomorphs in the lake sedimentary record could also indicate an increase in long-term or seasonal precipitation regimes and a subsequent expansion of wetlands and catchment surface areas dominated by C_3 grasses.

In addition, wind-pollinated grasses, sedges (Cyperaceae), and conifers produce large amounts of pollen and can, therefore, be overrepresented in sedimentary pollen grain assemblages. In contrast, herbs and most tropical rainforest angiosperms have low pollen production rates and are likely poorly represented in sedimentary records as this vegetation typically relies on animal vectors for pollination and successful reproduction (e.g., Ollerton et al., 2011).
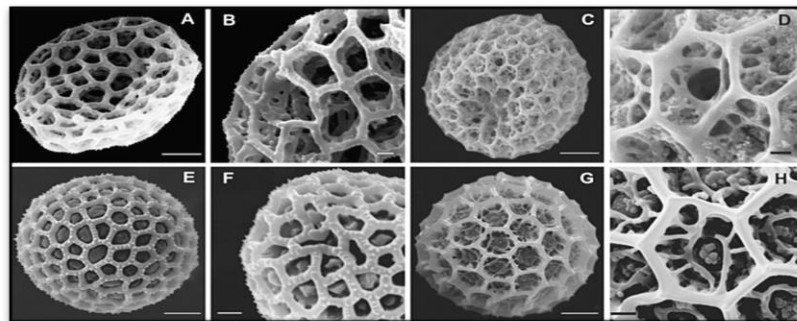
Figure 1.1 SEM images of the prehistoric pollen grains (A–D) and their closest modern counterparts with their morphology (E–H) (Palazzesi et al., 2012). *(A). Balbisia. Wendita type, (B). Balbisia, (C, D), Viviania marifolia type, (E). Balbisia calycina Sleumer 246, (F). Balbisia calycina, (G). Viviania ovata, (H). Viviania marifolia.*

Moreover, wind-dispersed pollen can travel long distances, which hampers the use of pollen records to reconstruct local vegetation changes (Parducci et al., 2015). Instead, pollen-based records mainly reflect landscape-scale changes in source plant composition within an area of ~10^5 km^2 (i.e., 300 x 300 km) (Cleal et al., 2021). Pollen grain analysis can also cover regional-scale plant diversity. This describes the diversity of plant fossils observed within a paleo-floristic province and most likely

reflects the source vegetation communities in an area larger than 10^5 km^2 (Cleal et al., 2021). In northern and temperate latitudes, Quaternary palynological data generally provide a good overview of regional-scale plant richness, being most robust for past tree vegetation (Reitalu et al., 2019).

1.2.2 Plant macrofossils mainly represent the localised allochthonous paleo-floristic community, generally dispersed over much smaller areas than pollen (Feurdean & Bennike, 2008; Birks, 2001). Stereomicroscopic determinations of leaves, needles, seeds, flower buds, bark, and rhizomes can be analysed in parallel to cross-validate palynology datasets to identify taxa that are usually overlooked from pollen for reasons outlined above, and assist in the identification of dominant cryptic pollen taxa (Parducci et al., 2015; Birks, 2003). Moreover, radiocarbon dating of macrofossils can generate accurate age models of sedimentary records. However, taphonomic factors may contribute to spurious diversity estimates, and variations in edaphic conditions can influence the level of post-mortem decay of plant tissue (Gestaldo and Demko, 2010). For instance, grasses, which are already challenging to classify using pollen, have a poor macrofossil record. Generally, vegetation growing further away from river or lake catchments is poorly represented as macrofossils. Nevertheless, plant remains from distant hinterland vegetation (albeit usually heavily fragmented) have been recorded from marine records and differed substantially in composition from the macrofossils of plant communities commonly observed in fluvio-lacustrine plant beds (Cleal et al., 2021 and references therein).

Figure 1.2 Plant macrofossil (modified after Denk et al., 2022).

1.2.3 Phytoliths (plant opals) are silicified microscopic plant remains accumulated in cell walls, cell cavities and intercellular spaces during growth. These plant diagnostic features can withstand up to 950^0 C (Piperno et al., 2006) and are released to the environment upon organic decay, burning, and digestion of the plant's vegetative parts. Upon burial in soil- and sedimentary records, phytoliths can be preserved for millions of years (An & Xie, 2022; Strømberg et al., 2013). Although not all plants produce phytoliths, grasses are notable phytolith producers. A subset of phytoliths are diagnostic at genus and species levels (Piperno, 2006) and can thus complement pollen spectra in identifying native grasses beyond the family level, as mentioned briefly above. Phytolith analysis from sedimentary records has been used to reconstruct paleoenvironmental and climatic perturbations, while residues of phytoliths associated with dental calculus, animal dung, and Neolithic and Bronze Age artefacts have revealed relevant insights into regional activities associated with early human settlement (i.e., agriculture, domestication of plants, dietary practices, and deforestation) (Lancelotti and Madella, 2018 and references therein). Several limitations regarding the interpretation of the phytolith assemblages still exist, such as subjectivity in morphological criteria and applying criteria from modern reference collections to archaeological assemblages and understanding taphonomy (Shillito, 2013). Moreover, in aquatic sedimentary records that are undersaturated in silica, these silicified features are prone to dissolution, which has also been frequently observed for silicified planktonic microfossils, notably diatom frustules (Ryves et al., 2001).
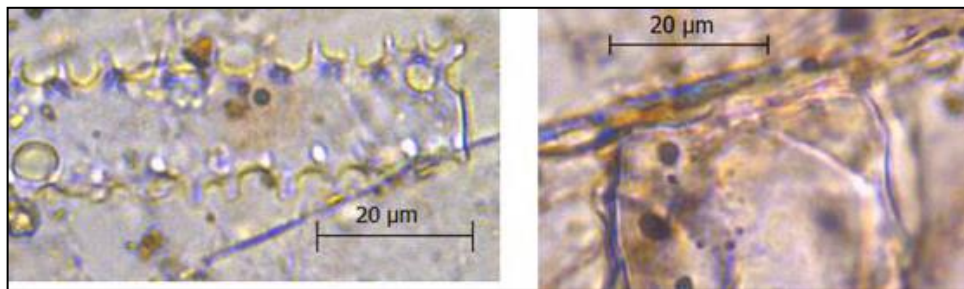
Figure 1.3 Epidermal phytolith morphotypes of conifers (*Picea* and *Pinus*) from An & Xie, 2022.

1.3 Stratigraphic analysis of ancient paleovegetation DNA

As mentioned above, several studies have shown that lacustrine (Capo et al., 2021 and references therein) and marine (Armbrecht et al., 2019 and references therein) sedimentary records also represent important archives of ancient vegetation DNA.

Extraction of this ancient sedimentary DNA (*sed*aDNA) and subsequent sequencing analysis of preserved vegetation metabarcoding genes has the potential to complement fossil pollen in reconstructing past vegetation assemblages and their responses to paleoenvironmental and more recent anthropogenic perturbations (e.g., Alsos et al., 2021; Courtin et al., 2021; Epp et al., 2015; Li et al., 2021; Niemeyer et al., 2017; Parducci et al., 2013; 2015; Pederson et al., 2013; Zimmermann et al., 2017). Since DNA degradation processes pose limits to the length of the fragments that can be retrieved from ancient specimens (Boere et al., 2011; Willerslev and Cooper, 2005), only stretches of cpDNA with less than 200 base pairs (bp) can be confidently analysed (Parducci et al., 2005; and illustrated in Fig. 1.4).

The short (10-143 bp; on average ~90 bp) variable P6-loop in the chloroplast *trn*L (UAA) intron (i.e., *trn*L-P6) (Taberlet et al., 2007) was found to be well preserved in the geological record (e.g., Capo et al., 2021 and references therein). The flanking regions are highly conserved so that most plants can be targeted for amplicon sequencing. A vast number of *trn*L-P6 sequences of contemporary Northern Hemisphere plant families are available in public databases such as NCBI's nonredundant nucleotides (nr/nt) database for comparison and taxonomic assignments of newly recovered environmental *trn*L-P6 sequences. Most vegetation can be identified at the family level, and in relatively low biodiversity environments, sequencing analysis of permafrost-preserved *trn*L-P6 outperformed the taxonomic resolution of pollen and resulted in the identification of ancient vegetation at the family level (100% of sequenced *trn*L-P6), 75% at the genus level, and 33% at the species level (Sonstebo et al., 2010).

Figure 1.4 Conceptual best practice workflow for sampling, processing, and analysing *sed*aDNA data (from Capo et al., 2022).

This combination of properties has made *trn*L-P6 one of the most frequently used plant metabarcoding genes in *sed*aDNA studies for reconstructing temporal changes in paleovegetation assemblages. Since chloroplasts are organelles found predominantly in plant leaves where most photosynthesis takes place, *sed*aDNA records targeting chloroplast-derived metabarcoding genes are thought to mainly represent catchment vegetation that drained into depositional basins as decaying chloroplast-rich plant litter via riverine- or terrestrial runoff (e.g., Alsos et al., 2018; Liu et al., 2020; Paus et al., 2015; Parducci et al., 2017; Voldstad et al., 2020). Lacustrine *sed*aDNA studies targeting cpDNA are considered particularly useful for reconstructing (semi) local scale paleovegetation assemblages.

Thus far, most terrestrial *sed*aDNA records have been generated from Holocene lakes located in high-latitude regions where relatively cold conditions contributed to promoting the long-term preservation of *sed*aDNA. For example, Clarke et al. (2020) generated a *sed*aDNA record of 24,000 years of vegetation dynamics in the Polar Urals, showing that Arctic-alpine species survived early-Holocene forest expansion in this heterogeneous landscape. In the European Alps, *sed*aDNA studies have provided new knowledge about the history of agricultural activities. For example, fruit trees absent from the pollen record were only detected

through *sed*aDNA metabarcoding (Bajard et al., 2017). Other *sed*aDNA studies have studied the effects of soil evolution, climate change, and pastoral activities on plant communities (e.g., Pansu et al., 2015). Metabarcoding approaches have also been used to identify vascular plants in Pleistocene permafrost soil samples (Jorgensen et al., 2012; Sonstebo et al., 2010).

Few studies have used *sed*aDNA to reconstruct tropical catchment vegetation changes (Boessenkool et al., 2014; Bremond et al., 2017; Dommain et al., 2020). These records only dated back several millennia and mainly comprised tropical lakes in cooler, high-altitude locations. Therefore, it remains to be seen how far back in time *sed*aDNA can be recovered and sequenced from tropical lakes after long-term exposure to less favorable, high *in situ* temperatures.

In addition, marine basins have thus far been greatly overlooked for reconstructing paleovegetation assemblages using *sed*aDNA approaches. Due to the greater distance to terrestrial source vegetation and a more complex and larger drainage area, marine *sed*aDNA records may represent the plant composition from the terrestrial hinterland at a larger landscape- or regional scale compared to inland lakes. Moreover, the quality and amount of sedimentary cpDNA in marine records may be substantially compromised due to the longer travel distance of drained chloroplast-rich plant litter from the source location and possibly longer exposure time to biotic and abiotic degradation processes before burial.

Several studies have also shown that soil-derived fungal DNA can be preserved in Holocene lacustrine records (Capo et al., 2016; Capo et al., 2021), permafrost soils (Bellemain et al., 2013; Lydolph et al., 2005), deep sea sediments (De Schepper et al., 2019), and cave sediments (Epure et al., 2014). Most recently, Hippel et al. (2021) reconstructed potential symbiotic, parasitic, and saprophytic fungal-plant associations using *sed*aDNA.

However, stratigraphic analysis of *sed*aDNA suffers from its drawbacks. For example, of all paleoecology proxies, DNA is likely the most labile biomolecule and most prone to post-mortem microbial attack and abiotic alterations during transportation and subsequent deposition and burial of the source organisms in the underlying sediments.

8

Exposure to unfavourable abiotic conditions such as elevated temperature, oxygen, ultraviolet radiation, and microbial attack during taphonomic processes leads to DNA damage (e.g., base pair substitutions), and fragmentation (Jia et al 2022). Postburial successive degradation of ancient genetic materials, such as deamination of cytosine, depurination, and fragmentation, increases with age, which could hamper the integrity of *sed*aDNA, resulting in spurious representations of compositional signals and temporal patterns of paleo-communities (Dalen et al., 2023). Adsorption to clay minerals can slow down the rate of degradation (Coolen and Overmann, 2007; Kanbar et al., 2020; Parducci et al., 2019), but the amount of genuine ancient genetic material that escaped downcore degradation to be targeted for reconstructing past aquatic and terrestrial ecosystems is often only present at trace levels in the sedimentary record, making this pool of DNA very prone to contamination with modern DNA. This requires stringent measures to minimise the chance of contamination offshore (during coring, subsampling, and transport) and onshore processing of samples in the laboratory, and the need to use proper controls to identify and eliminate contaminant sequences from the dataset (Fig. 1.4; Capo et al., 2022). For example, drilling muds are often used during coring as a lubricate to prevent the drilling bit from overheating. Microbial cell counts in these muds often exceed those of the low biomass deep subsurface environment by orders of magnitude and, therefore, considered a major potential source of contamination with intact cells from surface-dwelling microbial communities (e.g., Cockell et al., 2021; Friese et al., 2017; Inagaki et al., 2015). Fluorescent particles (tracers) which mimic the shape and size of bacterial cells are usually mixed with drilling fluids so that after core retrieval, sediment slices can be analysed microscopically to determine the extent and how deep these fluorescent tracers and possibly contaminant bacteria (could) have penetrated the core material (e.g., Friese et al., 2017). If fluorescent particles are absent, it is unlikely that larger eukaryotic unicellular plankton or pollen of modern origin have penetrated and contaminated the core material. Furthermore, amplicon sequencing of ancient genetic DNA from sediments does not provide reliable information about absolute quantitative community changes (Capo et al., 2021 and references therein). PCR bias can lead to a skewed over- or under-representation of taxa due to genomic-, cellular-, and species-specific variation in the number of targeted metabarcoding gene(s), sequence divergence in priming sites, and shifts of oligonucleotide tags among

amplicons during amplification (Rodriguez-Martinez et al., 2022, Krehenwinkel et al., 2017). Finally, ancient DNA authenticity and control over modern DNA depend on the use of proper bioinformatics methods to identify DNA damage pattern during post sequencing data processing (Slon et al 2017; Armbrecht et al., 2020).

1.4 Study locations

1.4.1 Tropical Lake Towuti (Sulawesi, Indonesia; *Research Chapters 2 and 3*)

The maximum 205-m-deep Lake Towuti (2.75° S, 121.5° E) is the oldest and largest (500 km^2 surface area) member of the tectonic Malili Lake complex, which furthermore comprises the smaller Matano- and Mahalona lakes (Figs. 1.5 and 1.6). The lake is positioned in a floristically biodiverse montane catchment area (~1144 km^2) at 318 meters above sea level (m.a.s.l.) (Russell et al., 2014) and in the centre of the Indo-Pacific Warm Pool (IPWP). The surface and bottom water temperatures of Lake Towuti are year-round ~31 and 28.5^0 C, respectively. The water column is thermally stratified, and anoxic conditions persist below 125 m (Fig. 1.5c). Due to the deficient sulphate concentrations and negligible activities of sulphate-reducing bacteria, the anoxic bottom waters are not sulfidic (Vuillemin et al., 2016). Precipitation within this tropical humid region at the lake's elevation averages 2,700 mm annually. It is strongly controlled by coupled interactions between the Australian-Indonesian winter and summer monsoons, regional sea surface temperatures, and the strength and position of the Intertropical Convergence Zone (ITCZ; Aldrian & Susanto, 2003; Hendon, 2003).
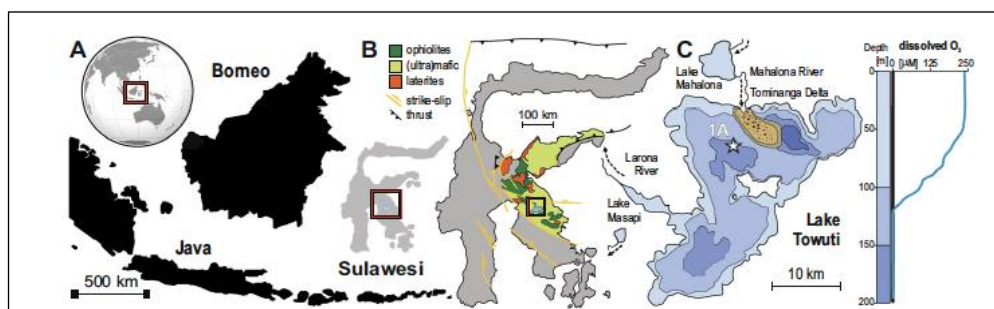
Figure 1.5 Location and geological setting of Lake Towuti. (A) Map showing the location of Lake Towuti in Sulawesi (Indonesia). and its position within the Malili Lake system and the main geological formations. (B) The island of Sulawesi and the geological formations surrounding Lake Towuti. (C) Bathygraphic map showing the coring location 1A where the water depth was 153 m. The oxygen profile on the right shows that the bottom waters were oxygen depleted at the coring location (after Friese et al., 2021).

Riverine catchment bedrock compositions leave a strong imprint on sediments in Lake Towuti (Costa et al., 2015; Goudge et al., 2017; Hasberg et al., 2019; Morlock et al., 2019; Sheppard et al., 2019; 2021). These studies reported that the Mahalona River and its largest tributary, the Lampenisu River, drain catchments primarily composed of serpentinised peridotite and ultramafic-derived Quaternary alluvium and supply most of the magnesium (Mg)- and serpentine-rich sediments into Lake Towuti's northern basin. Smaller rivers drain catchments dominated by ultramafic bedrock in the northeast and southwest and supply Lake Towuti with eroded topsoil enriched in iron (Fe), as well as potentially phytotoxic chromium (Cr) and nickel (Ni) (Russell et al., 2020).

The contribution of eroding topsoil and ultramafic substrates into Lake Towuti via these rivers is enhanced during drier and colder climate conditions, when lake level low stands, enhanced oxygenation of the water column, and efficient trapping of phosphate (P) to sedimentary iron hydroxy oxides leads to the formation of ultraoligotrophic conditions and low primary productivity (Crowe et al., 2008). Such conditions were most pronounced during the Last Glacial Maximum (LGM) when a much drier climate in Sulawesi than today resulted in a reduction of the lake water level by 10-35 m and deeper water column mixing (Vogel et al., 2015).
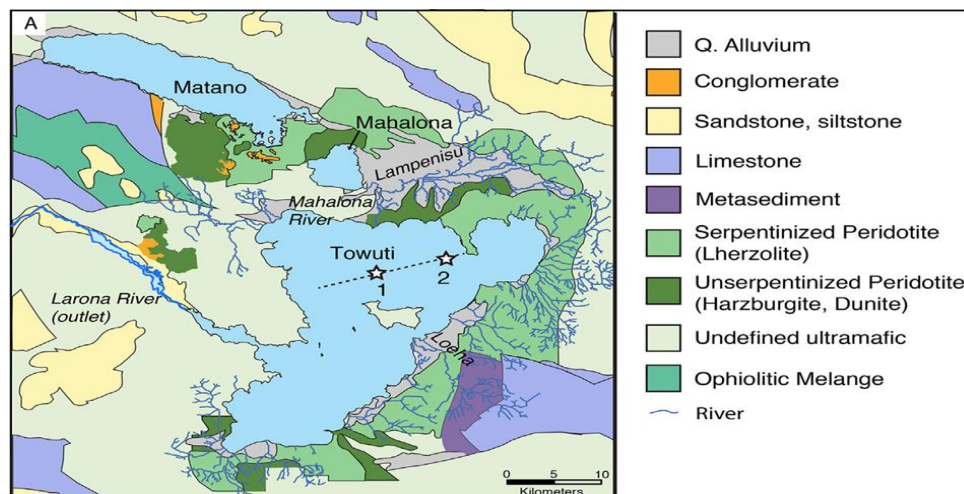
Figure 1.6 Detailed overview of the catchment geology of the Malili lake system and the location of the main rivers draining predominantly ultramafic (Mahalona- and Lampenisu Rivers) vs. felsic (Loeha River) catchment substrates into Lake Towuti. The white star (1) marks the location where core 1F for this thesis was obtained.

In contrast, the Loeha River draining a catchment of more felsic bedrock to the east of Lake Towuti, together with lateritic soils, which develop on ultramafic bedrock, deliver fine-grained sediments that are rich in kaolinite and quartz and are the most relevant sources of Titanium (Ti), Aluminium (Al), and potassium (K) to the deep northern lake basin where our core was recovered (Costa et al., 2015; Hasberg et al., 2019; Morlock et al., 2019). The erosion and sedimentation of laterite soil and Loeha River material are enhanced during warm and wet climate conditions. During increased precipitation and drainage from the Loeha River, Lake Towuti experiences lake-level high stands and the formation of a stratified water column and anoxic water anoxia. Under the reducing conditions, sedimentary-bound P is released to the photic zone, which promotes primary productivity, and such conditions prevailed during the relatively warm and wet Holocene (Russell et al., 2014; Costa et al., 2015; Vogel et al., 2015; Morlock et al., 2019; Russell et al., 2020).

In 2015, the Towuti Drilling Project (TDP), which involves a team of over 30 international researchers, recovered up to 120-m-long sediment cores from Lake Towuti aimed to reconstruct long-term environmental, climatic, and biological change in the tropical West Pacific (Russel et al., 2016; 2020). According to detailed geochronological, lithostratigraphic, mineralogical, and geochemical analysis spanning the entire sedimentary record, Lake Towuti emerged during accelerated tectonic subsidence from a landscape initially characterised by active river channels, shallow lakes, and swamps into a permanent lake ~1 Ma ago (Russell et al., 2020). Pre-lake sediments (Unit 2 or U2) mainly consist of alternating fluvial silty clays and peat layers. A thick peat interval between 101-98.8 mcd marks the transition into a permanent lake (Unit 1or U1). The U2/U1 boundary at 98.8 mcd was estimated to have occurred ~1 Ma ago through extrapolation of an accurately ^{40}Ar/^{39}Ar dated prominent tephra layer at 72.95 mcd which was deposited 797.3 ± 1.6 Ka (Russell et al., 2020). The lacustrine U1 sediments contain alternating red sideritic and green organic-rich clay intervals, which likely reflect orbital-scale cyclicity between drier/cooler/oxygenated/ultraoligotrophic and wetter/warmer/stratified/oligotrophic conditions, respectively (Russell et al., 2020). However, a more highly resolved age model from Unit 1 spanning marine isotope stages (MIS) 6 to 22 suggested that the transitions between Glacials and Interglacials do not per definition, always overlap with transitions between red and green clays (Ulfers et al., 2021).

Whereas Lake Towuti was ultraoligotrophic to oligotrophic during most of its history (Bramburger et al., 2008), long-term accumulation and subsequent weathering of tephra-bound P in the catchment may have contributed to the development of mesotrophic conditions and maximum productivity, which ultimately resulted in the deposition of two several-meters-thick diatomaceous oozes between 32-37 and 43-46 mcd (Russell et al., 2020). A low %Fe content and the presence of well-preserved sedimentary organic matter (SOM), as indicated by a high ratio of total extractable lipids (TLE) over total organic carbon (TOC) (i.e., a high TLE/TOC ratio), in the partly laminated oozes suggests that stratified conditions and bottom water anoxia also contributed to the release of sedimentary P and the increased primary productivity of diatoms (Russell et al., 2020).

At much longer timescales, the lacustrine record revealed three major shifts in paleodepositional and paleo-hydrological conditions. U1c (~98-76 mcd) shows frequent oscillations between more felsic (K-rich) and ultramafic (Mg-rich) sediments. These oscillations in sediment sources were likely caused by variable fault motion and a continued influence of tectonically driven changes in basin morphology and catchment hydrology (Russell et al., 2020). U1b (76-30 mcd) has low %Mg and undetectable amounts of serpentine. A combination of a higher contribution of green clays and elevated %K suggests an increased discharge of felsic sediments from the Loeha River and overall wetter/warmer conditions, lake-level high stands, and stratified and anoxic conditions that promoted primary productivity (Fig. 1.7). U1b is also the interval with the unique presence of the diatom oozes. The overlying U1a (top 30 m) shows a substantial increase in %Mg, indicative of a connection of the Lampenisu and Mahalona Rivers between Lakes Mahalona and Towuti (Russell et al., 2020).
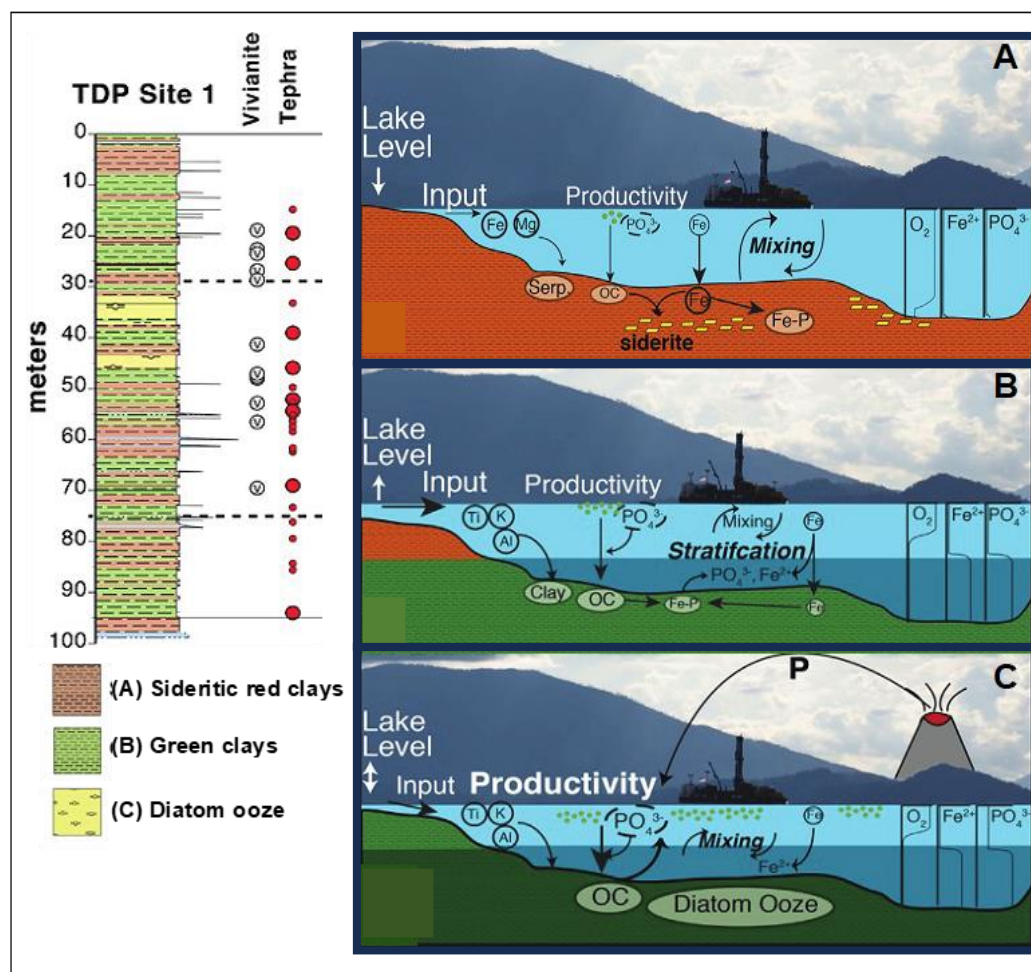
Figure 1.7 Schematic figures indicating inferred changes in lake level, water column mixing, oxygenation, nutrient concentrations, and biogeochemical cycling resulting in the formation of (A) red clays, (B) green clays, and (C) diatomaceous oozes in Lake Towuti. The composite lithostratigraphy from TDP Site 1 lacustrine Unit 1. Open circles with a V indicate the occurrence of macroscopic vivianites, and red circles indicate the presence of macroscopic tephra (Russell et al., 2020).

Moreover, the microbial composition and the role that microbial communities play in biogeochemical cycling in the low-oxygen ferruginous (iron-rich and sulphate-poor) sediments of Lake Towuti have been studied in detail by the TDP team (Friese et al., 2021; Vuillemin et al., 2016; 2017; 2018). These studies have provided important insights into how, for example, organic matter was mineralised under comparable conditions, which prevailed in the oxygen-depleted ferruginous Archaean and Proterozoic oceans (Friese et al., 2021). Fermentation and methanogenesis were shown to dominate sedimentary organic matter (SOM) mineralisation despite highly

abundant reactive ferric iron phases like goethite. This showed that ferric iron can be buried over geologic timescales even in the presence of labile organic carbon.

The coexistence of ferric iron with millimolar concentrations of methane further demonstrated a lack of iron-dependent methane oxidation (Friese et al., 2021). Despite ongoing microbial degradation of sedimentary organic matter (SOM) and long-term exposure to unfavourable high in-situ temperatures, extracellular microbial DNA was found to be preserved and successfully sequenced from the upper 35 m of analysed sediments (Vuillemin et al., 2017). Exogenous sources of extracellular sedimentary DNA were identified as those associated with soils reworked from the ferruginous catchment soils and adsorption to mineral and organic matrices most likely contributed to the long-term survival of the extracellular pool of sedimentary ancient DNA (Vuillemin et al., 2017).

The premise that extracellular microbial DNA can be recovered and sequenced from Lake Towuti sediments (Vuillemin et al., 2017), and the availability of geochemical proxy data have resulted in the vast knowledge about the lake's developmental history (e.g., Russell et al., 2020), created a unique opportunity to explore the suitability of *sed*aDNA for reconstructing terrestrial ecosystems in the tropics well beyond the Holocene era (Chapters 2 and 3 of this thesis) and to contribute to addressing one of the overarching aims of the TDP program: To understand long-term environmental, climatic, and biological changes in the tropical West Pacific.

1.4.2 The Black Sea (*the study location for thesis Chapter 4*)

Marine basins have thus far been under-sampled for reconstructing paleovegetation assemblages using *sed*aDNA approaches. Whereas vegetation DNA in lake sediments is considered predominantly of local origin, sediment records from more remote marine basins may represent paleo-genomic archives of local- or landscape-scale paleo-floristic diversity due to the much larger drainage area compared to inland lakes. It remains to be confirmed to what extent drained plant material reaches remote coring locations in marine basins and, upon burial, represents suitable archives of *sed*aDNA for reconstructing paleovegetation assemblages from the coastal hinterland.

The Black Sea was considered an ideal geological setting as a starting point to close this knowledge gap due to its sensitivity to climate-driven environmental and

hydrological changes, and the analysis of biogenic and geochemical proxies from the underlying late Glacial and Holocene sediments have provided a wealth of information about the paleo-environmental and paleo-ecological history of the eastern Mediterranean, one of the key centres of the agriculture revolution and civilization in the world (Giosan et al., 2012; Turney & Brown, 2007).

There are three late-Quaternary litho-stratigraphic units (Unit I, Unit II and Unit III) (Ross and De-gens, 1974), corresponding to the major stages of the Black Sea's environmental evolution. Calcite-rich and carbon-depleted Unit III sediments were deposited during the last Glacial when the Black was a landlocked fresh to a brackish lake (Ross & Degens, 1974; Yanchilina et al., 2017). Subsequent post-glacial sea level rise caused the Black Sea Lake to reconnect with the Mediterranean when the Bosporus sill was breached roughly 9,400 years ago. A positive freshwater budget controlled by the major rivers (notably the Danube), and direct precipitation led to the export of low-salinity water in the direction of the Mediterranean through the narrow and shallow Straits of Bosporus. In contrast, denser water from the Sea of Marmara flowed into the Black Sea as an undercurrent. This bi-directional flow of lower density fresher surface waters and more saline denser bottom waters resulted in permanent water column stratification, bottom water euxinia, and the deposition of the Unit II organic-rich sapropel ~ 7.6 ka BP. The timing of the onset of sapropel deposition overlaps with the start of the warm and moist Atlantic chronozone ~ 8 ka BP, which has been proposed to be the key trigger of the Neolithic culture transition in Europe (Ryan & Pitman, 1998; Turney & Brown, 2007). Sediments deposited since the last ~2,500 years ago comprise coccolith marl of Unit I when, according to alkenone D/H ratios (Van der Meer et al., 2008; Giosan et al., 2012; Huang et al., 2021), the Black Sea experienced a dramatic freshening throughout the entire basin which coincides with the onset of the Subatlantic climate (Wanner et al., 2008). The permanently stratified brackish Black Sea continues to be the largest anoxic basin in the world. Currently, only the upper ~100 m is fully oxygenated while a ~30-m-thick layer separates the oxygenated mixolimnion from the up to 2200 m deep permanently anoxic and sulfidic bottom waters (Volkov & Neretin, 2007; Dean & Arthur, 2010).

A subset of palynological studies has provided detailed information about multi-decadal to centennial-scale coastal vegetation and terrestrial climate variability in the Black Sea region as far back as the last glacial maximum (LGM) (Atanassova, 2005; Connor et al., 2013; Connor et al., 2007; Cordova et al., 2009; Filipova-Marinova, 2006; Filipova-Marinova et al., 2012; Mudie et al., 2007; Mudie et al., 2002; Shumilovskikh et al., 2012). Moreover, various studies have shown that all three sedimentary units represent rich archives of ancient plankton DNA, including those lacking preserved microfossils (Coolen, 2011; Coolen et al., 2013; Coolen et al., 2009; Corinaldesi et al., 2011; Giosan et al., 2012; Manske et al., 2008). In addition, temporal changes in plankton communities inferred from *sed*aDNA showed strong correlations with the palaeo-hydrological and palaeo-environmental conditions that prevailed at deposition (Giosan et al., 2012; Coolen et al., 2013).

These studies provided leverage for the likelihood that *sed*aDNA from terrestrial and aquatic vegetation could also be preserved in the sedimentary record of the Black Sea. The well-dated giant gravity core (GGC18) used for the latter studies was obtained from a water depth of 971 m, ~100 km offshore the western Black Sea slope (Bulgaria) during expedition AK06 on board the *R/V Akademik* (Institute of Oceanology, Bulgarian Academy of Sciences) (Fig. 1.8). *Genomic DNA from the same core GGC18 was used to generate the trnL-P6 amplicon sequencing dataset for Chapter 4 of this study.* The record of GGC18 covers the cold- and dry Younger Dryas, the deglacial (Preboreal), and the warmer and wetter Holocene.
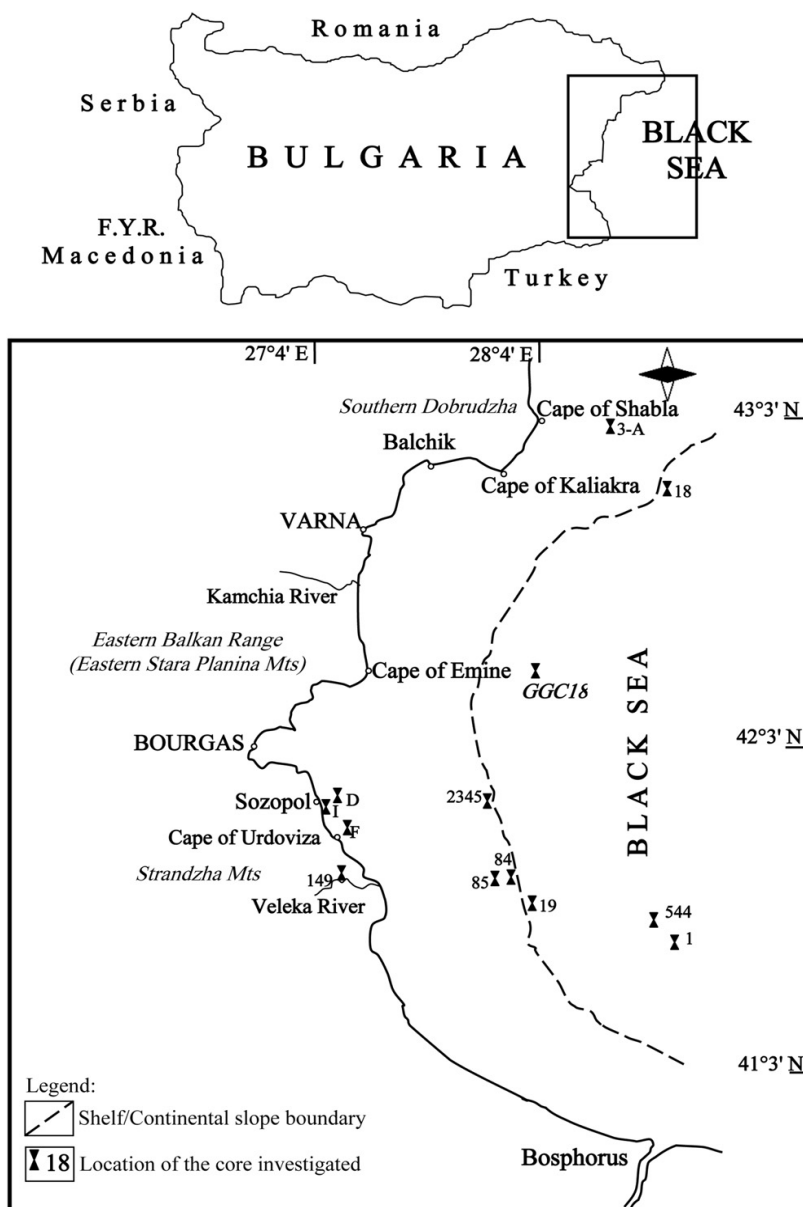
Figure 1.8 Map of Bulgaria (top figure) and a blown-up view of the western continental slope of the Black Sea showing the coring location (GGC18) and its position in relation to the continental slope and the Eastern Balkan Range, which is nowadays dominated by xerothermic forest vegetation. The study area constitutes the Black Sea region of the Euxinian province of European deciduous forest (Filipova-Marinova et al., 2012).

1.5 Re-cap of the RESEARCH AIMS involving chapters 2-4 of this thesis.

Chapter 2 describes sedimentary *trn*L-P6 amplicon sequencing to generate a record of Quaternary tropical catchment and aquatic vegetation changes associated with major transitions in limnological and hydrological changes throughout Lake Towuti's more than 1 Myr developmental history. Furthermore, the potential origins of the sedimentary chloroplast DNA were inferred from Pearson correlations between downcore relative changes in the *trn*L-P6-inferred paleovegetation assemblages and available (in)organic geochemical paleo-hydrological and paleo-environmental proxy data. *The results of this study address the following research questions:*

- *What is the preservation potential of sedaDNA in tropical lake records, and how far back in time can plant-specific metabarcoding genes be recovered and sequenced?*

- *Can metabarcoding of sedimentary chloroplast marker genes accurately describe the paleovegetation assemblages in tropical biodiversity hotspots?*

- *To what extent does the terrestrial paleovegetation sedaDNA record in tropical lakes inform about concomitant climate-induced changes in the paleodepositional environment?*

Chapter 3 uses 18S rRNA amplicon sequencing to compare the paleovegetation community composition with those described in Chapter 2 and to identify additional palaeo-environmentally relevant members of the Domain Eukarya throughout Lake Towuti's history. Since this analysis revealed an overwhelming predominance of fungal communities, Pearson correlation analysis between the *sed*imentary *trn*L-P6 (Chapter 2) and 18S rRNA (this chapter) was used to study the potential symbiotic, parasitic, and saprotrophic associations that existed between fungi and the local paleovegetation community. *This chapter aims to address the following specific research questions:*

- *What was the origin of the fungal taxa identified throughout Lake Towuti's record?*

- *Which fungal taxa represented symbiotic endophytes, ectomycorrhiza, plant pathogens, or lignin/cellulose degrading saprobes involved in wood, leaf, or soil organic matter degradation?*

- *Do saprobic fungi have the potential to continue decomposing sedimentary OM as anaerobic fermenters and form a symbiotic relationship with hydrogenotrophic methanogens?*

- *If so, can they still form an indirect genomic record of the role they played in the decomposition of dead wood or plant litter at the time of deposition?*

Chapter 4 describes a combined pollen and sedimentary *trn*L-P6 record of late-Glacial and Holocene vegetation changes in the Black Sea region at multi-decadal resolution. The Black Sea was chosen for this study due to the wealth of information that is available concerning its sensitivity to paleohydrological and paleo-environmental perturbations. The well-dated core used for this study (Fig. 1.9) was obtained from a water depth of 971 m, ~100 km offshore the western Black Sea slope (Bulgaria) and extensively studied previously for the reconstruction of plankton-climate interactions through paired stratigraphic analysis of *sed*aDNA and geochemical and isotopic paleo-environmental parameters. The record covers the cold and dry Younger Dryas, the deglacial, and the warmer and wetter Holocene. *This chapter aims to address the following knowledge gaps:*

- *Do remote marine basins with much larger and complicated catchment areas compared to inland lakes represent suitable sedimentary archives of terrestrial and marine paleovegetation communities?*

- *To what extent does the composition, relative read abundance, and geographic origin of the source vegetation overlap between sedaDNA and pollen datasets in marine sedimentary records?*

- *Can marine sedaDNA datasets complement, refine, or overturn pollen-inferred interpretations concerning the climatic or anthropogenic perturbations that may have contributed to changes in the regional paleo-floristic landscape?*

20

1.6 References

Aldrian, E. & Susanto, R.D. (2003). Identification of three dominant rainfall regions within Indonesia and their relationship to sea surface temperature. *International Journal of Climate, 23,*1435–1452.

Alsos, I. G., Lammers, Y., Kjellman, S. E., Merkel, M. K. F., Bender, E. M., Rouillard, A., Erlendsson, E., Guðmundsdóttir, E. R., Benediktsson, Í. Ö., Farnsworth, W. R., Brynjólfsson, S., Gísladóttir, G., Eddudóttir, S. D., & Schomacker, A. (2021). Ancient sedimentary DNA shows rapid post-glacial colonisation of Iceland followed by relatively stable vegetation until the Norse settlement (Landnám) AD 870. *Quaternary science reviews*, *259*, 106903.

Alsos, I. G., Lammers, Y., Yoccoz, N. G., Jørgensen, T., Sjögren, P., Gielly, L., & Edwards, M. E. (2018). Plant DNA metabarcoding of lake sediments: How does it represent the contemporary vegetation. *PLOS ONE, 13*(4), 0195403.

An, X., & Xie, B. (2022). Phytoliths from Woody Plants: A Review. *Diversity (Basel)*, *14*(5), 339.

Anshari, G., Kershaw, P., van der Kaars, S., & Jacobsen, G. (2004). Environmental change and peatland forest dynamics in the Lake Sentarum area, West Kalimantan, Indonesia. *Journal of Quaternary Science, 19*, 637-655.

Armbrecht, L., Weber, M. E., Raymo, M. E., Peck, V. L., Williams, T., Warnock, J., Kato, Y., Hernandez-Almeida, I., Hoem, F., Reilly, B., Hemming, S., Bailey, I., Martos, Y. M., Gutjahr, M., Percuoco, V., Allen, C., Brachfeld, S., Cardillo, F. G., Du, Z., . . . Zheng, X. (2022). Ancient marine sediment DNA reveals diatom transition in Antarctica. *Nature communications, 13*(5787), 5787-5787.

Atanassova, J. (2005). Palaeoecological setting of the western Black Sea area during the last 15 000 years. *Holocene, 15*(4), 576-584.

Bajard, M., Poulenard, J., Sabatier, P., Develle, A.-L., Giguet-Covex, C., Jacob, J., Crouzet, C., David, F., Pignol, C., Arnaud, F. (2017). Progressive and Regressive Soil Evolution Phases in the Anthropocene. *Catena, 150*, 39–52.

Bellemain, E., Davey, M. L., Kauserud, H., Epp, L. S., Boessenkool, S., Coissac, E., Geml, J., Edwards, M., Willerslev, E., Gussarova, G., Taberlet, P., Haile, J., & Brochmann, C. (2013). Fungal palaeodiversity revealed using high-throughput metabarcoding of ancient DNA from arctic permafrost. *Environ Microbiol*, *15*(4), 1176-1189.

Birks, H. H. (2001). Plant Macrofossils. In J. P. Smol, H. J. B. Birks, W. M. Last, R. S. Bradley, & K. Alverson (Eds.), *Tracking Environmental Change Using Lake Sediments: Terrestrial, Algal, and Siliceous Indicators* (pp. 49-74). Springer Netherlands.

Birks, H. H. (2003). The importance of plant macrofossils in the reconstruction of lateglacial vegetation and climate; examples from Scotland, western Norway, and Minnesota, USA. *Quaternary science reviews*, *22*(5-7), 453-473.

Boere, A. C., Sinninghe Damsté, J. S., Rijpstra, W. I. C., Volkman, J. K., & Coolen, M. J. L. (2011). Source-specific variability in post-depositional DNA preservation with potential implications for DNA based paleoecological records. *Organic geochemistry, 42*(10), 1216-1225.

Boessenkool, S., McGlynn, G., Epp, L. S., Taylor, D., Pimentel, M., Gizaw, A., Nemomissa, S., Brochmann, C., & Popp, M. (2014). Use of Ancient Sedimentary DNA as a Novel Conservation Tool for High-Altitude Tropical Biodiversity. *Conservation Biology, 28*(2), 446-455.

Bramburger, A.J., Hamilton, P.B., Hehanussa, P.E., Haffner, G.D. (2008). Processes regulating the community composition and relative read abundance of taxa in the diatom communities of the Malili Lakes, Sulawesi Island, Indonesia. *Hydrobiologia, 615,* 215–224.

Bremond, L., Favier, C., Ficetola, G. F., Tossou, M. G., Akouegninou, A., Gielly, L., Giguet-Covex, C., Oslisly, R., & Salzmann, U. (2017). Five thousand years of tropical lake sediment DNA records from Benin. *Quaternary Science Reviews, 170,* 203-211.

Capo, E., Giguet-Covex, C., Rouillard, A., Nota, K., Heintzman, P. D., Vuillemin, A., Ariztegui, D., Arnaud, F., Belle, S., Bertilsson, S., Bigler, C., Bindler, R., Brown, A. G., Clarke, C. L., Crump, S. E., Debroas, D., Englund, G., Ficetola, G. F., Garner, R. E., Gauthier, J., Gregory-Eaves, I., Heinecke, L., Herzschuh, U., Ibrahim, A., Kisand, V., Kjaer, K. H., Lammers, Y., Littlefair, J., Messager, E., Monchamp, M. E., Olajos, F., Orsi, W., Pedersen, M. W., Rijal, D. P., Rydberg, J., Spanbauer, T., Stoof-Leichsenring, K. R., Taberlet, P., Talas, L., Thomas, C., Walsh, D. A., Wang, Y. C., Willerslev, E., van Woerkom, A., Zimmermann, H. H., Coolen, M. J. L., Epp, L. S., Domaizon, I., Alsos, I. G., & Parducci, L. (2021). Lake Sedimentary DNA Research on Past Terrestrial and Aquatic Biodiversity. Overview and Recommendations. *Quaternary, 4*(1).

Capo, E., Monchamp, M.-E., Coolen, M., Domaizon, I., Armbrecht, L., & Bertilsson, S. (2022). Environmental paleomicrobiology: using DNA preserved in aquatic sediments to its full potential. *Environmental Microbiology*, *24*.

Capo, E., Debroas, D., Arnaud, F., Guillemot, T., Bichet, V., Millet, L., Gauthier, E., Massa, C., Develle, A. L., Pignol, C., Lejzerowicz, F., & Domaizon, I. (2016). Long-term dynamics in microbial eukaryotes communities: a palaeolimnological view based on sedimentary DNA. *Mol Ecol, 25*(23), 5925-5943.

Clarke, C. L., Alsos, I. G., Edwards, M. E., Paus, A., Gielly, L., Haflidason, H., Mangerud, J., Regnéll, C., Hughes, P. D. M., Svendsen, J. I., & Bjune, A. E. (2020). A 24,000-year ancient DNA and pollen record from the Polar Urals reveals temporal dynamics of arctic and boreal plant communities. *Quaternary science reviews, 247,* 106564.

Clarke, K. R., & Gorley, R. N. (2015). PRIMER v7: User Manual/Tutorial. PRIMER-E Ltd.

Cleal, C., Pardoe, H. S., Berry, C. M., Cascales-Minana, B., Davis, B. A. S., Diez, J. B., Filipova-Marinova, M. V., Giesecke, T., Hilton, J., Ivanov, D., Kustatscher, E., Leroy, S. A. G., McElwain, J. C., Oplustil, S., Popa, M. E.,

Seyfullah, L. J., Stolle, E., Thomas, B. A., & Uhl, D. (2021). Palaeobotanical experiences of plant diversity in deep time; 1, How well can we identify past plant diversity in the fossil record? *Palaeogeography, palaeoclimatology, palaeoecology, 576,* 110481.

Cockell, C. S., Schaefer, B., Wuchter, C., Coolen, M. J. L., Grice, K., Schnieders, L., Morgan, J. V., Gulick, S. P. S., Wittmann, A., Lofi, J., Christeson, G. L., Kring, D. A., Whalen, M. T., Bralower, T. J., Osinski, G. R., Claeys, P., Kaskes, P., de Graaff, S. J., Déhais, T. (2021). Shaping of the Present-Day Deep Biosphere at Chicxulub by the Impact Catastrophe That Ended the Cretaceous. *Frontiers in Microbiology*, *12*.

Connor, S. E., Ross, S. A., Sobotkova, A., Herries, A. I. R., Mooney, S. D., Longford, C., & Iliev, I. (2013). Environmental conditions in the SE Balkans since the Last Glacial Maximum and their influence on the spread of agriculture into Europe. *Quaternary Science Reviews*, *68*, 200-215.

Connor, S. E., Thomas, I., & Kvavadze, E. V. (2007). A 5600-yr history of changing vegetation, sea levels and human impacts from the Black Sea coast of Georgia. *Holocene, 17*(1), 25-36.

Coolen, M. J. L. (2011). 7000 years of *Emiliania huxleyi* viruses in the Black Sea. *Science, 333*(6041), 451-452.

Coolen, M. J. L., Orsi, W. D., Balkema, C., Quince, C. H., Keith, Sylva, S. P., Filipova-Marinova, M., & Giosan, L. (2013). Evolution of the plankton paleome in the Black Sea from the Deglacial to Anthropocene. *Proceedings of the National Academy of Sciences of the United States of America, 110*(21), 8609-8614.

Coolen, M. J. L., & Overmann, J. (2007). 217 000-year-old DNA sequences of green sulfur bacteria in Mediterranean sapropels and their implications for the paleoenvironment reconstruction. *Environmental Microbiology, 9*(1), 238-249.

Coolen, M. J. L., Saenz, J. P., Giosan, L., Trowbridge, N. Y., Dimitrov, P., Dimitrov, D., & Eglinton, T. I. (2009). DNA and lipid molecular stratigraphic records of haptophyte succession in the Black Sea during the Holocene. *Earth and Planetary Science Letters, 284*(3-4), 610-621.

Cordova, C. E., Harrison, S. P., Mudie, P. J., Riehl, S., Leroy, S. A. G., & Ortiz, N. (2009). Pollen, plant macrofossil and charcoal records for palaeovegetation reconstruction in the Mediterranean-Black Sea Corridor since the Last Glacial Maximum. *Quaternary International, 197*, 12-26.

Corinaldesi, C., Barucca, M., Luna, G. M., & Dell'Anno, A. (2011). Preservation, origin and genetic imprint of extracellular DNA in permanently anoxic deep-sea sediments. *Molecular Ecology, 20*(3), 642-654.

Costa, K. M., Russell, J. M., Vogel, H., & Bijaksana, S. (2015). Hydrological connectivity and mixing of Lake Towuti, Indonesia in response to paleoclimatic changes over the last 60,000 years. *Palaeogeography Palaeoclimatology Palaeoecology, 417,* 467-475.

Courtin, J., Andreev, A. A., Raschke, E., Bala, S., Biskaborn, B. K., Liu, S. S., Zimmermann, H., Diekmann, B., Stoof-Leichsenring, K. R., Pestryakova, L. A., & Herzschuh, U. (2021). Vegetation Changes in Southeastern Siberia During the Late Pleistocene and the Holocene. *Frontiers in Ecology and Evolution, 09*.

Crowe, S. A., O'Neill, A. H., Katsev, S., Hehanussa, P., Haffner, G. D., Sundby, B., Mucci, A., & Fowle, D. A. (2008). The biogeochemistry of tropical lakes: A case study from Lake Matano, Indonesia. *Limnology and Oceanography, 53*(1), 319-331.

Dalén, L., Heintzman, P. D., Kapp, J. D., & Shapiro, B. (2023). Deep-time paleogenomics and the limits of DNA survival. *Science, 382*(6666), 48-53.

De Schepper, S., Ray, J. L., Skaar, K. S., Sadatzki, H., Ijaz, U. Z., Stein, R., & Larsen, A. (2019). The potential of sedimentary ancient DNA for reconstructing past sea ice evolution. *The ISME Journal, 13*(10), 2566-2577.

Dean, W. E., & Arthur, M. A. (2010). *Geochemical characteristics of Holocene laminated sapropel (Unit II) and underlying lacustrine Unit III in the Black Sea*. US Department of the Interior, Geological Survey.

Dommain, R., Andama, M., McDonough, M. M., Prado, N. A., Goldhammer, T., Potts, R., Maldonado, J. E., Nkurunungi, J. B., & Campana, M. G. (2020). The

challenges of reconstructing tropical biodiversity with sedimentary ancient DNA: A 2200-year-long metagenomic record from Bwindi Impenetrable Forest, Uganda. *Frontiers in Ecology and Evolution, 8.*

Dong, W., Liu, J., Yu, J., Wang, L., & Zhou, S. (2012). Highly Variable Chloroplast Markers for Evaluating Plant Phylogeny at Low Taxonomic Levels and for DNA Barcoding. *PLOS ONE, 7*(4), 35071.

Doughty, C. E. (2013). Preindustrial Human Impacts on Global and Regional Environment. *Annual Review of Environment and Resources*, *38*(1), 503-527.

Epp, L. S., Gussarova, C., Boessenkool, S., Olsen, J., Haile, J., Schroder-Nielsen, A., Ludikova, A., Hassel, K., Stenoien, H. K., Funder, S., Willerslev, E., Kjaer, K., & Brochmann, C. (2015). Lake sediment multi-taxon DNA from North Greenland records early post-glacial appearance of vascular plants and accurately tracks environmental changes. *Quaternary Science Reviews, 117*, 152-163.

Epure, L., Meleg, I. N., Munteanu, C.-M., Roban, R. D., & Moldovan, O. T. (2014). Bacterial and Fungal Diversity of Quaternary Cave Sediment Deposits. *Geomicrobiology Journal*, *31*(2), 116-127.

Fernando, W. G. (2012). Plants: An International Scientific Open Access Journal to Publish All Facets of Plants, Their Functions and Interactions with the Environment and Other Living Organisms. *Plants (Basel)*, *1*(1), 1-5.

Feurdean, A., & Bennike, O. (2008). Plant macrofossils analysis from Steregoiu NW Romania: taphonomy, representation, and comparison with pollen analysis. *Studia Universitatis Babeş-Bolyai. Geologia*, *53*(1), 5-10.

Filipova-Marinova, M. (2006). Palynostratigraphy of Pleistocene and Holocene sediments from the western Black Sea area. *Comptes Rendus De L Academie Bulgare Des Sciences, 60*(3), 279-290.

Filipova-Marinova, M., Pavlov, D., Coolen, M. J. L., & Giosan, L. (2012). First high-resolution marinopalynological stratigraphy of Late Quaternary sediments from

the central part of the Bulgarian Black Sea area. *Quaternary International, 293*, 170-183.

Friese, A., Kallmeyer, J., Kitte, J., Montaño Martinez, I., Bijaksana, S., & Wagner, D. (2017). A simple and inexpensive technique for assessing contamination during drilling operations. *Limnology and Oceanography: Methods, 15*.

Friese, A., Bauer, K., Glombitza, C., Ordoñez, L., Ariztegui, D., Heuer, V. B., Vuillemin, A., Henny, C., Nomosatryo, S., & Simister, R. (2021). Organic matter mineralization in modern and ancient ferruginous sediments. *Nature communications*, *12*(1), 2216.

Gastaldo, R. A., & Demko, T. M. (2010). The Relationship Between Continental Landscape Evolution and the Plant-Fossil Record: Long Term Hydrologic Controls on Preservation. In (pp. 249-285). Springer Netherlands.

Giesecke, T., Davis, B., Brewer, S., Finsinger, W., Wolters, S., Blaauw, M., de Beaulieu, J.-L., Binney, H., Fyfe, R. M., Gaillard, M.-J., Gil-Romera, G., van der Knaap, W. O., Kuneš, P., Kühl, N., van Leeuwen, J. F. N., Leydet, M., Lotter, A. F., Ortu, E., Semmler, M., & Bradshaw, R. H. W. (2014). Towards mapping the late Quaternary vegetation change of Europe. *Vegetation history and archaeobotany*, *23*(1), 75-86.

Giosan, L., Coolen, M. J. L., Kaplan, J. O., Constantinescu, S., Filip, F., Filipova-Marinova, M., Kettner, A. J., & Thom, N. (2012). Early anthropogenic transformation of the danube-black sea system. *Scientific reports, 2*(1), 582-582.

Gobet, E., Tinner, W., Bigler, C., Hochuli, P. A., & Ammann, B. (2005). Early-Holocene afforestation processes in the lower subalpine belt of the Central Swiss Alps as inferred from macrofossil and pollen records. *The Holocene*, *15*(5), 672-686.

Golovnina, K. A., Glushkov, S. A., Blinov, A. G., Mayorov, V. I., Adkison, L. R., & Goncharov, N. P. (2007). Molecular phylogeny of the genus Triticum L. *Plant Systematics and Evolution, 264*(3-4), 195-216.

Goudge, T. A., Russell, J. M., Mustard, J. F., Head, J. W., & Bijaksana, S. (2017). A 40,000 yr record of clay mineralogy at Lake Towuti, Indonesia: Paleoclimate

reconstruction from reflectance spectroscopy and perspectives on paleolakes on Mars. *Bulletin*, *129*(7-8), 806-819.

Hamilton, R., Stevenson, J., Li, B., & Bijaksana, S. (2019). A 16,000-year record of climate, vegetation and fire from Wallacean lowland tropical forests. *Quaternary Science Reviews, 224,* 105929.

Hasberg, A. K. M., Bijaksana, S., Held, P., Just, J., Melles, M., Morlock, M. A., Opitz, S., Russell, J. M., Vogel, H., & Wennrich, V. (2019). Modern sedimentation processes in Lake Towuti, Indonesia, revealed by the composition of surface sediments. *Sedimentology, 66*(2), 675-698.

Hendon, H.H. (2003). Indonesian rainfall variability: impacts of ENSO and local air-sea interaction. *Journal of Climate, 16,* 1775–1790.

Hippel, V. B., Stoof-Leichsenring, K. R., Schulte, L., Seeber, P., Epp, L. S., Biskaborn, B. K., Diekmann, B., Melles, M., Pestryakova, L., & Herzschuh, U. (2022). Long-term fungus–plant covariation from multi-site sedimentary ancient DNA metabarcoding. *Quaternary science reviews, 295,* 107758.

Hope, G. (2001). Environmental change in the Late Pleistocene and later Holocene at Wanda site, Soroako, South Sulawesi, Indonesia. *Palaeogeography, palaeoclimatology, palaeoecology, 171*(3), 129-145.

Horrocks, M. (2020). Recovering Plant Microfossils from Archaeological and other Palaeoenvironmental Deposits: A Practical Guide Developed from Pacific Region Experience. *Asian perspectives (Honolulu)*, *59*(1), 186-207.

Huang, Y., Zheng, Y., Heng, P., Giosan, L., & Coolen, M. J. L. (2021). Black Sea paleosalinity evolution since the last deglaciation reconstructed from alkenone-inferred Isochrysidales diversity. *Earth and planetary science letters, 564,* 116881.

Inagaki, F., Hinrichs, K.-U., Kubo, Y., Bowles, M., Heuer, V., Hong, W.-L., Hoshino, T., Ijiri, A., Imachi, H., Ito, M., Kaneko, M., Lever, M., Lin, Y.-S., Methé, B., Morita, S., Morono, Y., Tanikawa, W., Bihan, M., Bowden, S., & Yamada, Y. (2015). Exploring deep microbial life in coal-bearing sediment down to ~2.5 km below the ocean floor. *Science, 349,* 420-424.

Jia, W., Liu, X., Kathleen R. Stoof-Leichsenring, Liu, S., Li, K., & Herzschuh, U. (2022). Preservation of sedimentary plant DNA is related to lake water chemistry. *Environmental DNA, 4*(2), 425-439.

Jorgensen, T., Haile, J., MÖLler, P. E. R., Andreev, A., Boessenkool, S., Rasmussen, M., Kienast, F., Coissac, E., Taberlet, P., Brochmann, C., Bigelow, N. H., Andersen, K., Orlando, L., Gilbert, M. T. P., & Willerslev, E. (2012). A comparative study of ancient sedimentary DNA, pollen and macrofossils from permafrost sediments of northern Siberia reveals long-term vegetational stability: Comparative Study of Ancient Sedimentary DNA, Pollen AND Macrofossil. *Molecular ecology*, *21*(8), 1989-2003.

Kanbar, H., Olajos, F., Englund, G., & Holmboe, M. (2020). Geochemical identification of potential DNA-hotspots and DNA-infrared fingerprints in lake sediments. *Applied Geochemistry, 122*, 104728.

Krehenwinkel, H., Wolf, M., & Lim, J.Y. (2017). Estimating and mitigating amplification bias in qualitative and quantitative arthropod metabarcoding. *Scientific Reports, 7*, 17668.

Lancelotti, C., & Madella, M. (2018). Phytoliths and the Human Past: Archaeology, Ethnoarchaeology and Palaeoenvironmental Studies.

Li, K., Stoof-Leichsenring, K. R., Liu, S. S., Jia, W. H., Liao, M. N., Liu, X. Q., Ni, J., & Herzschuh, U. (2021). Plant sedimentary DNA as a proxy for vegetation reconstruction in eastern and northern Asia. *Ecological Indicators, 132*.

Lisztes-Szabó, Z., Braun, M., Csík, A., & Pető, Á. (2019). Phytoliths of six woody species important in the Carpathians: characteristic phytoliths in Norway spruce needles. *Vegetation history and archaeobotany*, *28*(6), 649-662.

Liu, S. S., Stoof-Leichsenring, K. R., Kruse, S., Pestryakova, L. A., & Herzschuh, U. (2020). Holocene vegetation and plant diversity changes in the Northeastern Siberian treeline region from pollen and sedimentary ancient DNA. *Frontiers in Ecology and Evolution, 8*.

Lydolph, M. C., Jacobsen, J., Arctander, P., Gilbert, M. T., Gilichinsky, D. A., Hansen, A. J., Willerslev, E., & Lange, L. (2005). Beringian paleoecology inferred

from permafrost-preserved fungal DNA. *Appl Environ Microbiol*, *71*(2), 1012-1017.

Mander, L., & Punyasena, S. W. (2014). On the taxonomic resolution of pollen and spore records of earth's vegetation. *International Journal of Plant Sciences, 175*(8), 931-945.

Manske, A. K., Henssge, U., Glaeser, J., & Overmann, J. (2008). Subfossil 16S rRNA gene sequences of green sulfur bacteria in the Black Sea and their implications for past photic zone anoxia. *Applied and Environmental Microbiology, 74*, 624-632.

Melinda, P. (2018). Characteristics of Collapsing Ecosystems and Main Factors of Collapses. In H. Levente (Ed.), *Ecosystem Services and Global Ecology* (pp. Ch. 2). IntechOpen.

Morlock, M. A., Vogel, H., Nigg, V., Ordonez, L., Hasberg, A. K. M., Melles, M., Russell, J. M., Bijaksana, S., & Team, T. D. P. S. (2019). Climatic and tectonic controls on source-to-sink processes in the tropical, ultramafic catchment of Lake Towuti, Indonesia. *Journal of Paleolimnology, 61*(3), 279-295.

Mudie, P. J., Marret, F., Aksu, A. E., Hiscott, R. N., & Gillespie, H. (2007). Palynological evidence for climatic change, anthropogenic activity and outflow of Black Sea water during late Pleistocene and Holocene: Centennial-to decadal-scale records from the Black and Marmara Seas. *Quaternary International, 167*, 73-90.

Mudie, P. J., Rochon, A., & Aksu, A. E. (2002). Pollen stratigraphy of Late Quaternary cores from Marmara Sea: land-sea correlation and paleoclimatic history. *Marine Geology, 190*(1-2), 233-260.

Niemeyer, B., Epp, L. S., Stoof-Leichsenring, K. R., Pestryakova, L. A., & Herzschuh, U. (2017). A comparison of sedimentary DNA and pollen from lake sediments in recording vegetation composition at the Siberian treeline. *Molecular Ecology Resources, 17*(6), 46-62.

Ollerton, J., Winfree, R., & Tarrant, S. (2011). How many flowering plants are pollinated by animals? *Oikos, 120*(3), 321-326.

Palazzesi, L., Gottschling, M., Barreda, V., & Weigend, M. (2012). First Miocene fossils of Vivianiaceae shed new light on phylogeny, divergence times, and historical biogeography of Geraniales. *Biological Journal of the Linnean Society*, *107*(1), 67-85.

Palmer, J. D., Jansen, R. K., Michaels, H. J., Chase, M. W., & Manhart, J. R. (1988). Chloroplast DNA variation and plant phylogeny. *Annals of the Missouri Botanical Garden, 75*(4), 1180-1206.

Pansu, J., Giguet-Covex, C., Ficetola, G.F., Gielly, L., Boyer, F., Zinger, L., Arnaud, F., Poulenard, J., Taberlet, P., Choler, P. (2015). Reconstructing Long-Term Human Impacts on Plant Communities: An Ecological Approach Based on Lake Sediment DNA. *Molecular Ecology, 24*, 1485–1498.

Parducci, L., Bennett, K. D., Ficetola, G. F., Alsos, I. G., Suyama, Y., Wood, J. R., & Pedersen, M. W. (2017). *Ancient plant DNA in lake sediments. New Phytologist, 214*(3), 924-942.

Parducci, L., Matetovici, I., Fontana, S. L., Bennett, K. D., Suyama, Y., Haile, J., Kjaer, K. H., Larsen, N. K., Drouzas, A. D., & Willerslev, E. (2013). Molecular- and pollen-based vegetation analysis in lake sediments from central Scandinavia. *Molecular Ecology, 22*(13), 3511-3524.

Parducci, L., Suyama, Y., Lascoux, M., & Bennett, K. D. (2005). Ancient DNA from pollen: a genetic record of population history in Scots pine. *Molecular Ecology, 14*(9), 2873-2882.

Parducci, L., Valiranta, M., Salonen, J. S., Ronkainen, T., Matetovici, I., Fontana, S. L., Eskola, T., Sarala, P., & Suyama, Y. (2015). Proxy comparison in ancient peat sediments: pollen, macrofossil, and plant DNA. *Philosophical transactions of the Royal Society of London Series B, Biological sciences, 370*(1660), 20130382.

Paus, A., Boessenkool, S., Brochmann, C., Epp, L. S., Fabel, D., Haflidason, H., & Linge, H. (2015). Lake Store Finnsjoen - a key for understanding Lateglacial/early Holocene vegetation and ice sheet dynamics in the central Scandes Mountains. *Quaternary Science Reviews, 121*, 36-51.

Pedersen, M. W., Ginolhac, A., Orlando, L., Olsen, J., Andersen, K., Holm, J., Funder, S., Willerslev, E., & Kjaer, K. H. (2013). A comparative study of ancient environmental DNA to pollen and macrofossils from lake sediments reveals taxonomic overlap and additional plant taxa. *Quaternary Science Reviews, 75*, 161-168.

Piperno, D. R. (2006). *Phytoliths: a comprehensive guide for archaeologists and paleoecologists*. Rowman Altamira.

Reitalu, T., Bjune, A. E., Blaus, A., Giesecke, T., Helm, A., Matthias, I., Peglar, S. M., Salonen, J. S., Seppä, H., Väli, V., Birks, H. J. B., Palaeo, e., Coastal dynamics, F. s., & Global, c. (2019). Patterns of modern pollen and plant richness across northern Europe. *The Journal of ecology, 107*(4), 1662-1677.

Rodriguez-Martinez, S., Klaminder, J., Morlock, M. A., Dalén, L., & Yu-Tuan Huang, D. (2023). The topological nature of tag jumping in environmental DNA metabarcoding studies. *Molecular Ecology Resources, 23*(3), 621-631.

Ross, DA.& Degens, ET. (1974). Recent sediments of Black Sea. *AAPG Bull, 20*, 183–199.

Rull, V. (2022). Biodiversity crisis or sixth mass extinction? Does the current anthropogenic biodiversity crisis really qualify as a mass extinction? *EMBO reports*, *23*(1), 54193.

Russell, J. M., Vogel, H., Bijaksana, S., Melles, M., Deino, A., Hafidz, A., Haffner, D., Hasberg, A. K. M., Morlock, M., von Rintelen, T., Sheppard, R., Stelbrink, B., & Stevenson, J. (2020). The late quaternary tectonic, biogeochemical, and environmental evolution of ferruginous Lake Towuti, Indonesia. *Palaeogeography Palaeoclimatology Palaeoecology, 556*.

Russell, J. M., Vogel, H., Konecky, B. L., Bijaksana, S., Huang, Y. S., Melles, M., Wattrus, N., Costa, K., & King, J. W. (2014). Glacial forcing of central Indonesian hydroclimate since 60,000 y BP. *Proceedings of the National Academy of Sciences of the United States of America, 111*(14), 5100-5105.

Ryan, W. B. F., & Pitman, W. C. (1998). *Noah's Flood: The New Scientific Discoveries about the Event that Changed History*. Simon & Schuster.

Ryves, D. B., Juggins, S., Fritz, S. C., & Battarbee, R. W. (2001). Experimental diatom dissolution and the quantification of microfossil preservation in sediments. *Palaeogeography, palaeoclimatology, palaeoecology, 172*(1-2), 99-113.

Sheppard, R. Y., Milliken, R. E., Russell, J. M., Dyar, M. D., Sklute, E. C., Vogel, H., Melles, M., Bijaksana, S., Morlock, M. A., & Hasberg, A. K. M. (2019). Characterization of Iron in Lake Towuti sediment. *Chemical Geology, 512,* 11-30.

Sheppard, R. Y., Milliken, R. E., Russell, J. M., Sklute, E. C., Dyar, M. D., Vogel, H., Melles, M., Bijaksana, S., Hasberg, A. K. M., & Morlock, M. A. (2021). Iron Mineralogy and Sediment Colour in a 100 m Drill Core from Lake Towuti, Indonesia Reflect Catchment and Diagenetic Conditions. *Geochemistry Geophysics Geosystems, 22*(8).

Shillito, L.-M. (2013). Grains of truth or transparent blindfolds? A review of current debates in archaeological phytolith analysis. *Vegetation history and archaeobotany*, *22*(1), 71-82.

Shumilovskikh, L. S., Tarasov, P., Arz, H. W., Fleitmann, D., Marret, F., Nowaczyk, N., Plessen, B., Schluetz, F., & Behling, H. (2012). Vegetation and environmental dynamics in the southern Black Sea region since 18 kyr BP derived from the marine core 22-GC3. *Palaeogeography Palaeoclimatology Palaeoecology, 337*, 177-193.

Slon, V., Hopfe, C., Weiss, C. L., Mafessoni, F., de la Rasilla, M., Lalueza-Fox, C., & Meyer, M. (2017). Neandertal and denisovan DNA from Pleistocene sediments. *Science, 356*(6338), 605–608.

Sonstebo, J. H., Gielly, L., Brysting, A. K., Elven, R., Edwards, M., Haile, J., Willerslev, E., Coissac, E., Rioux, D., Sannier, J., Taberlet, P., & Brochmann, C. (2010). Using next-generation sequencing for molecular reconstruction of past Arctic vegetation and climate. *Molecular ecology resources*, *10*(6), 1009-1018.

Souto, M., Castro, D., García-Rodeja, E., & Pontevedra-Pombal, X. (2019). The Use of Plant Macrofossils for Paleoenvironmental Reconstructions in Southern European Peatlands. *Quaternary*, *2*(4), 34.

Steffen, W., Grinevald, J., Crutzen, P., & McNeill, J. (2011). The Anthropocene; conceptual and historical perspectives. *Philosophical transactions of the Royal Society of London. Series A: Mathematical, physical, and engineering sciences*, *369*(1938), 842-867.

Stevenson, J. (2018). Vegetation and climate of the Last Glacial Maximum in Sulawesi. In S. O. orcid, D. B. orcid, J. Meyer (Eds.), *The Archaeology of Sulawesi. Current Research on the Pleistocene to the Historic Period* (pp. 17-29). ANU Press.

Strömberg, C. A., Dunn, R. E., Madden, R. H., Kohn, M. J., & Carlini, A. A. (2013). Decoupling the spread of grasslands from the evolution of grazer-type herbivores in South America. *Nature communications*, *4*(1), 1478.

Taberlet, P., Coissac, E., Pompanon, F., Gielly, L., Miquel, C., Valentini, A., Vermat, T., Corthier, G., Brochmann, C., & Willerslev, E. (2007). Power and limitations of the chloroplast trnL (UAA) intron for plant DNA barcoding. *Nucleic Acids Research, 35*(3), 14.

Turney, C. S. M., & Brown, H. (2007). Catastrophic early Holocene sea level rise, human migration and the Neolithic transition in Europe. *Quaternary science reviews*, *26*(17), 2036-2041.

Ulfers, A., Hesse, K., Zeeden, C., Russell, J. M., Vogel, H., Bijaksana, S., & Wonik, T. (2021). Cyclostratigraphy and paleoenvironmental inference from downhole logging of sediments in tropical Lake Towuti, Indonesia. *Journal of paleolimnology*, *65*, 377-392.

van der Meer, M. T. J., Sangiorgi, F., Baas, M., Brinkhuis, H., Sinninghe Damste, J. S., & Schouten, S. (2008). Molecular isotopic and dinoflagellate evidence for late Holocene freshening of the Black Sea. *Earth and planetary science letters, 267*(3-4), 426-434.

Vogel, H., Russell, J., Cahyarini, S., Bijaksana, S., Wattrus, N., Rethemeyer, J., & Melles, M. (2015). Depositional modes and lake-level variability at Lake Towuti, Indonesia, during the past similar to 29 kyr BP. *Journal of Paleolimnology, 54*(4), 359-377.

Voldstad, L. H., Alsos, I. G., Farnsworth, W. R., Heintzman, P. D., Hakansson, L., Kjellman, S. E., Rouillard, A., Schomacker, A., & Eidesen, P. B. (2020). A complete Holocene lake sediment ancient DNA record reveals long-standing high Arctic plant diversity hotspot in northern Svalbard. *Quaternary Science Reviews, 234*.

Volkov, I., & L.N, N. (2007). Hydrogen Sulfide in the Black Sea. In (Vol. 5, pp. 309-331).

Vuillemin, A., Friese, A., Alawi, M., Henny, C., Nomosatryo, S., Wagner, D., Crowe, S. A., & Kallmeyer, J. (2016). Geomicrobiological Features of Ferruginous Sediments from Lake Towuti, Indonesia. *Front Microbiol, 7*, 1007.

Vuillemin, A., Horn, F., Alawi, M., Henny, C., Wagner, D., Crowe, S. A., & Kallmeyer, J. (2017). Preservation and Significance of Extracellular DNA in Ferruginous Sediments from Lake Towuti, Indonesia. *Frontiers in Microbiology, 8*.

Vuillemin, A., Horn, F., Friese, A., Winkel, M., Alawi, M., Wagner, D., Henny, C., Orsi, W. D., Crowe, S. A., & Kallmeyer, J. (2018). Metabolic potential of microbial communities from ferruginous sediments. *Environmental Microbiology, 20*(12), 4297-4313.

Wanner, H., Beer, J., Buetikofer, J., Crowley, T. J., Cubasch, U., Flueckiger, J., Goosse, H., Grosjean, M., Joos, F., Kaplan, J. O., Kuettel, M., Mueller, S. A., Prentice, I. C., Solomina, O., Stocker, T. F., Tarasov, P., Wagner, M., &

Widmann, M. (2008). Mid- to Late Holocene climate change: an overview. *Quaternary Science Reviews, 27*(19-20), 1791-1828.

Willerslev, E., & Cooper, A. (2005). Ancient DNA. *Proceedings of the Royal Society of London Series B-Biological Sciences, 272*(1558), 3-16.

Yanchilina, A. G., Ryan, W. B., McManus, J. F., Dimitrov, P., Dimitrov, D., Slavova, K., & Filipova-Marinova, M. (2017). Compilation of geophysical, geochronological, and geochemical evidence indicates a rapid Mediterranean-derived submergence of the Black Sea's shelf and subsequent substantial salinification in the early Holocene. *Marine Geology*, *383*, 14-34.

Zimmermann, H. H., Raschke, E., Epp, L. S., Stoof-Leichsenring, K. R., Schwamborn, G., Schirrmeister, L., Overduin, P. P., & Herzschuh, U. (2017). Sedimentary ancient DNA and pollen reveal the composition of plant organic matter in Late Quaternary permafrost sediments of the Buor Khaya Peninsula (northeastern Siberia). *Biogeosciences, 14*(3), 575-596.

Chapter 2

A 1Ma sedimentary ancient DNA (*sed*aDNA) record of catchment vegetation changes and the developmental history of tropical Lake Towuti (Sulawesi, Indonesia).

2.1 Abstract

Studying past ecosystems from ancient environmental DNA preserved in lake sediments (*sed*aDNA) is a rapidly expanding field. This research has mainly involved Holocene sediments from lakes in cool climates, with little known about the suitability of *sed*aDNA to reconstruct substantially older ecosystems in the warm tropics. Here, we report the successful recovery of chloroplast *trn*L (UAA) sequences (*trn*L-P6 loop) from the sedimentary record of Lake Towuti (Sulawesi, Indonesia) to elucidate changes in regional tropical vegetation assemblages during the lake's Late Quaternary paleodepositional history. After the stringent removal of contaminants and sequence artefacts, taxonomic assignment of the remaining genuine *trn*L-P6 reads showed that native nitrogen-fixing legumes, C_3 grasses, and shallow wetland vegetation (*Alocasia*) were most strongly associated with > one-million-year-old (>1 Ma) peats and silts (114-98.8 meters composite depth; mcd), which were deposited in a landscape of active river channels, shallow lakes, and peat-swamps. A statistically significant shift towards partly submerged shoreline vegetation that was likely rooted in anoxic muddy soils (i.e., peatland forest trees and wetland C_3 grasses (Oryzaceae) and nutrient-demanding aquatic herbs (presumably *Oenanthe javanica*) occurred at 76 mcd (~0.8 Ma), ~0.2 Ma after the transition into a permanent lake. This wetland vegetation was most strongly associated with diatom ooze (46-37 mcd), thought to be deposited during maximum nutrient availability and primary productivity. Herbs (Brassicaceae), trees/shrubs (Fabaceae, Theaceae), and C_3 grasses correlated with inorganic parameters, indicating increased drainage of ultramafic sediments and laterite soils from the lakes' catchment, particularly at times of inferred drying. Downcore variability in *trn*L-P6 from tropical forest trees (*Toona*), shady ground cover herbs (Zingiberaceae), and tree orchids (*Luisia*) most strongly correlated with sediments of a predominantly felsic signature considered to be originating from the catchment of the Loeha River draining into Lake

Towuti during wetter climate conditions. However, the co-correlation with dry climate-adapted trees (i.e., *Castanopsis* or *Lithocarpus*) plus C_4 grasses suggests that increased precipitation seasonality also contributed to the increased drainage of felsic Loeha River sediments. This multiproxy approach shows that despite elevated preservation conditions under the prevailing high *in-situ* temperatures, tropical lake sediments can provide long-term of ancient environmental DNA for reconstructing ecosystems, which warrants further exploration.

2.2 Introduction

Fossil pollen and spores provide a valuable record of the evolutionary history of vegetation and their response to past climate change (e.g., Anshari et al., 2004; Hamilton et al., 2019a; Hope, 2001; Stevenson, 2018), but overlapping morphological features can complicate the identification of various plant families at lower taxonomic levels. Notably, similar fossil pollen morphologies between genera of true grasses (Poaceae) make it impossible to distinguish between wet climate C_3 versus dry climate C_4 grasses and grasses that can switch between C_3 and C_4 carbon fixation pathways (Mander & Punyasena, 2014 and references therein). The same problem stands for dominant tropical tree families, which can only be separated into broad habitat types with time intensive morphological research (e.g., Hamilton et al., 2019b). Moreover, landscape reconstruction from pollen analysis is complicated by the variable production and transportation of pollen from different genera. For instance, the origin of pollen from wind-pollinated plants can be obscured by long distances, sometimes even cross-continental transportation (Gregory, 1978). Additionally, and problematically for tropical landscape reconstruction, rainforest angiosperms have low pollen production rates as they typically rely on animal vectors for pollination and successful reproduction (e.g., Ollerton et al., 2011). Such vegetation is, therefore, likely to be poorly represented in the fossil pollen record.

Several studies have shown that lacustrine sedimentary records also represent important archives of ancient vegetation DNA (Capo et al., 2021 and references therein) that can expand on and resolve critical issues from pollen-based reconstructions. Extraction of ancient sedimentary DNA (*sed*aDNA) and subsequent sequencing analysis of preserved vegetation metabarcoding genes, notably the short 10-134 base pair (bp) P6 loop of the chloroplast *trn*L (UAA) intron (Taberlet et al., 2007), can complement fossil pollen in reconstructing local vegetation communities

and their responses to paleoenvironmental and more recent anthropogenic perturbations (e.g., Alsos et al., 2021; Courtin et al., 2021; Epp et al., 2015; Li et al., 2021; Niemeyer et al., 2017; Parducci et al., 2013; 2015; Pederson et al., 2013; Zimmermann et al., 2017). Namely, since chloroplasts are organelles found predominantly in plant leaves where most photosynthesis takes place, *sed*aDNA records targeting chloroplast-derived metabarcoding genes are thought to mainly represent ancient local catchment vegetation that entered lake basins as decaying plant litter via riverine- or terrestrial runoff (e.g., Alsos et al., 2018; Liu et al., 2020; Paus et al., 2015; Parducci et al., 2017; Voldstad et al., 2020). Stratigraphic analysis of *Sed*aDNA thus has the potential to be an excellent archive of local vegetation change.

DNA from past phytoplankton communities has been extracted and sequenced from up to 2 Ma-old deep-sea sediments (Kirkpatrick et al., 2016; Armbrecht et al., 2022) and from up to 270 Kyr-old lake sediments (i.e., Lake Van, Turkey) (Randlett et al., 2014). However, most terrestrial *sed*aDNA records have been generated from Holocene lakes located in high-latitude regions where relatively cold conditions can promote the long-term preservation of *sed*aDNA (Capo et al., 2021 and references therein). A few recent studies have used *sed*aDNA to reconstruct tropical catchment vegetation change (Boessenkool et al., 2014; Bremond et al., 2017; Dommain et al., 2020). However, these records only date back several millennia and comprise tropical lakes in cooler, high-altitude locations. Therefore, it remains to be seen how far back in time *sed*aDNA can be recovered and sequenced from tropical lakes after long-term exposure to less favorable, high *in situ* temperatures.

During the 2015 Towuti Drilling Project (Russell et al., 2016), sediment cores spanning more than 1 Ma of deposition (Russell et al., 2020) were obtained from Lake Towuti (Sulawesi, Indonesia) (Fig. 2.1) to reconstruct aquatic and terrestrial ecosystem responses to late-Quaternary environmental and climate variability in the tropical western Pacific. The 205 m-deep Lake Towuti (2.75° S, 121.5° E) is the largest (500 km^2 surface area) member of the tectonic Malili Lake complex (which includes the smaller Matano- and Mahalona lakes) (Fig. 2.1) and is positioned in a floristically biodiverse catchment area (~1144 km^2) (Cannon et al., 2009; Whitten et al., 1988). The lakes' surface and bottom water temperatures were ~31 and 28.5 °C, respectively. The uninterrupted continuous record from Lake Towuti, which extends well beyond the Holocene (Russell et al., 2020), offers a unique opportunity to study

the long-term preservation potential of *sed*aDNA in tropical lakes and its suitability to reconstruct past vegetation change.

According to detailed geochronological, lithostratigraphic, mineralogical, and geochemical analysis spanning the entire sedimentary record, Lake Towuti emerged during accelerated tectonic subsidence from a landscape initially characterised by active river channels, shallow lakes, and swamps and became a permanent lake at ~1 Ma (Russell et al., 2020). Drilling recovered cores from holes up to ~150 m deep, with sediment subdivided into two main stratigraphic units. The deeper sediment sequence, Unit 2, consists of alternating fluvial silty clays and peat layers (Russell et al., 2020). A thick peat interval between 101-98.8 mcd marks the transition into a permanent lake (Unit 1; U1). The U2/U1 transition at 98.8 mcd was estimated 1 Ma ago by extrapolating an accurately $^{40}Ar/^{39}Ar$ dated tephra layer at 72.95 mcd (i.e., 797.3 ± 1.6 Ka) (Russell et al., 2020). The lacustrine U1 sediments contain alternating red sideritic and green organic-rich clay intervals, likely to reflect orbital scale alterations between cooler, drier climates that promoted lower lake levels, lake mixing, and ultraoligotrophic conditions due to phosphate trapping by sedimentary iron oxyhydroxides (red sideritic clays) versus warmer, wetter climate stages that promoted a more productive lake through the release of sedimentary P and ferrous iron under seasonally stratified and anoxic conditions (green clays) (Russell et al., 2020).

At much longer timescales, the lacustrine record reveals three major shifts in paleodepositional and paleohydrological conditions. Unit 1c (~98-76 mcd) shows frequent oscillations between more felsic (K-rich) and ultramafic (Mg-rich) sediments. The oscillations in sediments were likely caused by variable fault motion and a continued influence of tectonically driven changes in basin morphology and catchment hydrology (Russell et al., 2020). Unit 1b (76-30 mcd) has low %Mg and undetectable amounts of serpentine. A combination of a higher contribution of green clays and elevated %K in U1b suggests increased discharge of felsic sediments from the Loeha River to the east of Lake Towuti during warmer, wetter climates that promoted a more productive stratified lake. Long-term accumulation and weathering of tephra-bound P in the catchment may also have contributed to the development of mesotrophic conditions and maximum productivity, which ultimately resulted in the

deposition of two several-meters-thick diatomaceous oozes between 32-37 and 43-46 mcd (Russell et al., 2020). The overlying U1a (top 30 m) shows a substantial increase in %Mg, indicating a connection of the Lampenisu and Mahalona Rivers between Lakes Mahalona and Towuti (Russell et al., 2020).

Here we used sedimentary *trn*L-P6 amplicon sequencing (Taberlet et al., 2007) to generate a record of Quaternary tropical catchment and aquatic vegetation changes associated with the well-described transitions in limnological and hydrological changes throughout the lakes' more than 1 Ma history. Furthermore, the potential origin of the sedimentary chloroplast DNA was inferred from Pearson correlations between downcore relative changes in the *trn*L-P6-inferred paleovegetation assemblages and the previously analysed (in)organic geochemical paleohydrological and paleoenvironmental parameters.

2.3 Material and Methods

2.3.1 Sampling

Drilling commenced at Site 1 (Fig. 2.1) on 23 May 2015 using the ICDP Deep Lakes Drilling System (DLDS) operated by DOSECC Exploration Services.
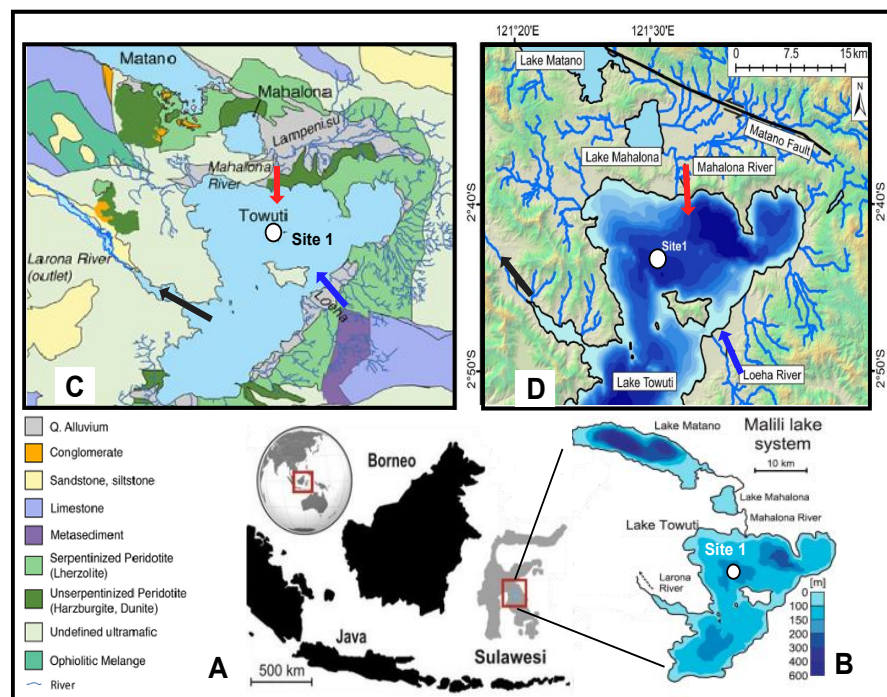
Figure 2.1 General overview of the sampling location. (A) Location of Lake Towuti on the Indonesian Island of Sulawesi as part of the Malili Lake system (modified after Friese et al., 2021). (B) Bathymetry of Lake Mahalona, Lake Mahalona, and Lake Towuti (changed from Russell et al., 2016). (C) Map of

the local bedrock geology with legend below (modified from Costa et al.,2015). (D) A detailed map of the main rivers draining into Lake Towuti (modified from Morlock et al., 2021). Note the locations of ultramafic rocks, the source of Mg-rich eroded catchment material that nowadays drains into the lake via the Mahalona River (North-East of Lake Towuti) (red arrow in c and d) during periods of reduced precipitation resulting in low lake water stands vs limestone and metasedimentary bedrock as the source of K-rich eroded catchment material, which drains into the lake via the Loeha River (South-East of Lake Towuti) (blue arrow in c and d) during wetter conditions and high lake level stands (Russell et al., 2020). The direction of Lake surface water outflow via the Larona River is indicated with a black arrow in c and d. The coring location 1 is marked with a white circle in (B-D).

This priority coring site was chosen for highly resolved paleoclimate and paleoecology reconstructions spanning the entire history of Lake Towuti, as it is relatively free of thick turbidites and located in the proximity of core IDLE-TOW10-9B, which yielded high-quality paleoclimate data for the last 60 ka (Russell et al., 2014; 2020). Core 1F used for this study was from site IDLE-TOW10, obtained at a water depth of 156 m (Fig. 2.1) using a PQ (122.6 mm hole, 66 mm core) diameter drill string with a hydraulic piston corer (HPC) for soft lacustrine sediments of Unit 1. Alien rotating coring, which required the addition of drilling fluid to lubricate the drill bit, was used to recover the more resistant lithologies of pre-lake U2 and a 2-m-thick interval of lacustrine red clays between 70.5 and 72.5 (Fig. 2.1). The upper 114 meters of this core were analysed. Upon completion of the coring expedition in June 2015, the 3-m-long whole-round core sections were shipped inside standard capped butyrate liners via air freight to LacCORE (the National Lacustrine Core Facility) at the University of Minnesota, MN, USA, for processing, description, scanning, and subsampling (Russell et al., 2016). Sediment samples for DNA analysis (n=146) were obtained at ~10 ka resolution from freshly split core sections between 2.95 and 114.75 mcd after Coolen et al. (2013) and transported inside sterile Whirl Pac bags to the 5.1. quarantine trace DNA lab facility (Australian Department of Agriculture Approved Arrangement # W3032), located within the Western Australia Organic and Isotope Geochemistry Centre (WA-OIGC) at Curtin University in Perth, where the samples were stored at -80 °C until DNA extraction.

2.3.2 Sedimentary DNA extraction

Depending on availability, both intracellular and mineral-adsorbed extracellular DNA was extracted from 2 to 8 grams of sediment inside a bleach- and UV-sterilized HEPA-filtered horizontal laminar flow bench within lab W3032 using the DN*easy* Powermax Soil DNA extraction kit (Qiagen) with modifications after Direito et al. (2012) to efficiently release mineral-adsorbed extracellular DNA (Orsi et al., 2017). The

concentration of extracted DNA was quantified fluorometrically using the Quant-iT™ Picogreen dsDNA Assay Kit (Thermo Fisher Scientific, Scoresby, VIC, Australia). Co-extracted PCR-inhibiting substances such as humic acids were removed using the OneStep PCR Inhibitor Removal Kit (Zymo Research, Irvine, CA, USA). Reagent mixtures without sediment were extracted and purified in parallel and served as controls for contamination during the lab procedures (extraction blanks; n=4).

2.3.3 Illumina MiSeq amplicon sequencing of sedimentary *trn*L-P6

In a general molecular biology lab that is physically separated from the trace DNA clean lab, PCR reactions were prepared using the SYBR Premix Ex Taq kit (Takara, Bio Inc.). One µL of extracted and purified DNA (~2-25 ng) was added to a total volume of 20 µL reaction mixture and amplified (in triplicate) using a Realplex quantitative PCR system (Eppendorf, Hauppauge, NY). The PCR reactions were stopped in the exponential phase or after a maximum of 33 cycles to prevent overamplification and minimize the production of PCR artefacts such as primer dimers. Each PCR cycle included a denaturation step (5 sec at 95 °C), primer annealing (30 sec at 51 °C), and primer extension plus imaging (15 sec at 72 °C) of newly formed SYBR®green labelled double-stranded DNA. The short chloroplast ~10-134 bp *trn*L-P6 loop (Taberlet et al., 2007) was amplified using modified eco-PCR tested primers after Riaz et al. (2011): *trn*L-G2 (5'-GGG CAA TCCT GAG CCA A-3') and *trn*L-H2 (5'-TTG AGT CTC TGC ACC TAT C-3') since this primer combination yielded the least amount of primer dimers. Each initial round of PCR included triplicate reactions with 1 µL of each extraction blank and two reactions without template DNA present (background blanks).

The quality of the amplicons was evaluated by agarose gel electrophoresis. 131 out of 146 samples between 3.64 and 114.57 mcd revealed the expected average amplicon size of ~90 bp. Unfortunately, the expected amplicon size of ~95 bp could not be obtained from the two shallowest available samples (2.95 and 3.12 mcd). One microliter of 131 *trn*L-P6 amplicons and the amplified background and extraction blanks served as a template for a nested PCR using the same primers carrying the required Illumina adapters. In addition, the reverse primers in the nested PCR carried

12 bp Golay barcodes after Caporaso et al. (2012) to support the pooling of samples and contamination controls for subsequent MiSeq Illumina sequencing. Identical barcodes were used for triplicate reactions of each sample and background vs extraction blanks. The nested PCR reactions were also followed in real-time and stopped after reaching the end of the exponential phase (12 cycles) to prevent over-amplification and minimise the formation of PCR artefacts (More et al., 2018). The concentration of each barcoded amplicon was quantified fluorometrically (Quanti-iT^{TM} PicoGreen TM ds DNA reagent; Thermo Scientific, Scoresby, VIC, Australia), and equimolar amounts were pooled and concentrated using an Amicon Ultra centrifugal system (3 KDa). The concentrated barcoded library was run on a sterile 2% agarose gel at 120V for 60 min, and the expected fragment was excised and gel-purified using the Monarch gel extraction kit (New England Biolabs). The DNA concentration of the concentrated and gel-purified library was measured again fluorometrically and sent for Illumina MiSeq paired-end sequencing (2x75 bp/150 cycles) at the Australian Genome Research Facility (AGRF) in Perth.

2.3.4 Taxonomic assignments and removal of unassigned reads plus contaminants

Using ObiTools (Boyer et al., 2016), raw sequences were paired with an alignment score threshold of 20, assigned to samples, and de-replicated. Low-count sequences (< 10) and short reads (<10 nucleotides) were removed using obigrep, and PCR errors were removed using obiclean. Ecotag was used for taxonomic assignment of remaining unique and genuine ASVs. The *trn*L reference database for taxonomic assignment of the ASVs was created using ecoPCR from release 143 of the European Nucleotide Archive. Before downstream analysis, unassigned and contaminant reads that occurred in both the samples and in extraction- and background amplification blanks were removed, and the remaining error- and contaminant-free datasets were used for downstream bioinformatic- and biostatistical analysis. We considered all ASVs assigned at the same lowest reliable taxonomic rank as a unique taxon, and the sum of reads of each taxon formed the species abundance matrix for ordination and biostatistical analyses described below.

2.3.5 Bioinformatics and biostatistics of the clean *trn*L-P6 datasets

Relative read abundance and presence/absence matrices of ASVs that could be identified at the same lowest reliable taxonomic levels (i.e., family, clade, subfamily, tribe, genus, or species level) formed the template for downstream bioinformatics and biostatistical analysis. Partial Least Square-Discriminant Analysis (PLSDA) (Sisk-Hackworth & Kelly, 2020) was performed in the R package MixOmics (Rohart et al., 2017) as a sensitive ordination tool to visualise the level of dissimilarities in paleovegetation communities between samples and sample groups (i.e., paleodepositional units and main lithologies). Before this analysis, zero entries in the species abundance matrix were offset by 1 to allow a centred log-ratio (CLR) transformation (Lee et al., 2017). Global and pairwise similarity analysis (ANOSIM) was used to determine if *trn*L-P6 paleovegetation communities differed significantly between paleodepositional units and main lithologies. This analysis used Bray Curtis dissimilarities of square root transformed relative read abundance data and Sørensen dissimilarities of presence/absence data in PRIMER-e v7 (Clarke & Gorley, 2015). Indicator Species Analysis (ISA) was performed using the R package IndicSpecies (De Caceres & Legendre, 2009) to reveal the significant association of *trn*L-P6 vegetation (classified at the lowest reliable taxonomic levels) with paleodepositional units and sediment lithologies. In addition, a similarity of percentage (SIMPER) analysis was performed in PRIMER-e v7 to identify the taxa that contributed most to group similarities or dissimilarities between groups that contained significantly different (ANOSIM $p < 0.05$) paleovegetation communities.

A Clustered Image Map (CIM) of Pearson correlations between *trn*L-P6-inferred paleovegetation and previously analysed (in)organic geochemical parameters for changes in Lake Towuti's paleohydrology and paleoenvironment (Morlock et al., 2021; Russell et al., 2020; Sheppard et al., 2021) was performed in MixOmics to infer the origins of the different types of vegetation that drained into Lake Towuti in the form of chloroplast-rich plant litter. These parameters included:

(i)   **Cr and Ni** (as oxides) - potentially phototoxic.

(ii) **Fe and Mn** (as oxides)- redox-sensitive and enriched in the Mahalona and Lampenisu Rivers draining ultramafic bedrock catchments and laterite soils, respectively.

(iii) **Mg** - discharged into Lake Towuti as Mg-rich serpentines via the Mahalona River (Morlock et al., 2019; Russell et al., 2020).

(iv) **K, Al, Ti (as oxides) and increased Al/Mg ratio** – indicative of increased erosion and sedimentation of laterite soils and drainage of felsic bedrock material from the Loeha River to the east (Morlock et al., 2019).

(v) **TOC** - elevated due to enhanced primary productivity, increased terrestrial OM influx, or increased SOM preservation during stratified and anoxic conditions.

(vi) **δ^{13}C of bulk SOM** - enriched in case of increased influx of OM from C_4 vegetation (Russell et al., 2020).

(vii) **TLE/TOC ratio** - elevated in the case of increased preservation of SOM under stratified and reducing anoxic conditions and signifying high lake-level stands and a wetter climate (Russell et al., 2020).

(viii) **%SiO$_2$** – Diatom ooze indicating mesotrophic conditions caused by long-term leaching of P from tephra, which contributed to the deposition of the several-meter-thick diatom oozes (Russell et al., 2020).

Bubble plots were prepared using the packages reshape2 and ggplot2 (Wickham, 2016) in R (https://www.R-project.org/) to visualise downcore changes in the relative read abundance of the *trn*L-P6 inferred vegetation.

2.4 Results

2.4.1 General overview of the downcore distribution of eDNA content and sequence data

The total amount of extracted environmental DNA (eDNA), which likely comprises a complex mixture of extant and past biological sources, notably bacteria, varied

substantially between the analysed intervals of the same lithologies (see Fig. 2.2A and Table S2.1 for details).
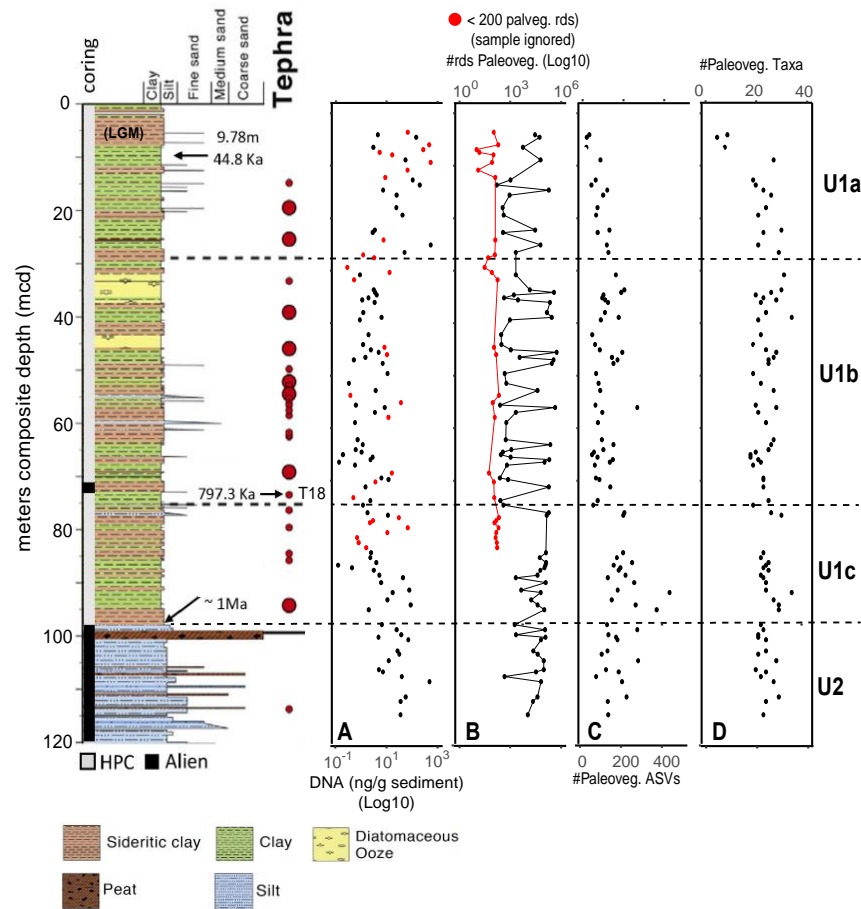
Figure 2.2 Total environmental DNA (eDNA) concentration and general overview of the recovered Paleogenic sequence data: (A) Amount of extracted total eDNA (ng/g sediment). (B) The total number of reads from paleovegetation. Samples containing fewer than 200 *trn*L-P6 reads of paleovegetation, which were excluded from further analysis are indicated in red. (C) Total number of ASVs that could be assigned to paleovegetation at family, clade, subfamily, tribe, or genus levels. (D) The number of taxa inferred from the sum of ASVs assigned to the same taxonomic ranks in the 82 remaining analysed sediment intervals. See Figs. S2.1-S2.3 for an overview of the contaminants and unassigned ASVs or sequencing artefacts removed from the dataset before processing. The lithology graph left of panel A shows the alternating deposition of silty clay and peat intervals during the pre-lake stage (Unit 2), followed by permanent lacustrine conditions above the U2/U1 transition at 98 mcd. See Russell et al. (2020) and results and discussion in the main text for a detailed description of the main lithologies (lacustrine green clays, red sideritic clays, and diatom ooze intervals vs pre-lake fluvial silts and peats) and for the paleohydrological/paleodepositional conditions that were used to define the major pre-lake U2 and lacustrine U1a-, U1b-, and U1c stages and their transitions. The lithology graph further shows composite sediment depth (mcd), coring method (hydraulic piston vs Alien), the position of tephra deposits T1-T23 and sediment ages. Radiocarbon dating on the bulk organic matter at 9.79 mcd revealed a sediment age of ~44.7 Ka, whereas ^{40}Ar/^{39}Ar dating of the tephra T18 layer at 72.95 mcd revealed a sediment age of 797.3 ± 1.6 Ka. The U2/U1c transition at ~98.8 mcd was estimated to have occurred 1 Ma ago through extrapolation (see Russell et al., 2020 for details).

Sedimentary *trn*L-P6 was successfully amplified from 113 out of 143 extracted intervals, and subsequent amplicon sequencing yielded 10^3 to 4 x 10^5 sequence reads per sample (Fig. S2.1A). In total, 2770 ASVs were assigned from all samples combined. Aligning the recovered ASVs with available *trn*L-P6 sequences in the EMBL plant sequence database revealed that roughly one-third of these ASVs (962 out of 2770) could only be identified at subphylum or higher taxonomic ranks and were not considered for further analysis. While this may be attributed to a lack of available closely related *trn*L-P6 sequences, similarity analysis using the Basic Local Alignment Search (BLAST) tool showed that 899 out of the 962 poorly assigned ASVs did not show any closely matching sequences available in NCBI's (National Center for Biotechnology Information) nucleotide collection (nr/nt) database (https://blast.ncbi.nlm.nih.gov). The remaining 63 ASVs showed the highest similarities with sequences of bacterial origin (Fig. S2.1).

The parallel amplified and sequenced background- and extraction blanks (BGB and EB) yielded a combined total of 227 ASVs that could be assigned to the common lab contaminants *Musa* (a genus of the family Musaceae that includes banana) and northern hemisphere temperate climate conifers (Pinaceae; *Pinus* and *Picea*) (Boessenkool et al., 2014; Pedersen et al., 2013), as well as unusual contaminants, notably unclassified Asparagaceae (subfamily Nolinoideae) (Fig. S2.2). The remainder of relatively less abundant contaminant ASVs represented non-native taxa showing the highest sequence similarities (>96%) with *Allium* (a genus of herbs of the family Amaryllidaceae that comprises garlic and onion), *Arachis* (a genus of herbs of the legume family Fabaceae that includes peanuts), *Callitris* (conifers indigenous to Australia), and *Alnus* (deciduous trees of the family Betulaceae, native to temperate regions of the northern hemisphere) (Fig. S2.2). In agreement with this result, Musaceae, Pinaceae, and Asparagaceae also represented the relatively most abundant assigned contaminants in many samples throughout the record, with minor contributions of *Allium*, *Arachis*, *Callitris,* and *Alnus* (Fig. S2.3). In addition, 216 out of the 962 unassigned ASVs were found to be relatively abundant contaminants in the blanks and many of the samples (Box B of Fig. S2.3) and were removed from the

48

dataset. The remaining 1375 ASVs, considered to be sourced from paleovegetation, could be assigned at taxonomic ranks low enough (i.e., family, clade, subfamily, tribe, or genus levels) for meaningful paleoenvironmental interpretations (Fig. 2.3).

We decided to exclude thirty-one sediment intervals which, after the stringent removal of contaminants and unassigned reads, yielded less than 200 *trn*L-P6 sequences from taxonomically assigned paleovegetation in total (i.e., 18 red clays, 12 green clays, and one silty clay (i.e., the red labelled intervals in Fig. 2.2B). Using the definition of depositional units after Russell et al. (2020), the remaining 82 intervals comprised fourteen U2 intervals (five peats and nine silty clays), seventeen U1c intervals (six red clays and 11 green clays), thirty-seven U1b intervals (one silty clay, ten red clays, 17 green clays, and nine diatom oozes), and fourteen intervals of U1a (five red clays and nine green clays) (Fig. 2.3). The thick interval of siderite red clays between ~3 and 7 mcd of unit 1a span the Last Glacial Maximum (~15-30 cal. Ka BP) (Russell et al., 2020). Eight red clay samples from the LGM (2.95, 3.12, 3.64, 4.12, 4.6, 6.03, 6.51 and 6.94 mcd) were initially available for DNA extraction. However, only three red clays (4.12, 4.6, and 6.51 mcd), which were deposited during the LGM, were found suitable for downstream analysis as they yielded more than 200 *trn*L-P6 reads from paleovegetation that could be identified at family or lower taxonomic ranks (Figs. 2.2, 2.3). Only 61 additional ASVs were lost after excluding 31 intervals with fewer than 200 paleovegetation reads.
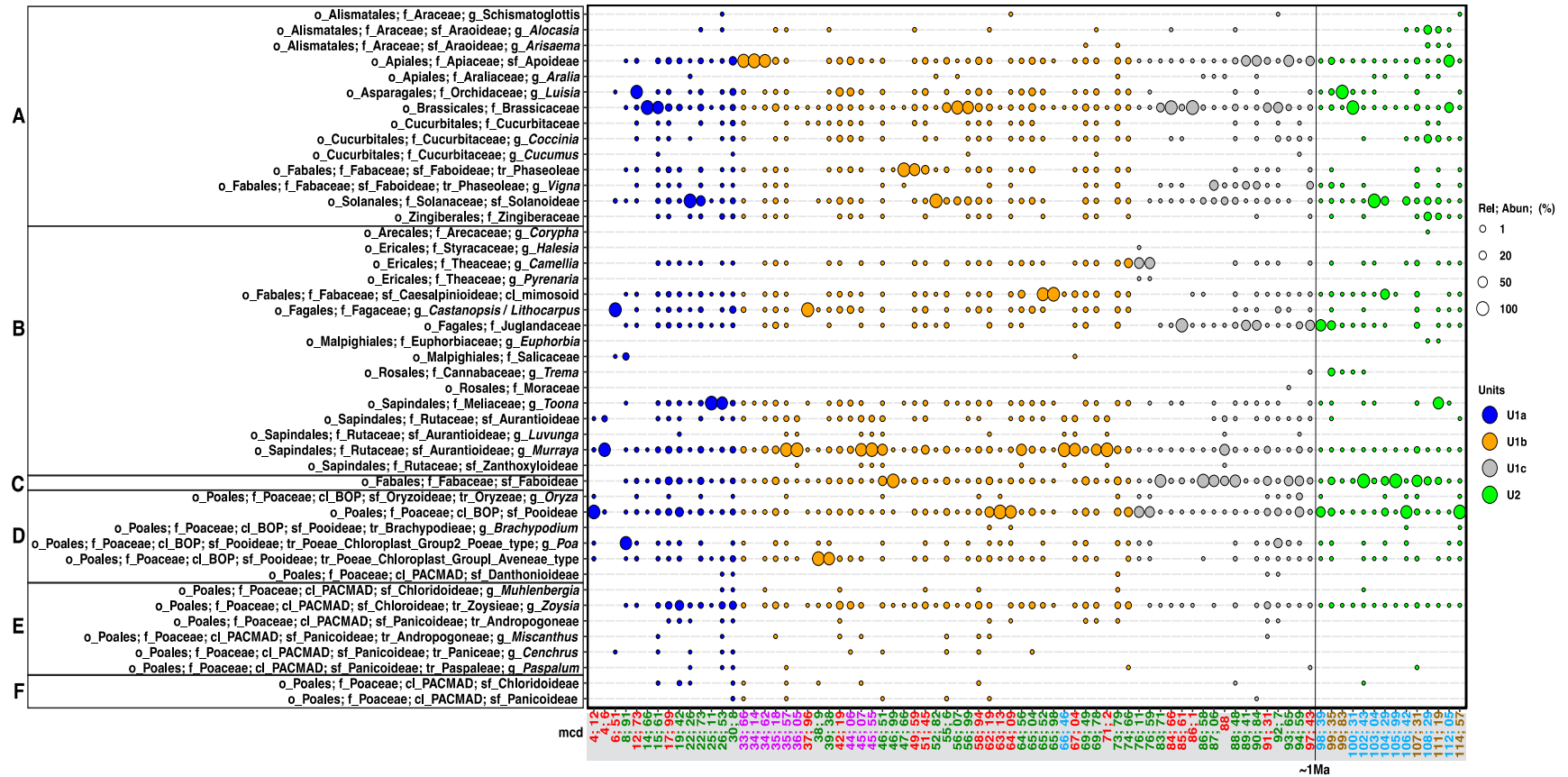
Figure 2.3 Bubble plot showing the downcore distribution of *trn*L-P6-inferred paleovegetation. Only samples are shown that contained more than 200 *trn*L-P6 reads from past taxa after removal of contaminants, poorly classified reads (i.e., subphylum or higher) in the EMBL plant database or represent artefact reads that did not return any significant similarities after blasting against the NCBI's nr database. The taxonomic levels include order (o_), family (f_), subfamily (sf_), clade (cl_), tribe (tr_), and genus (g_). The size of the bubbles indicates the relative read abundance at 1%, 20%, 50%, and 100% scale. The vegetation is ordered alphabetically within the following boxed categories: A (herbs), B (TRSH), C (herbs or TRSH), D (C₃ grasses), E (C₄ grasses), and F (C₃/C₄ grasses). See Russell et al. (2020) and the main text for details about the lithologies and depositional units. The x-axis denotes meters composite depths (mcd) of the analysed sediment intervals. The samples have been colour-coded according to the main lithology types. (See the caption of Fig. 2.2 for additional overlapping details).

50

After these measures, 1364 remaining ASVs were selected for downstream data analysis. The number of ASVs varied greatly throughout the core, being lowest in the red clays of the LGM (14-28 ASVs per interval) and highest in the older red clays of U1 (42-418 ASVs) and green clays (38-355 ASVs). See Table S 2.1 for further details. The plant lists for Sulawesi were sourced from a digitised herbarium list of 28,000 specimens collected from Sulawesi and compiled by the Naturalis Biodiversity Center in Leiden, The Netherlands. Plant function types were determined by assessment of the specimen notes in the herbarium list as well as published data (Whitten et al., 1988; Kessler et al., 2002; IUCN, 2019). The ASVs could be assigned to herbs (n=12), trees or shrubs (TRSH; n=18, C_3 grasses (n=6), C_4 grasses (n=6), and C_3 or C_4 grasses (n=2) (Fig.2.3) at taxonomic ranks (family or lower) native to Sulawesi. In addition, unclassified Fabaceae (Faboideae) formed a separate category since they may represent herbs and TRSH (Figs. 2.3, 2.4). Roughly four times fewer paleovegetation taxa were identified from the LGM section of U1a (n=6.3 ± 2.1) than in the older red clays of U1 (n=22.5 ± 3.5) (Table S2.1; 82 intervals). A comparable average number of taxa were identified from green clays (23.4 ± 3.9), diatom oozes (23.4 ± 3.8), clayey silts (22.9 ± 2.5), and peat intervals (22.2 ± 3.3) (Fig. 2.2, Fig. S2.1, and Table S2.1). Herbs and TRSH showed the highest relative read abundances throughout the record, followed by C_3 grasses. Obligate C_4 grasses comprised less than 10% throughout the core, reaching the highest levels in the green clays, notably in section U1b (Fig. 2.4).
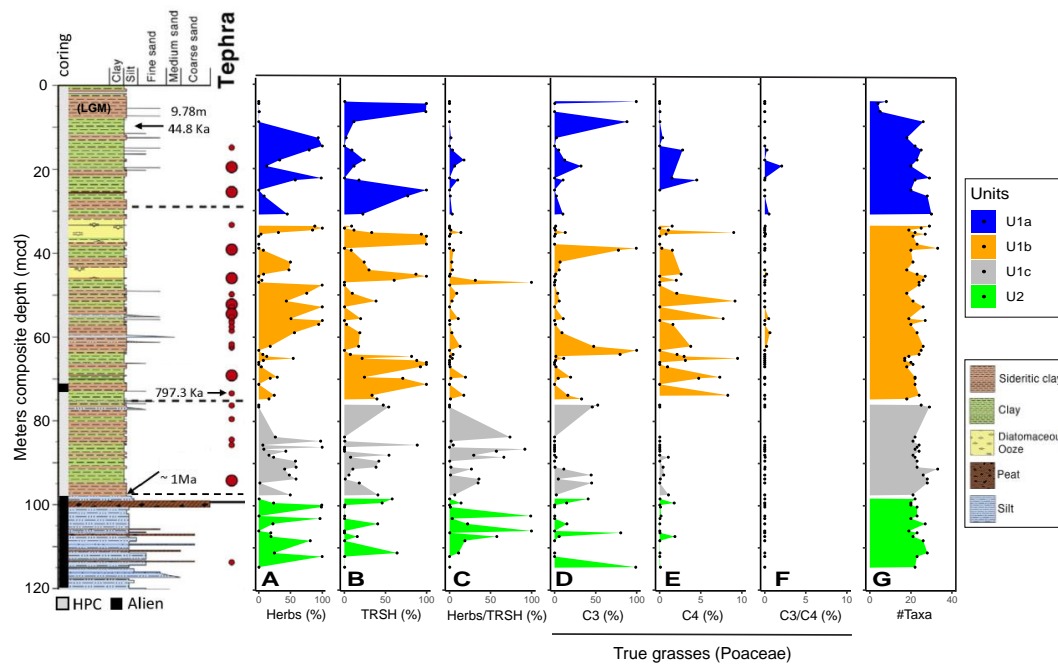
Figure 2.4 Downcore variability in *trn*L-P6 inferred paleovegetation. Relative read abundance of *trn*L-P6 from (A) Herbs; (B) evergreen trees and shrubs (TRSH); (C) Faboideae that could be herbs and/or TRSH; (D) true grasses (Poaceae) that use the C_3 carbon fixation pathway (BOP clade and the subfamily Danthonioideae of the PACMAD clade; (E) genera of true grasses within the PACMAD subfamilies Chloridoideae and Panicoideaea that only use the C_4 carbon fixation pathway as an adaption to drier conditions; (F) PACMAD subfamilies that could not be assigned at genus level and may have been using C_3 as well as C_4 carbon fixation pathways; (G) The number of *trn*L-P6 paleovegetation taxa identified at the lowest reliable taxonomic ranks. The paleodepositional units were defined by Russell et al. (2020). (See the caption of Fig. 2.2 for overlapping details).

2.4.2 Classification of samples using Partial Least Square Discriminant Analysis (PLSDA)

PLSDA enables selecting the most predictive or discriminative features in data to help classify samples (Sisk-Hackworth & Kelly, 2020). Due to the dissimilarities in the composition and relative read abundance of paleovegetation (n=45 taxa in 82 intervals), PLSDA analysis resulted in the formation of spatially separated clusters for each of the four previously defined major paleodepositional categories (i.e., pre-lake U2, and lacustrine U1c,1b, and 1a) (Fig. S2.4). Subsequent analysis of similarities (ANOSIM) using Bray-Curtis Dissimilarity of standardized and square root transformed relative read abundance data as well as using Euclidean Dissimilarity of presence-absence (PA) data, showed that the taxa identified through sedimentary *trn*L-P6 profiling differed significantly between these paleodepositional units (global test: $r = 0.148$; $p = 0.003$ vs $r = 0.150$; $p = 0.001$) (Table 2.1). No significant differences in

paleovegetation taxa were observed using Bray-Curtis vs Euclidean dissimilarities (global ANOSIM test) between pre-lake U2 and the entire lacustrine U1 section (top row in Table 2.1). Pairwise ANOSIM using all four paleodepositional categories showed that the Bray Curtis dissimilarities in community composition were highest between U1a and U1c ($r= 0.153$; $p=0.002$), between U1b and U1c ($r=0.186$; $p=0.012$), and between U1b and U2 ($r=0.196$, $p=0.024$) (Table 2.1). Highly significant differences in paleovegetation were observed between U1a and U2 only based on Euclidian analysis of presence/absence data ($p=0.001$) vs a marginally significant difference ($p=0.024$) using Bray-Curtis analysis of square root transformed quantitative sequence data. Paleovegetation assemblages between U1a and U1b and U1c and U2 did not differ significantly (Table 2.1). Treating diatom oozes and the clays from U1b as two separate sample categories for ANOSIM analysis resulted in higher global r- and lower global p-values mainly driven by the greater significant dissimilarities in vegetation assemblages between the diatom ooze and U1c ($r= 0.306$; $p=0.001$) vs U2 ($r= 0.374$; $p=0.001$). Paleovegetation assemblages did not differ significantly between diatom ooze and lacustrine clays, which is likely due to the imbalance in the availability of samples in favour of the clays. Treating diatom oozes and clays of U1b as two separate sample categories resulted in more significant dissimilarities in the presence/absence of paleovegetation, most notably between U1a and U2 (Table 2.1). Global and pairwise ANOSIM performed on the main lithologies revealed that paleovegetation assemblages only differed significantly between samples of the peat and clayey silt intervals of U2 and the diatom oozes of U1b (See Table 2.1 for further details).

Table 2.1 Global and pairwise analysis of similarities (ANOSIM) showing significant dissimilarities in paleovegetation between sample categories: (i) pre-lake Unit 2 x lacustrine Unit 1; (ii) paleodepositional units (four categories; U2, U1c, U1b, U1a); (iii) paleodepositional units with the diatom ooze considered as a separate sample category of Unit 1b (U2, U1c, U1b$_{DO}$, U1b$_{RC+GC}$, U1a).

Categories	Global vs. pairwise tests	SQRT+Bray-Curtis			PA + Euclidian		
		R	P	Sign. Level	R	P	Sign. Level
Stages (pre-lake x lake)	Global test	0.063	0.226	NS	0.05	0.268	NS
Paleodepositional units (U1a,U1b,U1c,U2)	Global test	0.148	0.003	**	0.15	0.001	***
	U1a x U1b	0.117	0.094	NS	0.204	0.02	*
	U1a x U1c	0.153	0.002	**	0.119	0.009	**
	U1a x U2	0.11	0.036	*	0.137	0.003	**
	U1b x U1c	0.186	0.012	*	0.101	0.06	NS
	U1b x U2	0.196	0.024	*	0.185	0.01	*
	U1c x U2	0.021	0.256	NS	0.072	0.063	NS
Paleodepositional units (U1a,U1b(RC+GC),U1b(DO), U1c,U2)	Global test	0.193	0.001	***	0.123	0.002	***
	U1a x U1b(DO)	0.018	0.364	NS	-0.063	0.8	NS
	U1a x U1b(RC+GC)	0.074	0.179	NS	0.193	0.01	*
	U1a x U1c	0.153	0.006	**	0.119	0.009	**
	U1a x U2	0.08	0.024	*	0.137	0.001	***
	U1b(DO) x U1b(RC+GC)	0.04	0.349	NS	0.017	0.399	NS
	U1b(DO) x U1c	0.306	0.001	***	0.068	0.184	NS
	U1b(DO) x U2	0.374	0.001	***	0.151	0.044	*
	U1b(RC+GC) x U1c	0.161	0.006	**	0.114	0.028	*
	U1b(RC+GC) x U2	0.138	0.041	*	0.201	0.004	**
	U1c x U2	0.021	0.28	NS	0.072	0.063	NS
Main lithologies	Global test	0.044	0.212	NS	0.034	0.265	NS
	RC x GC	0.023	0.281	NS	0.056	0.138	NS
	RC x DO	-0.043	0.628	NS	-0.082	0.784	NS
	RC x silt	0.122	0.099	NS	0.004	0.444	NS
	RC x peat	-0.018	0.519	NS	-0.004	0.582	NS
	GC x DO	0.051	0.319	NS	-0.03	0.582	NS
	GC x silt	0.044	0.330	NS	0.085	0.185	NS
	GC x peat	-0.052	0.595	NS	0.069	0.335	NS
	DO x silt	0.487	0.001	***	0.12	0.028	*
	DO x peat	0.4	0.002	**	0.082	0.236	NS
	silt x peat	-0.078	0.718	NS	-0.136	0.897	NS

Note: ANOSIM results were compared using Bray-Curtis vs Euclidian dissimilarities of normalised and square root-transformed relative read abundance- vs presence-absence data of paleovegetation communities identified at the lowest reliable taxonomic levels. R shows the mean of ranked dissimilarities between categories to the mean of ranked dissimilarities within categories. $P < 0.05$ indicates significantly different global and pairwise ANOSIM tests. Significance levels: 0 '***' 0.001 '**' 0.01 '*' 0.05 and not significant (NS). Only samples with >200 total reads of genuine paleovegetation after removal of the artefact- and contaminant *trn*L-P6 reads were used for ANOSIM analysis (Fig. 2.3). See Table 2.2, listing the significant indicator species assigned to the developmental stages, and Fig. 2.5 for an overview of taxa with the highest percentage associated with the five depositional stages (i.e., SIMPER analysis).

2.4.3 Identification of past vegetation through sedimentary *trn*L-P6 profiling

Herbs currently native to Sulawesi: Wetland herbs of the order Allismatales (Arecaceae), notably *Alocasia* ("Elephant Ear") that grows from rhizomes and is native to tropical and subtropical Asia, including Sulawesi (http://www.powo.science.kew.org), were primarily identified in the peats and silts at the base of the studied interval (Fig. 2.3). Indicator Species Analysis revealed that another genus *Arisaema* in this family of wetland herbs was significantly associated with this depositional stage ($r = 0.477$; $p = 0.008$; Table 2.2).

Table 2.2 Overview of taxa that differed significantly between paleodepositional units.

	Indicator species	Category	A	B	stat	p.value	Sign. Level
A U1a, U1b, U1c, U2	o_Poales; f_Poaceae; cl_PACMAD; sf_Panicoideae; tr_Paniceae; g_*Cenchrus*	U1a	0.5857	0.9	0.726	0.048	*
	o_Cucurbitales; f_Cucurbitaceae	U1b	0.4497	0.8108	0.604	0.032	*
	o_Fabales; f_Fabaceae; sf_Faboideae; tr_Phaseoleae	U1b	0.5997	0.973	0.764	0.004	**
	o_Poales; f_Poaceae; cl_BOP; sf_Pooideae; tr_Poeae_Chloroplast_GroupI_Aveneae_type	U1b	0.5168	0.973	0.709	0.041	*
	o_Sapindales; f_Rutaceae; sf_Aurantioideae	U1b	0.5103	0.8649	0.664	0.007	**
	o_Sapindales; f_Rutaceae; sf_Aurantioideae; g_*Murraya*	U1b	0.5248	1	0.724	0.001	***
	o_Fabales; f_Fabaceae; sf_Faboideae; tr_Phaseoleae; g_*Vigna*	U1c	0.6186	1	0.786	0.001	***
	o_Fagales; f_Juglandaceae	U1c	0.4891	1	0.699	0.021	*
	o_Alismatales; f_Araceae; sf_Araoideae; g_*Arisaema*	U2	0.7978	0.2857	0.477	0.008	**
	o_Malpighiales; f_Euphorbiaceae; g_*Euphorbia*	U2	0.9872	0.1429	0.376	0.041	*
	o_Rosales; f_Cannabaceae; g_*Trema*	U2	0.8742	0.4286	0.612	0.01	**
	Indicator species	**Category**	**A**	**B**	**stat**	**p.value**	**Sign. Level**
B U1a, U1b(RC+GC), U1b(DO), U1c, U2	N/A	U1a	-	-	-	-	-
	o_Cucurbitales; f_Cucurbitaceae	U1b (RC+GC)	0.3585	0.8571	0.554	0.045	*
	o_Fabales; f_Fabaceae; sf_Faboideae; tr_Phaseoleae	U1b (RC+GC)	0.5091	0.9643	0.701	0.023	*
	o_Apiales; f_Apiaceae; sf_Apoideae	U1b (DO)	0.4312	1	0.657	0.002	**
	o_Sapindales; f_Rutaceae; sf_Aurantioideae	U1b (DO)	0.4903	1	0.7	0.001	***
	o_Sapindales; f_Rutaceae; sf_Aurantioideae; g_*Luvunga*	U1b (DO)	0.5085	0.4444	0.475	0.041	*
	o_Sapindales; f_Rutaceae; sf_Aurantioideae; g_*Murraya*	U1b (DO)	0.4603	1	0.678	0.001	***
	o_Fabales; f_Fabaceae; sf_Faboideae	U1c	0.3388	1	0.582	0.035	*
	o_Fabales; f_Fabaceae; sf_Faboideae; tr_Phaseoleae; g_*Vigna*	U1c	0.5733	1	0.757	0.002	**
	o_Fagales; f_Juglandaceae	U1c	0.4407	1	0.664	0.022	*
	o_Alismatales; f_Araceae; sf_Araoideae; g_*Arisaema*	U2	0.7491	0.2857	0.463	0.019	*
	o_Rosales; f_Cannabaceae; g_*Trema*	U2	0.8707	0.4286	0.611	0.025	*

Note: Indicator Species Analysis (ISA) was performed with (**A**) lacustrine subunits U1a, U1b (all lithologies), U1c and pre-lake U2; (**B**) U1a, U1b (RC+GC separated from DO intervals), U1c, and U2. The best indicator species are those found only in samples/intervals belonging to one group/category (A=1) and are present in all samples within that group (B=1). Only taxa with *p* values < 0.05 are shown in the table. Significance levels (*r*): 0 '***' 0.001 '**' 0.01 '*' 0.05. Taxonomic levels: o_(order); f_(family); sf_(subfamily); tr_(tribe); cl_(clade), g_(genus). Note that the indicator species in each sample category are ordered alphabetically.

Putative N-fixing legumes (Fabaceae) were relatively abundant throughout U2 and U1c. They also showed equally highest percentage associations (SIMPER; ~38%) with both depositional units (Fig. 2.5) but represented only significant indicator taxa for U1c (Table 2.2). Unclassified Faboideae made the highest contribution among

group members of U2 and U1c. Since this subfamily of Fabaceae could not be classified at lower taxonomic levels, they may also represent TRSH and, therefore, were grouped as Herbs and TRSH (vegetation category C in Figs. 2.2-2.4). ASVs of the cosmopolitan nightshade family Solanaceae, predominantly assigned to the native genus *Solanum* (http://www.powo.science.kew.org), were found to be associated with all subunits but did not show any association with diatom oozes. In contrast, the herb family Brassicaceae (Brassicales) showed the highest percentage associations with U1c and U1a and the lowest association with the diatom ooze intervals (Fig. 2.5). Moreover, ASVs assigned to herbs of the family Apiaceae (subfamily Apoideae) showed up to 100% sequence similarity with Java water dropwort (i.e., *Oenanthe javanica*). This native edible aquatic herb, which can be abundant in freshwater environments throughout Southeast Asia, showed the highest associations with U1b diatom oozes (SIMPER; 18%) (Fig. 2.5) and represented a significant indicator species for this sample category (ANOSIM; r=0.657; p=0.02) (Table 2.2).
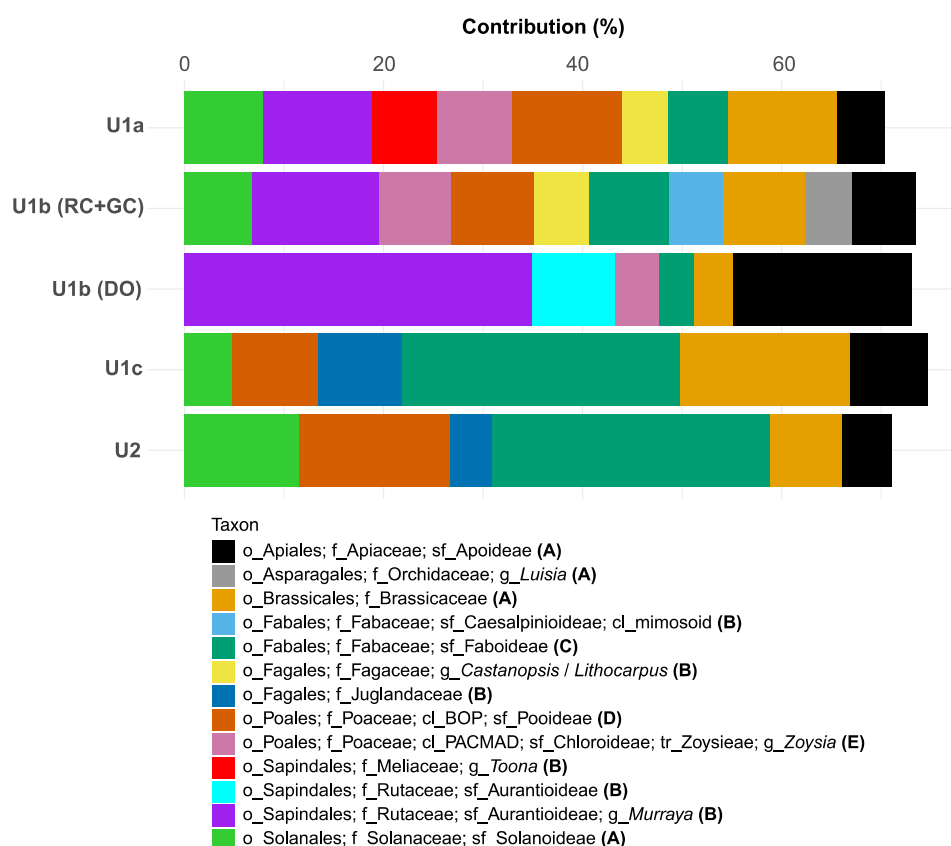
Figure 2.5 Similarity percentages (SIMPER) analysis showing the taxa that made the highest % contribution to the (Bray-Curtis) similarities observed within group members (cut-off = 70%): Pre-lake U2 vs the lacustrine subunits U1a, U1b (RC and GC), U1b (DO), and U1c. (A) herbs; (B) (TRSH); (C) herbs and/or TRSH of Faboideae; (D) C$_3$ grasses; (E) C$_4$ grasses. (See the caption of Fig. 2.2 and the main text for a detailed description of the depositional stages).

Trees and shrubs (TRSH): ASVs assigned to Juglandaceae (Fagales) were present in most pre-LGM intervals but were found to be a significant indicator taxon for U1c (Table 2.1) and revealed the highest SIMPER associations with this early lacustrine depositional unit (Fig. 2.5). Although genus level identification was not possible, it may represent *Engelhardia*, a native evergreen tree of Sulawesi often associated with dense primary forests on mountain slopes between 300 and 1600 meters above sea level (Kessler et al., 2002), and fossil pollen type recorded within nearby lake sediment records (Hamilton et al., 2019a). ASVs with 99-100% sequence similarities to *Toona ciliata*, a large native tropical forest tree of the Mahogany family (Meliaceae), were recovered from intervals throughout the record, except for the LGM red clays. *Toona* was most consistently identified from U1a (Table 2.2) and showed the highest SIMPER association with this depositional unit (Fig. 2.5). ASVs related to Caesalpinioideae (Fabaceae), a subfamily of the Mimosoid clade, were most consistently identified from green clays (Fig. 2.3). Although not a significant indicator taxon for any of the depositional units (Table 2.2), Caesalpinoideae were found to be only associated with clays of U1b in the case where these lithologies were treated as a separate group from diatom oozes (Fig. 2.5). ASVs of this subfamily of Fabaceae showed ~98-100% sequence similarity with the native genus *Parkia*, which can be found in various tropical habitats, including moist lowland forests and swamps (Hopkins, 1994). *Castanopsis* and/or *Lithocarpus* (Fagaceae) were most consistently present in U1a and U1b intervals, including the LGM (Fig. 2.3), and revealed relatively low percentage associations (SIMPER: 5-7%) with the clays of these subunits when diatom ooze was treated as a separate category (Fig. 2.5). These drought-tolerant tropical evergreen trees now dominate at lower/mid-montane elevations in Sulawesi (Biagioni et al., 2015; Culmsee et al., 2010) and have been described from fossil pollen in the adjacent TOW-9 and satellite lake (Lantoa) records (Hamilton et al., 2019a; Stevenson, 2018). ASVs with up to 100% sequence similarity to native genera (*Murraya* and *Luvunga*) belonging to the Rutaceae subfamily Aurantioideae (http://www.powo.science.kew.org) were present in the majority of analysed intervals, including LGM red clays. However, the relative read abundance of

57

Aurantioideae (notably *Murraya* that mainly inhabits peatland) was highest in the diatom oozes and showed very high association with this lithology (43%) and showed lower percentage associations with the clays of U1b and U1a. However, no substantial associations were observed with U2 and U1c (Fig. 2.5). As expected, the Aurantioideae represented highly significant indicator taxa for the diatom oozes (Table 2.2). ASVs identified as *Trema* (Cannabaceae) were only detected in four consecutive intervals above the U2/U1c transition (Fig. 2.3). In agreement with this result, *Trema* was a significant indicator taxon for U2 (Table 2.2) but was not substantially associated with this interval (Fig. 2.5).

True grasses (Poaceae): Sedimentary *trn*L-P6 profiling allowed us to distinguish between wet climate C_3 and dry climate C_4 grasses. Pooid grasses belonging to the BOP clade (Fig. 2.3), which exclusively use the C_3 carbon fixation pathway (Chang et al., 2013), predominated over C_4 grasses in all analysed intervals, including the LGM (Fig. 2.4). These C_3 grasses included the Pooideae subtribes Poeae and Aveneae (type *Avena* L) found in cooler climate regions of the world as well as in tropical mountains (Lasut, 2009). According to SIMPER analysis, Pooideae revealed relatively high percentage associations with all depositional units except for the diatom ooze intervals. Native C_3 wetland grasses (*Oryza*) were sporadically found in green clays shortly after the U2/U1c transition and in green clays plus diatom ooze (Fig. 2.3). A subfamily of PACMAD grasses that exclusively use the C_3 carbon fixation pathway (Danthanoideae), were also sporadically detected (Fig. 2.3). *Zoysia* (subfamily Chloroideae) a genus of exclusively C_4 grasses within the PACMAD clade (Aliscioni et al., 2012) was detected throughout the record, except for the LGM red clays (Fig. 2.3). Other C_4 grasses of the PACMAD clade (*Muhlenbergia*, *Miscanthus*, *Cenchrus*, and *Paspalum*) were only sporadically detected throughout the core, but most frequently in the green clay intervals of U1a and U1b, where they reached relative read abundances of up to 10% of the total vegetation assemblages (Fig. 2.4).

2.4.4 Pearson correlations between *trn*L-P6 vegetation and geochemical parameters

The cluster heatmap of Fig. 2.6 shows Pearson correlations (Pearson's *r* values) between downcore changes in the relative read abundance of taxa that comprised at least 1% of the *trn*L-P6 assemblage and previously analyzed (in)organic paleoenvironmental parameters. This analysis revealed three clusters of paleovegetation: Juglandaceae and the putative N-fixing legumes (Cluster A), were predominantly identified from and associated with the pre-lake landscape and early lake development (U2 and U1c). This cluster of pioneer forest vegetation revealed the highest positive Pearson correlation with sedimentary calcium content, which, according to end member (EM) modeling, indicates increased tectonic movement and a high-energy depositional environment at the coring site (Morlock et al., 2021). Cluster B includes taxa that showed highly significant SIMPER associations with the organic-rich diatom ooze intervals of U1b (Fig. 2.5), deposited during elevated nutrient availability and primary productivity. Notable examples are *Murraya* (Rutaceae), which includes small native peatland forest trees that were most likely growing in organic-rich and anoxic muddy sediments along the lake's shoreline (i.e., in a similar fashion as mangrove vegetation), and aquatic herbs within the Apiaceae subfamily Apoideae related to nutrient-demanding water dropwort (*Oenanthe javanica*). The concomitant highest negative Pearson correlations with $\delta^{13}C_{org}$ and highest positive Pearson correlations with %TOC, TLE/TOC, and %Si (Fig. 2.6) suggest that chloroplast-rich litter from this local C_3 paleovegetation contributed substantially to the immature (well-preserved) and ^{13}C-depleted sedimentary OM in the diatom oozes.
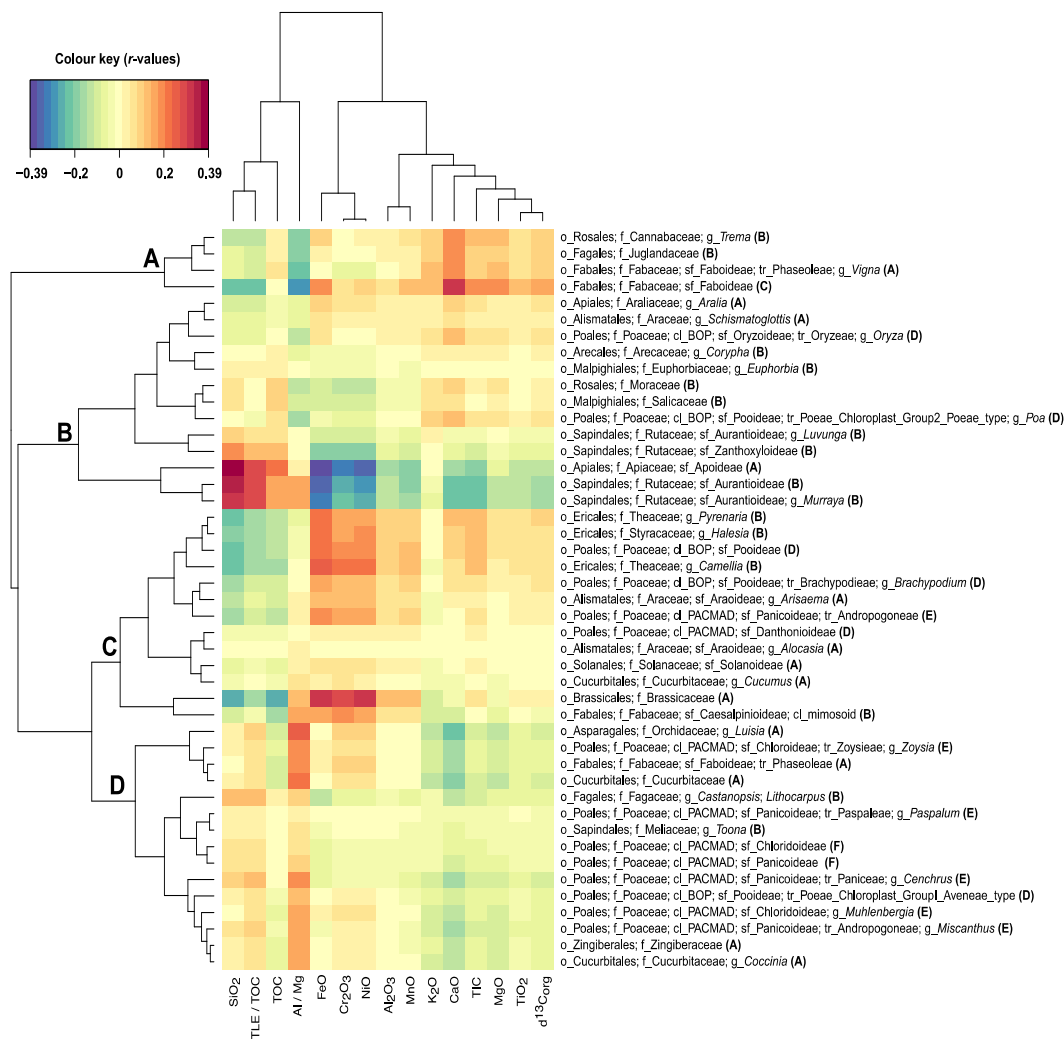
Figure 2.6 Cluster Image Map (CIM) showing Pearson correlations (*r* values in colour key) between relative changes in *trn*L-P6-inferred paleovegetation communities and previously analysed geochemical proxy data. Cluster A correlated most strongly with %Ca and comprised pioneering N-fixing trees of the legume family Fabaceae and N-fixing *Trema* (Cannabaceae) that prevailed during the pre-lake landscape characterized by active river channels, shallow lakes, and swamps. The upper part of Cluster B includes partially submerged vegetation that was likely rooted in muddy anoxic shoreline soils (e.g., *Oryza*, Alismatales) during early Lake Towuti. The lower part of Cluster B comprises peat swamp catchment vegetation (Rutaceae, notably *Murraya*) and nutrient-demanding aquatics (Apiaceae). This local vegetation prevailed during high nutrient availability that resulted in the subsequent deposition of diatom oozes (i.e., strong Pearson correlation with %Si) and when frequent stratified conditions and bottom water anoxia resulted in excellent preservation of SOM (high positive Pearson correlation with the TLE/TOC ratio, and %TOC). Cluster C comprises herbs (e.g., Brassicaceae), TRSH (e.g., Theaceae, Fabaceae), and mainly C_3 grasses (Poaceae), which most likely drained into Lake Towuti in the form of chloroplast-rich plant litter as the source of sedimentary *trn*L-P6 along with eroded ultramafic bedrock (Mg) and topsoil rich in Fe, Ni, and Cr during periods of reduced precipitation and low lake stands. The paleovegetation forming cluster D showed the highest positive Pearson correlations with the AL/Mg ratio indicative of predominant drainage from the Loeha River (Morlock et al., 2019) during elevated precipitation or periods of increased seasonality. (See the main text for a more detailed discussion about the potential origin of the identified paleovegetation and inferred changes in the paleodepositional environment, plus the caption of Fig. 2.2 for overlapping details and abbreviations).

In contrast, Cluster C consisted of herbs (Brassicaceae, Fabaceae), TRSH (Theaceae), and C_3 grasses (Poaceae) that most strongly (positively) correlated with sediments of a predominantly ultramafic signature (Fe-, Cr-, Ni-, Mg-, and Mn oxides) (Fig. 2.5).

Lastly, paleovegetation of cluster D comprised predominantly lower montane, large evergreen rainforest trees, ground cover herbs that spread via rhizomes and prefer moist and shady closed canopy conditions (Zingiberaceae), as well as tree orchids (*Luisia*). The vegetation of Cluster D is most strongly correlated with the Al/Mg ratio, indicating a more substantial contribution to the drainage of sediments from the Loeha River during periods of increased precipitation (Morlock et al., 2019). A possible explanation for why this cluster contains most of the assumed C_4 grasses of the PACMAD clade will be discussed below. See Fig. 2.6 for a complete overview of the Pearson correlations between downcore changes in paleovegetation assemblages and inorganic and isotopic for past changes in paleohydrology, paleoecology, and the paleodepositional development of late-Pleistocene Lake Towuti.

2.5 Discussion

2.5.1 Origin of contaminants and proof of concept for the successful and strict removal of contaminants

In deep biosphere studies, drilling muds are often used during coring as a lubricate to prevent the drilling bit from overheating. Microbial cell counts in these muds often exceed those of the low biomass deep subsurface environment by orders of magnitude and, therefore, considered a major potential source of contamination with intact cells from surface-dwelling microbial communities (e.g., Cockell et al., 2021; Friese et al., 2017; Inagaki et al., 2015). Fluorescent particles (tracers) which mimic the shape and size of bacterial cells are usually mixed with drilling fluids so that after core retrieval, sediment slices can be analysed microscopically to determine the extent and how deep these fluorescent tracers and possibly contaminant bacteria (could) have penetrated the core material (e.g., Friese et al., 2017). Drilling fluids were only required to lubricate the drill bit during Alien rotating coring to recover the more resistant

lithologies of Unit 2 plus the 2-m-thick red clay interval between 70.5-72.5 mcd. Therefore, contamination of the lacustrine sediments of Unit 1 with drilling fluids can be excluded and would not have impacted the observed Pearson correlations between relative changes in the *trn*L-P6 paleovegetation community composition and the geochemical parameters (Fig. 6), which informed about concomitant changes in the paleodepositional environment of Towuti Lake.

While fluorescent tracers have not been used during coring of 1F, microscopic analysis performed on U1 sediments from a parallel core from site 1 (core 1A) showed that bacterial cell-sized fluorescent tracer particles only penetrated the outer few mm of sediment (Friese et al., 2017). Pollen grains represent the smallest plant diagnostic morphological features as a potential source of contamination with chloroplast DNA during coring. Being substantially larger than bacterial cells renders it highly unlikely that modern pollen sourced from the water column or from surface sediments would have penetrated and contaminated the centre of the core, which was exclusively subsampled for DNA extraction in this study. In contrast, contamination with airborne pollen during subsampling or DNA extraction and sequence library preparation is a well-known concern in *sed*aDNA studies. Most notably, Gymnosperms (conifers) are a common source of contamination as this tree vegetation produces vast amounts of airborne pollen that can travel large distances (e.g., Boessenkool et al., 2014; Pedersen et al., 2013). Stevenson (2018) reported that native montane conifers (*Agathis*, *Dacrydium*, *Phyllocladus*, and *Podocarpus*) combined comprised up to ~30% of the total pollen count in the Glacial and Holocene sediments from the TOW-09 record previously obtained from the same coring location. However, none of the *trn*L-P6 reads in the samples and controls could be assigned to these genera or their respective families. Therefore, chloroplast-rich plant litter from local catchment vegetation was the predominant source of paleovegetation identified in this study, which rules out the possibility that locally or remotely produced modern pollen represented a source of contamination during coring. Instead, all identified reads that occurred in both samples as well as in the background and extraction blanks were assigned to taxa not native to Sulawesi and/or are the common lab contaminants *Musa* (Musaceae), Nolinoideae

(Asparagaceae), and *Pinus*/*Picea* (Pinaceae) (Boessenkool et al., 2014; Pedersen et al., 2013). Indirect evidence that the randomly distributed contaminants were accurately identified and stringently removed from the *trn*L-P6 data was provided by (a) the significant concomitant shifts in *trn*L-P6-inferred paleovegetation with transitions in the paleodepositional environment of Lake Towuti and (b) the identification of plausible significant indicator taxa associated with paleodepositional categories. Further evidence for a non-random downcore distribution of *trn*L-P6 from native taxa was provided by (c) the moderately strong Pearson correlations between relative changes in paleovegetation assemblages and geochemical parameters, indicative of simultaneous changes in the paleohydrology and paleodepositional environment of Lake Towuti as discussed in more detail below.

2.5.2 Factors contributing to the long-term preservation of vegetation *sed*aDNA in Lake Towuti

Bacteria, archaea, and eukaryotes contribute to lake sediments' total pool of extractable DNA. They include a mix of intracellular DNA associated with intact cells and extracellular DNA released into the environment after the lysis of dead cells (e.g., Vuillemin et al., 2017; Parducci et al., 2017 and references therein). Intracellular DNA from intact and physiologically active microbial communities dominated the total pool of extractable DNA in the surface sediments, while the relative read abundance of extracellular sedimentary environmental DNA from dead bacterial biomass increased with sediment depth in Lake Towuti (Vuillemin et al., 2017; 2019). These findings showed that a substantial amount of *sed*aDNA escaped initial microbial degradation in the surface sediments of Lake Towuti.

Since we used a non-selective destructive DNA extraction approach, it was impossible to verify whether plant taxa were identified from the pool of mineral-adsorbed extracellular DNA or DNA associated with intact chloroplasts in plant litter still undergoing microbial decomposition. Upon burial in the sedimentary record, microbial communities would be expected to preferentially degrade more reactive plant litter (e.g., leaves) and its associated DNA, favouring the preservation of more

recalcitrant wood structures. However, bias caused by preferential preservation of *sed*aDNA from woody plants and trees is unlikely to have played a substantial role in the outcomes of this study. Namely, leaves were likely the most abundant form of drained and sequestered plant biomass for all identified plant categories (herbs, TRSH, and grasses) and the richest source of chloroplasts per volume of plant remains. Moreover, leafy herbs and TRSH were equally well presented throughout the record (Figs. 2.3, 2.4).

Mineral adsorption of the negatively charged phosphate group in DNA contributes to extracellular DNA's immediate- and long-term protection against degradation by microbial nucleases (e.g., Coolen & Overmann, 2007; Demaneche et al., 2001; Freeman et al., 2023; Pietramellara et al., 2009; Vuillemin et al., 2017). Mineral adsorption in Lake Towuti's sediment is mainly facilitated due to the high amounts of ferruginous clays and clay-sized particles (Vuillemin et al., 2017), making up >60% of the sediment particle composition (Hasberg et al., 2019). Similarly, efficient adsorption of phosphate by sedimentary iron hydroxides, especially in a low sulphate environment like Lake Towuti, is thought to have contributed to ultraoligotrophic conditions and concomitant low primary productivity in the oxygenated sunlit surface waters of Lake Towuti during the deposition of the sideritic red clays (Caraco et al., 1986; Crowe et al., 2008).

In addition, as has been reported from many other stratified and anoxic basins (e.g., Coolen and Overmann, 2007; Coolen et al., 2004; 2013), bottom water anoxia in a stratified Lake Towuti would have resulted in lower microbial mineralisation rates, and hence, an increase in the accumulation of sedimentary OM and the fraction of *sed*aDNA that escaped early degradation during the deposition of the green clays as compared to red clays, which were deposited in a fully mixed and oxygenated water column (Russel et al., 2020).

Positively charged mineral surfaces generally exhibit a high affinity for DNA in any environment. In contrast, DNA binds to negatively charged surfaces, like nonclay silicates, via a cation bridge, and desorption will occur if the concentration or the ionic

64

potential of the immediate environment is decreased (e.g., Pastré et al., 2006). Therefore, the adsorption strength of *sed*aDNA to the silicified diatom ooze material is likely lower than that of the clays. In that case, a low microbial mineralisation rate under prevailing anoxic conditions was likely the main factor contributing to the accumulation of the immature/labile OM and the long-term survival of *sed*aDNA against microbial attack in the diatom ooze intervals.

We recovered *trn*L-P6 of wetland herbs such as *Alocasia* and Zingiberaceae in the oldest peat intervals of U2. This partially submerged vegetation was likely rooted in anoxic muddy soils in the peatland-dominated pre-lake landscape and could have survived waterlogged conditions through plant-mediated rhizosphere oxygenation (e.g., Nyburg et al., 1997; Koop-Jacobsen et al., 2021). Low microbial activities likely prevailed in the bulk of anoxic soils not associated with the oxygenated rhizosphere. Since the DNA adsorption capacity of sedimentary OM is deficient (Coolen and Overmann, 2007), reduced microbial mineralisation rates under oxygen-depleted conditions likely also contributed most to the accumulation of organic matter and more labile biomolecules, including DNA in the peats of U2.

The strong mineral adsorption to the ferruginous clays most likely contributed uniquely to the long-term preservation of *sed*aDNA in tropical Lake Towuti (Friese et al., 2017). However, even in relatively productive and fully mixed oxygenated tropical lakes, oxygen as the highest energy-yielding electron acceptor usually becomes depleted in the top few cm of sediments (e.g., Wang et al., 2022). Therefore, even if mineral adsorption did not play a substantial role in the long-term preservation of *sed*aDNA, reduced rates of microbial mineralisation leading to sedimentary OM accumulation and enhanced preservation of *sed*aDNA in anaerobic subsurface sediments is likely to be relatively widespread in mesotrophic and eutrophic tropical lake environments and warrants further investigation.

2.5.3 Insights into the developmental history of Lake Towuti from *sed*aDNA-inferred changes in catchment vegetation

(i) Taxa associated with the pre-lake landscape (U2) and early lacustrine development of Lake Towuti (U1C)

In agreement with previous mineralogical and geochemical findings (Russell et al., 2020), the paleovegetation identified from U2 indicates a pre-lake landscape characterised by shallow lakes and swamps before transitioning into a permanent Lake Towuti. For example, *Alocasia* was most consistently detected in U2. These wetland herbs prefer partial shade, spread through rhizomes, and can be invasive in swampy areas, but they need shallow waters and will not survive when submerged (Markesteijn et al., 2007). In addition, the presence of N-fixing pioneer vegetation indicates the presence of relatively disturbed and nutrient-depleted soils before developing a partly forested peat swamp. For example, *Trema* (Cannabaceae) was a source of sedimentary *trn*L-P6 in four consecutive intervals, marking the U2/U1c boundary and a significant indicator species for U2. ASVs derived from *Trema* cp DNA showed >99% similarity with *Trema orientale*, a fast-growing, N-fixing pioneer tree native to Sulawesi, which can tolerate poor soils and is often found in disturbed areas and tropical forest margins. It can provide shade and improve soil fertility to stimulate the germination of seedlings of secondary tropical hardwood trees (Haberle et al., 2006). *Trema* was accompanied by N-fixing pioneer herbs of the legume family Fabaceae (i.e., *Vigna*), which continued to be consistent throughout lacustrine U1c until ~76 mcd (i.e., ~0.8 Ma).

The timing of this shift in paleovegetation assemblages coincided with the U1c/U1b boundary (Russell et al., 2020). This drastic change in the paleodepositional development of Lake Towuti seems to have had a more considerable impact on the local catchment vegetation that entered the lake in the form of chloroplast-rich litter than the transition into the permanent lake (i.e., U2/U1c boundary), which did not result in significant changes in *trn*L-P6 inferred paleovegetation assemblages. We infer that considerable tectonic movements and catchment morphological adjustments continued well past the U2/U1c boundary until ~0.8 Ma.

(ii) Paleovegetation associated with increased drainage of (ultra)mafic substrates.

Serpentine or ultramafic substrates are harsh environments for vegetation due to their low nutrient content (N, P, and K), the imbalance of Ca and Mg, and the presence of a high concentration of potentially phytotoxic trace elements, notably Ni and Cr (Garnier et al., 2021; Kazakou et al., 2008). Nevertheless, ultramafic ecosystems are often biodiversity hotspots and host numerous endemic species (Myers et al., 2000). These include vegetation types that have developed strategies such as drastically lowering the impact of phytotoxic trace elements through hyperaccumulation of heavy metals (Prasad & Freitas, 2003) and the release of exudates in the rhizosphere to solubilise iron minerals to release Fe^{2+} needed for several processes including photosynthesis (Morrissey & Guerinot, 2009 and references therein). Brassicaceae, followed by Poaceae, the unclassified Faboideae (Fabaceae), and Theaceae had the strongest positive Pearson correlations with %Fe, %Ni, and %Cr derived from drainage of ultramafic rocks from the lake catchment. These plant families are known to include many highly efficient taxa in extracting bioavailable Fe^{2+} from soils containing only biologically inert iron minerals (Morrissey & Guerinot, 2009 and references therein). Moreover, Brassicaceae has the highest number of species capable of hyperaccumulating Ni and Cr (Prasad & Freitas, 2003). The strong Pearson correlations between downcore changes in the relative read abundances of these taxa and %Ni, %Cr, and %Fe suggest that their chloroplast-rich plant litter drained into Lake Towuti mixed with eroded ultramafic sediment.

Ultramafic sediments rich in Ni, Cr, and Fe are deposited in Lake Towuti under drier conditions and lower lake levels (Russell et al., 2020). Drier conditions were pronounced during the LGM when the lake water level was 10-35 m lower than today (Vogel et al., 2015). The strong drying signal is derived primarily from the stable isotope measurements of terrestrial leaf waxes ($\delta^{13}C_{wax}$) (Russell et al., 2014). Vegetation utilising the C_3 photosynthetic pathway (the bulk of herbaceous and woody plant life) has $\delta^{13}C$ values between –29‰ to –38‰, whereas plants utilising the C_4 pathway (primarily tropical and warm season grasses) have $\delta^{13}C$ values of –14‰ to –26‰ (Bi et al. 2005, Chikaraishi & Naraoka 2003). Therefore, the observed enrichment of 15‰

over the LGM from approximately –40‰ to –25‰ was interpreted as an expansion of C_4 grasses in a savanna-like landscape with reduced tree cover (Russell et al., 2014).

In contrast, the pollen record from core TOW-09 revealed that tropical lowland tree forest vegetation was still abundantly present during the LGM, while Cyperaceae (sedges) outcompeted grasses as the most abundant C_4 vegetation (Stevenson, 2018). Therefore, instead of a widespread savanna-type open landscape, the pronounced lake-level low stands during the LGM most likely resulted in the expansion of the lakes' foreshore surface area covered by sedges as the predominant C_4 plants (Stevenson, 2018). Moreover, a local record of the deglacial period showed limited evidence for the presence of broad-scale grasslands in the lowlands (Hamilton et al., 2019a). Similarly, in this study, we do not find support for an expansion of C_4 grasses in the region during the LGM. Instead, the LGM red clays revealed the presence of sedimentary *trn*L-P6 assigned to wet climate C_3 grasses. The inundation regime is a main driver shaping the vegetation community structure in wetlands (Baldwin et al., 1996). Most likely, the C_3 vegetation identified using *trn*L-P6 metabarcoding was adapted to or could have tolerated long-term exposure to flooding and inundation near the deeper coring location. Cyperaceae produce large amounts of wind-fertilized pollen that can travel long distances (Stevenson, 2018). The inability to detect the chloroplast marker gene assigned to Cyperaceae in our dataset implies that this vegetation was zoned further away from the coring location at more elevated, drier areas of the lakes' foreshore.

(iii) Paleovegetation associated with increased drainage of lateritic soils and felsic substrates from the Loeha River

The paleovegetation forming cluster D (Fig. 2.6) showed the strongest positive Pearson correlations with the Al/Mg ratio, indicating increased drainage of lateritic soils and felsic substrates from the Loeha River to the east of Lake Towuti. Previous studies (Morlock et al., 2019; Russell et al., 2020) inferred that these sediments were deposited during increased precipitation and lake-level high stands. The vegetation that forms cluster D indicates a warm, humid paleoenvironment with tropical evergreen trees (*Toona*) that created a closed canopy offering shady and moist conditions for tree orchids (*Luisia*) and ground cover herbs (Zingiberaceae), known to spread via rhizomes. The association between cluster D and the Al/Mg ratio indicates that this vegetation was widespread in the catchment area of the Loeha River.

However, cluster D also included the PACMAD grasses identified as genera of the subfamilies Chloridoideae and Panicoideae that exclusively use the C_4 carbon fixation pathway (e.g., *Zoysia*, *Muhlenbergia*). In addition, cluster D included *trn*L-P6 assigned to *Castanopsis* and/or *Lithocarpus* that was most consistently present in U1a and U1b intervals, including the red clays from the LGM. As mentioned earlier, the presence of these drought-tolerant tropical evergreen trees that now dominate at lower/mid-montane elevations in Sulawesi (Biagioni et al., 2015; Culmsee et al., 2010) during the LGM was independently confirmed from adjacent fossil pollen records (Hamilton et al., 2019a; Stevenson, 2018). A mixture of *trn*L-P6 sourced from C_3 and C_4 vegetation in cluster D implies that periods of increased seasonal rainfall prevailed and contributed to a predominance of felsic drainage.

2.5.4 Nutrient-demanding aquatic herbs and partially submerged shoreline vegetation during stratification, mesotrophic conditions, and the deposition of diatom oozes

Rutaceae (subfamily Aurantioideae) and Apiaceae (subfamily Apoideae) were notable representatives of Cluster B paleovegetation. ASVs assigned to Aurantioideae showed the highest sequence similarities with *Murraya* and *Luvunga*, small SE Asian swamp woodland trees native to Sulawesi (Kessler et al., 2002), while ASVs assigned to Apoideae showed up to 100% sequence similarity to *trn*L-P6 of native Java water dropwort (*Oenanthe javanica*). This perennial aquatic herb is widespread in Southeast Asia (http://www.powo.science.kew.org), where it is found in grassy forest margins, marshes, wet meadows, lake shores, and muddy rivers or stream banks and can become somewhat invasive when rooting in nutrient-rich soils or sediments. The upper part of cluster B also included *Oryza*, a genus of wetland C_3 grasses native to Sulawesi. The positive Pearson correlations between relative changes in their *trn*L-P6 content with %TOC and the TLE/TOC ratio suggests that his vegetation was rooted in muddy organic-rich shoreline sediments. Stratified and anoxic conditions likely contributed to preserving the labile sedimentary OM, and bioavailable Fe(II) would have been abundant. An increase in nutrient availability combined with the slow release of tephra-bound phosphorus (Russell et al., 2020) could have contributed to the expansion of Java water dropwort, which coincided with the formation of diatom blooms, as evident from the correlation between changes in the relative read

abundance of sedimentary *trn*L-P6 of this aquatic herb with silica content. The fact that sedimentary *trn*L-P6 from this shoreline vegetation and not that of Cyperaceae could be identified from the sedimentary record implies that the chloroplast-rich litter from the vegetation of cluster D was more efficiently transported to the coring location because lake levels were higher than during the dry LGM.

2.6 Conclusions

We successfully amplified and sequenced sedimentary *trn*L-P6 from up to 114 m deep and over 1 Ma-old tropical Lake Towuti sediments. After stringent removal of contaminants and unassigned/poorly classified ASVs, the remaining ASVs could be assigned to at least 45 native taxa at family or lower taxonomic ranks. Downcore changes in the relative read abundance of these paleovegetation assemblages reflected changes in the paleodepositional environment as inferred from Pearson correlations with previously analysed organic and inorganic parameters during the lakes' more than 1 Myr history. Nitrogen-fixing pioneer vegetation and shallow wetland herbs were most strongly associated with > 1 Ma-old peats and silts deposited in a tectonically active landscape of active river channels, shallow lakes, and peat swamps. A statistically significant shift in the paleovegetation was observed ~200 ka after the transition into a permanent lake (i.e., ~800 kyr ago), which coincided with a decrease in tectonic activity and catchment adjustments. Most notably, the newly emerged shoreline vegetation comprised putative peatland forest trees and partially submerged C_3 grasses (Oryzaceae). Positive Pearson correlations between relative changes in their *trn*L-P6 content with %TOC and the TLE/TOC ratio suggest that this vegetation grew and rooted in muddy organic-rich shoreline sediments. Stratified and anoxic conditions likely contributed to preserving the labile sedimentary OM, and bioavailable Fe(II) would have been readily available. An increase in nutrient availability from frequent turnover of the water column combined with the slow release of tephra-bound phosphorus could have contributed to the expansion of Java water dropwort, which coincided with the formation of diatom blooms, as evident from the correlation between changes in the relative read abundance of sedimentary *trn*L-P6 of this aquatic herb with silica content. In contrast, herbs (Brassicaceae, Fabaceae), trees/shrubs (Theaceae), and C_3 grasses (Pooideae) showed the highest positive Pearson correlations with sediments of an ultramafic signature (e.g., rich in

Fe, Ni and Cr). These plant families include the highest number of taxa with highly efficient strategies to extract bioavailable Fe(II) from iron-rich rocks and are capable of hyperaccumulation of phytotoxic metals, including Ni and Cr. Therefore, this vegetation was likely adapted to grow on the ultramafic rocks within the lake's catchment, and their chloroplast-rich biomass drained into Lake Towuti mixed with eroded ultramafic substrates during drier periods. Rainforest trees (e.g., *Toona*), shady ground cover herbs (Zingiberaceae), and tree orchids (*Luisia*) showed the highest Pearson correlations with inorganic parameters indicating increased drainage of felsic substrates from the Loeha River to the east of Lake Towuti during periods of increased precipitation. However, the co-presence of sedimentary *trn*L-P6 from dry climate-adapted vegetation (i.e., C$_4$ grasses and *Castanopsis/Lithocarpus*) implies that more seasonal climates also resulted in a predominance of felsic drainage, not just wetter conditions.

While the strong mineral adsorption to the ferruginous clays most likely uniquely contributed to the long-term preservation of *sed*aDNA in Lake Towuti, enhanced preservation of *sed*aDNA in anaerobic and organic-rich subsurface sediments is likely to be relatively widespread in mesotrophic and eutrophic tropical lake environments. Therefore, to what extent tropical lake *sed*aDNA records could complement existing proxies in reconstructing local terrestrial and aquatic ecosystem changes and their responses to paleoenvironmental perturbations warrants further investigation. The limited availability of reference sequences of metabarcoding genes from tropical forest vegetation in public databases, notably from this tropical biodiversity hotspot, could explain why roughly half of the ASVs did not have close similarities with any of the vast amount of DNA sequences available in the NCBI nr database. In addition, a subset of unassigned ASVs could also represent PCR artefacts. Future studies could use hybridisation capture targeting multiple metabarcoding genes (e.g., Foster et al., 2022) to eliminate PCR bias and to improve the overall taxonomic resolution of tropical paleovegetation.

2.7 References

Aliscioni, S., Bell, H. L., Besnard, G., Christin, P. A., Columbus, J. T., Duvall, M. R., Edwards, E. J., Giussani, L., Hasenstab-Lehman, K., Hilu, K. W., Hodkinson, T. R., Ingram, A. L., Kellogg, E. A., Mashayekhi, S., Morrone, O., Osborne, C. P., Salamin, N., Schaefer, H., Spriggs, E., Smith, S. A., Zuloaga, F., & Grass Phylogeny Working, G., II. (2012). New grass phylogeny resolves deep evolutionary relationships and discovers C4 origins. *New Phytologist, 193*(2), 304-312.

Alsos, I. G., Lammers, Y., Kjellman, S. E., Merkel, M. K. F., Bender, E. M., Rouillard, A., Erlendsson, E., Gudmundsdottir, E. R., Benediktsson, I. O., Farnsworth, W. R., Brynjolfsson, S., Gisladottir, G., Eddudottir, S. D., & Schomacker, A. (2021). Ancient sedimentary DNA shows rapid post-glacial colonization of Iceland followed by relatively stable vegetation until the Norse settlement (Landnam) AD 870. *Quaternary Science Reviews, 259*.

Alsos, I. G., Lammers, Y., Yoccoz, N. G., Jorgensen, T., Sjogren, P., Gielly, L., & Edwards, M. E. (2018). Plant DNA metabarcoding of lake sediments: How does it represent the contemporary vegetation. *Plos One, 13*(4).

Anshari, G., Kershaw, P., van der Kaars, S., & Jacobsen, G. (2004). Environmental change and peatland forest dynamics in the Lake Sentarum area, West Kalimantan, Indonesia. *Journal of Quaternary Science, 19,* 637-655.

Armbrecht, L., Weber, M. E., Raymo, M. E., Peck, V. L., Williams, T., Warnock, J., Kato, Y., Hernández-Almeida, I., Hoem, F., Reilly, B., Hemming, S., Bailey, I., Martos, Y. M., Gutjahr, M., Percuoco, V., Allen, C., Brachfeld, S., Cardillo, F. G., Du, Z., Fauth, G., Fogwill, C., Garcia, M., Glüder, A., Guitard, M., Hwang, J.-H., Iizuka, M., Kenlee, B., O'Connell, S., Pérez, L. F., Ronge, T. A., Seki, O., Tauxe, L., Tripathi, S., & Zheng, X. (2022). Ancient marine sediment DNA reveals diatom transition in Antarctica. *Nature Communications, 13*(1), 5787.

Baldwin, A. H., McKee, K. L., & Mendelsohn, I. A. (1996). The influence of vegetation, salinity, and inundation on seed banks of oligohaline coastal marshes. *American Journal of Botany*, *83*, 470-479.

Bi, X., Sheng, G., Liu, X., Li, C., & Fu, J. (2005). Molecular and carbon and hydrogen isotopic composition of n-alkanes in plant leaf waxes. *Organic Geochemistry, 36*(10), 1405–1417.

Biagioni, S., Wundsch, M., Haberzettl, T., & Behling, H. (2015). Assessing resilience/ sensitivity of tropical mountain rainforests towards climate variability of the last 1500 years: The long-term perspective at Lake Kalimpaa (Sulawesi, Indonesia). *Review of Palaeobotany and Palynology, 213,* 42-53.

Boessenkool, S., McGlynn, G., Epp, L. S., Taylor, D., Pimentel, M., Gizaw, A., Nemomissa, S., Brochmann, C., & Popp, M. (2014). Use of Ancient Sedimentary DNA as a Novel Conservation Tool for High-Altitude Tropical Biodiversity. *Conservation Biology, 28*(2), 446-455.

Boyer, F., Mercier, C., Bonin, A., Le Bras, Y., Taberlet, P., & Coissac, E. (2016). OBITOOLS: a UNIX-inspired software package for DNA metabarcoding. *Molecular Ecology Resources, 16*(1), 176-182.

Bremond, L., Favier, C., Ficetola, G. F., Tossou, M. G., Akouegninou, A., Gielly, L., Giguet-Covex, C., Oslisly, R., & Salzmann, U. (2017). Five thousand years of tropical lake sediment DNA records from Benin. *Quaternary Science Reviews, 170,* 203-211.

Cannon, C.H., Morley, R.J., & Bush, A.B. (2009). The current refugial rainforests of Sundaland are unrepresentative of their biogeographic past and highly vulnerable to disturbance. *Proceedings of the National Academy of Sciences*, *106*(27), 11188–11193.

Capo, E., Giguet-Covex, C., Rouillard, A., Nota, K., Heintzman, P. D., Vuillemin, A., Ariztegui, D., Arnaud, F., Belle, S., Bertilsson, S., Bigler, C., Bindler, R., Brown, A. G., Clarke, C. L., Crump, S. E., Debroas, D., Englund, G., Ficetola, G. F., Garner, R. E., Gauthier, J., Gregory-Eaves, I., Heinecke, L., Herzschuh, U., Ibrahim, A., Kisand, V., Kjaer, K. H., Lammers, Y., Littlefair, J., Messager, E., Monchamp, M. E., Olajos, F., Orsi, W., Pedersen, M. W., Rijal, D. P., Rydberg, J., Spanbauer, T., Stoof-Leichsenring, K. R., Taberlet, P., Talas, L., Thomas, C., Walsh, D. A., Wang, Y. C., Willerslev, E., van Woerkom, A., Zimmermann, H. H., Coolen, M. J. L., Epp, L. S., Domaizon, I., Alsos, I. G., & Parducci, L. (2021).

Lake Sedimentary DNA Research on Past Terrestrial and Aquatic Biodiversity. *Overview and Recommendations: Quaternary, 4*(1).

Caporaso, J. G., Lauber, C. L., Walters, W. A., Berg-Lyons, D., Huntley, J., Fierer, N., Owens, S. M., Betley, J., Fraser, L., Bauer, M., Gormley, N., Gilbert, J. A., Smith, G., & Knight, R. (2012). Ultra-high-throughput microbial community analysis on the Illumina HiSeq and MiSeq platforms. *Isme Journal, 6*(8), 1621-1624.

Caraco, N. F., Cole, J. J., & Likens, G. E. (1989). Evidence for sulfate-controlled phosphorus release from sediments of aquatic systems. *Nature, 341*(6240), 316-318.

Chang, Y. M., Chang, C. L., Li, W. H., & Shih, A. C. C. (2013). Historical profiling of maize duplicate genes shed light on the evolution of C4 photosynthesis in grasses. *Molecular Phylogenetics and Evolution, 66*(2), 453-462.

Chikaraishi, Y. & Naraoka, H, (2003). Compound-specific δD–$\delta 13C$ analyses of n-alkanes extracted from terrestrial and aquatic plants. *Phytochemistry*, *63*(3), 361–371.

Clarke, K. R., & Gorley, R. N. (2015). *PRIMER v7: User Manual/Tutorial.* PRIMER-E Ltd. https://www.primer-e.com/our-software/primer-version-7/

Cockell, C. S., Schaefer, B., Wuchter, C., Coolen, M. J. L., Grice, K., Schnieders, L., Morgan, J. V., Gulick, S. P. S., Wittmann, A., Lofi, J., Christeson, G. L., Kring, D. A., Whalen, M. T., Bralower, T. J., Osinski, G. R., Claeys, P., Kaskes, P., de Graaff, S. J., Déhais, T. (2021). Shaping of the Present-Day Deep Biosphere at Chicxulub by the Impact Catastrophe That Ended the Cretaceous. *Frontiers in Microbiology*, *12*.

Coolen, M. J. L., & Overmann, J. (2007). 217 000-year-old DNA sequences of green sulfur bacteria in Mediterranean sapropels and their implications for the paleoenvironment reconstruction. *Environmental Microbiology, 9*(1), 238-249.

Coolen, M. J. L., Muyzer, G., Rijpstra, W. I. C., Schouten, S., Volkman, J. K., & Damste, J. S. S. (2004). Combined DNA and lipid analyses of sediments reveal changes in Holocene haptophyte and diatom populations in an Antarctic lake. *Earth and Planetary Science Letters, 223*(1-2), 225-239.

Coolen, M. J. L., Orsi, W. D., Balkema, C., Quince, C., Harris, K., Sylva, S. P., Filipova-Marinova, M., & Giosan, L. (2013). Evolution of the plankton paleome in the Black Sea from the Deglacial to Anthropocene. *Proceedings of the National Academy of Sciences of the United States of America, 110*(21), 8609-8614.

Costa, K. M., Russell, J. M., Vogel, H., & Bijaksana, S. (2015). Hydrological connectivity and mixing of Lake Towuti, Indonesia in response to paleoclimatic changes over the last 60,000 years. *Palaeogeography Palaeoclimatology Palaeoecology, 417,* 467-475.

Courtin, J., Andreev, A. A., Raschke, E., Bala, S., Biskaborn, B. K., Liu, S. S., Zimmermann, H., Diekmann, B., Stoof-Leichsenring, K. R., Pestryakova, L. A., & Herzschuh, U. (2021). Vegetation Changes in Southeastern Siberia During the Late Pleistocene and the Holocene. *Frontiers in Ecology and Evolution, 09.*

Crowe, S. A., O'Neill, A. H., Katsev, S., Hehanussa, P., Haffner, G. D., Sundby, B., Mucci, A., & Fowle, D. A. (2008). The biogeochemistry of tropical lakes: A case study from Lake Matano, Indonesia. *Limnology and Oceanography, 53*(1), 319-331.

Culmsee, H., Leuschner, C., Moser, G., & Pitopang, R. (2010). Forest aboveground biomass along an elevational transect in Sulawesi, Indonesia, and the role of Fagaceae in tropical montane rain forests. *Journal of Biogeography, 37*(5), 960-974.

De Caceres, M., & Legendre, P. (2009). Associations between species and groups of sites: indices and statistical inference. *Ecology, 90*(12), 3566-3574.

Demaneche, S., Jocteur-Monrozier, L., Quiquampoix, H., & Simonet, P. (2001). Evaluation of biological and physical protection against nuclease degradation of clay-bound plasmid DNA. *Applied and Environmental Microbiology, 67*(1), 293-299.

Direito, S. O. L., Marees, A., & Roling, W. F. M. (2012). Sensitive life-detection strategies for low-biomass environments: optimizing the extraction of nucleic acids adsorbing to terrestrial and Mars analogue minerals. *FEMS Microbiology Ecology, 81*(1), 111-123.

Dommain, R., Andama, M., McDonough, M. M., Prado, N. A., Goldhammer, T., Potts, R., Maldonado, J. E., Nkurunungi, J. B., & Campana, M. G. (2020). The challenges of reconstructing tropical biodiversity with sedimentary ancient DNA: A 2200-year-long metagenomic record from Bwindi Impenetrable Forest, Uganda. *Frontiers in Ecology and Evolution, 8.*

Epp, L. S., Gussarova, C., Boessenkool, S., Olsen, J., Haile, J., Schroder-Nielsen, A., Ludikova, A., Hassel, K., Stenoien, H. K., Funder, S., Willerslev, E., Kjaer, K., & Brochmann, C. (2015). Lake sediment multi-taxon DNA from North Greenland records early post-glacial appearance of vascular plants and accurately tracks environmental changes. *Quaternary Science Reviews, 117,* 152-163.

Foster, N. R., van Dijk, K. J., Biffin, E., Young, J. M., Thomson, V. A., Gillanders, B. M., Jones, A. R., & Waycott, M. (2022). A targeted capture approach to generating reference sequence databases for chloroplast gene regions. *Ecology and Evolution, 12*(4), 8816.

Freeman, C. L., Dieudonné, L., Agbaje, O. B. A., Žure, M., Sanz, J. Q., Collins, M., & Sand, K. K. (2023). Survival of environmental DNA in sediments: Mineralogic control on DNA taphonomy. *Environmental DNA*, *00*, 1–15.

Friese, A., Kallmeyer, J., Kitte, J., Montaño Martinez, I., Bijaksana, S., & Wagner, D. (2017). A simple and inexpensive technique for assessing contamination during drilling operations. *Limnology and Oceanography: Methods, 15.*

Garnier, J., Quantin, C., Raous, S., Guimaraes, E., & Becquer, T. (2021). Field availability and mobility of metals in Ferralsols developed on ultramafic rock of Niquelandia, Brazil. *Brazilian Journal of Geology, 51*(1).

Gregory, P. H. (1978). Distribution of airborne pollen and spores and their long-distance transport. *Pure and Applied Geophysics PAGEOPH, 116*(2-3), 309-315.

Haberle, S. G., Tibby, J., Dimitriadis, S., & Heijnis, H. (2006). The impact of European occupation on terrestrial and aquatic ecosystem dynamics in an Australian tropical rain forest. *Journal of Ecology, 94*(5), 987-1002.

Hamilton, R., Hall, T., Stevenson, J., & Penny, D. (2019b). Distinguishing the pollen of Dipterocarpaceae from the seasonally dry and moist tropics of south-east Asia using light microscopy. *Review of Palaeobotany and Palynology, 263,*117-133.

Hamilton, R., Stevenson, J., Li, B., & Bijaksana, S. (2019a). A 16,000-year record of climate, vegetation and fire from Wallacean lowland tropical forests. *Quaternary Science Reviews, 224,* 105929.

Hasberg, A. K. M., Bijaksana, S., Held, P., Just, J., Melles, M., Morlock, M. A., Opitz, S., Russell, J. M., Vogel, H., & Wennrich, V. (2019). Modern sedimentation processes in Lake Towuti, Indonesia, revealed by the composition of surface sediments. *Sedimentology, 66*(2), 675-698.

Hope, G. (2001). Environmental change in the Late Pleistocene and later Holocene at Wanda site, Soroako, South Sulawesi, Indonesia. *Palaeogeography Palaeoclimatology Palaeoecology, 171*(3-4), 129-145.

Hopkins, H.C.F. (1994). The Indo-Pacific Species of Parkia (Leguminosae: Mimosoideae). *Kew Bulletin, 49*(2), 181-234.

Inagaki, F., Hinrichs, K.-U., Kubo, Y., Bowles, M., Heuer, V., Hong, W.-L., Hoshino, T., Ijiri, A., Imachi, H., Ito, M., Kaneko, M., Lever, M., Lin, Y.-S., Methé, B., Morita, S., Morono, Y., Tanikawa, W., Bihan, M., Bowden, S., & Yamada, Y. (2015). Exploring deep microbial life in coal-bearing sediment down to ~2.5 km below the ocean floor. *Science, 349,* 420-424.

IUCN. (2019). International Union for Conservation of Nature annual report 2019.

Kazakou, E., Dimitrakopoulos, P. G., Baker, A. J. M., Reeves, R. D., & Troumbis, A. Y. (2008). Hypotheses, mechanisms, and trade-offs of tolerance and adaptation

to serpentine soils from species to ecosystem level. *Biological Reviews, 83*(4), 495-508.

Kessler, P. J. A., Bos, M., Sierra+Daza, S. E. C., Kop, A., Willemse, L., Pitopang, R., & Gradstein, S. (2002). Checklist of woody plants of Sulawesi, Indonesia. *Blumea journal of plant taxonomy and plant geography, 14*, 1-160.

Kirkpatrick, J. B., Walsh, E. A., & D'Hondt, S. (2016). Fossil DNA persistence and decay in marine sediment over hundred-thousand-year to million-year time scales. *Geology, 44*(8), 615-618.

Koop-Jakobsen, K., Meier, R.J., Mueller, P. (2021). Plant-mediated rhizosphere oxygenation in the native invasive salt marsh grass Elymus athericus. *Frontiers in Plant Sciences, 10*(12), 66975.

Lasut, M. T. (2009). The floristic study of herbaceous grasses in Sulawesi. http://repository.ipb.ac.id/handle/123456789/22507

Lee, C., Lee, S., & Park, T. (2017). Statistical methods for metagenomics data analysis. *International Journal of Data Mining and Bioinformatics, 19*(4), 366-385.

Li, K., Stoof-Leichsenring, K. R., Liu, S. S., Jia, W. H., Liao, M. N., Liu, X. Q., Ni, J., & Herzschuh, U. (2021). Plant sedimentary DNA as a proxy for vegetation reconstruction in eastern and northern Asia. *Ecological Indicators, 132*.

Liu, S. S., Stoof-Leichsenring, K. R., Kruse, S., Pestryakova, L. A., & Herzschuh, U. (2020). Holocene vegetation and plant diversity changes in the Northeastern Siberian treeline region from pollen and sedimentary ancient DNA. *Frontiers in Ecology and Evolution, 8*.

Mander, L., & Punyasena, S. W. (2014). On the taxonomic resolution of pollen and spore records of earth's vegetation. *International Journal of Plant Sciences, 175*(8), 931-945.

Markesteijn, L., Poorter, L., & Bongers, F. (2007). Light-dependent leaf trait variation in 43 tropical dry forest tree species. *American Journal of Botany, 94*(4), 515-525.

More, K. D., Orsi, W. D., Galy, V., Giosan, L., He, L. J., Grice, K., & Coolen, M. J. L. (2018). A 43 kyr record of protist communities and their response to oxygen minimum zone variability in the Northeastern Arabian Sea. *Earth and Planetary Science Letters, 496*, 248-256.

Morlock, M. A., Vogel, H., Nigg, V., Ordonez, L., Hasberg, A. K. M., Melles, M., Russell, J. M., Bijaksana, S., & Team, T. D. P. S. (2019). Climatic and tectonic controls on source-to-sink processes in the tropical, ultramafic catchment of Lake Towuti, Indonesia. *Journal of Paleolimnology, 61*(3), 279-295.

Morlock, M.A., Vogel, H., Russell, J.M., Anselmetti, F.S., & Bijaksana, S. (2021). Quaternary environmental changes in tropical Lake Towuti, Indonesia, inferred from end-member modelling of X-ray fluorescence core-scanning data. *Journal of Quaternary Science, 36*, 1040–1051.

Morrissey, J., & Guerinot, M. L. (2009). Iron uptake and transport in plants: The good, the bad, and the ionome. *Chemical Reviews, 109*(10), 4553-4567.

Myers, N., Mittermeier, R. A., Mittermeier, C. G., da Fonseca, G. A. B., & Kent, J. (2000). Biodiversity hotspots for conservation priorities. *Nature, 403*(6772), 853-858.

Niemeyer, B., Epp, L. S., Stoof-Leichsenring, K. R., Pestryakova, L. A., & Herzschuh, U. (2017). A comparison of sedimentary DNA and pollen from lake sediments in recording vegetation composition at the Siberian treeline. *Molecular Ecology Resources, 17*(6), 46-62.

Nijburg, J.W., Coolen, M.J.L., Gerards, S., Gunnewiek, P.J.A.K., & Laanbroek, H.J. (1997). Effects of nitrate availability and the presence of Glyceria maxima on the composition and activity of the dissimilatory nitrate-reducing bacterial community. *Applied and Environmental Microbiology*, *63*(3), 931-937.

Ollerton, J., Winfree, R., & Tarrant, S. (2011). How many flowering plants are pollinated by animals? *Oikos, 120*(3), 321-326.

Orsi, W. D., Coolen, M. J. L., Wuchter, C., He, L. J., More, K. D., Irigoien, X., Chust, G., Johnson, C., Hemingway, J. D., Lee, M., Galy, V., & Giosan, L. (2017).

Climate oscillations reflected within the microbiome of Arabian Sea sediments. *Scientific Reports, 7.*

Parducci, L., Bennett, K. D., Ficetola, G. F., Alsos, I. G., Suyama, Y., Wood, J. R., & Pedersen, M. W. (2017). Ancient plant DNA in lake sediments. *New Phytologist, 214*(3), 924-942.

Parducci, L., Matetovici, I., Fontana, S. L., Bennett, K. D., Suyama, Y., Haile, J., Kjaer, K. H., Larsen, N. K., Drouzas, A. D., & Willerslev, E. (2013). Molecular- and pollen-based vegetation analysis in lake sediments from central Scandinavia. *Molecular Ecology, 22*(13), 3511-3524.

Parducci, L., Valiranta, M., Salonen, J. S., Ronkainen, T., Matetovici, I., Fontana, S. L., Eskola, T., Sarala, P., & Suyama, Y. (2015). Proxy comparison in ancient peat sediments: pollen, macrofossil, and plant DNA. *Philosophical transactions of the Royal Society of London Series B, Biological sciences, 370*(1660), 20130382.

Pastré, D., Hamon, L., Landousy, F., Sorel, I., David, M.-O., Zozime, A., Le Cam, E., & Piétrement, O. (2006). Anionic polyelectrolyte adsorption on mica mediated by multivalent cations: A solution to DNA imaging by atomic force microscopy under high ionic strengths. *Langmuir, 22*(15)*, 6651–6660.*

Paus, A., Boessenkool, S., Brochmann, C., Epp, L. S., Fabel, D., Haflidason, H., & Linge, H. (2015). Lake Store Finnsjoen - a key for understanding Lateglacial/early Holocene vegetation and ice sheet dynamics in the central Scandes Mountains. *Quaternary Science Reviews, 121,* 36-51.

Pedersen, M. W., Ginolhac, A., Orlando, L., Olsen, J., Andersen, K., Holm, J., Funder, S., Willerslev, E., & Kjaeer, K. H. (2013). A comparative study of ancient environmental DNA to pollen and macrofossils from lake sediments reveals taxonomic overlap and additional plant taxa. *Quaternary Science Reviews, 75,* 161-168.

Pietramellara, G., Ascher, J., Borgogni, F., Ceccherini, M. T., Guerri, G., & Nannipieri, P. (2009). Extracellular DNA in soil and sediment: fate and ecological relevance. *Biology and Fertility of Soils, 45*(3), 219-235.

Prasad, M. N. V., & Freitas, H. M. D. (2003). Metal hyperaccumulation in plants - Biodiversity prospecting for phytoremediation technology. *Electronic Journal of Biotechnology, 6*(3), 285-321.

Randlett, M. E., Coolen, M. J. L., Stockhecke, M., Pickarski, N., Litt, T., Balkema, C., Kwiecien, O., Tomonaga, Y., Wehrli, B., & Schubert, C. J. (2014). Alkenone distribution in Lake Van sediment over the last 270 ka: influence of temperature and haptophyte species composition. *Quaternary Science Reviews, 104,* 53-62.

Riaz, T., Shehzad, W., Viari, A., Pompanon, F., Taberlet, P., & Coissac, E. (2011). ecoPrimers: inference of new DNA barcode markers from whole-genome sequence analysis. *Nucleic acids research, 39*(21), 145-145.

Rohart, F., Gautier, B., Singh, A., & Le Cao, K. A. (2017). mixOmics: An R package for 'omics feature selection and multiple data integration. *Plos Computational Biology, 13*(11).

Russell, J. M., Bijaksana, S., Vogel, H., Melles, M., Kallmeyer, J., Ariztegui, D., Crowe, S., Fajar, S., Hafidz, A., Haffner, D., Hasberg, A., Ivory, S., Kelly, C., King, J., Kirana, K., Morlock, M., Noren, A., O'Grady, R., Ordonez, L., Stevenson, J., von Rintelen, T., Vuillemin, A., Watkinson, I., Wattrus, N., Wicaksono, S., Wonik, T., Bauer, K., Deino, A., Friese, A., Henny, C., Imran, Marwoto, R., Ngkoimani, L., Nomosatryo, S., Safiuddin, L., Simister, R., & Tamuntuan, G. (2016). The Towuti Drilling Project: paleoenvironments, biological evolution, and geomicrobiology of a tropical Pacific lake. *Scientific Drilling, 21,* 29-40.

Russell, J. M., Vogel, H., Bijaksana, S., Melles, M., Deino, A., Hafidz, A., Haffner, D., Hasberg, A. K. M., Morlock, M., von Rintelen, T., Sheppard, R., Stelbrink, B., & Stevenson, J. (2020). The late quaternary tectonic, biogeochemical, and environmental evolution of ferruginous Lake Towuti, Indonesia. *Palaeogeography Palaeoclimatology Palaeoecology, 556.*

Russell, J. M., Vogel, H., Konecky, B. L., Bijaksana, S., Huang, Y. S., Melles, M., Wattrus, N., Costa, K., & King, J. W. (2014). Glacial forcing of central Indonesian hydroclimate since 60,000 y BP. *Proceedings of the National Academy of Sciences of the United States of America, 111*(14), 5100-5105.

Sheppard, R. Y., Milliken, R. E., Russell, J. M., Sklute, E. C., Dyar, M. D., Vogel, H., Melles, M., Bijaksana, S., Hasberg, A. K. M., & Morlock, M. A. (2021). Iron

Mineralogy and Sediment Colour in a 100 m Drill Core from Lake Towuti, Indonesia Reflect Catchment and Diagenetic Conditions. *Geochemistry Geophysics Geosystems, 22*(8).

Sisk-Hackworth, L., & Kelley, S. T. (2020). An application of compositional data analysis to multiomic time-series data. *Nar Genomics and Bioinformatics, 2*(4).

Stevenson, J. (2018). Vegetation and climate of the Last Glacial Maximum in Sulawesi: The Archaeology of Sulawesi. Current Research on the Pleistocene to the Historic Period. ANU Press.

Taberlet, P., Coissac, E., Pompanon, F., Gielly, L., Miquel, C., Valentini, A., Vermat, T., Corthier, G., Brochmann, C., & Willerslev, E. (2006). Power and limitations of the chloroplast trn L (UAA) intron for plant DNA barcoding. *Nucleic Acids Research, 35*(3), e14-e14.

Vogel, H., Russell, J., Cahyarini, S., Bijaksana, S., Wattrus, N., Rethemeyer, J., & Melles, M. (2015). Depositional modes and lake-level variability at Lake Towuti, Indonesia, during the past similar to 29 kyr BP. *Journal of Paleolimnology, 54*(4), 359-377.

Voldstad, L. H., Alsos, I. G., Farnsworth, W. R., Heintzman, P. D., Hakansson, L., Kjellman, S. E., Rouillard, A., Schomacker, A., & Eidesen, P. B. (2020). A complete Holocene lake sediment ancient DNA record reveals long-standing high Arctic plant diversity hotspot in northern Svalbard. *Quaternary Science Reviews, 234.*

Vuillemin, A., Horn, F., Alawi, M., Henny, C., Wagner, D., Crowe, S. A., & Kallmeyer, J. (2017). Preservation and Significance of Extracellular DNA in Ferruginous Sediments from Lake Towuti, Indonesia. *Frontiers in Microbiology, 8.*

Vuillemin, A., Wirth, R., Kemnitz, H., Schleicher, A. M., Friese, A., Bauer, K. W., Simister, R., Nomosatryo, S., Ordonez, L., Ariztegui, D., Henny, C., Crowe, S. A., Benning, L. G., Kallmeyer, J., Russell, J. M., Bijaksana, S., Vogel, H., & Towuti Drilling Project Sci, T. (2019). Formation of diagenetic siderite in modern ferruginous sediments. *Geology, 47*(6), 540-544.

Wang, Z., Wang, C., & Liu, H. (2022). Higher dissolved oxygen levels promote downward migration of phosphorus in the sediment profile: Implications for lake restoration. *Chemosphere*, *301*,134705.

Whitten, A.J., Mustafa, M., & Henderson, G.S. (1988). *The Ecology of Sulawesi.* Gadjah Mada University Press, Indonesia.

Wickham, H. (2016). *Ggplot2: Elegant graphics for data analysis* (2nd ed.). Springer-Verlag New York.

Zimmermann, H. H., Raschke, E., Epp, L. S., Stoof-Leichsenring, K. R., Schwamborn, G., Schirrmeister, L., Overduin, P. P., & Herzschuh, U. (2017). Sedimentary ancient DNA and pollen reveal the composition of plant organic matter in Late Quaternary permafrost sediments of the Buor Khaya Peninsula (north-eastern Siberia). *Biogeosciences, 14*(3), 575-596.

2.8 Supplementary materials
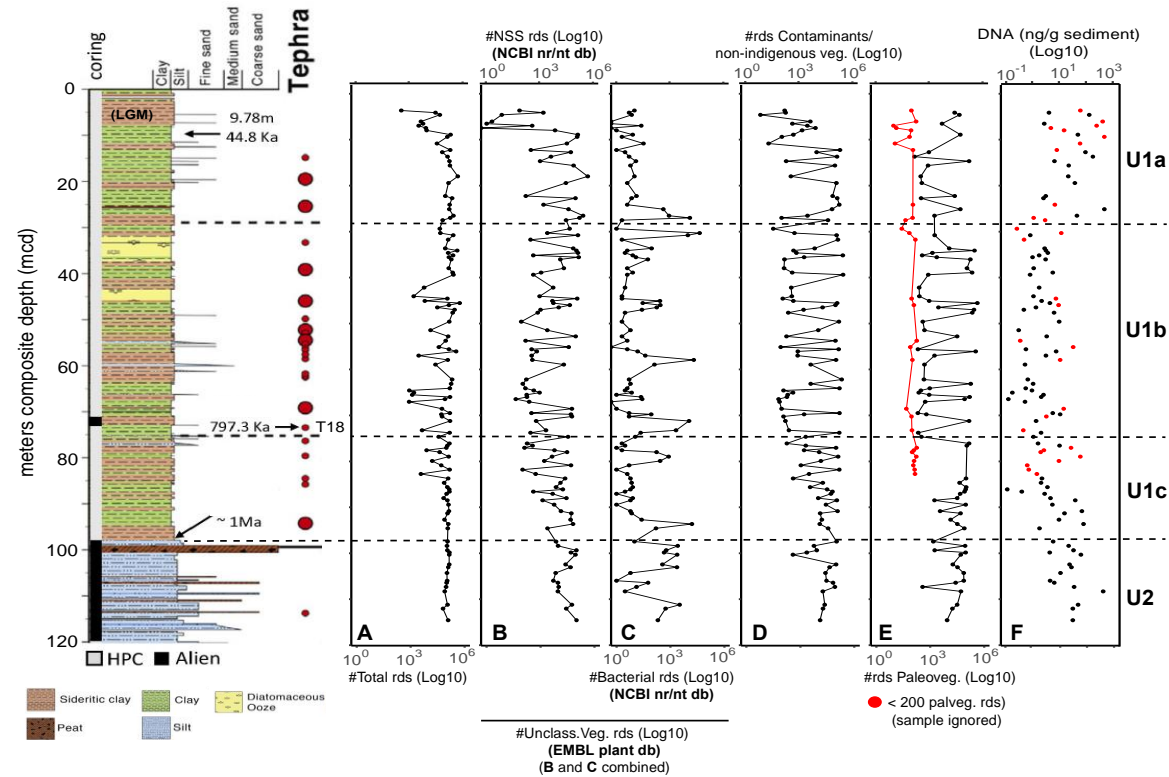
Figure S2.1 Total environmental DNA (eDNA) concentration and general overview of the recovered sequence data: (A) Total number of reads per analysed interval comprising: (B) reads with no significant similarities (NSS); or (C) that were identified as bacterial artifacts according to blast results against all sequences available in NCBI's nr/nt database. The sequences from panels B and C combined could not be assigned to vegetation at taxonomic ranks lower than subphylum level when compared with *trn*L-P6 sequences available in the EMBL plant database; (D) Contaminant reads of non-indigenous vegetation that could be assigned to family rank or lower, which were present in a subset of samples and in the background- and extraction blanks. See Fig. S2.2-S2.4 for an overview of the non-native taxa and typical lab contaminants identified from the PCR controls; (E) Remaining non-contaminant *trn*L-P6 reads from native paleovegetation that could be identified at family, clade, subfamily, tribe, and genus levels. Samples containing fewer than 200 *trn*L-P6 reads of paleovegetation excluded from the further analysis are indicated with red symbols. (F) shows the amount of extracted eDNA (ng/g sediment), including from the 31 intervals that were not considered for further analysis due to the low recovery of sequences from genuine paleovegetation (red symbols).

Classified contaminants

- 🟧 o_Asparagales;f_Amaryllidaceae;g_*Allium*
- 🟩 o_Asparagales;f_Asparagaceae;sf_Nolinoideae
- 🟪 o_Cupressales;f_Cupressaceae;g_*Callitris*
- ⬜ o_Fabales;f_Fabaceae;sf_Faboideae_tr_Dalbergieae;cl_Pterocarpus;g_*Arachis*
- 🟨 o_Fagales;f_Betulaceae
- 🟥 o_Pinales;f_Pinaceae;g_*Pinus + Picea*
- ⬛ o_Zingiberales;f_Musaceae;g_*Musa*
- 🟦 Sum of other rare contaminants

Total reads in sequenced controls:
BGB1: 2.3×10^1
EB1: 2.5×10^3
EB2: 7.9×10^2
EB3: 2.1×10^5
EB4: 2.3×10^3
EB5: 1.1×10^2

Figure S2.2 Stacked bar graph showing only the relative read abundance (sum = 100%) of non-native vegetation (see Fig. S2.2) identified at family, subfamily, or genus level from the PCR amplified and sequenced background- and extraction blanks. The total number of recovered reads from these taxonomically assigned contaminants in each blank is shown below the colour key. Notably, the relatively most abundant classified contaminants (Musaceae, Pinaceae, and Asparagaceae) and those present at very low abundances (e.g., *Allium*) were identified, irrespective of the several orders of magnitude differences in the total number of contaminant sequences present in these blanks. (See Fig. S2.3 for an overview of the relative read abundances of unidentified vegetation (EMBL plant database) or that had no significant similarity with any sequences present in NCBI's nr/nt database in the background- and extraction controls).
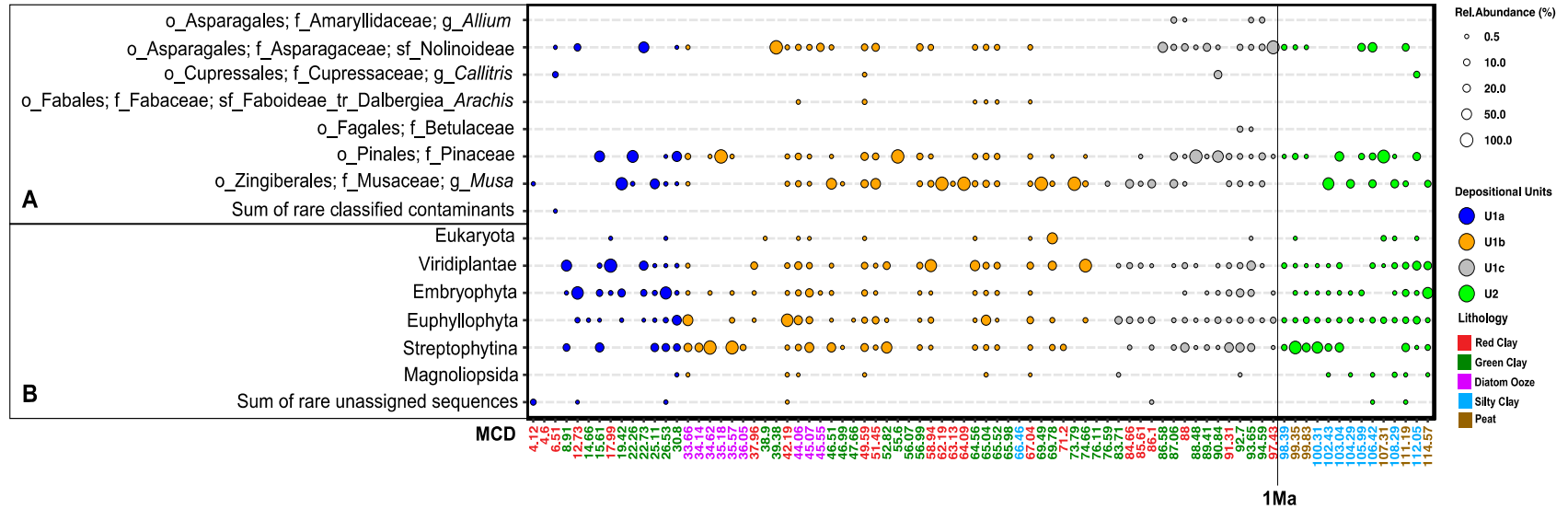
Figure S2.3 Bubble plot showing the relative read abundance of putative contaminants from (A) taxa not native to Sulawesi at the identified taxonomic ranks and (B) poorly classified vegetation or sequencing artifacts. All ASVs involved were removed from sample data, irrespective of their presence or absence from the background and extraction blanks (See Fig. S2.2 comparison and further details).

Proof of concept that fossil pollen is no source of sedimentary *trn*L-P6 in Lake Towuti

Mature pollen from species with maternal inheritance of cpDNA (most of the angiosperms) contain, at maturation, a regular amount of both genomes in the vegetative cell and a decreased amount in the generative cells (Parducci et al., 2017 and reference therein). A reduced amount of cpDNA in the generative cells makes it more likely that the non-native Musaceae, Asparagaceae, and Betulaceae found in both samples and blanks represented lab contaminants instead of contaminant DNA introduced from chloroplast-rich airborne pollen. In contrast, mature pollen from species with paternal cpDNA inheritance (most conifers) contain a regular amount of cpDNA in the vegetative cell and increased cpDNA in the generative cell (Parducci et al., 2017 and reference therein). As a result, conifers incl. Pinaceae and Cupressaceae produce mass amounts of airborne pollen rich in paternally inherited cpDNA, which increases the chance of cross-contamination during sampling and processing sediment samples for *sed*aDNA analysis. However, contamination with airborne pollen from these conifers can also be ruled out since only *Pinus merkusii* is native to Indonesia, with Sumatra as the closest possible origin. Moreover, Stevenson (2018) reported that native montane conifers (*Agathis*, *Dacrydium*, *Phyllocladus*, and *Podocarpus*) combined comprised up to ~30% of the total pollen count in the Glacial to Holocene sediments of TOW-09 near core 1F. Since none of the *trn*L-P6 reads in the samples and controls could be assigned to these genera or their respective families, chloroplast-rich biomass of (local) catchment vegetation instead of locally or remotely produced pollen was the predominant source of the taxa identified in this study.
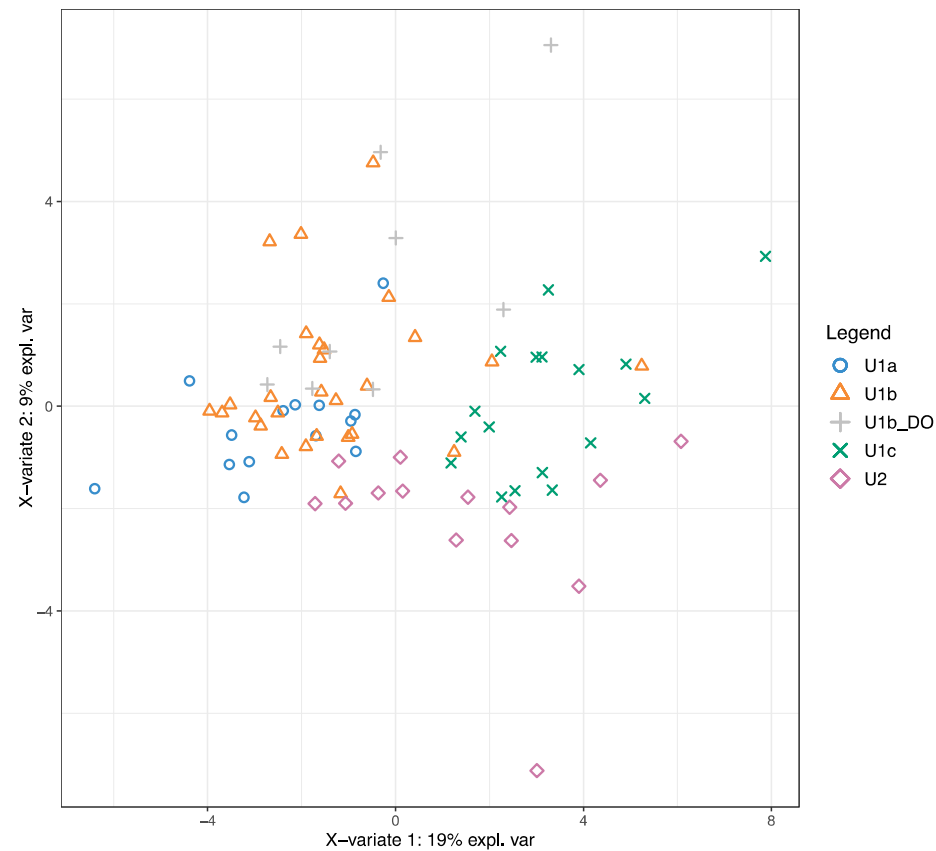
Figure S2.4 PLSDA plots showing separation of samples associated with the lacustrine and pre-lake depositional units after Russell et al. (2000) based on dissimilarities in authentic *trn*L-P6 inferred paleovegetation (n=45 taxa). Pre-lake Unit2 (>98 mcd; purple diamonds), lacustrine U1c (98-76 mcd; grey cross signs), U1b (76-31 mcd) separated into diatom oozes (U1b$_{DO}$; grey plus signs), and red + green clays combined (U1b$_{RC+GC}$; orange triangles), and U1a (31-4 mcd; blue circles): Only the 82 samples were included that contained more than 200 *trn*L-P6 reads from genuine paleovegetation after removing potential contaminants and poorly classified or artifact reads. See global and pairwise ANOSIM test results (Table 2.1 in the main manuscript) to verify significant differences in paleovegetation between sample categories. (See the caption of Fig. 2.2 and the main text for a detailed description of the sample categories).

Table S2.1 General overview of environmental DNA content and sequencing results. The average DNA concentration (nanograms per gram sediment), standard deviation, and the range in DNA concentration within intervals belonging to the various lacustrine (U1) and pre-lake (U2) lithologies are shown for the 113 intervals that contained *trn*L-P6 amplicons vs. the 82 out of 113 intervals that yielded at least 200 total paleovegetation reads after the stringent removal of poorly classified /artifacts and contaminant reads. Only shown for the 82 analysed intervals are the number of paleovegetation ASVs, and the number of taxa that could be classified at family, subfamily, clade, tribe, and genus ranks. The number of intervals belonging to each lithology is shown as well. RC (red clays) deposited during the last glacial maximum (LGM) vs. red clays that were deposited within the deeper lacustrine unit (older than LGM). GC (green lacustrine clays), DO (diatom oozes of U1b). See Fig. 2.2 of the main manuscript for the downcore profiles of these three datasets.

	Core Lithologies	113 intervals (with trnL-P6 amplicons)				82 intervals (with > 200 paleovegetation reads)									
			DNA (ng/g sed)				DNA (ng/g sed)			# paleoveg. ASVs			# Paleoveg. Taxa		
		# Intervals	Average	Sd	Range	# Intervals	Average	Sd	Range	Average	Sd	Range	Average	Sd	Range
U1	RC (LGM)	8	100.6	136.9	2.6-379	3	41.8	66.9	2.6-119.1	19.3	7.6	14-28	6.3	2.1	4-8
	RC (older than LGM)	31	9.6	18.7	0.1-87.4	18	8.6	20.4	0.1-87.4	126.2	90.3	42-418	22.5	3.5	4-33
	GC	49	31.8	88.6	0.1-438.2	37	26.7	75.1	0.1-438.2	129.8	71.1	38-355	23.4	3.9	17-33
	DO	9	2.4	1.1	1.0-4.1	9	2.4	1.1	1.0-4.1	124.0	52.3	56-198	23.4	3.8	18-29
	Clayey silt	2	1.3	1.7	0.1-2.5	1	NA	NA	0.1	NA	NA	128	NA	NA	21
U2	Clayey silt	9	63.4	124.5	4.2-392.5	9	63.4	124.5	4.2-392.5	164.4	64.6	88-265	22.9	2.5	19-27
	Peat	5	28.8	15.4	4.1-46.6	5	28.8	15.4	4.1-46.6	133.8	54.5	61-209	22.2	3.3	20-28
		113				82									

Chapter 3

A 1 Ma sedimentary ancient DNA (*sed*aDNA) record of tropical paleovegetation assemblages and their associations with parasitic, endophytic, and saprophytic fungi.

3.1 Abstract

Fungi have a global distribution and exhibit diverse functional traits that are pivotal in driving terrestrial ecosystem dynamics. Short-term time series experiments have shown that the diversity and composition of soil fungi are subject to change in a global warming scenario, with potentially significant implications for the resilience of forest functioning, plant diversity, and soil processes. However, the analysis of geobiological archives (e.g., lake sediments) is required to cover climate-induced compositional changes of vegetation and associated fungal communities that take place at decadal to millennial timescales. Unfortunately, unlike pollen palynomorphs, diagnostic morphological features of fungi are rarely present. Sedimentary ancient DNA (*sed*aDNA) metabarcoding offers the opportunity to reconstruct past ecosystems, including taxa that lack morphological remains. This approach was recently used to reconstruct Quaternary fungal associations with Arctic tundra vegetation. However, similar studies have yet to be performed from tropical lake records where high *in situ* temperatures are expected to be unsuitable for the long-term preservation of *sed*aDNA. Here, we used 18S rRNA gene metabarcoding to study the eukaryotic community composition at millennium-scale resolution in ca. 1 Ma-year-old sediments from tropical Lake Towuti (Sulawesi, Indonesia). Fungi comprised >96% of the eukaryotic reads in all 82 sediment intervals. All identified fungal taxa belonged to Ascomycota (mainly Dothiodeomycetes, Eurotiomycetes, and Leotiomycetes) and Basidiomycota (dominated by Agaricomycetes). Most taxa were related to soil organic matter (OM) and wood decaying saprotrophs and, to a lesser extent, with ectomycorrhizal or necrotrophic phytopathogens. Pearson correlation analysis between relative changes in fungi (this study) and geochemical parameters vs. *trn*L-P6 paleovegetation communities (Chapter 2) showed that the downcore distribution of the fungal community composition was mainly shaped by soil mineral composition, the amount and maturity of sedimentary OM, and paleovegetation categories that differ in their

lignocellulosic fibre content. Didymellaceae (Dothideomycetes) and Basidiomycota most strongly correlated with trees and woody shrubs (TRSH) and were most likely involved in lignocellulosic wood decay. Ascomycota belonging to the soil clade GS35, Eurotiomycetes (Aspergillaceae and Herpotrichiellaceae) and Leotiomycetes (Pseudeurotiaceae and Gelatiodiscaceae) most strongly correlated with grasses and may have been part of the rhizosphere or as free-living saprotrophic soil OM degraders. Leptospheriaceae and Phaeosphaeriaceae (Dothideomycetes) most likely formed a close association with herbs as necrotrophic phytopathogens, and their combined biomass was mixed in with felsic substrates, which drained into Lake Towuti from the Loeha River catchment during prolonged periods of elevated precipitation and seasonality. The strongest Pearson correlation was observed between *Exophiala* (Herpotrichiellaceae) and organic-rich diatom ooze intervals, where these putative anaerobic fermenters may continue to form a syntrophic partnership with hydrogenotrophic methanogens. Altogether, our data show that tropical lakes can form long-term genomic archives of direct- (phytopathogenic, mycorrhizal) and indirect- (soil-, wood- and sedimentary OM decomposing) fungal-plant-soil (paleo) associations.

3.2 Introduction

Fungi have a global distribution and exhibit diverse functional traits that are pivotal in driving terrestrial ecosystem dynamics. Fungi are known to form close interactions with plants. The most common functional fungal guilds in forests are saprotrophic, mycorrhizal, pathogenic/parasitic, and endophytic. Saprotrophic (or saprobic) fungi obtain energy and nutrients from the decomposition of dead organic plant material and, therefore, play an essential role in the recycling of complex lignocellulosic plant fibres (Dighton et al., 2016 and references therein). Mycorrhizal fungi colonise plant roots and grow into the rhizosphere, forming a mutualistic partnership with terrestrial plants. They are essential in mobilising soil-bound minerals and the plant's ability to acquire these solubilised nutrients. At the same time, these root-associated fungi receive carbohydrates from the host plants in return (Finlay, 2008). This partnership is especially beneficial for plants growing in nutrient-poor soils. Endophytes differ from mycorrhizal fungi in that they reside entirely within plant tissues and grow inside

roots, stems, and leaves. Endophytes also increase plant fitness by, for example, activating host defence mechanisms against virulent pathogens, increasing the host plant's tolerance to drought or exposure to phototoxic heavy metals in soils (Solaiman et al., 2015). Plant parasitic fungi can be grouped as biotrophs feeding on living tissue, while necrotrophic fungi penetrate the plant, destroy the tissue, and subsequently provoke plant death (Naranjo-Ortiz & Gabaldón, 2019).

Several experimental time-series studies have shown that climate change-induced warming leads to changes in soil fungal community compositions. For example, warming of tundra soils resulted in a decrease in mycorrhizal fungi and a concomitant increase in saprotrophic, pathogenic, and root endophytic fungal richness (Geml et al., 2015; Mundra et al., 2016). A two-year time series experiment furthermore showed that the warming of tropical soils caused a progressive decline in tropical soil microbial diversity, with possible substantial implications for the resilience of tropical forest functioning, plant diversity, and soil processes (Nottingham et al., 2022). The latter study revealed a decrease in the relative read abundance of Basidiomycota, including the diverse order of Agaricales, which comprises important saprophytic and ectomycorrhizal taxa. At the same time, several orders in the phylum Ascomycota increased in relative read abundance, which comprises thermotolerant saprophytic and pathogenic fungi (e.g., Aurotiales, Hypocreales, and Pezizales) and yeasts (Saccharomycetales). These changes were accompanied by an accelerated rate of soil OM decomposition and the amount of CO_2 released (Nottingham et al., 2022).

However, time-series experiments must be extended to cover compositional changes of vegetation and associated fungal communities, which take place over much longer decadal, centennial, or even millennial timescales. Hence, the analysis of geobiological archives is required to study the long-term impact of environmental changes on fungi-soil-plant interactions. Lake sediments provide long-term records of pollen palynomorphs to study temporal changes in regional vegetation assemblages (Anshari et al., 2004; Hamilton et al., 2019; Hope, 2001; Stevenson, 2018). In contrast, a limited number of diagnostic fungal morphologic features (e.g., non-pollen

palynomorphs) (Van Geel, 2001) can be retrieved from sedimentary records to provide a comprehensive (parallel) overview of temporal changes in fungal community compositions (Loughlin et al., 2018; Quamar & Stivrinsz, 2021) and to infer concomitant changes in the terrestrial paleoenvironment.

Sedimentary ancient DNA (*sed*aDNA) metabarcoding, which studies past biodiversity based on sequencing analysis of taxonomically informative marker genes, is a molecular palaeoecological proxy rapidly increasing in popularity (Capo et al., 2021). A key benefit of this approach is the ability to identify taxa that did not form or left behind microscopic or macroscopic diagnostic features in the sedimentary record (e.g., Coolen, 2011). Extraction of sedimentary DNA and subsequent amplicon sequencing analysis of preserved vegetation metabarcoding genes, notably the chloroplast *trn*L-P6 loop marker (Taberlet et al., 2007), has been shown to complement fossil pollen in reconstructing local vegetation communities and their responses to paleo-environmental and more recent anthropogenic perturbations (e.g., Alsos et al., 2021; Courtin et al., 2021; Epp et al., 2015; Li et al., 2021; Niemeyer et al., 2017; Parducci et al., 2013; 2015; Pederson et al., 2013; Zimmermann et al., 2017).

A few studies have also used molecular tools to assess past fungal community compositions in permafrost soils and aquatic sediments (Bellemain et al., 2013; Hippel et al., 2022; Talas et al., 2021). For example, ITS metabarcoding on Late-Holocene Arctic Lake sediments recorded major shifts in mycorrhizal fungi and those taxonomically related to known plankton parasites. It was suggested that the predicted fungal ecophysiology and host specificity could be used to reconstruct aquatic and regional terrestrial ecosystems and their responses to environmental change (Talas et al., 2021). Hippel et al. (2022) went a step further. They performed a combined sedimentary *trn*L-P6 and ITS metabarcoding approach to reconstruct fungal community changes and their predicted saprotrophic, mycorrhizal, and parasitic paleo-associations with tundra and boreal forest vegetation spanning the last 47 kyr. These results showed, for example, that the expansion of woody forest vegetation with postglacial warming led to an increase in the abundance of fungi phylogenetically related to known mycorrhizae, lichens, and phytopathogens and a decline in yeasts

and saprotrophs (Hippel et al., 2022). Based on these observations, it was concluded that changes in the soil fungal community composition and their ecophysiological properties under future warming will likely affect forest expansion, plant species diversity and ecosystem stability in the Arctic (Hippel et al., 2022).

For *sed*aDNA studies aimed to reconstruct ecosystem responses to paleo-environmental perturbations, it is essential to target organisms that, upon burial in the sedimentary record, are no longer capable of thriving under the prevailing environmental conditions (Coolen et al., 2004). Plants are an excellent example of forming reliable non-living archives of *sed*aDNA since light is no longer available in subsurface sediments for photosynthesis to sustain their obligate photoautotrophic lifestyle. Oxygen, the highest energy-yielding electron acceptor for microbial respiration of organic matter (OM), usually becomes depleted below the top few cm of sediments (Orsi et al., 2017). Obligate aerobic organisms such as macroscopic zooplankton would not be able to survive in the oxygen-depleted subsurface sediments (Kiko et al., 2018) and, therefore, also form reliable sources of *sed*aDNA. However, unlike the examples outlined above, fungi are metabolically versatile, and a subset of the population in sedimentary records may continue to be shaped by the modern environmental conditions prevailing *in situ*, which then could lead to spurious paleo-ecological and paleo-environmental data interpretations. For example, while fungi are generally considered to be aerobes, it is well known that agricultural soils harbour many facultative anaerobic fungi, capable of anaerobic respiration of OM using nitrate instead of oxygen as the terminal electron acceptor (i.e., denitrification), including members of the widespread phytopathogenic genus *Fusarium* (Shoun & Tanimoto, 1991).

Moreover, evidence is emerging that various anoxic habitats are not only inhabited by anaerobic prokaryotes but also by obligate anaerobic fungi. Anaerobic fungi have most extensively been studied from the rumen of herbivores, where they play a crucial role in the highly efficient breakdown of recalcitrant lignocellulosic plant fibres (e.g., Khejornsart & Wanapat, 2010). Anaerobic fungi have also been reported from landfills (McDonald et al., 2012), biogas reactors (Haitjema et al., 2014), freshwater lakes (McDonald et al., 2012), anoxic deep-sea sediments (Nagano & Nagahama, 2012), and even from anoxic provinces of the deep oceanic crust (Ivarsson et al., 2016).

Fungal DNA records (with or without parallel vegetation *sed*aDNA metabarcoding) have so far been obtained from terrestrial settings in cold, high-latitude environments where low temperatures would have contributed to the long-term preservation of subsurface environmental DNA. It is generally assumed that post-depositional exposure to less favourable, high *in situ* temperatures prevents the long-term preservation of *sed*aDNA in tropical settings. Nevertheless, a few recent studies have shown that trace amounts of plant DNA can be recovered from late-Holocene (Boessenkool et al., 2014; Bremond et al., 2017; Dommain et al., 2020) and even late-Pleistocene tropical lake sediments (Chapter 2 of this thesis). However, it remains unknown how far back in time fungal DNA can be recovered and sequenced from tropical lakes and to what extent parallel metabarcoding of fungal and plant in tropical lake settings can be used to reconstruct fungal-plant associations and to infer concomitant changes in the paleodepositional environment.

The late-Pleistocene sedimentary record from Lake Towuti (Sulawesi, Indonesia) that was used to generate a 1Myr record of vegetation changes through *trn*L-P6 barcoding (Chapter 2 of this thesis) offered a unique opportunity to study (a) how far back in time fungal DNA can also be recovered and sequenced from tropical lakes and (b) to what extent parallel metabarcoding of fungal and plant in tropical lake settings can be used to reconstruct fungal-plant associations and to infer concomitant changes in the paleodepositional environment.

To address these aims, we used the available DNA extracts from the Lake Towuti record (Chapter 2) for 18S rRNA gene amplicon sequencing targeting the short (~130 bp) hypervariable V9 region (Amaral-Zettler et al., 2009). This general eukaryotic metabarcoding gene was initially chosen to generate a holistic overview of members of the Domain Eukarya, not limited to fungi, that could provide information about changes in the paleodepositional environment of Lake Towuti and to compare the relative read abundance of plant- vs fungal 18SV9 reads in each sample. Pearson correlation analysis between downcore changes in the relative read abundance of the identified fungal taxa (this study) and the geochemical parameters vs. paleovegetation assemblages identified through *trn*L-P6 metabarcoding (Chapter 2) was performed to infer the origin and association of the fungal community members with (a) ultramafic substrates which drained into lake Towuti from the Mahalona River during drier

climate stages, (b) felsic substrates, which drained into lake Towuti via the Loeha River during wetter conditions, and with (c) anoxic muddy soils of the lakes' catchment at times of increased primary productivity and concomitant diatom ooze formation.

We postulate that fungal taxa showing elevated positive Pearson correlations with the paleodepositional geochemical parameters represented soil OM decomposing saprotrophs or mycorrhizae. In contrast, we hypothesise that fungal taxa showing positive Pearson correlations with paleovegetation assemblages are most closely related to wood-decaying saprotrophs, phytopathogens, or endophytes, which formed direct associations with their host plants.

3.3 Material and Methods

3.3.1 Coring, subsampling, and DNA extraction

All DNA extracts available from Lake Towuti's Core 1F and used for amplicon sequencing of the chloroplast plant marker gene *trn*L-P6 (Chapter 2) served as the template for sedimentary 18S rRNA gene profiling (this study). Please see the Materials and Methods section of Chapter 2 for a detailed description of the coring, sampling, and DNA recovery procedures.

3.3.2 Illumina MiSeq amplicon sequencing of sedimentary 18SV9

PCR reaction mixtures were prepared within the clean lab and inside a UV-sterilized, HEPA-filtered horizontal laminar flow bench. Before use, all working surfaces and equipment inside the HLF bench were cleaned with RNase AWAY™ as an additional measure to remove possible traces of foreign DNA. The recovered purified sedimentary DNA was quantified fluorometrically using Quant-iT PicoGreen™ double-stranded DNA (dsDNA) Reagent (Invitrogen). Each PCR reaction contained ~20 nanograms of template DNA, 1xSYBR Premix Ex Taq kit (Takara, Bio Inc.), and 0.2 µM final concentration of domain-specific primers targeting the hypervariable V9 region of the 18S rRNA gene: Euk1380F (5′-CCCTGCCHTTTGTACACAC) and Euk1510R (5′-CCTTCYGCAGGTTCACCTAC) (Amaral-Zettler et al., 2009). The total volume of each reaction was adjusted to 20 µL using PCR-grade water (Amicon). Newly formed SYBR-green-stained dsDNA in each reaction was followed in real-time using a Real-Plex quantitative PCR (qPCR) system (Eppendorf, Hauppauge,

NY). We initially performed a test run to determine how many cycles were needed for each sample to reach the end of the exponential phase and to prevent overamplification and subsequent formation of PCR artefacts such as primer dimers. Based on these results, separate qPCR runs were performed to accommodate samples that required 25, 30, 35 or 40 cycles to reach the end of the exponential phase. Background- and extraction blanks were run alongside the samples using the same number of cycles. The amplification steps were as follows: initial denaturation at 95 ℃ for 60 sec, followed by 25-40 cycles of denaturation (5 sec at 95 ℃), primer annealing (5 sec at 66 ℃), and primer extension plus imaging of newly formed SYBR®green stained dsDNA (30 sec at 72 ℃). The correct fragment length of each amplicon was verified by agarose gel electrophoresis amended with SYBR green. A dark reader (Qiagen) was used to visualise the SYBR®green stained DNA. Only the expected ~130-bp-long amplified fragments were excised from the gel using flame-sterilised scalpels. DNA was eluted from the fragments in 75 uL molecular-grade TE buffer pH 8 (8h at 4 ℃). Twenty nanograms of the eluted DNA fragments were subjected to a second round of PCR (12 cycles) using the same conditions as described above, except that the template-specific reverse primers included sample-specific 12 bp Golay barcode indices plus adapter and pad regions (modified after Caporaso et al., 2012) for Illumina MiSeq sequencing. Equimolar amounts of the indexed amplicons were pooled, concentrated using an Amicon Ultra 0.5 mL 30 kDa Centrifugal Filter (Millipore Sigma) and subjected to agarose gel electrophoresis (50 min at 120 V). After electrophoresis, the library of the expected length was excised from the gel using a heat-sterilised scalpel, gel-purified using the Monarch DNA Gel Extraction Kit (New England Biolabs), concentrated, quantified, and sequenced (paired-end; 150 cycles; Illumina MiSeq) at the Australian Genome Research Facility (AGRF) in Perth (WA, Australia) using the sequencing facilities default procedures (agrf.com.au).

3.3.3 Bioinformatics and Biostatistics

Paired-end reads were imported, aligned, and demultiplexed using Quantitative Insights into Microbial Ecology (QIIME2; V 2021.11) (Bolyen et al., 2019). The raw paired-end reads were demultiplexed using q2-demux. Primer and Illumina adapter sequences were removed using q2-cutadapt (Ryberg & Matheny, 2011), followed by denoising and chimaera removal using the Divisive Amplicon Denoising Algorithm

(DADA2) plugin (Callahan et al., 2016). QIIME2 feature-classifier classify-sklearn (Pedregosa et al., 2011) was used for the taxonomic annotation of the high-quality Amplicon Sequence Variants (ASVs) against the SILVA 138 database (Hadziavdic et al., 2014). ASVs present in samples and in background- and extraction blanks were considered contaminants and removed from the dataset.

Global and pairwise similarity analysis (ANOSIM) was used to determine if the fungal and amoebozoan assemblages differed significantly between sample categories: (i) pre-lake vs. lacustrine stages, (ii) paleodepositional units, and (iii) sediment lithologies (Russell et al., 2020 and Chapter 2 of this thesis). This analysis was performed in PRIMER-e v7 (Clarke & Gorley, 2015) using Bray Curtis dissimilarities of square root transformed relative read abundance data and Sørensen dissimilarities of presence/absence data. Indicator Species Analysis (ISA) (Dufrene & Legendre, 1997) was performed using the R package IndicSpecies (De Caceres & Legendre, 2009) to reveal significant associations of fungi and amoebozoans (classified at the lowest reliable taxonomic levels) with these three sample categories. In addition, similarity of percentage (SIMPER) analysis was performed in PRIMER-e v7 to identify taxa that contributed most to group similarities or dissimilarities between groups that contained significantly different (ANOSIM p<0.05) paleovegetation communities.

A Clustered Image Map (CIM) was created in MixOmics (Kim-Anh Le Cao et al., 2016) to infer the predominant origins (i.e., local lake catchment and ultramafic vs. felsic substrates from the Mahalona and Loeha Rivers, respectively) of the subsurface fungal assemblages based on the Pearson correlation strength between temporal changes in their relative read abundance and previously analysed (in)organic geochemical parameters (Morlock et al., 2021; Russell et al., 2020; Sheppard et al., 2021). See the methods section of Chapter 2 of this thesis for a complete overview and description of the geochemical parameters included in the analysis. In addition, Pearson *r*-values between downcore changes in the fungal assemblages and *trn*L-P6 inferred paleovegetation categories (herbs, grasses, TRSH) (Chapter 2) were visualised using CIM to predict beneficial vs. parasitic fungal-paleovegetation interactions throughout Lake Towuti's paleodepositional history.

3.4 Results

3.4.1 General overview of the downcore distribution of DNA content and sequence data

The total DNA content varied up to three orders of magnitude throughout the core (Fig. 3.1). Most sedimentary DNA was likely of bacterial origin since eukaryotic 18SV9 could only be amplified and sequenced from 82 out of 146 available sediment intervals, irrespective of total DNA content. We recovered 7,076,835 high-quality reads, ranging between 5.8×10^5 and 9.8×10^5 per interval (Fig. 3.1).
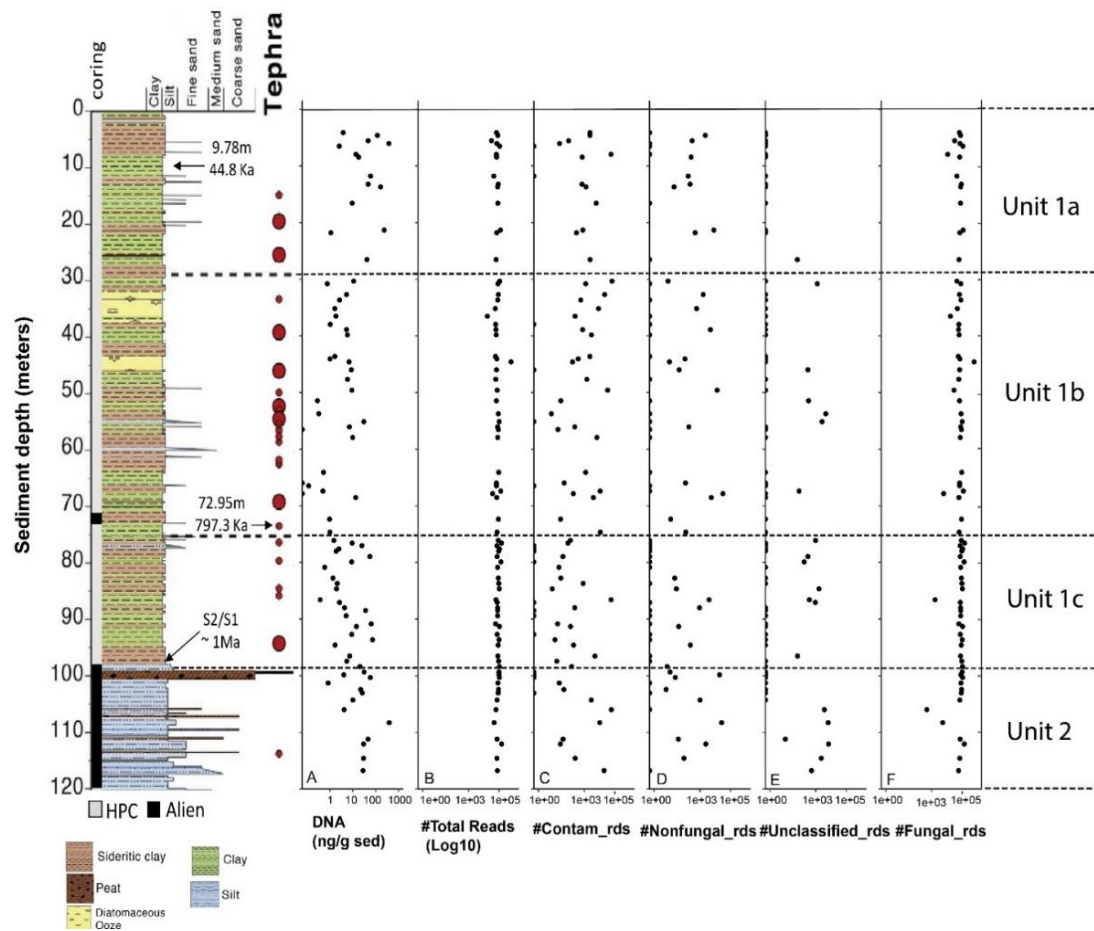
Figure 3.1 General overview of core 1F and recovered sequence data. The lithology graph further shows composite sediment depth (mcd), coring method (hydraulic piston vs Alien), the position of tephra deposits T1-T23 and sediment ages. Radiocarbon dating on the bulk organic matter at 9.79 mcd revealed a sediment age of ~44.7 Ka, whereas $^{40}Ar/^{39}Ar$ dating of the tephra T18 layer at 72.95 mcd revealed a sediment age of 797.3 ± 1.6 Ka. The U2/U1c transition at ~98.8 mcd was estimated to have occurred 1 Ma ago through extrapolation (see Russell et al., 2020 for details). (A) Total extracted sedimentary DNA content (nanograms per gram sediment) (B) Total number of reads comprising: (C) lab contaminants reads that were also or only identified in amplified and sequenced extraction- and background blanks (D) Reads identified as human pathogens, insects, or plants (E) Unclassified reads. These reads were excluded from downstream analysis. (F) Number of genuine paleo-fungal reads that was used for downstream analysis in this study. All panels show quantities in Log10 scale.

99

Before downstream analysis, 621,396 reads were removed from the datasets, which included contaminants (n=444,837 reads), and putative ancient eukaryotic communities other than fungi, but out of scope for this study: amoebozoans (n=152,860), arthropods (n =9,322), and vegetation (n=14,827) (Figs. S3.1, S3.2). The remaining 6,455,439 fungal reads (Fig. 3.1) were assigned to 78 ASVs, which were classified as 38 individual fungal taxa belonging to the phyla Ascomycota (sac fungi; n=25) and Basidiomycota (club fungi; n =13) (Fig. 3.2., Table. 3.1) as detailed below.
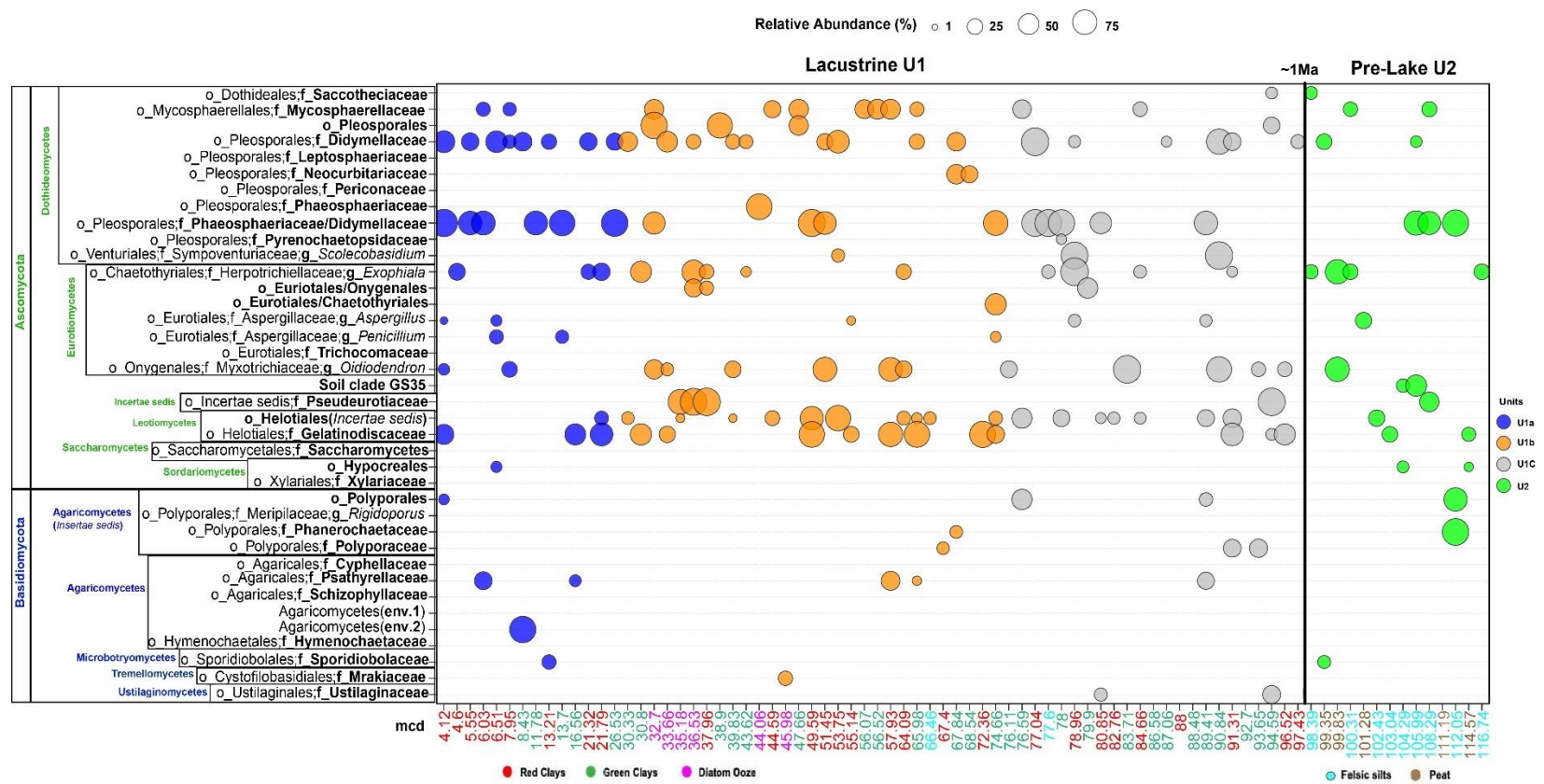
Figure 3.2 Bubble Plot showing the downcore changes in the relative read abundance of Ascomycota (n=25 taxa), Basidiomycota (n=13) identified at the lowest reliable taxonomic ranks throughout the 117 m-long sediment record of Lake Towuti (n=80 intervals). Taxa identified at order (o_), family (f_), or genus (g_) levels that belong to the same Ascomycete or Basidiomycete classes are grouped inside rectangular boxes. The legend on the y-axis refers to the colour coding for the bubbles to mark the depositional units and their transitions. The x-axis shows the meter composite depths (mcd) of each sample and have been colour-coded according to lithology types: Lacustrine red clays (red), green clays (green), diatom ooze (purple); Pre-lake U2 felsic silts (blue), and peat (brown). The vertical line marks the transition into a permanent Lake Towuti ~1 Myr ago.

101

Table 3.1 General overview of recovered fungal ASVs, their taxonomic assignments, and their potential environmental niche and functions. Lowest reliable taxonomic taxonomic ranks were achieved down to family level (except for the genera *Exophiala*, *Aspergillus*, *Penicillium*, and *Oidiodendron*). See the cluster image maps of the main Figures 3.4 and 3.5 for the interpretation of the information shown in the columns labelled "Geochem Cluster"," Geochem Category", and "Vegetation type".

ASV#	phylum	class	order	family	env. clones + genera that include species with >99.3 % seq. similarity in NCBI's nr/nt database		Geochem Fig. 3	Plant cat.	Environmental clones/isolates (100% identity)
					Lowest reliable taxonomic ranks		**Highest pos. Pearson-*r***		
1	Ascomycota	Dothideomycetes	Dothideales	Saccotheciaceae	*Aureobasidium*	B	Neutral	Grasses	Saprobes; endophytes; phytopathogens
2	Ascomycota	Dothideomycetes	Mycosphaerellales	Mycosphaerellaceae	*Ramularia* & *Zymoseptoria*	B	Ultramafic	Herbs	Nectrotrophic phytopathogens with diverse host plant range
3, 4, 5, 6, 7	Ascomycota	Dothideomycetes	Pleosporales	NA	NA	B	Felsic	TRSH & Grasses	Unknown function (potential saprotroph)
8, 9, 10, 11, 12, 13, 14	Ascomycota	Dothideomycetes	Pleosporales	Didymellaceae	*Didymella* & *Phoma herbarium*	A	Ultramafic	TRSH	DSE (antimycobacterial in diverse plant tissue/ saprobes soil plant litter / parasitic (stem blight in herbs) / HM accumulator (e.g. Mg-, Fe-, Ti-, Al-, Ca-, K-oxides)
15, 16	Ascomycota	Dothideomycetes	Pleosporales	Leptosphaeriaceae	*Plenodomus* & *Leptosphaeria*	B	Felsic	TRSH	DSE (nectrotrophic phytopathogens)
17	Ascomycota	Dothideomycetes	Pleosporales	Neocurbitariaceae	*Neocucurbitaria*	A	Neutral	TRSH & Grasses	Potential saprotrophs
18	Ascomycota	Dothideomycetes	Pleosporales	Periconaceae	*Periconia*	B	Felsic	TRSH	DSE (antimycobacterial)
19, 20	Ascomycota	Dothideomycetes	Pleosporales	Phaeosphaeriaceae	*Phaeosphaeria* & *Ophiosphaerella*	B	Felsic	Herbs	Mostly phytopathogens (herbs and grasses)
21, 22, 23	Ascomycota	Dothideomycetes	Pleosporales	Phaeosphaeriaceae, Didymellaceae	*Paraphoma* & *Phaeosphaeriopsis* vs. *Phoma* & *Didymella*	B	Felsic	Herbs	DSE (phytopthogens; crown & root rot & leaf spot disease; saprobes complex hydrocarbon degraders; associated with submerged wood in FW lakes
24	Ascomycota	Dothideomycetes	Pleosporales	Pyrenochaetopsidaceae	*Pyrenochaetopsis*	B	Neutral	Herbs	Plant pathogens; saprophytes; endophytes
25, 26, 27, 28, 29, 30	Ascomycota	Eurotiomycetes	Chaetothyriales	Herpotrichiellaceae	***Exophiala*** (*E. xenobiotica*)	C	Mesotrophic	Grasses	DSE; putative anaerobic fermenters; lignolitic saprobes; present in TOC-rich soils; antimycobial against root rot fungi.
31	Ascomycota	Eurotiomycetes	Euriotales, Onygenales	NA	NA	C	Mesotrophic	Grasses	Saprotrophes (cellulotypic, in moist low pH soils
32, 33	Ascomycota	Eurotiomycetes	Euriotales, Chaetothyriales	NA	NA	B	Neutral	Neutral	Unknown function
34, 35, 36	Ascomycota	Eurotiomycetes	Euriotales	Aspergillaceae	***Aspergillus***	A	Ultramafic	Grasses	Unknown function (potential saprotroph)
37, 38, 39, 40, 41	Ascomycota	Eurotiomycetes	Euriotales	Aspergillaceae	***Penicillium***	A	Neutral	Grasses	Putative saprotrops, ubiquitous in soils
42	Ascomycota	Eurotiomycetes	Euriotales	Trichocomaceae	NA	> 95 mcd	No data	Herbs	Putative saprotrops, ubiquitous in soils
43, 44, 45, 46, 47, 48, 49	Ascomycota	Eurotiomycetes	Onygenales	Myxotrichaceae	***Oidiodendron***	A	Neutral	Neutral	Ectomycorrhizal
50	Ascomycota	GS35_soil clade	GS35_soil clade	GS35_soil clade	Clone GL37478_S201 (UDB014907)	> 95 mcd	No data	Grasses	Broad habitat most common in grass- and shrubland soils
51	Ascomycota	Leotiomycetes	Thelebolales	Pseudeurotiaceae	NA	A	Ultramafic	Grasses	Saprobes soil plant litter
52	Ascomycota	Leotiomycetes	Helotiales *incertae sedis*	NA	Uncultured fungal isolate_UPSC_H2_67 (GU564949)	A	Neutral	TRSH & Herbs	Endophytes
53, 54, 55	Ascomycota	Leotiomycetes	Helotiales	Gelatinodiscaceae	*Neobulgaria*	A	Ultramafic	Grasses	Saprobes_wood decay
56, 57	Ascomycota	Saccharomycetes	Saccharomycetales	Saccharomycetaceae	*Candida* & *Myerozyma*	A	Ultramafic	Neutral	yeasts (soils in extreme environments)
58, 59	Ascomycota	Sordariomycetes	Hypocreales	NA	NA	B	Neutral	Neutral	putative anaerobic fermenter (sporadic presence)
60	Ascomycota	Sordariomycetes	Xylariales	Xylariaceae	*Nemania* & *Spirririma*	A	Neutral	TRSH	Saprobes (wood decay)
61	Basidiomycota	Agaricomycetes *Incertae sedis*	Polyporales	NA	NA	A	Neutral	Neutral	Saprobes (lignolitic wood decomposers)
62	Basidiomycota	Agaricomycetes *Incertae sedis*	Polyporales	Meripilaceae	*Rigidoporus*	A	Ultramafic	TRSH	Saprobes (lignolitic wood decomposers)
63, 64	Basidiomycota	Agaricomycetes *Incertae sedis*	Polyporales	Phanerochaetaceae	*Bjerkandera*	A	Neutral	TRSH & Grasses	Saprobes (lignolitic wood decomposers)
65	Basidiomycota	Agaricomycetes *Incertae sedis*	Polyporales	Polyporaceae	*Perenniporia*	A	Neutral	TRSH	Saprobes (lignolitic wood decomposers)
66, 67	Basidiomycota	Agaricomycetes	Env.1	Env.1	clone G-jav2-SSU2_OTU-0-241_4 (MF343933)	A	Neutral	TRSH	Rhizosphere orchids (Mycoheterotrophic Gastrodia)
68	Basidiomycota	Agaricomycetes	Env.2	Env.2	clone CMH121 (KF800212)	B	Neutral	Neutral	Saprobes soil plant litter
69, 70	Basidiomycota	Agaricomycetes	Agaricales	Psathyrellaceae	*Psathyrella* & *Coprinellus*	C	Mesotrophic	TRSH & Grasses	Saprobic on fallen wood
71	Basidiomycota	Agaricomycetes	Agaricales	Cyphellaceae	*Chondrostereum*	A	Neutral	TRSH	Saprobic on fallen wood
72	Basidiomycota	Agaricomycetes	Agaricales	Schizophyllaceae	*Schizophyllum*	A	Neutral	TRSH	Saprobic on fallen wood
73, 74, 75, 76, 77	Basidiomycota	Agaricomycetes	Hymenochaetales	Hymenochaetaceae	*Inonotus* & *Phellinus*	A	Neutral	Neutral	Parasitic on trees causing white rot
78	Basidiomycota	Microbotryomycetes	Sporidiobolales	Sporidiobolaceae	*Rhodotorula*	A	Ultramafic	Grasses	non-Saccharomyces yeast isolated from soil (e.g. Brazilianrain forest) capable of anaerobic fermentation (sporadic distribution)

102

3.4.2 Downcore distribution of taxa belonging to Ascomycota and Basidiomycota

3.4.2.1 Ascomycota

We identified six classes, 14 orders, 16 families of Ascomycota (Fig. 3.2). Five taxa could be identified at genus level (Fig. 3.2). Dothiodeomycetes and Eurotiomycetes were the most abundant classes and were observed throughout the record (Fig. 3.2). Pleosporales was the most diverse and frequently observed order of Dothiodeomycetes and was mainly represented by the families Phaeosphaeriaceae (consistently present throughout U1 and U2), and Didymellaceae (most consistently present in U1) (Fig. 3.2, Table 3.1). The ASVs classified as Didymellaceae showed 99-100% sequence homology with species of the genus *Didymella* and *Phoma herbarum* (Table 3.1). Whereas members of both genera are most often considered important plant pathogens, these soil-borne fungi are also known as leaf-decaying saprobes and as plant-beneficial endophytes involved in antimycobacterial biocontrol (e.g., Braga et al., 2018). ASVs 21-23 classified as Phaeospaeriaceae revealed >97.08% sequence similarity with species of *Paraphoma*, which were found throughout the record, including the pre-lake U2 interval. Members of *Paraphoma* are dark septate endophytes (DSE) and have also most frequently been reported as plant pathogens (causing crown and root rot or leaf spot disease) (Moslemi et al., 2016). In addition, *Paraphoma* spp. are known for degrading recalcitrant hydrocarbons, including plastic and have also been reported from submerged wood in freshwater lakes (El-Elimat et al., 2014) (Table 3.1). However, these ASVs revealed the same sequence homology with *Didymella* and *Phoma* and may also represent Didymellaceae. ASVs 19,20 could be exclusively classified as Phaeosphaeriaceae as they showed >99.27% sequence similarity to members of *Phaeosphaeria* and/or *Ophiospaerella* within this family. *Phaeosphaeria* species are saprobes capable of lignin degradation or pathogens on wild herbaceous and woody plants (Ferrari et al., 2021).

Eurotiomycetes (predominantly black yeasts) was the next most diverse class of Ascomycota and comprised of three orders that could be classified to genus level using the short but hypervariable 18S rRNA V9 region: Chaetothyriales (Herpotrichiellaceae; *Exophiala*), Onygenales (Myxotrhichaceae; g_*Oidiodendron*), and Eurotiales (f_Aspergillaceae; g_*Aspergillus* and g_*Penicillium*) (Fig. 3.2). *Oidiodendron* (possibly ectomycorrhizal) was most consistently present throughout U1, followed by *Exophiala* (saprobes or endophytes) (Fig. 3.2., Table 3.1).

Leotiomycetes included Heliotales (Gelatinodiscaceae; ASVs 53-55) and Thelobolales (Pseudeurotiaceae; ASV51). Gelatinodiscaceae were most consistently detected in the felsic silts of U2 and green clays of U1 and least frequent in the organic-rich U2 peat and U1 diatom ooze intervals (Fig. 3.2). The genus *Neobulgaria* showed the highest sequence similarity with Gelatinodiscaceae (Table 3.1) and includes saprobes involved in wood decay (Kwasna et al., 2021). Pseudeurotiaceae (ASV51) was recovered throughout the sedimentary record of Lake Towuti and showed 100% sequence similarity with the metabolically and environmentally diverse soil fungus *Pseudogymnoascus pannorum* M1372 (Chaturvedi et al., 2018). Pseudeurotiaceae were also the dominant source of fungal ITS sequences in Glacial sediments of Arctic tundra lakes (Hippel et al., 2022)

Clade GS35 was only found in a continuous set of silty clays of U2. This soil clade is phylogenetically related to the classes Leotiomycetes and Sordariomycetes (with low support) and distributed globally in very broad ecoregions concerning climate and soil pH (Tedersoo et al., 2017; Zhang & Wang, 2015). Saccharomycetes (Saccharomycetales; Saccharomycetaceae) with 100% sequence homology with fermenting yeasts of the genera *Candida* and *Myerozyma*, and Sordariomycetes (Hypocreales and Xylariales; Xylariaceae) were only sporadically detected classes of Ascomycota throughout the core (Fig. 3.2).

3.4.2.2 Basidiomycota

Basidomycota were less frequently detected throughout the core compared to Ascomycota. The most prominent class were Agaricomycetes and was mainly represented by the order Agaricales, most notably the family Psathyrellaceae, possibly represented by wood-decaying saprobes *Psathyrella* and *Corpinellus* (Fig.3.2). Hymenochaetales (Hymenochaetaceae) most closely related to parasitic, ligninolytic white rot fungi (*Innonotus* and *Phellinus*) were only identified in green clays deeper than 68 mcd and in the oldest peat (Fig. 3.2). Polyporales belonging to Agaricomycetes with uncertain placement (*incertae sedis*) were also most frequently recovered at depths below 66 mcd (Fig. 3.2) and most closely related to putative ligninolytic wood decomposing saprobes within the families Phanerochaetaceae, Polyporaceae, and

Meripillaceae (Table 3.1). The remaining classes of Basidiomycota, Microbotryomycetes (saprobic and phytopathogenic yeasts), Tremellomycetes (dimorphic fungi) and Ustilaginomycetes (smut fungi) were only present in a few intervals (Fig. 3.2).

3.4.3 Significant differences in fungal communities between paleo-depositional units and primary core lithologies

Global and pairwise ANOSIM tests using presence/absence data of the subsurface fungi generally resulted in higher significance levels compared to Bray-Curtis dissimilarities of normalised and square root-transformed relative read abundance data (Table 3.2). Therefore, the ANOSIM results described below are based on presence/absence data (see Table 3.2 for ANOSIM test results based on relative read abundance data). Global ANOSIM showed that the overall fungal assemblages differed significantly between intervals from pre-lake vs. lacustrine stages (r=0.296; p =0.001), depositional units (r =0.108; p =0.002), and (c) lithologies (r =0.140; p =0.003) (Table 3.2). Pairwise ANOSIM tests involving depositional units, the largest dissimilarities between the subsurface fungal assemblages were observed between U1c vs. U2 (r = 0.35; p=0.001) and U1b vs. U2 (r = 0.214; p=0.002). Fungal assemblages did not differ significantly between U1a vs. U1b and U1b vs. U1c (Table 3.2). Pairwise ANOSIM tests showed that only fungi associated with green or red clays differed significantly from those identified in the felsic silts and peats of U2 (Table 3.2).

Table 3.2 Global and pairwise analysis of similarities (ANOSIM) showing significant ($p < 0.05$) and non-significant ($p > 0.05$) dissimilarities in the paleo-fungal community composition (n=38 taxa) between paleodepositional units (U) and main sediment lithologies. ANOSIM was compared based on Sørensen dissimilarities of presence/absence data **(A, B)** and Bray-Curtis dissimilarities of normalised and square root-transformed (SQRT) relative read abundance data **(C, D)**. U1 (lacustrine subunits 1a, 1b, 1c); U2 (pre-lake unit). The main lithologies of U1 are Red Clays (RC), Green Clays (GC), and Diatom Ooze (DO). The main lithologies of U2 are felsic silts and peats. **(E)** Indicator Species Analysis showing taxa significantly associated with the entire lacustrine U1 or with pre-lake U2 deposits based on normalised and square root-transformed relative read abundance data. Significant indicator taxa with an A-value of 1.0 (100%) only occur in samples of the group to which they are significantly associated. The B-value is 1.0 in case the indicator species is present in all samples of the group to which they are significantly associated. See the results and discussion sections of the main text for details. Significance levels (p): 0 '***' 0.001 '**' 0.01 '*' 0.05 and not significant (NS).

A — Precense/Absence + Sørensen) (Developmental units)

Groups	*r*-value	*p*-value	Sign.level
U2 x U1	0.296	0.001	***
Global test	0.108	0.002	**
U1a x U1b	-0.044	0.750	NS
U1a x U1C	0.109	0.041	*
U1a x U2	0.161	0.002	**
U1b x U1C	0.023	0.195	NS
U1b x U2	0.214	0.002	**
U1C x U2	0.35	0.001	***

C — Rel.abund. Norm+SQRT+Bary-Curtis (Developmental units)

Groups	*r*-value	*p*-value	Sign.level
U2 x U1	0.133	0.028	*
Global test	0.041	0.099	NS
U1a x U1b	-0.073	0.889	NS
U1a x U1C	0.063	0.103	NS
U1a x U2	0.153	0.01	**
U1b x U1C	-0.001	0.45	NS
U1b x U2	0.1	0.062	NS
U1C x U2	0.124	0.024	*

B — Precense/Absence + Sørensen) (Lithologies)

Groups	*r*-value	*p*-value	Sign.level
U2 x U1	0.296	0.001	***
Global test	0.14	0.003	**
RC x GC	-0.017	0.758	NS
RC x DO	0.136	0.155	NS
RC x Silt	0.309	0.002	**
RC x Peat	0.287	0.037	*
GC x DO	0.04	0.353	NS
GC x Silt	0.302	0.001	***
GC x Peat	0.257	0.035	*
DO x Silt	0.224	0.054	.
DO x Peat	0.105	0.16	NS
Silt x Peat	-0.05	0.586	NS

D — Rel.abund. Norm+SQRT+Bary-Curtis (Main lithologies)

Groups	*r*-value	*p*-value	Sign.level
U2 x U1	0.133	0.028	*
Global test	0.1	0.099	NS
RC x GC	-0.012	0.64	NS
RC x DO	0.212	0.031	*
RC x Silt	0.128	0.068	NS
RC x Peat	0.173	0.091	NS
GC x DO	0.103	0.141	NS
GC x Silt	0.162	0.021	*
GC x Peat	0.207	0.034	*
DO x Silt	0.268	0.010	*
DO x Peat	0.296	0.037	*
Silt x Peat	0.074	0.27	NS

E

Taxonomy (all p_Ascomycota)	Group	A	B	*r*-value	*p*-value	Sign.level
c_Dothideomycetes; o_Pleosporales; f_Didymellaceae	Unit 1	0.7387	0.8209	0.779	0.041	*
c_Eurotiomycetes; o_Onygenales; f_Myxotrichaceae; g_*Oidiodendron*	Unit 1	0.9366	0.791	0.861	0.001	***
Soil clade_GS35	Unit 2	1	0.3077	0.555	0.002	**
c_Dothideomycetes; o_Mycosphaerellales; f_Mycosphaerellaceae	Unit 2	0.918	0.3846	0.594	0.025	*
c_Dothideomycetes; o_Dothideales; f_Saccotheciaceae	Unit 2	0.9805	0.1538	0.388	0.029	*
c_Eurotiomycetes; o_Eurotiales; f_Aspergillaceae; g_*Aspergillus*	Unit 2	0.8608	0.3077	0.515	0.026	*
c_Leotiomycetes; o_Helotiales; f_Gelatinodiscaceae	Unit 2	0.8128	0.6154	0.707	0.038	*
c_Sordariomycetes; o_Hypocreales	Unit 2	0.9242	0.1538	0.377	0.035	*

3.4.4 Similarity percentages (SIMPER) associations of fungal taxa to the depositional units and lithologies of Lake Towuti

Using a 90% cut-off for SIMPER analyses, eight fungal taxa contributed most to the similarities observed among samples belonging to the same paleodepositional units and lithologies (Fig. 3.3). Phaeosphaeriaceae contributed between 10 and 85% to within-group similarities in all lithologies, being highest in peat intervals of U2 and lowest in organic-rich diatom ooze. Among depositional units, the lowest contribution was observed within the sideritic red clays of U1a (Fig. 3.3). Pseudeurotiaceae also contributed to within-group similarities in all units and lithologies but showed a reverse trend, with the highest % associations being highest for U1a and red clays and lowest for the organic-rich diatom ooze and peat intervals (Fig. 3.3). Didymellaceae only showed SIMPER associations with the felsic silts of U2 and the clays of U1. Their % association with U2 and U1b were relatively low compared to the lack of association observed with peat and diatom ooze intervals (Fig. 3.3). Gelatinodiscaceae and Mycosphaerellaceae lacked associations with the lacustrine units and lithologies and were the remaining fungi that showed relatively low % associations with U2 lithologies (i.e., limited to the felsic silts). *Oidiodendron* contributed 5-20% associations with all three lacustrine units and lithologies, highest in green clays and U1a. *Exophiala* showed very high % associations with diatom ooze (SIMPER 60%) and, to a lesser extent, with green clays (SIMPER =3%) and no association with red clays. The relatively low % association of *Exophiala* with U1b can be explained by the predominance of green clays over diatom ooze in this lacustrine interval (Fig. 3.3). Psathyrellaceae (Basiciomycota) were also most strongly associated with diatom ooze (SIMPER = 13%) and only with green clays (Simper =2%) (Fig. 3.3).
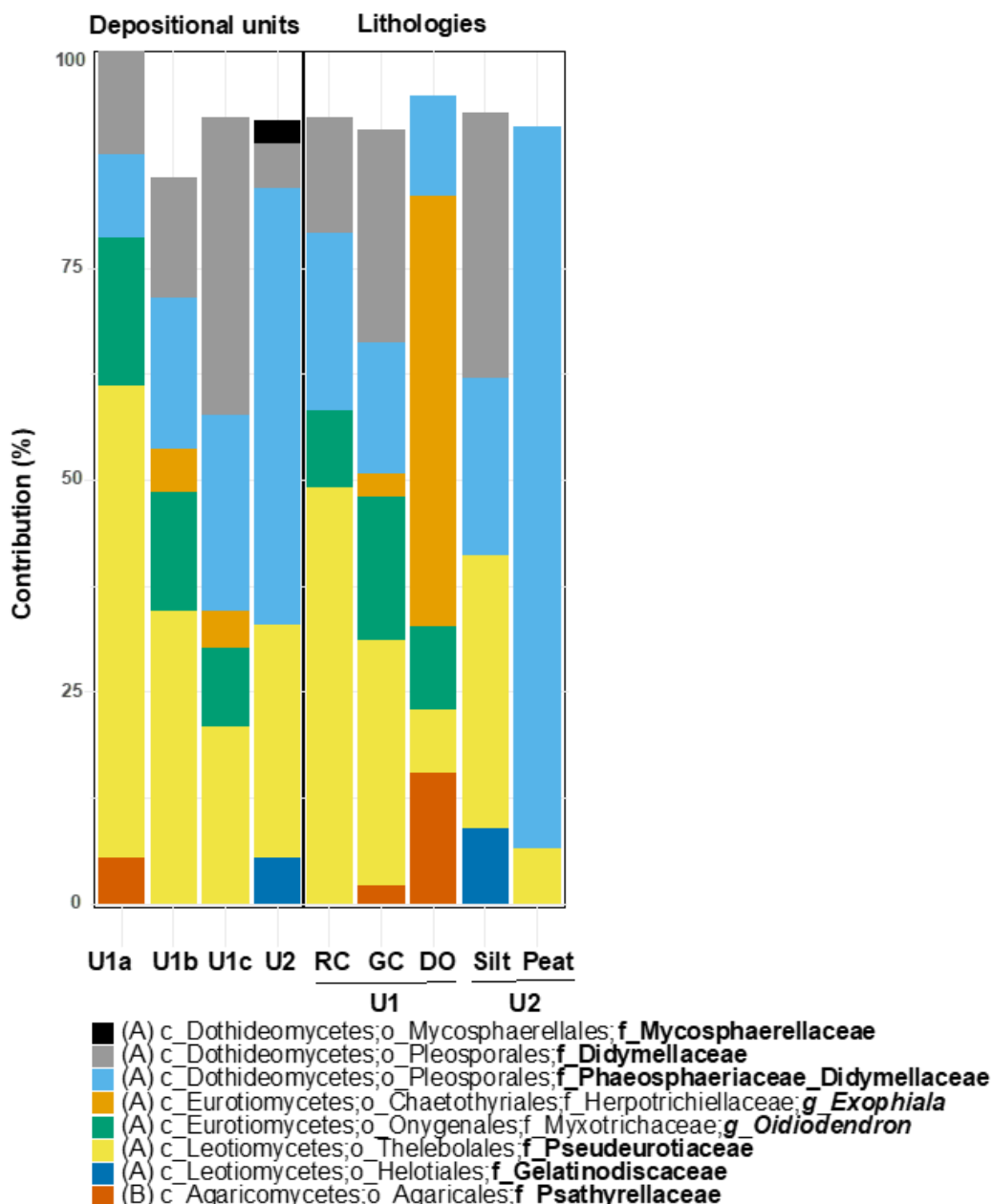
Figure 3.3 Similarity percentages (SIMPER) results showing the top 8 fungal taxa and their percentage contribution to the (Bray-Curtis) similarities (cut-off = 90%) observed between samples belonging to the lacustrine (U1a, U1b, U1c) and pre-lake (U2) depositional stages vs. the main sediment lithologies: sideritic Red Clays (RC), Green Clays (GC), and Diatom Ooze (DO) of Unit 1, and felsic silts and peats of Unit 2.

3.4.5 Pearson correlations strength between fungal taxa and geochemical parameters.

The Cluster Image Map (CIM) of Fig. 3.4 shows the Pearson correlation strength between relative changes in the downcore distribution of fungal taxa and previously analysed geochemical data and resulted in the formation of three distinct clusters (Fig. 3.4). Cluster A comprised taxa with neutral to weakly positive Pearson *r*-values with inorganic parameters (oxides of Fe, Mg, Mn, Ni, Cr) indicative of increased drainage of ultramafic sediments and laterite soils from the lakes' catchment, particularly at times of inferred drying (Russell et al., 2020). See Chapter 2 for a detailed description of the relationship between these inorganic proxies and associated paleo-environmental and paleohydrological conditions. Didymellaceae revealed the highest Pearson *r* values with the ultramafic markers denoted as "U (++)". Please note that the *r* values shown in Fig. 3.4 should be interpreted descriptively, as they do not necessarily indicate significant associations. Two subclusters labelled as "U (+)" contain taxa with low but still positive Pearson *r* values with ultramafic markers, including Pseudeurotiaceae and Gelatinodiscaeae (Leotiomycetes), which showed high SIMPER associations with U2 felsic silts vs. red clays of U1a, respectively. Taxa that showed neutral Pearson correlations with ultramafic markers predominantly represented Basidiomycota (Fig. 3.4).

Cluster B represented taxa that showed the highest positive Pearson *r* values with inorganic markers indicative of an increased contribution of the Loeha River (increased Al/Mg ratio), which drained felsic substrates rich in K_2O from the NE catchment of Lake Towuti during wetter climate conditions. The cluster showing the highest Pearson *r* values with these felsic markers was exclusively represented by families belonging to the Dothiodeomycetes order Pleosporales (i.e., Phaeosphaeriaceae and Laptospheriaceae). Other members of this class also predominated in the lower subcluster of B despite the near-to-neutral and weak positive Pearson correlation strength with K_2O and the Al/Mg ratio (Fig. 3.4).

Cluster C comprised Psathyrellaceae and *Exophiala*. In agreement with their highest SIMPER association with diatom ooze intervals (Fig. 3.3), these fungi showed low- to medium-strong Pearson correlations with the TLE/TOC ratio, %TOC, and

silica content as markers for increased deposition and burial of relatively labile sedimentary OM during mesotrophic conditions, which ultimately led to the development of diatom blooms and subsequent deposition of the silica-rich diatom ooze intervals (Russell et al 2020, Fig. 3.4).
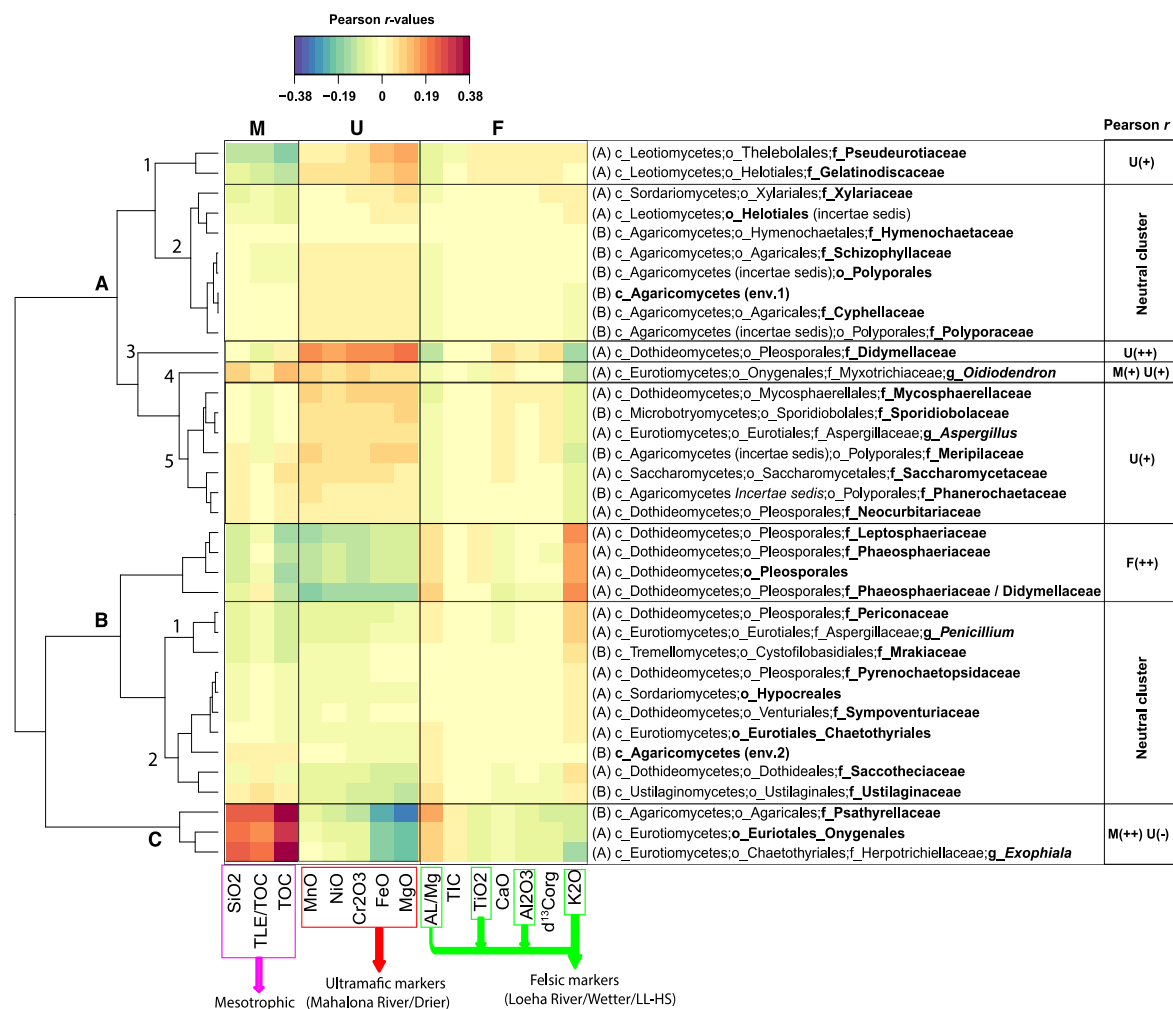
Figure 3.4 Cluster Image Map (CIM) showing Pearson correlations (*r* values shown in colour key) between relative changes in the downcore distribution of fungal taxa and previously analysed geochemical proxy data (Russell et al., 2020; Sheppard et al., 2021). See Results and Discussion sections of this chapter for data interpretation. Cluster A shows taxa with neutral- to weakly positive Pearson correlation strength with ultramafic (U) parameters, being highest for Didymellaceae, while *Oidiodendron* shows positive Pearson *r* values with ultramafic and mesotrophic (M) parameters. Cluster B included fungal taxa with neutral- to weakly positive Pearson *r*-values with felsic (F) parameters. Taxa in Cluster C show medium-strong Pearson correlation strength with mesotrophic parameters. The taxonomic levels of the fungal phyla Ascomycota (A) and Basidiomycota (B) are denoted as: class (c_), order (o_), family (f_), and genus (g_). Note that the soil clade GS35 was only found at depths >96 mcd for which no geochemical data is available and, therefore, missing from this figure.

3.4.6 Pearson correlations strength between fungal taxa (this chapter) and paleo-vegetation categories (Chapter 2)

The Cluster Image Map of Fig. 3.5 shows the Pearson correlation strength between relative changes in the downcore distribution of fungal taxa (this chapter) and the main categories (i.e., herbs, trees & shrubs "TRSH", and grasses) identified through *trn*L-P6 amplicon sequencing (Chapter 2). This resulted in the forming of three main clusters with fungi that most strongly correlated with each of the primary vegetation categories (Fig. 3.5). Didymellaceae showed the highest, medium-strong Pearson correlation with TRSH (Subcluster A3). Whereas a subset of fungal taxa in Cluster A did not exclusively show low positive Pearson r values with TRSH, most of these fungi represented saprobic Basidiomycetes and Ascomycetes involved in wood degradation (Table 3.1).

Cluster B exclusively comprised Ascomycota, which only showed low to medium-strong Pearson correlations with grasses. The soil clade GS35 and Euotiomycetes (i.e., unclassified Eurotiales or Onygenales) in subcluster B1 revealed the highest positive Pearson *r* values with grasses. Cluster B2 included Leotiomycetes (Gelatinodiscaceae and Pseudeurotiaceae), Eurotiomycetes (*Aspergillus*, *Penicillium* and *Exophiala*), as well as Dothideomycetes (Saccotheciaceae) showing low positive Pearson *r* values with grasses.

Cluster C included Ascomycota with medium strong Pearson correlations solely with herbs (i.e., Phaeosphaeriaceae and Leptosphaeriaceae belonging to the class Dothideomycetes in subcluster C2). Both taxa revealed medium strong negative correlations with grasses. Mycosphaerellaceae (also belonging to the class Dothideomyetes) and Trichomonaceae (Eurotiomycetes) formed subcluster C2, showing low positive Pearson *r* values only with herbs (Fig. 3.5). Cluster C1 showed neutral correlations with all vegetation categories and mainly included Basidiomycota.
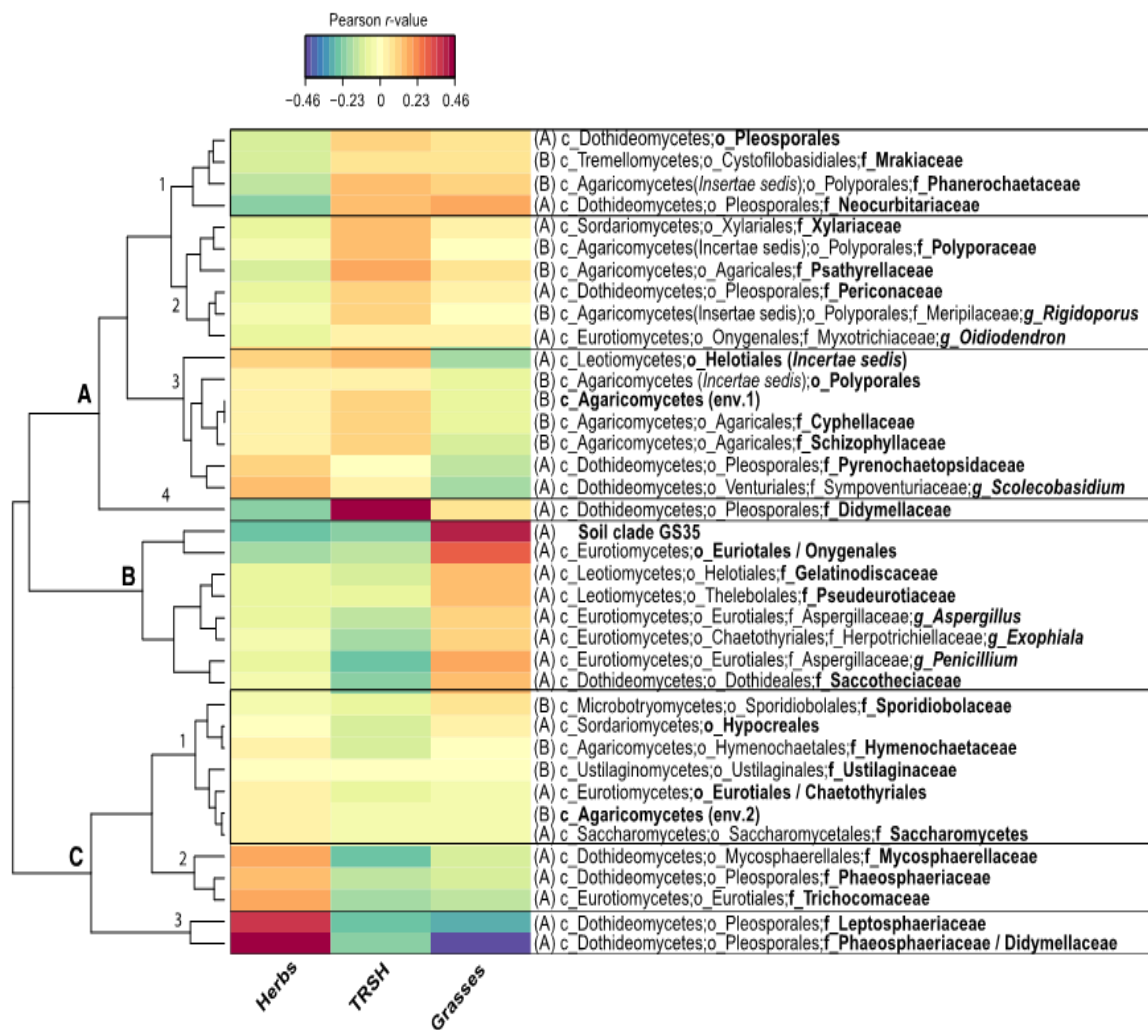
Figure 3.5. CIM representing Pearson correlations (*r* values shown in colour key) between downcore changes in the relative read abundance of fungal taxa (this chapter) and the main paleovegetation categories inferred from the paired sedimentary *trn*L-P6 profiling depicted from Thesis Chapter 2. Separate clusters were formed with fungal taxa that showed weak to moderate positive Pearson correlations with TRSH & grasses (A1), TRSH only (A2&A4), TRSH & herbs (A3); grasses only (Cluster B), and herbs only (Cluster C2 and C3). Cluster C1 contains fungal taxa that showed neutral *r* values for all vegetation categories. The taxonomic levels of the fungal phyla Ascomycota (A) and Basidiomycota (B) are denoted as class (c_), order (o_), family (f_), and genus (g_). The soil clade GS35 has only been classified at the phylum level (Ascomycota). (See the results and discussion sections of the main text for further details).

3.5 Discussion

3.5.1 Origin of Fungi in the deep subsurface deposits of Lake Towuti

Our data revealed that the overall fungal community composition differed significantly between pre-lake and lake deposits. Indicator species analysis revealed

that *Oidiodendron* (Onygonales; Myxotrhichiaceae) represented the most significant indicator taxon for the entire U1 lake core section. *Oidiodendron* showed a relatively high percentage of associations with all three U1 lithologies and depositional subunits and no associations with U2. It was the only taxon showing weak- but positive Pearson correlations with ultramafic and mesotrophic conditions. Near-to-neutral Pearson *r* values were observed between *Oidiodendron* and all three vegetation categories. *Oidiodendron* spp. are well-known ectomycorrhiza, and their lack of association with the U2 silts and peats may imply that the host vegetation was not present or at a far lower density in the pre-lake landscape. The Pleosporales family Didymellaceae, most likely represented by the genus *Didymella*, was also a significant indicator taxon for U1. Didymellaceae revealed high percentage associations with the U2 felsic silts and clays of U1, but no associations were observed with the organic-rich peat and diatom ooze. They furthermore showed weak- and medium-strength positive Pearson correlations with ultramafic substrates and TRSH, respectively. Didymellaceae include known endophytes of diverse plant tissue and can be beneficial for plant growth as anti-microbial bio-controlling agents but can also emerge as plant parasites causing stem blight in herbs (Jogaiah et al., 2004). Didymellaceae are furthermore known saprobes of soil plant litter. Given their dominance in U1 and their association with ultramafic inorganic parameters and cpDNA from TRSH, Didymellaceae in our record most likely represented saprobes in soils from the lakes' ultramafic catchment, which predominantly drained into Lake Towuti during increased runoff from the Mahalona River during prolonged periods of drier conditions.

The soil clade GS35 represented the best and most significant indicator taxon for U2 but was only found in a sequence of four felsic silt samples. This clade that has yet to be classified has a widespread distribution but is mainly found in grassland soils. Open grassland vegetation would have been widespread in a dynamic and disturbed pre-lake landscape dominated by many small rivers and shallow lakes. Soil and wood-decaying saprobes (Saccotheciaceae, Gelatinodiscaceae, and *Aspergillus*) and necrotrophic phytopathogens (Mycosphaerellaceae) represented marginally significant additional indicator taxa for U2.

Chapter 3

A 1 Ma sedimentary ancient DNA (sedaDNA) record of tropical paleovegetation assemblages and their associations with parasitic, endophytic, and saprophytic fungi

As detailed in Chapter 2, the paleodepositional subunits of U1 (U1a, U1b, U1c) and their transitions have been defined previously based on downcore changes in physical, geochemical, and sedimentological parameters. However, we did not find evidence of significantly different fungal assemblages associated with these stages and boundaries. Nevertheless, Pearson correlation analysis between relative changes in the downcore distribution of fungal taxa and geochemical parameters revealed separate clusters that can be attributed to drier and wetter climate stages and elevated primary productivity during the evolution of the lake.

Minerals with an ultramafic signature (Fig. 3.4, red cluster) indicative of increased drainage from the largest Mahalona and Lampenisu rivers NW of Lake Towuti during drier conditions correlated positively with, most notably, Pseudeurotiaceae as well as with Didymellaceae, which was a significant indicator taxon for U1 and already discussed above. *Pseudogymnoascus pannorum*, the most closely related member of Pseudeurotiaceae in the Lake Towuti record, is widely distributed in soils such as caves and mines (Chaturvedi et al., 2018). Like ultramafic soil, mine soil substrates can also be rich in heavy metals, which suggests that the Pseudeurotiaceae were indeed associated with the drained ultramafic sediments where they were capable of tolerating exposure to toxic elements like Ni and Cr through hyperaccumulation. *P. annorum* can grow at psychrophilic and mesophilic temperature ranges (Christen-Zaech et al., 2008). Being tolerant to colder temperatures may explain its continuous presence in the red clays deposited during the dry and cold LGM. *P. pannorum* also tolerates a wide acidity range, has an extreme tolerance to many xenobiotics, demonstrated extensive saprotrophic enzymatic activities, and is capable of utilising complex carbohydrates and metabolising an extensive range of carbon intermediates (Chaturvedi et al., 2018). This suggests that the Pseudeurotiaceae most closely related to *P. pannorum* in our record represented soil litter decomposers. The capability of these extremophiles to adapt to a wide range of environmental conditions would explain why 18S rRNA gene sequences of Pseudeurotiaceae were identified in all but three sediment intervals. Pseudeurotiaceae of unknown function have also been recovered from Holocene Artic Lake sediments (Hippel et al., 2022) where they may have represented soil saprobes.

Furthermore, mainly taxa from the class Dothideomycetes were positively correlated with felsic markers indicative of increased drainage of felsic substrates from the NE Loeha River during wetter conditions and increased seasonality. Notable examples are putative necrotrophic phytopathogens of the families Leptosphaeriaceae (possibly *Leptosphaeria*) and Mycosphaerellaceae (possibly *Ramularia*) and putative phytopathogens of herbs and grasses (Phaeosphaeriaceae; possibly *Phaeosphaeria*). These fungal taxa furthermore showed the highest positive Pearson correlations with herbs. These pathogens could have formed a relatively large pool of fungal biomass associated with the host plants' necro mass, which, at times of increased precipitation, would have efficiently drained into Lake Towuti mixed in with felsic substrates.

A separate cluster comprised of *Exophiala*, Psathyrellaceae, and Onygenales. These taxa correlated most strongly with geochemical markers indicative of increased nutrient input and paleo-productivity and the subsequent deposition of the organic-rich diatom ooze intervals of Unit 1b (Fig. 3.4, Mesotrophic conditions; purple cluster). *Exophiala* are black yeast that possess ligninolytic enzymes and are commonly found in organic-rich soils (Rustler et al., 2008; Prenafeta-Boldú et al., 2006). Onygenales are often considered cellulolytic saprobes in moist and low-pH soils (Greif & Currah, 2007). Psathyrellaceae (Basidiomycota) grow as lignin-degrading saprobes on fallen wood (Krik et al., 2008; Osono,2019). As expected, the latter showed the highest positive Pearson *r* values with TRSH. Instead, Onygenales and *Exophiala* revealed the highest positive Pearson correlations with grasses. Wood and grasses are rich sources of lignocellulosic fibres, and these results suggest that diatom ooze intervals comprise a mix of OM derived from these two vegetation categories.

We propose that the fungal taxa, which positively correlated with the ultramafic and felsic geochemical markers, represented saprobes, (necrotrophic) phytopathogens, and ectomycorrhiza. Mixed in with the ultramafic and felsic substrates, these fungal communities, along with decaying plant litter, drained into Lake Towuti via the Mahalona and Loeha Rivers, which contributed most to the sedimentation processes during long-term periods of drier and wetter conditions,

respectively. The most consistent direct fungal-host-substrate associations were observed between the putative necrotrophic phytopathogens, herbs as the main host vegetation category, and felsic substrates on which this vegetation grew. In contrast, the composition of saprobic fungal communities, notably those involved in soil OM decomposition, would have been mainly shaped by the vegetation that colonised a particular soil type. This implies an indirect correlation between saprobic fungi, paleovegetation, and the type of drained sedimentary substrates. As discussed in Chapter 2, during the mesotrophic stage of Lake Towuti, the most prominent paleovegetation identified through sedimentary *trn*L-P6 barcoding was most likely locally sourced from the lakes' muddy anoxic catchment soils and within-lake aquatic herbs. We speculate that facultative-obligate anaerobic fungi, associated initially with anoxic littoral sediments, may still be involved in the decomposition of OM in the sapropelic diatom ooze deposits, as discussed in more detail in section 3.4.2.

In addition, several taxa showed a lack of correlation with any of the analysed geochemical parameters (Fig. 3.4). These mainly comprised lignin-degrading Basidiomycota that were only occasionally detected throughout the record. Their sporadic occurrence suggests that relatively low amounts of biomass of wood-colonising Basidiomycota were drained into Lake Towuti and were also less evenly distributed across the lakebed compared to Ascomycota, which mainly drained into the lake mixed in with sedimentary substrates. In addition, the flux of biomass from obligate aquatic fungi, which are often taxonomically related and difficult to differentiate from soil-derived fungi (Calabon et al. 2022), would most likely also have been marginal in comparison and could be among the sparsely distributed taxa that lacked any correlation with the geochemical parameters.

3.5.2 Presence of fungi in the deposits of Lake Towuti and their potential physiological role in ongoing organic carbon transformation

For *sed*aDNA studies aimed to reconstruct ecosystem responses to paleo-environmental perturbations, it is essential to target organisms that are incapable of surviving or adapting their physiological properties upon burial (Coolen et al., 2004). Oxygen, the highest energy-yielding electron receptor for microbial respiration of

OM, usually becomes depleted below the top few cm of sediments (Orsi et al., 2017). Obligate aerobic organisms such as zooplankton cannot thrive under oxygen-depleted conditions and are, therefore, considered to form genuine records of *sed*aDNA in anaerobic subsurface sediments (Kiko et al., 2018). Since most fungi are considered aerobic heterotrophs, oxygen-depleted lake records are also assumed to represent *sed*aDNA archives of soil-derived or aquatic fungi that inform about terrestrial paleo-environmental conditions.

However, evidence is emerging that a substantial fraction of fungi can dwell under oxygen-depleted conditions as facultative- or even obligate anaerobes (Hess et al., 2020; Iversson et al., 2016 and reference therein). Although our study does not provide conclusive evidence for the presence of viable and physiologically active fungi in the deep subsurface sediments of Lake Towuti, porewaters within the upper 12 m of sediment were shown to contain relatively high concentrations of formate, acetate, lactate, and propionate (Friese et al., 2021). These four volatile fatty acids (VFAs) are the primary metabolites of microbial fermentation, constituting a key step in OM mineralisation. Furthermore, the authors found that methanogenesis is a dominant carbon mineralisation pathway in the sediments of Lake Towuti. Hydrogen, acetate, and formate are the main fungal fermentation products, and anaerobic fungi are known to form a syntrophic partnership with methanogenic archaea capable of utilising these fungal metabolites to produce methane (Teunissen et al.,1992). This syntrophic partnership was first described to occur in the rumen of herbivores, where anaerobic fungi play a vital role in the breakdown of recalcitrant lignocellulosic plant fibres (Khejornsart & Wanapat, 2010; Hess et al., 2020). Anaerobic fungi described from oxygen-depleted environments other than rumens of herbivores mainly belong to Ascomycota. Most Ascomycota sequences detected in the Lake Towuti record were closely related to known saprobes capable of decomposing complex carbon compounds such as lignin, cellulose, and aromatics. *Aspergillus* and *Penicillium* (Aspergillaceae), *Candida* (Saccharomyecateae), and *Exophiala* (Herpotrichiellaceae) (Gancedo, 1998; Kurakov et al., 2008; Ivarsson et al., 2020) are notable examples of confirmed facultative- and obligate anaerobic saprobic fungi in our record. Of those, *Exophiala*, which possesses ligninolytic enzymes and has been frequently reported from organic-rich soils (Isola et al., 2021), was most consistently identified throughout

117

the record (including the red clays of the LGM) but showed the highest percentage association with the TOC-rich anaerobic diatom ooze intervals. *Exophiala* has also been reported and isolated from Mid-Atlantic igneous crusts underlying anaerobic provinces (Hirayama et al., 2015), where they were thought to form a syntrophic relationship with hydrogenotrophic methanogens (Ivarsson et al., 2020).

Thus, it is feasible that a fraction of the detected fungal microbial community is still physiologically active and may continue to play a role in the transformation of OM in a syntrophic partnership with hydrogenotrophic and/or acetoclastic methanogens, thereby maintaining an anaerobic environment. If so, these living soil-derived fungi form an indirect long-term genomic record of concomitant terrestrial environmental conditions that prevailed at deposition. Indirect paleo-environmental conditions were previously successfully recorded from shotgun metagenomic sequence data of living subseafloor bacteria in the Arabian Sea (Orsi et al., 2017). Roughly 15% of the subseafloor microbiome in the latter study was seeded from the overlying water column, where they were likely involved in denitrification during Monsoon-triggered periods of oxygen minimum zone expansion. These taxa possessed the genetic machinery capable of switching to a fermentative lifestyle upon burial in the sedimentary record (Orsi et al., 2017).

3.6 Conclusions

Here, we used 18S rRNA gene metabarcoding to study the eukaryotic community composition at millennium-scale resolution in ca. 1 Ma-year-old sediments from tropical Lake Towuti (Sulawesi, Indonesia). Fungi comprised >96% of the eukaryotic reads in all 82 sediment intervals. All identified fungal taxa belonged to Ascomycota (mainly Dothiodeomycetes, Eurotiomycetes, and Leotiomycetes) and Basidiomycota (dominated by Agaricomycetes). Most taxa were related to soil OM and wood decaying saprotrophs and, to a lesser extent, with ectomycorrhizal or necrotrophic phytopathogens. Pearson correlation analysis between relative changes in fungi and geochemical parameters vs. *trn*L-P6 paleovegetation communities (chapter 2) showed that the downcore distribution of the fungal community composition was mainly shaped by soil mineral composition, the amount and maturity of sedimentary OM, and paleovegetation categories that differ in their lignocellulosic fibre content. Didymellaceae (Dothideomycetes) and Basidiomycota most strongly correlated with

TRSH and were most likely involved in lignocellulosic wood decay. Ascomycota belonging to the soil clade GS35, Eurotiomycetes (Aspergillaceae and Herpotrichiellaceae) and Leotiomycetes (Pseudeurotiaceae and Gelatiodiscaceae) most strongly correlated with grasses and may have been part of the rhizosphere or as free-living saprotrophic soil OM degraders. Leptospheriaceae and Phaeosphaeriaceae (Dothideomycetes) most likely formed a close association with herbs as necrotrophic phytopathogens, and their combined biomass was mixed in with felsic substrates, which drained into Lake Towuti from the Loeha River catchment during prolonged periods of elevated precipitation and seasonality. The strongest Pearson correlation was observed between *Exophiala* (Herpotrichiellaceae) and organic-rich diatom ooze intervals, where these putative anaerobic fermenters may continue to form a syntrophic partnership with hydrogenotrophic methanogens. Altogether, our data show that tropical lakes can form long-term genomic archives of direct- (phytopathogenic, mycorrhizal) and indirect- (soil-, wood-, and sedimentary OM decomposing) fungal-plant-soil (paleo)associations.

A drawback of our study was that we used 18SV9 as a metabarcoding gene, initially aimed to provide a comprehensive overview of the total composition of eukaryotes. At best, 18SV9 can identify fungal taxa at the genus level, while ITS has become the best practice metabarcoding gene to identify fungal taxa down to the species level. Repeating the study using ITS as the ideal fungal metabarcoding would not only lower the taxonomic resolution but likely also result in a more precise prediction of their ecophysiological guilds and an increase in the number of taxa that likely had direct endomycorrhizal, phytopathogenic, or plant-beneficial endosymbiotic associations with plants.

3.7 References

Alsos, I. G., Sjögren, P., Edwards, M. E., Landvik, J. Y., Gielly, L., Forwick, M., Coissac, E., Brown, A. G., Jakobsen, L. V., Føreid, M. K., & Pedersen, M. W. (2016). Sedimentary ancient DNA from Lake Skartjørna, Svalbard: Assessing the resilience of arctic flora to Holocene climate change. *The Holocene, 26*(4), 627-642.

Amaral-Zettler, L. A., McCliment, E. A., Ducklow, H. W., & Huse, S. M. (2009). A Method for Studying Protistan Diversity Using Massively Parallel Sequencing of V9 Hypervariable Regions of Small-Subunit Ribosomal RNA Genes. *PLOS ONE, 4*(7), e6372.

Anshari, G., Kershaw, P., van der Kaars, S., & Jacobsen, G. (2004). Environmental change and peatland forest dynamics in the Lake Sentarum area, West Kalimantan, Indonesia. *Journal of Quaternary Science, 19*, 637-655.

Bellemain, E., Davey, M. L., Kauserud, H., Epp, L. S., Boessenkool, S., Coissac, E., Geml, J., Edwards, M., Willerslev, E., Gussarova, G., Taberlet, P., Haile, J., & Brochmann, C. (2013). Fungal palaeodiversity revealed using high-throughput metabarcoding of ancient DNA from arctic permafrost. *Environ Microbiol*, *15*(4), 1176-1189.

Boessenkool, S., Mcglynn, G., Epp, L. S., Taylor, D., Pimentel, M., Gizaw, A., Nemomissa, S., Brochmann, C., & Popp, M. (2014). Use of ancient sedimentary DNA as a novel conservation tool for high-altitude tropical biodiversity. *Conservation biology, 28*(2), 446-455.

Bolyen, E., Rideout, J. R., Dillon, M. R., Bokulich, N. A., Abnet, C. C., Al-Ghalith, G. A., Alexander, H., Alm, E. J., Arumugam, M., Asnicar, F., Bai, Y., Bisanz, J. E., Bittinger, K., Brejnrod, A., Brislawn, C. J., Brown, C. T., Callahan, B. J., Caraballo-Rodríguez, A. M., Chase, J., . . . Caporaso, J. G. (2019). Reproducible, interactive, scalable and extensible microbiome data science using QIIME 2. *Nature Biotechnology*, *37*(8), 852-857.

Braga, R. M., Padilla, G., & Araújo, W. L. (2018). The biotechnological potential of Epicoccum spp.: diversity of secondary metabolites. *Critical Reviews in Microbiology*, *44*(6), 759-778.

Bremond, L., Favier, C., Ficetola, G. F., Tossou, M. G., Akouégninou, A., Gielly, L., Giguet-Covex, C., Oslisly, R., & Salzmann, U. (2017). Five thousand years of tropical lake sediment DNA records from Benin. *Quaternary Science Reviews, 170*, 203-211.

Calabon, M., Hyde, K., Jones, E., Bao, D.-F., Bhunjun, C. S., Phukhamsakda, C., Shen, H.-W., Gentekaki, E., Al Sharie, A., Barros, J., Chandrasiri, S., Hu, D.-M., Hurdeal, V., Rossi, W., Guardia Valle, L., Zhang, H., Figueroa, M., Raja, H., Sahadevan, S., & Balasuriya, A. (2023). *Freshwater fungal biology, 14*, 195–413.

Callahan, B. J., McMurdie, P. J., Rosen, M. J., Han, A. W., Johnson, A. J. A., & Holmes, S. P. (2016). DADA2: High-resolution sample inference from Illumina amplicon data. *Nature Methods*, *13*(7), 581-583.

Capo, E., Giguet-Covex, C., Rouillard, A., Nota, K., Heintzman, P. D., Vuillemin, A., Ariztegui, D., Arnaud, F., Belle, S., Bertilsson, S., Bigler, C., Bindler, R., Brown, A. G., Clarke, C. L., Crump, S. E., Debroas, D., Englund, G., Ficetola, G. F., Garner, R. E., . . . Parducci, L. (2021). Lake Sedimentary DNA Research on Past Terrestrial and Aquatic Biodiversity: Overview and Recommendations. *Quaternary*, *4*(1), 6.

Caporaso, J. G., Lauber, C. L., Walters, W. A., Berg-Lyons, D., Huntley, J., Fierer, N., Owens, S. M., Betley, J., Fraser, L., Bauer, M., Gormley, N., Gilbert, J. A., Smith, G., & Knight, R. (2012). Ultra-high-throughput microbial community analysis on the Illumina HiSeq and MiSeq platforms. *Isme Journal, 6*(8), 1621-1624.

Chaturvedi, V., DeFiglio, H., & Chaturvedi, S. (2018). Phenotype profiling of white-nose syndrome pathogen Pseudogymnoascus destructans and closely-related Pseudogymnoascus pannorum reveals metabolic differences underlying fungal lifestyles. *F1000Res*, *7*, 665.

Christen-Zaech, S., Patel, S., & Mancini, A. J. (2008). Recurrent cutaneous Geomyces pannorum infection in three brothers with ichthyosis. *J Am Acad Dermatol*, *58*(5), S112-113.

Clarke, K. R., Gorley, R. N. (2015). PRIMER v7: User Manual/Tutorial. PRIMER-E Ltd.

Coolen, M. J. L. (2011). 7000 years of Emiliania huxleyi viruses in the Black Sea. *Science, 333*(6041), 451-452.

Coolen, M. J. L., Hopmans, E. C., Rijpstra, W. I. C., Muyzer, G., Schouten, S., Volkman, J. K., & Sinninghe Damsté, J. S. (2004). Evolution of the methane cycle in Ace Lake (Antarctica) during the Holocene: response of methanogens and methanotrophs to environmental change. *Organic geochemistry*, *35*(10), 1151-1167.

Courtin, J., Andreev, A. A., Raschke, E., Bala, S., Biskaborn, B. K., Liu, S. S., Zimmermann, H., Diekmann, B., Stoof-Leichsenring, K. R., Pestryakova, L. A., and Herzschuh, U. (2021). Vegetation Changes in Southeastern Siberia During the Late Pleistocene and the Holocene. *Frontiers in Ecology and Evolution, 09*.

De Caceres, M., and Legendre, P. (2009). Associations between species and groups of sites: indices and statistical inference. *Ecology, 90*(12), 3566-3574.

Dighton, J. (2016). *Fungi in Ecosystem Processes, 2nd Edition*.

Dommain, R., Andama, M., McDonough, M. M., Prado, N. A., Goldhammer, T., Potts, R., Maldonado, J. E., Nkurunungi, J. B., & Campana, M. G. (2020). The challenges of reconstructing tropical biodiversity with sedimentary ancient DNA: A 2200-year-long metagenomic record from Bwindi impenetrable forest, Uganda. *Frontiers in Ecology and Evolution, 8*, 218.

Dufrene, M., & Legendre, P. (1997). Species assemblages and indicator species: The need for a flexible asymmetrical approach. *Ecological Monographs, 67*(3), 345-366.

El-Elimat, T., Raja, H. A., Figueroa, M., Falkinham III, J. O., & Oberlies, N. H. (2014). Isochromenones, isobenzofuranone, and tetrahydronaphthalenes produced by Paraphoma radicina, a fungus isolated from a freshwater habitat. *Phytochemistry*, *104*, 114-120.

Epp, L. S., Gussarova, C., Boessenkool, S., Olsen, J., Haile, J., Schroder-Nielsen, A., Ludikova, A., Hassel, K., Stenoien, H. K., Funder, S., Willerslev, E., Kjaer, K., and Brochmann, C. (2015). Lake sediment multi-taxon DNA from North Greenland records early post-glacial appearance of vascular plants and accurately tracks environmental changes. *Quaternary Science Reviews, 117*, 152-163.

Ferrari, R., Gautier, V., & Silar, P. (2021). Chapter Three - Lignin degradation by ascomycetes. In M. Morel-Rouhier & R. Sormani (Eds.), *Advances in Botanical Research* (Vol. 99, pp. 77-113). Academic Press.

Finlay, R. D. (2008). Ecological aspects of mycorrhizal symbiosis: with special emphasis on the functional diversity of interactions involving the extraradical mycelium. *Journal of Experimental Botany*, *59*(5), 1115-1126.

Friese, A., Bauer, K., Glombitza, C., Ordoñez, L., Ariztegui, D., Heuer, V. B., Vuillemin, A., Henny, C., Nomosatryo, S., & Simister, R. (2021). Organic matter mineralization in modern and ancient ferruginous sediments. *Nature communications, 12*(1), 2216.

Gancedo, J. M. (1998). Yeast carbon catabolite repression. *Microbiology and molecular biology reviews, 62*(2), 334-361.

Geel, B. (2006). Non-Pollen Palynomorphs. In (Vol. 3, pp. 99-119).

Geml, J., Morgado, L. N., Semenova, T. A., Welker, J. M., Walker, M. D., & Smets, E. (2015). Long-term warming alters richness and composition of taxonomic and functional groups of arctic fungi. *FEMS Microbiology Ecology*, *91*(8), 095.

Greif, M. D., & Currah, R. S. (2007). Patterns in the occurrence of saprophytic fungi carried by arthropods caught in traps baited with rotted wood and dung. *Mycologia*, *99*(1), 7-19.

Hadziavdic, K., Lekang, K., Lanzen, A., Jonassen, I., Thompson, E. M., & Troedsson, C. (2014). Characterization of the 18S rRNA gene for designing universal eukaryote specific primers. *PLoS One*, *9*(2), 87624.

Haitjema, C. H., Solomon, K. V., Henske, J. K., Theodorou, M. K., & O'Malley, M. A. (2014). Anaerobic gut fungi: Advances in isolation, culture, and cellulolytic enzyme discovery for biofuel production. *Biotechnol Bioeng*, *111*(8), 1471-1482.

Hamilton, R., Stevenson, J., Li, B., & Bijaksana, S. (2019). A 16,000-year record of climate, vegetation and fire from Wallacean lowland tropical forests. *Quaternary Science Reviews, 224*, 105929.

Hess, M., Paul, S. S., Puniya, A. K., van der Giezen, M., Shaw, C., Edwards, J. E., & Fliegerová, K. (2020). Anaerobic Fungi: Past, Present, and Future. *Front Microbiol*, *11*, 584893.

Hippel, V. B., Stoof-Leichsenring, K. R., Schulte, L., Seeber, P., Epp, L. S., Biskaborn, B. K., Diekmann, B., Melles, M., Pestryakova, L., & Herzschuh, U. (2022). Long-term fungus–plant covariation from multi-site sedimentary ancient DNA metabarcoding. *Quaternary science reviews, 295,* 107758.

Hirayama, H., Abe, M., Miyazaki, J., Sakai, S., & Takai, K. (2015). Data report: cultivation of microorganisms from basaltic rock and sediment cores from the North Pond on the western flank of the Mid-Atlantic Ridge, IODP Expedition 336. *Sci Technol (JAMSTEC)*, *2*, 15.

Hope, G. (2001). Environmental change in the Late Pleistocene and later Holocene at Wanda site, Soroako, South Sulawesi, Indonesia. *Palaeogeography Palaeoclimatology Palaeoecology, 171*(3-4), 129-145.

Isola, D., Scano, A., Orrù, G., Prenafeta-Boldú, F. X., & Zucconi, L. (2021). Hydrocarbon-contaminated sites: Is there something more than Exophiala

xenobiotica? New insights into black fungal diversity using the long cold incubation method. *Journal of Fungi, 7*(10), 817.

Ivarsson, M., Bengtson, S., & Neubeck, A. (2016). The igneous oceanic crust – Earth's largest fungal habitat? *Fungal ecology*, *20*, 249-255.

Jogaiah, S., Kumar, T., Niranjana, S., & Shetty, S. (2004). First report of gummy stem blight caused by Didymella bryoniae on muskmelon (Cucumis melo) in India. *Plant Pathology*, *53*, 364-369.

Khejornsart, P., & Wanapat, M. (2010). Diversity of Rumen Anaerobic Fungi and Methanogenic Archaea in Swamp Buffalo Influenced by Various Diets. *Journal of Animal and Veterinary Advances*, *9*, 3062-3069.

Kiko, R., & Hauss, H. (2019). On the Estimation of Zooplankton-Mediated Active Fluxes in Oxygen Minimum Zone Regions. *Frontiers in Marine Science*, *6*.

Kirk, P., Cannon, P., Minter, D., & Stalpers, J. (2008). *Ainsworth and Bisby's Dictionary of the Fungi*. Cabi.

Kurakov, A. V., Lavrent'ev, R. B., Nechitailo, T. Y., Golyshin, P. N., & Zvyagintsev, D. G. (2008). Diversity of facultatively anaerobic microscopic mycelial fungi in soils. *Microbiology, 77*(1), 90-98.

Kwaśna, H., Szewczyk, W., Baranowska, M., Gallas, E., Wiśniewska, M., & Behnke-Borowczyk, J. (2021). Mycobiota Associated with the Vascular Wilt of Poplar. *Plants*, *10*(5), 892.

Lê Cao, K.-A., Costello, M.-E., Lakis, V. A., Bartolo, F., Chua, X.-Y., Brazeilles, R., & Rondeau, P. (2016). MixMC: A Multivariate Statistical Framework to Gain Insight into Microbial Communities. *PLOS ONE*, *11*(8), 0160169.

Li, K., Stoof-Leichsenring, K. R., Liu, S. S., Jia, W. H., Liao, M. N., Liu, X. Q., Ni, J., and Herzschuh, U. (2021). Plant sedimentary DNA as a proxy for vegetation reconstruction in eastern and northern Asia. *Ecological Indicators, 132*.

Loughlin, N., Gosling, W., & Montoya, E. (2017). Identifying environmental drivers of fungal non-pollen palynomorphs in the montane forest of the eastern Andean flank, Ecuador. *Quaternary Research*, *89*, 1-15.

McDonald, J. E., Houghton, J. N., Rooks, D. J., Allison, H. E., & McCarthy, A. J. (2012). The microbial ecology of anaerobic cellulose degradation in municipal waste landfill sites: evidence of a role for fibrobacters. *Environ Microbiol*, *14*(4), 1077-1087.

Morlock, M.A., Vogel, H., Russell, J.M., Anselmetti, F.S., Bijaksana, S. (2021). Quaternary environmental changes in tropical Lake Towuti, Indonesia, inferred from end-member modelling of X-ray fluorescence core-scanning data. *Journal of Quaternary Science, 36*, 1040–1051.

Moslemi, A., Ades, P. K., Groom, T., Crous, P. W., Nicolas, M. E., & Taylor, P. W. (2016). Paraphoma crown rot of pyrethrum (Tanacetum cinerariifolium). *Plant Disease*, *100*(12), 2363-2369.

Mundra, S., Bahram, M., & Eidesen, P. B. (2016). Alpine bistort (Bistorta vivipara) in edge habitat associates with fewer but distinct ectomycorrhizal fungal species: a comparative study of three contrasting soil environments in Svalbard. *Mycorrhiza*, *26*(8), 809-818.

Nagano, Y., Nagahama, T., Hatada, Y., Nunoura, T., Takami, H., Miyazaki, J., Takai, K., & Horikoshi, K. (2010). Fungal diversity in deep-sea sediments – the presence of novel fungal groups. *Fungal Ecol.*, *3*, 316-325.

Naranjo-Ortiz, M. A., & Gabaldón, T. (2019). Fungal evolution: diversity, taxonomy and phylogeny of the Fungi. *Biol Rev Camb Philos Soc*, *94*(6), 2101-2137.

Niemeyer, B., Epp, L. S., Stoof-Leichsenring, K. R., Pestryakova, L. A., and Herzschuh, U. (2017). A comparison of sedimentary DNA and pollen from lake sediments in recording vegetation composition at the Siberian treeline. *Molecular Ecology Resources, 17*(6), 46-62.

Nottingham, A., Scott, J. J., Saltonstall, K., Broders, K., Montero-Sanchez, M., Püspök, J., Bååth, E., & Meir, P. (2022). Microbial diversity decline and

community response are decoupled from increased respiration in warmed tropical forest soil. *Nature Microbiology*, *7*, 1650-1660.

Orsi, W. D., Coolen, M. J. L., Wuchter, C., He, L., More, K. D., Irigoien, X., Chust, G., Johnson, C., Hemingway, J. D., Lee, M., Galy, V., & Giosan, L. (2017). Climate oscillations reflected within the microbiome of Arabian Sea sediments. *Scientific Reports*, *7*(1), 6040.

Osono, T. (2019). Functional diversity of ligninolytic fungi associated with leaf litter decomposition. *Ecological Research*, *35*.

Parducci, L., Matetovici, I., Fontana, S. L., Bennett, K. D., Suyama, Y., Haile, J., Kjaer, K. H., Larsen, N. K., Drouzas, A. D., and Willerslev, E. (2013). Molecular- and pollen-based vegetation analysis in lake sediments from central Scandinavia. *Molecular Ecology, 22*(13), 3511-3524.

Parducci, L., Valiranta, M., Salonen, J. S., Ronkainen, T., Matetovici, I., Fontana, S. L., Eskola, T., Sarala, P., and Suyama, Y. (2015). Proxy comparison in ancient peat sediments: pollen, macrofossil, and plant DNA. *Philosophical transactions of the Royal Society of London Series B, Biological sciences, 370*(1660), 20130382.

Pedersen, M. W., Ginolhac, A., Orlando, L., Olsen, J., Andersen, K., Holm, J., Funder, S., Willerslev, E., & Kjaeer, K. H. (2013). A comparative study of ancient environmental DNA to pollen and macrofossils from lake sediments reveals taxonomic overlap and additional plant taxa. *Quaternary Science Reviews, 75*, 161-168.

Pedregosa, F., Varoquaux, G., Gramfort, A., Michel, V., Thirion, B., Grisel, O., Blondel, M., Prettenhofer, P., Weiss, R., Dubourg, V., Vanderplas, J., Passos, A., Cournapeau, D., Brucher, M., Perrot, M., & Duchesnay, É. (2011). Scikit-learn: Machine Learning in Python. *J. Mach. Learn. Res.*, *12*, 2825–2830.

Phookamsak, R., Liu, J.-K., McKenzie, E. H. C., Manamgoda, D. S., Ariyawansa, H., Thambugala, K. M., Dai, D.-Q., Camporesi, E., Chukeatirote, E.,

Wijayawardene, N. N., Bahkali, A. H., Mortimer, P. E., Xu, J.-C., & Hyde, K. D. (2014). Revision of Phaeosphaeriaceae. *Fungal Diversity*, *68*(1), 159-238.

Prenafeta-Boldú, F. X., Summerbell, R., & Sybren de Hoog, G. (2006). Fungi growing on aromatic hydrocarbons: biotechnology's unexpected encounter with biohazard? *FEMS Microbiol Rev*, *30*(1), 109-130.

Quamar, M. F., & Stivrins, N. (2021). Modern pollen and non-pollen palynomorphs along an altitudinal transect in Jammu and Kashmir (Western Himalaya), India. *Palynology*, *45*(4), 669-684.

Russell, J. M., Vogel, H., Bijaksana, S., Melles, M., Deino, A., Hafidz, A., Haffner, D., Hasberg, A. K. M., Morlock, M., von Rintelen, T., Sheppard, R., Stelbrink, B., and Stevenson, J. (2020). The late quaternary tectonic, biogeochemical, and environmental evolution of ferruginous Lake Towuti, Indonesia. *Palaeogeography Palaeoclimatology Palaeoecology,* 556.

Rustler, S., Chmura, A., Sheldon, R. A., & Stolz, A. (2008). Characterisation of the substrate specificity of the nitrile hydrolyzing system of the acidotolerant black yeast Exophiala oligosperma R1. *Stud Mycol*, *61*, 165-174.

Ryberg, M., & Matheny, P. B. (2011). Asynchronous origins of ectomycorrhizal clades of Agaricales. *Proceedings of the Royal Society B: Biological Sciences*, *279*, 2003 - 2011.

Sheppard, R. Y., Milliken, R. E., Russell, J. M., Sklute, E. C., Dyar, M. D., Vogel, H., Melles, M., Bijaksana, S., Hasberg, A. K. M., and Morlock, M. A. (2021). Iron Mineralogy and Sediment Colour in a 100 m Drill Core from Lake Towuti, Indonesia Reflect Catchment and Diagenetic Conditions. *Geochemistry Geophysics Geosystems, 22*(8).

Shoun, H., & Tanimoto, T. (1991). Denitrification by the fungus Fusarium oxysporum and involvement of cytochrome P-450 in the respiratory nitrite reduction. *J Biol Chem, 266*(17), 11078-11082.

Solaiman, Z. M., Abbott, L. K., & Varma, A. (2015). Role of Mycorrhizal Fungi in the Alleviation of Heavy Metal Toxicity in Plants. In (Vol. 41, pp. 241-258). Springer Berlin / Heidelberg.

Stevenson, J. (2018). Vegetation and climate of the Last Glacial Maximum in Sulawesi. In S. O. orcid, D. B. orcid, J. Meyer (Eds.), The Archaeology of Sulawesi. Current Research on the Pleistocene to the Historic Period (pp. 17-29). ANU Press.

Taberlet, P., Coissac, E., Pompanon, F., Gielly, L., Miquel, C., Valentini, A., Vermat, T., Corthier, G., Brochmann, C., & Willerslev, E. (2007). Power and limitations of the chloroplast trnL (UAA) intron for plant DNA barcoding. *Nucleic Acids Res*, *35*(3), e14.

Talas, L., Stivrins, N., Veski, S., Tedersoo, L., & Kisand, V. (2021). Sedimentary Ancient DNA (sedaDNA) Reveals Fungal Diversity and Environmental Drivers of Community Changes throughout the Holocene in the Present Boreal Lake Lielais Svētiņu (Eastern Latvia). *Microorganisms*, *9*(4).

Tedersoo, L., Bahram, M., Puusepp, R., Nilsson, R. H., & James, T. (2017). Novel soil-inhabiting clades fill gaps in the fungal tree of life. *Microbiome*, *5*.

Teunissen, M., Kets, E., Op den Camp, H., Huis in't Veld, J., & Vogels, G. (1992). Effect of coculture of anaerobic fungi isolated from ruminants and non-ruminants with methanogenic bacteria on cellulolytic and xylanolytic enzyme activities. *Archives of microbiology, 157*, 176-182.

Wang, S. N., Fan, Y. G., & Yan, J. Q. (2022). Iugisporipsathyrareticulopilea gen. et sp. nov. (Agaricales, Psathyrellaceae) from tropical China produces unique ridge-ornamented spores with an obvious suprahilar plage. *MycoKeys*, *90*, 147-162.

Zhang, N., & Wang, Z. (2015). 3 Pezizomycotina: Sordariomycetes and Leotiomycetes. In (pp. 57-88).

Zimmermann, H. H., Raschke, E., Epp, L. S., Stoof-Leichsenring, K. R., Schwamborn, G., Schirrmeister, L., Overduin, P. P., and Herzschuh, U. (2017). Sedimentary ancient DNA and pollen reveal the composition of plant organic matter in Late Quaternary permafrost sediments of the Buor Khaya Peninsula (northeastern Siberia). *Biogeosciences, 14*(3), 575-596.

3.8 Supplementary materials
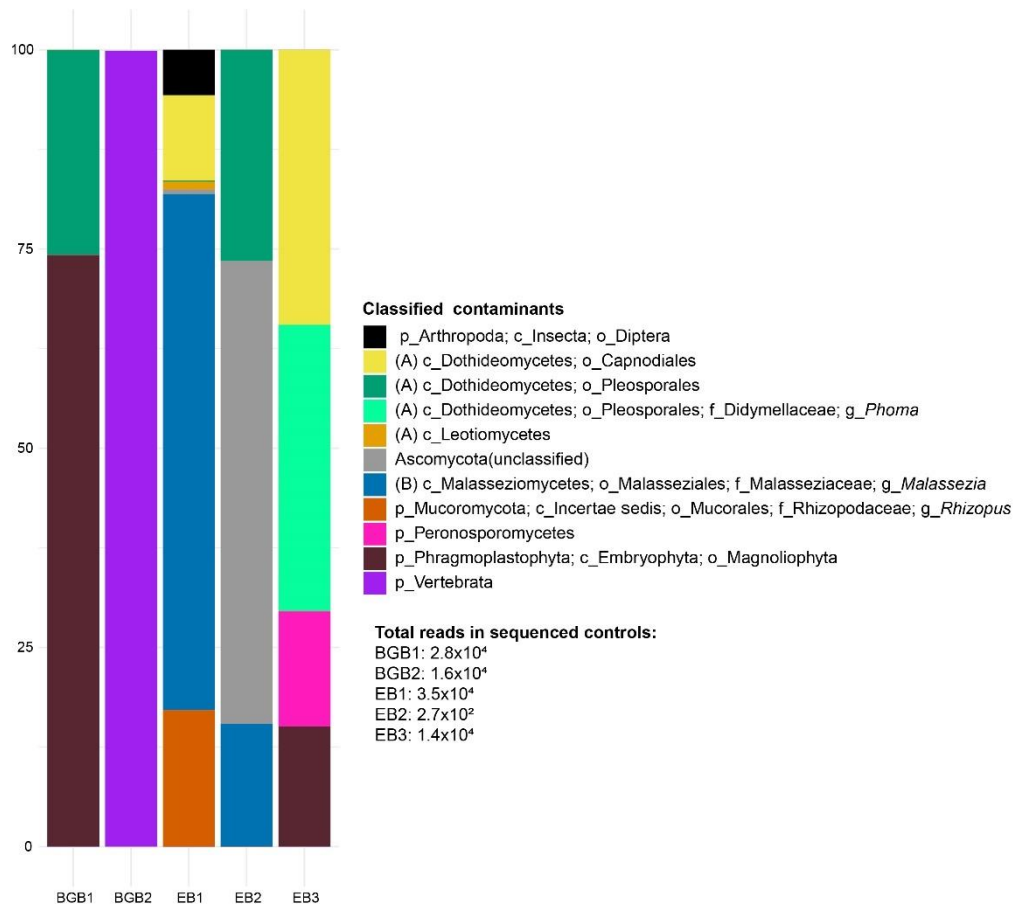
Figure S3.1 Stacked bar graph showing only the relative read abundance (sum=100%) of contaminants from the sequenced background- and extraction blanks. The total number of recovered reads from these taxonomically assigned contaminants in each blank is shown below the colour key. See Fig. S3.2 for an overview of the relative read abundance of contaminants in the background- and extraction controls.
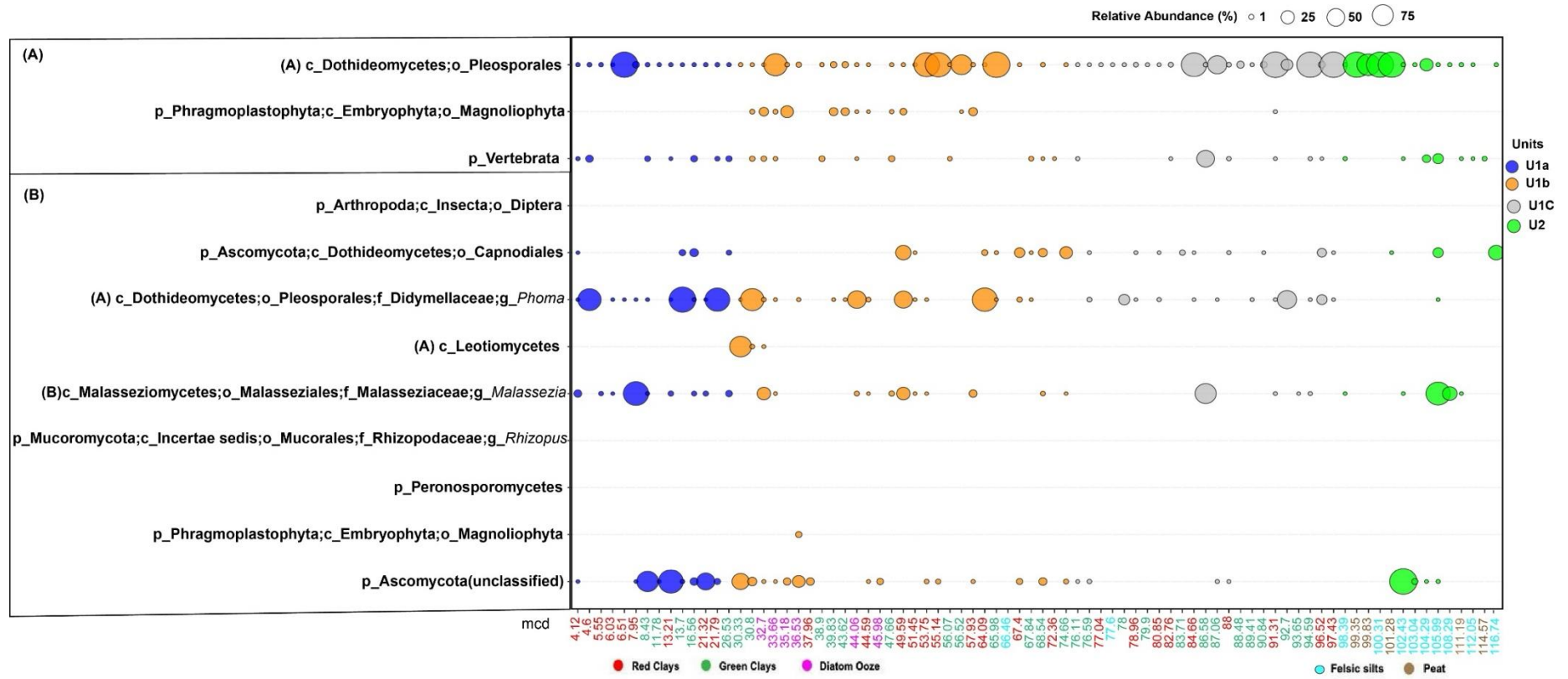
Figure S3.2. Bubble plot showing the relative read abundance of putative contaminants from (A) taxa identified from background blanks and (B) taxa identified from extraction blanks. All ASVs assigned to these taxa were removed from the sample data before downstream analysis.

Chapter 4

A combined pollen and sedimentary ancient DNA (*sed*aDNA) record of late-Glacial and Holocene vegetation changes in the Black Sea region.

This chapter has been submitted to a peer-reviewed international journal.

4.1 Abstract

Several studies have shown that lake sediments represent valuable archives of ancient plant DNA that can be extracted and sequenced to complement palynological studies in reconstructing past vegetation assemblages and their responses to paleoenvironmental and more recent anthropogenic perturbations. However, similar studies have yet to be performed in detail from marine basins. This study used amplicon sequencing analysis of the chloroplast marker gene *trn*L-P6 to reconstruct late-Glacial and Holocene vegetation changes in the southwestern Black Sea region. Parallel pollen identified a predominance of xerophytic herbs (e.g., *Artemisia*), which dominated the steppe landscape of the coastal plains surrounding the Black Sea during the late Glacial and early Holocene. According to the pollen analysis, the warm and wet conditions with the onset of the Atlantic (~ 8 ka cal. BP) expanded arboreal oak forest vegetation. Furthermore, putative anthropophytes such as cultivated cereals (*Triticum* and cereale-type pollen) and ruderals (e.g., *Filipendula*) indicative of early farming practices were most consistently present during the Bronze Age, overlapping with the most recent Subatlantic chronozone.

High pollen-producing xerophytic steppe vegetation such as *Artemisia* were minor contributors to the *trn*L-P6 pool during the late Glacial and early Holocene. Instead, the *trn*L-P6 approach recorded a predominance of C_4 grasses (Panicoideae) and native C_3 Pooid grasses within the wheat tribe Triticeae, which may have been used for the cultivation of cereal crops by Neolithic, Iron-, or Bronze Age farmers. Moreover, nitrogen-fixing pioneer vegetation (Fabaceae, *Alnus*, and *Populus*) were relatively abundant sources of the cpDNA marker gene that may have occupied the coastal freshwater catchment before the reconnection with the Mediterranean Sea ~9 ka cal. BP. The onset of the Atlantic saw a drastic increase in the relative read

abundance of *trn*L-P6 from the native marshland inhabiting halophyte *Artemisia maritima* as the possible source of *Artemisia* pollen, which would explain why *Artemisia* remained a relatively abundant pollen source throughout the wetter Holocene.

Moreover, softwood arboreal taxa (*Alnus*, *Salix*, *Populus*, and *Tilia*), which usually occupy nutrient-rich alluvial sediments closest to the rivers that are often inundated, predominated the *trn*L-P6 pool over hardwood taxa (*Ulmus, Carpinus betulus, Quercus*, and *Acer*), which are usually zoned on less frequently inundated elevations further away from the riverbanks. Lastly, sedimentary *trn*L-P6 metabarcoding identified native *Athyrium filix-femina* (lady fern) and *Filipendula ulmaria* (meadowsweet). These taxa can be abundant members of the low diversity ground cover vegetation in moist riparian forests, arguing against *Filipendula* being an anthropophyte used as a ruderal during prehistoric agricultural activities. This study shows that marine basins can provide valuable long-term archives of *sed*aDNA from paleovegetation and can improve the identification of the origin of host plants of fossil pollen and improve pollen-based interpretations about to what extent climatic vs anthropogenically perturbations played a role in shaping the paleo-floristic landscape of the coastal hinterland.

4.2 Introduction

Fossil pollen and spores provide a valuable record of Quaternary paleovegetation assemblages and landscape changes in the context of past climate- and/or more recent anthropogenic perturbations (e.g., Anshari et al., 2004; Hope, 2001; Stevenson, 2018). Palynological studies focus mainly on differentiating paleovegetation at family or genus levels. Overlapping morphological features can complicate the identification of closely related plant species (Mander & Punyasena, 2014) even for Quaternary paleovegetation assemblages despite the relatively well-known relationship between pollen and source plants compared to older records (e.g., Giesecke et al., 2014). Species-level characterisation of pollen can also become too time-consuming, especially in highly resolved temporal records, and the best praxis approach would require cross-validation of the data by independent palynologists (Cleal et al., 2021). Notably, the similarity in fossil pollen morphology between genera of true grasses

(Poaceae) complicates the ability to distinguish between wet climate C_3 vs. dry climate C_4 grasses and grasses that can switch between C_3 and C_4 carbon fixation pathways (Mander & Punyasena, 2014). Therefore, grasses are usually grouped as Poaceae or Graminae in pollen-based paleovegetation and paleoclimate studies (e.g., Connor et al., 2013; Filipova-Marinova et al., 2012; Mudie et al., 2007; Shumilovskikh et al., 2012). A notable exception is the ability to identify cultivated cereals at the genus level, which has been used to reconstruct the arrival of humans and the onset of regional agricultural activities during the Holocene (e.g., Filipova et al., 2006; 2012). However, identification at the species level would be needed to distinguish between cultivated crops and closely related native wild-type species of the same genus. For example, the genus *Triticum* within the wheat tribe Triticeae includes the cultivated bread wheat species *T. aestivum* L. and closely related wild-type species of *Triticum* native to countries surrounding the Black Sea, including *Bulgaria* (POWO,2023).

Moreover, the origin of airborne pollen and spores can sometimes not be inferred as they can travel long distances. As a result, pollen-based palynological studies mainly reflect landscape-scale diversity of plant fossils observed within a depositional basin representing the source plant composition within an area of $\sim 10^5$ km^2 (i.e., 300 x 300 km) (Cleal et al., 2021). In addition, palynological analysis can also cover regional-scale diversity. This describes the diversity of plant fossils observed within a paleo-floristic province and most likely reflects the source vegetation communities in an area larger than 10^5 km^2 (Cleal et al., 2021).

Another issue is the variability in pollen productivity between different plant taxa. Quaternary palynological data sets from northern and temperate latitudes provide robust information about the richness of wind-pollinated taxa and most tree species at landscape and regional scales (Reitalu et al., 2019). Poaceae and Cyperaceae are the most abundant wind-pollinated herbs. This vegetation can occupy a wide range of habitats, and their pollen can be widely dispersed, making it difficult to determine the origin of Poaceae and Cyperaceae in palynological studies. Most other herbs are underrepresented in pollen spectra since they produce fewer pollen that different

vectors can disperse, and their fossil pollen are generally less well preserved (Leroy & Roiron, 1996).

DNA-barcoding approaches utilising a variety of variable regions of chloroplast DNA (cpDNA) are also widely used to study phylogenetic and evolutionary relationships of numerous plant taxa (Dong et al., 2012; Palmer et al., 1988). The non-coding cpDNA regions are phylogenetically more informative than the coding regions at lower taxonomic levels because they are under less functional constraints and evolve rapidly (Gielly & Taberlet, 1994). For example, cpDNA barcoding methods have been developed to study the evolution and phylogeny of the genus *Triticum*, which includes the bread wheat species *T. aestivum* L., and other cultivated and wild-type species (Golovnina et al., 2007). Such detailed species-level taxonomic resolution for *Triticum* is not possible based on pollen. Several studies have shown that lacustrine sedimentary records also represent important archives of ancient vegetation DNA (Capo et al., 2021 and references therein). Extraction of this ancient sedimentary DNA (*sed*aDNA) and subsequent sequencing analysis of preserved vegetation metabarcoding genes has the potential to complement fossil pollen in reconstructing past vegetation assemblages and their responses to paleoenvironmental and more recent anthropogenic perturbations (e.g., Alsos et al., 2021; Courtin et al., 2021; Epp et al., 2015; Li et al., 2021; Niemeyer et al., 2017; Parducci et al., 2013; 2015; Pederson et al., 2013; Zimmermann et al., 2017). Since DNA degradation processes limit the length of the fragments that can be retrieved from ancient specimens (Boere et al., 2011; Willerslev & Cooper, 2005), only stretches of cpDNA with less than 200 base pairs (bp) can be confidently analysed (Parducci et al., 2005). The short (10-143 bp; on average ~90 bp) variable P6-loop in the chloroplast *trn*L (UAA) intron (i.e., *trn*L-P6) (Taberlet et al., 2007) was found to be well preserved in the geological record (e.g., Capo et al., 2021 and references therein). The flanking regions are highly conserved so that most plants can be targeted for amplicon sequencing. A vast number of *trn*L-P6 sequences of contemporary Northern Hemisphere plant families are available in public databases such as NCBI's nonredundant nucleotides (nr/nt) database for comparison and taxonomic assignments of newly recovered environmental *trn*L-P6 sequences. Most vegetation can be identified at the family

level, and in relatively low biodiversity environments, sequencing analysis of permafrost-preserved *trn*L-P6 outperformed the taxonomic resolution of pollen and resulted in the identification of ancient vegetation at the family level (100% of sequenced *trn*L-P6), 75% at the genus level, and 33% at the species level (Sonstebo et al., 2010).

This combination of properties has made *trn*L-P6 one of the most frequently used plant metabarcoding genes in *sed*aDNA studies for reconstructing temporal changes in paleovegetation assemblages (Capo et al., 2021, and references therein). Since chloroplasts are organelles found predominantly in plant leaves where most photosynthesis takes place, *sed*aDNA records targeting chloroplast-derived metabarcoding genes are thought to mainly represent catchment vegetation that drained into depositional basins as decaying chloroplast-rich plant litter via riverine- or terrestrial runoff (e.g., Alsos et al., 2018; Liu et al., 2020; Paus et al., 2015; Parducci et al., 2017; Voldstad et al., 2020). Lacustrine *sed*aDNA studies targeting cpDNA are, therefore, considered particularly useful for reconstructing paleovegetation assemblages at a more localised landscape scale.

In contrast, marine basins have thus far been greatly overlooked for reconstructing paleovegetation assemblages using *sed*aDNA approaches. Due to the greater distance to terrestrial source vegetation and a more complex and larger drainage area, marine *sed*aDNA records may represent the plant composition from the terrestrial hinterland at a larger landscape- or regional scale compared to inland lakes. On the other hand, the quality and amount of sedimentary cpDNA in marine records may be substantially compromised due to the longer travel distance of drained chloroplast-rich plant litter from the source location and possibly longer exposure time to biotic and abiotic degradation processes before burial.

The semi-isolated Black Sea is an excellent location to close this knowledge gap. For example, the Black Sea is sensitive to climate-driven environmental changes, and the underlying sediments represent high-resolution geobiological and geochemical archives of continental climate variability and concurrent terrestrial and aquatic ecosystem responses to hydrological and environmental conditions that prevailed at

the time of deposition (Coolen et al., 2013; Hoyle et al., 2021).

For example, a subset of palynological studies has provided detailed information about multi-decadal to centennial-scale coastal vegetation and terrestrial climate variability in the Black Sea region as far back as the last glacial maximum (LGM) (Atanassova, 2005; Connor et al., 2013; Connor et al., 2007; Cordova et al., 2009; Filipova-Marinova, 2007; Filipova-Marinova et al., 2012; Mudie et al., 2007; Mudie et al., 2002; Shumilovskikh et al., 2012). Moreover, various studies have shown that both organic carbon depleted and oxygenated late Glacial lacustrine sediments and the overlying organic-rich sediments that were deposited during permanent stratified and euxinic conditions, which had developed after the marine reconnection, represent rich archives of ancient genetic material from past plankton species including those lacking preserved microfossils (Coolen, 2011; Coolen et al., 2013; Coolen et al., 2009; Corinaldesi et al., 2011; Giosan et al., 2012; Manske et al., 2008). Moreover, temporal changes in plankton communities inferred from *sed*aDNA showed strong correlations with the paleohydrological and paleoenvironmental conditions that prevailed at deposition (Giosan et al., 2012; Coolen et al., 2013). These studies provided enough leverage to assume that *sed*aDNA from terrestrial and aquatic vegetation could also be preserved in the sedimentary record of the Black Sea.

For this study, we performed amplicon sequencing of sedimentary *trn*L-P6 to reconstruct terrestrial vegetation changes in the western Black Sea region in response to multi-decadal scale late-glacial and Holocene climate variability. The 295-cm-long giant gravity core (GGC-18) used for this study was recovered from a water depth of 971m in the western basin of the Black Sea (42°46.569N:28°40.647E) in September 2006. The coring location falls within the Black Sea region of the Euxinian province of the European deciduous forest. The eastern Balkan Range area (Eastern Stara Planina Mts., Cape Emine area) is dominated by xerothermic forest vegetation (Filipova-Marinova et al., 2012).

GGC-18 comprises an uninterrupted and near-to-continuous record of the Younger Dryas cold stadial, deglacial (Preboreal), and the Holocene. Pollen and non-pollen palynomorphs have been analysed in detail from the bottom 195 cm (11,600-94 a cal. BP; Preboreal to recent) of the same sediment record (Filipova-Marinova et al., 2012). In addition, the same sediment record has been analysed extensively using

multiproxy approaches, including isotope lipid biomarker geochemistry to reconstruct sea surface temperature and salinity (SST and SSS), to identify sediment intervals corresponding to the late-glacial and Holocene climate stages and to study the response of the Black Sea's planktonic populations to the late-glacial and Holocene climate stages and stage transitions using *sed*aDNA (Coolen et al., 2013).

The overarching aims of this study were to elucidate if marine basins provide archives of *sed*aDNA from distant paleo-floristic ecosystems and to what extent sequencing analysis of sedimentary chloroplast marker genes (i.e., *trn*L-P6) can complement fossil pollen in reconstructing landscape- and/or regional scale vegetation changes in the context of well-described paleohydrological conditions that prevailed during key climate stages covering the late-Glacial and Holocene.

4.3 Material and Methods

4.3.1 Sediment sampling, description of environmental stages, and age models

The *sed*aDNA record of past vegetation changes (this study) and previously analysed pollen grain and geochemical datasets presented in this study stem from late Glacial and Holocene sediments of Giant Gravity Core GGC18 (total length of 287 cm) (Coolen et al., 2006; Filipova-Marinova et al., 2012). GGC18 was recovered from a water depth of 971m in the western basin of the Black Sea (42°46.569" N:28°40.647" E) during cruise AK06 on the *R/V Akademik* (Institute of Oceanology, Bulgarian Academy of Sciences; IOBAS) in September 2006. The coring location falls within the Black Sea region of the Euxinian province of the European deciduous forest. The eastern Balkan Range area (Eastern Stara Planina Mts., Cape Emine area) is dominated by xerothermic forest vegetation (Filipova-Marinova et al., 2012).

On board the R/V Akademik, the core was cut into five core sections, and a circular saw was used to cut the core liners on both sides simultaneously. A piano wire was used to cut the sediment cores in half. Sterile knives were used to remove the top 0.5 cm of sediment from split core sections. Then, samples were obtained using sterile headless 3 mL syringes with one cm diameter. The top 0.5 cm in these "mini corers" were also discarded to minimise the chance of contamination. The upper 8 cm of sediments representing the last 450 years of deposition was recovered using a multi-

corer, but this material was no longer available for this study. Samples from GGC18 were obtained at one cm resolution between 8 and 123 cm, thirty-three one-cm intervals were acquired between 123 and 193 cm (roughly every other cm), and every other 10 cm was sampled from the remainder of the core (i.e., 174 intervals in total). Detailed information about the age model of the sedimentary record and sampling procedures, including precautions taken to prevent (cross) contamination with foreign DNA, can be found elsewhere (Coolen et al., 2009; 2013; Giosan et al., 2012).

4.3.2 DNA extraction and amplicon sequencing of sedimentary *trn*L-P6

Genomic DNA was extracted from 8-10 grams of wet-weight sediment using the PowerMax™ Soil DNA Isolation Kit (Mobio, Carlsbad, CA) inside a horizontal laminar flow bench in a clean lab following the manufacturer's protocol. Beforehand, the horizontal flow bench was UV-sterilized, and all surfaces inside were decontaminated with DNase-Away solution (Coolen et al., 2013). Co-extracted humic acids were removed from the 172 DNA extracts using the One-Step PCR-inhibitor Removal Kit (Zymoresearch), and the lack of PCR inhibition was confirmed by Coolen et al. (2013). The concentrations of the purified DNA extracts were quantified fluorometrically using the Quant-iT™Picogreen dsDNA Assay Kit (Molecular Probes). Genomic DNA extracted from all 172 available sediment intervals spanning the last 13,000 years of deposition served as the template for *trn*L-P6 library preparation. In addition, extractions were performed without the addition of sediment as controls for contamination during DNA extraction. Aliquots of these Extraction Blanks (EB) and background blanks (no template present) were amplified and sequenced in parallel. Equimolar amounts of gel-purified individually barcoded *trn*L-P6 amplicons were pooled for paired-end sequencing (2x75 bp/150 cycles) on an Illumina MiSeq instrument at the Australian Genome Research Facility (AGRF) in Perth following AGRF's standardised protocol. See the materials and methods section of Chapter 2 of this thesis for further details about the protocols involving library preparation and amplicon sequencing of sedimentary *trn*L-P6.

4.3.3 Taxonomic assignments and removal of unassigned reads plus contaminants

As described in the Materials and Methods section of Chapter 2, using ObiTools (Boyer et al., 2016), raw sequences were paired with an alignment score threshold of 20, assigned to samples, and de-replicated. Low-count sequences (<10) and short reads (<10 nucleotides) were removed using obigrep, and PCR errors were removed using obiclean. Ecotag was used for the taxonomic assignment of remaining unique and genuine ASVs. The *trn*L reference database for taxonomic assignment of the ASVs was created using ecoPCR from release 143 of the European Nucleotide Archive. Contaminant ASVs that appeared in the samples, extraction blanks, and background amplification blanks were removed from the dataset, and only ASVs that represented genuine paleovegetation and could be identified at ranks low enough for meaningful paleoenvironmental interpretations were considered for downstream analysis (i.e., family, clade, subfamily, tribe, genus, or species level). We considered all ASVs assigned at the same lowest reliable taxonomic rank as a unique taxon, and the sum of reads of each taxon formed the species abundance matrix for ordination and biostatistical analyses described below.

4.3.4 Bioinformatics and biostatistics of the clean *trn*L-P6 datasets

Canonical analysis of principal coordinates (CAP) was performed in PRIMER-e v.7 (Clarke & Gorley, 2015) as a sensitive ordination tool to visualise the level of Bray-Curtis dissimilarities in paleovegetation communities (taxa) between samples and the climate stages as shown in Fig. 1). Before Bray-Curtis dissimilarity analysis, the *trn*L-P6 and pollen-inferred paleovegetation abundance matrices (taxon levels) were normalised to 100%, and square root transformed. The transitions between the climate stages in the sedimentary record of GGC18 were defined previously from the observed shifts in pollen-inferred paleovegetation (Filipova-Marinova et al., 2012; and this thesis chapter). Then, global- and pairwise analysis of similarity (ANOSIM) was performed in PRIMER-e v.7 to determine if the paleovegetation assemblages identified through stratigraphic analysis of *trn*L-P6 and pollen differed significantly between climate stages. Indicator Species Analysis (ISA) was performed using the R package IndicSpecies (De Caceres & Legendre, 2009) to reveal the significant association of *trn*L-P6 vs. pollen-identified taxa with the Late-Glacial and Holocene climate stages. Fossil pollen assemblages were previously analysed in 53 overlapping

sediment intervals of GGC18 (Filipova-Marinova et al., 2012), and this dataset was used for comparison of the paleovegetation inferred from sedimentary *trn*L-P6 metabarcoding (this study).

4.4 Results and Discussion

4.4.1 Core lithology and description of chronozones

Calcium- and total organic matter (TOC) content follows distinct profiles in sedimentary records from the Black Sea obtained at greater water depth (>100 m) where permanent stratification and bottom water euxinia prevailed at the time of deposition (Murray et al., 1989). Therefore, the downcore distribution of Ca and TOC content of GGC18 (Coolen et al., 2013) was used for this study to characterise the core lithostratigraphy further and to verify the age model (Fig. 4.1). The oldest section of the core (> 11,400 calendar years before the present; 11.4 ka Cal. BP) consists of glacial-type sediments deposited during the dry and cold Younger Dryas stadial when lower primary productivity most likely resulted in the deposition of TOC depleted sediments with relatively low authigenic calcite content (Fig. 4.1) (Bahr et al., 2005; Major et al., 2002).
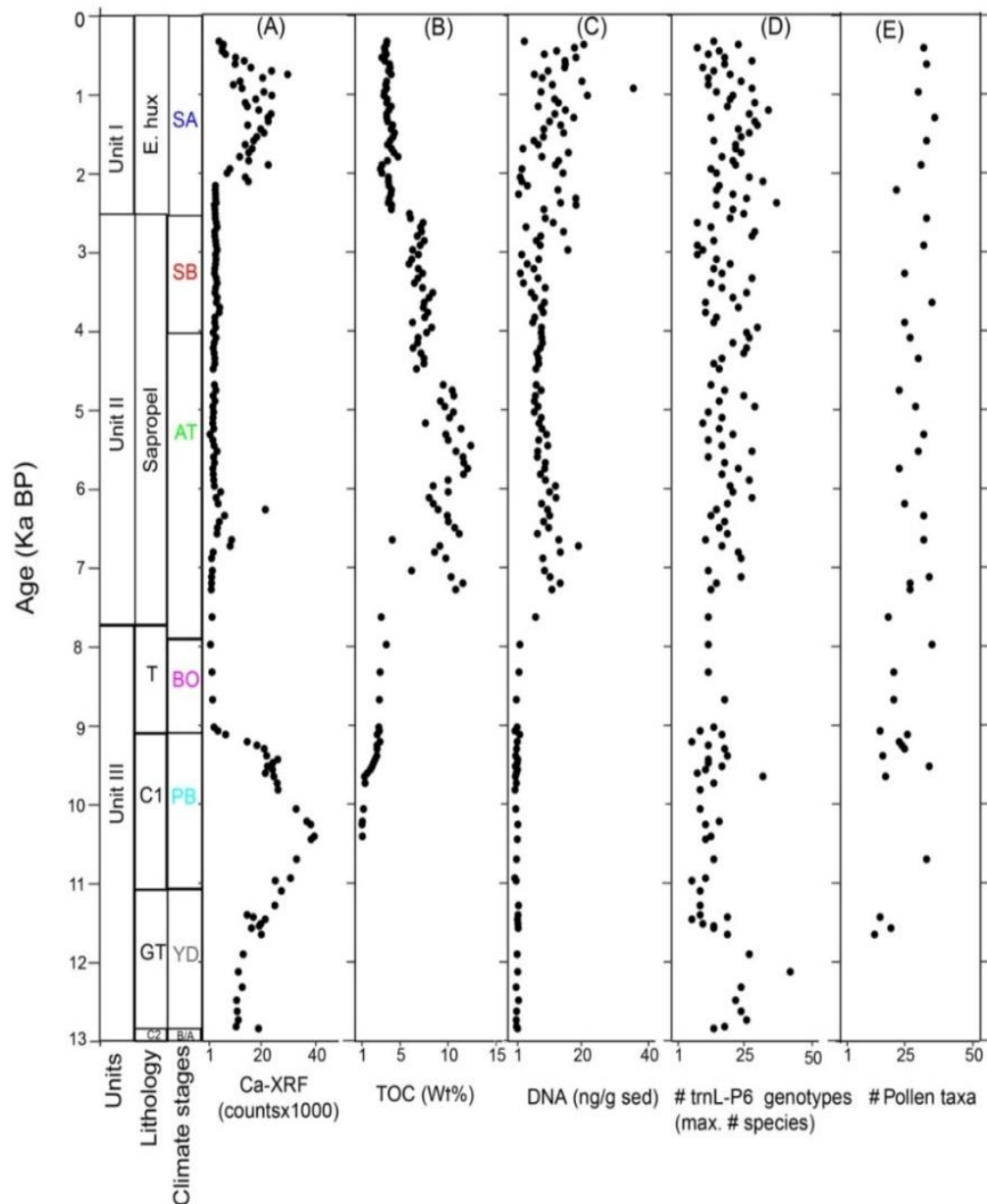
Figure 4.1 Core lithology, and climate stages of MC19 and GGC18. Changes in the paleodepositional environment was partly inferred from the sedimentary calcium (A) and TOC content (B) and shown for comparison alongside the amount of extracted DNA (C) and the number of plant taxa inferred from *trn*L-P6 genotyping (D) vs. pollen (E). See Filipova-Marinova et al. (2012) for a detailed overview of the plant taxa identified through pollen from the exact same core and sediment intervals. Abbreviations of the climate stages: SA (Subatlantic; ~2515 a BP until the present), SB (Subboreal; ~2515 to ~4086 a BP), AT (Atlantic; ~4086 to ~7628 a BP), (Boreal; ~7628 to ~9388 BP), PB (Preboreal; ~9,388 to ~11,100 a BP) and YD (Younger Dryas; ~11,100 to ~12,800 a BP). (See results for a detailed description of these climate stages and sediment lithologies).

The Younger Dryas caused pronounced cooling everywhere in Europe and is recognised as the last most significant stage of climate deterioration before the onset of the Holocene interstadial (Berglund et al., 1994; Mudie et al., 2007; Wick et al., 2003). Section C1 (~11.4-9.4 ka cal. BP) overlapped with the Preboreal when warmer but still relatively dry climate conditions led to elevated primary productivity and a return in maximum calcite deposition (Fig. 4.1). The relatively organic-rich (2.4 ± 0.8 wt% TOC) transition sapropel (T-interval; ~9,4-8 ka cal. BP) was deposited during the Boreal chronozone when an increase in humidity combined with relatively warm conditions caused a further increase in primary productivity (Major et al., 2002). Moreover, the onset of the Boreal marks the timing of the postglacial reconnection with the Mediterranean Sea and the initial influx of saline waters (Coolen et al., 2013; Mudie et al., 2007) via the Bosporus Straight.

A significant change in climate conditions occurred with the transition into the Atlantic chronozone (~ 8-5 ka cal. BP). The Atlantic was the warmest and most humid climate stage of the Holocene. It started when high humidity, regulated by the transport of air masses from the Atlantic Ocean, reached the Balkan Peninsula (Tonkov & Bozilova (1995). The interplay between an increase in precipitation and riverine drainage of freshwater, mainly from the Danube River to the east, and the inflow of saline bottom waters through the Bosporus Strait during this chronozone led to permanent water column stratification, bottom water euxinia, and the deposition of the organic-rich (TOC > 15 wt %) laminated sapropel of Unit II (Hay, 1988), a few centuries later (~7.6 ka Cal. BP) (Fig. 4.1). The deposition of the organic-rich sapropel continued during the relatively warm and dry Subboreal (5-2.5 ka cal. BP) that followed. The relatively organic-rich (3.8% ± 0.5% TOC) laminated coccolith marl of Unit I (last 2.5 kyr) was deposited during the cool and wet Subatlantic chronozone (Wanner et al., 2008) during which the Black Sea experienced a freshening throughout the entire basin (e.g., Coolen et al., 2013; Van der Meer et al., 2008) and a gradual decline in sea surface temperature (SST) from ~20 °C to 17 °C (Coolen et al., 2013). However, recent alkenone D/H ratios performed on sediments from GGC18 suggest that a substantial freshening of the Black Sea started roughly 1000 years earlier with the onset of the Bronze Age (Huang et al., 2021). In addition, sedimentary and

144

paleoenvironmental analysis of GGC18 suggests that intensified land use and deforestation over the last ~3000 years led to an increased drainage of sediments from the Danube River and a rapid increase in its delta (Giosan et al., 2012). These man-made environmental changes most likely also contributed to an increased freshening of the Black Sea during the Subatlantic chronozone. Changes in these hydrological balances since the Late Glacial and during the Holocene are relevant for our discussion below about the origin of chloroplast-rich plant litter as the primary source for the sedimentary *trn*L-P6 plant metabarcoding gene. For the most part, these chronozones overlap with the local pollen assemblage zones (LPAZ) (Fig. 4.1), which were previously identified in GGC18 based on clustering analysis of relative changes in pollen spectra (Filipova-Marinova et al., 2012): LPAZ-1 (Younger Dryas), LPAZ-2 (Preboreal), LPAZ-3 (Boreal), LPAZ-4 (Atlantic and the first one kyr of the Subboreal), LPA-5 (remainder of the Subboreal), and LPAZ-6 (Subatlantic) (Fig. 4.1).

4.4.2 Recovery of sedimentary *trn*L-P6 amplicons

In the organic-rich marine sediments (U2+U1), which were deposited during permanently stratified conditions and bottom water euxinia (i.e., spanning LPAZ-4 to LPAZ-6), the DNA content was on average 20 times higher (~20 ng/g sediment) than in the transition sapropel (LPAZ-3) and throughout the TOC-depleted lacustrine Unit III sediments spanning LPAZ-1 and 2. (Fig. 4.1). Unit III was deposited under fully oxygenated conditions, considered less favourable for preserving organic matter. However, we previously reported the presence of relatively long (~500 bp) marker genes assigned to freshwater plankton in the TOC-poor Unit III intervals and that adsorption to clay minerals likely aided in long-term DNA preservation (Coolen et al., 2013). Therefore, we initially tried to amplify relatively long (~450 bp) *trn*L gene fragments using primers *trn*L-G combined with primer *trn*L-D (Taberlet et al., 2007), but this resulted in successful PCR amplification in only 40 % of the samples with most failed attempts in the oldest TOC-poor Unit III sediments. Instead, the much shorter P6 loop in the *trn*L (UAA) intron could be amplified and sequenced at multi-decadal resolution in 155 out of 178 available sediment intervals (i.e., 78% success rate). The higher success in amplifying shorter *trn*L fragments suggests that a substantial portion of the sedimentary chloroplast DNA had undergone postmortem

degradation and originated from paleovegetation sources. On average, we recovered 10^4 *trn*L-P6 reads per sample. Before downstream analysis, up to 10% of reads that also occurred in the background and/or extraction blanks (Fig. S4.1) were removed. The remaining genuine reads were assigned to 389 amplicon sequence variants (ASVs). Taxonomic classification of these ASVs revealed 55 native taxa of paleoenvironmental relevance that could be identified at the family level or lower (see Fig. 4.2 and Table S4.1 for further details). Forty-eight out of 55 *trn*L-P6 taxa were previously identified through fossil (n=72 pollen taxa) in 53 intervals spanning the entire record of GGC 18 (Filipova-Marinova et al., 2012). A similar bubble plot was used to represent the downcore distribution of the pollen composition (Fig. 4.3) for direct comparison with the community composition identified through sedimentary *trn*L-P6 metabarcoding. The green-marked text in the figures refers to the taxonomic levels shared between both proxies (Figs. 4.2 and 4.3). Both proxies revealed a comparable downcore distribution in the average number of taxa (n= ~25) per analysed interval (Fig. 4.1). The paleovegetation categories included aquatics (n=5 taxa for *trn*L-P6 vs n= 2 for pollen), ferns (n=1 vs n=3), sedges (n=1 taxa for both proxies), grasses (n=5 vs n=4), herbs (n=17 vs n=40), angiosperm trees and shrubs (TRSH; n=20 for both proxies), and conifers (n=6 vs n=4).
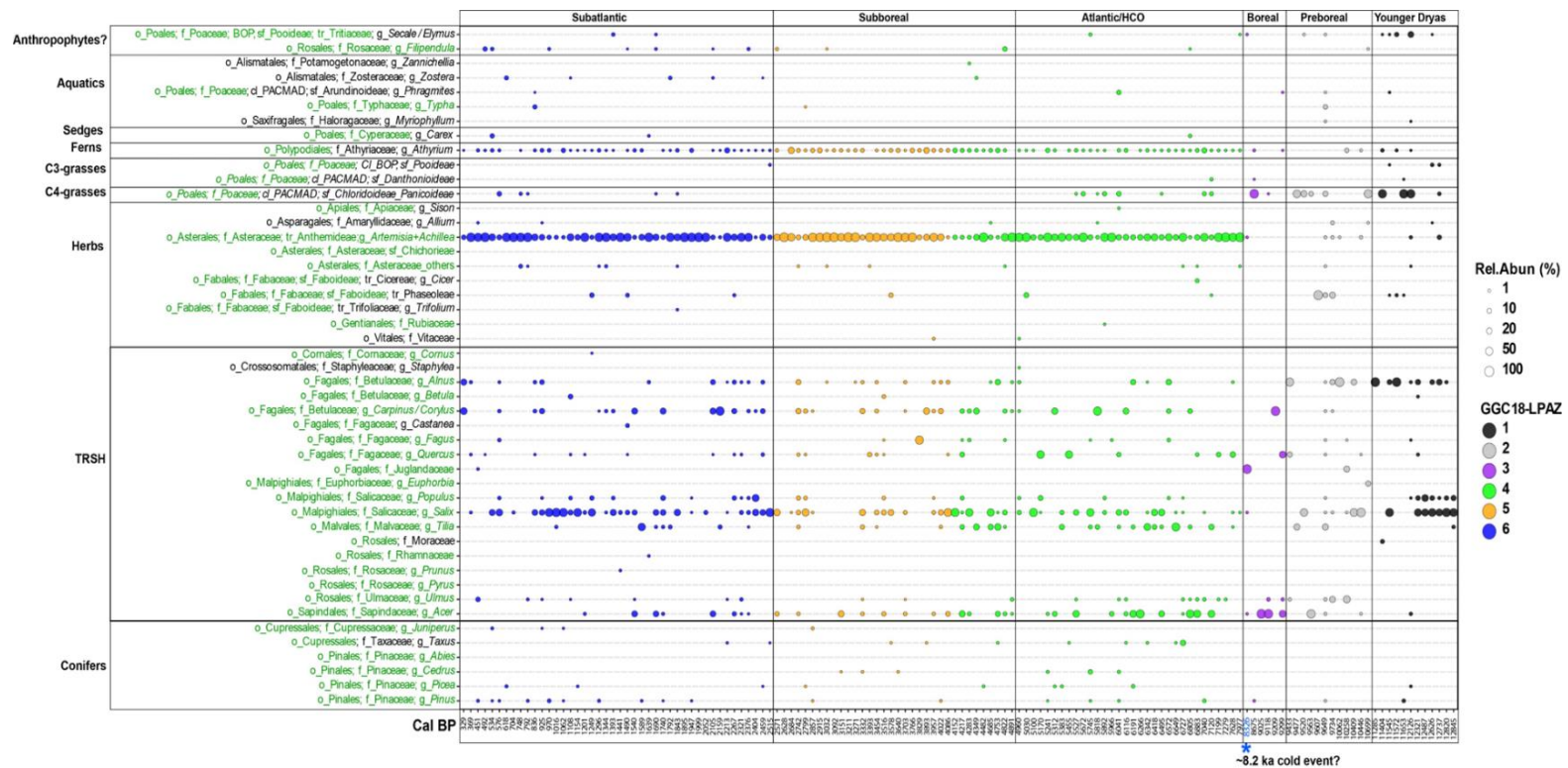
Figure 4.2 Paleovegetation assemblages in GGC18 inferred from sedimentary *trn*L-P6 metabarcoding. The relative read abundance data only includes taxa assigned at family or lower taxonomic ranks suitable for paleoenvironmental interpretations: Order (o_), family (f_), clade (cl_), subfamily (sf_), tribe (tr_), genus (g_). The identified taxa are in alphabetical order and grouped based on vegetation type: putative anthropophytes, aquatics, sedges, ferns, sum of C$_3$ grasses of the BOP- and PACMAD (Danthoniadeae) clades vs. C$_4$ grasses of the PACMAD clade; see Table S4.1 for a full overview of grasses identified at genus level, herbs, trees and/or shrubs (TRSH), and conifers. Green text refers to the taxonomic ranks that were also identified through the parallel analysis of fossil pollen (Filipova-Marinova et al., 2012; and Fig. 4.3). Bubble size and colour refer to the relative read abundance of taxa and Local Pollen Assemblage Zones (GGC18-LPAZ; Filipova-Marinova et al., 2012), respectively. The calendar ages of the analysed intervals are indicated on the x-axis. The vertical lines mark the transitions between the late-Glacial and Holocene climate stages after Coolen et al. (2013), which greatly overlap with the LPAZ's except for the transition between the Holocene Climate Optimum (HCO; also known as Atlantic chronozone) and the Preboreal. The x-axis shows the calendar ages of the analysed sediment intervals. A high relative read abundance of Juglandaceae was observed at ~8.3 ka BP, which may represent the well-known 8.2 ka cold event.
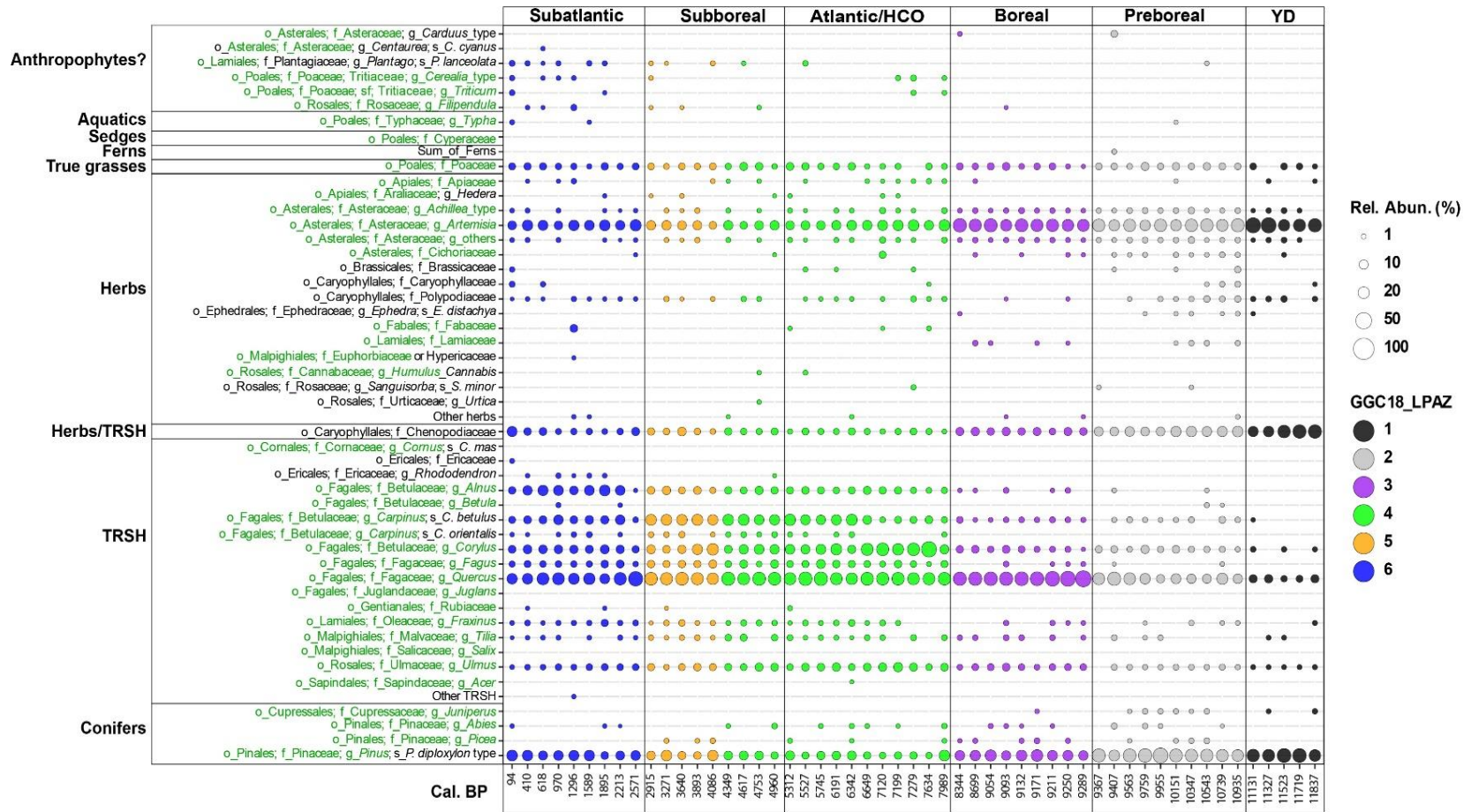
Figure 4.3 Paleovegetation pollen assemblages in GGC18 (modified from Filipova et al., 2012). Green text refers to the taxonomic ranks that were also identified through sedimentary *trn*L-P6 metabarcoding (Fig. 4.2). (See caption of Fig. 4.2 for overlapping details).

148

Before detailing the temporal changes in the various taxa identified using both approaches, it is important to stress that quantitative changes of *trn*L-P6 vegetation should be interpreted with caution due to the possibility of methodological bias (e.g., PCR efficiency) and differences in preservation of DNA among the type of plant material (Capo et al., 2021 and references therein). These issues could have contributed to the far lower consistency in the downcore distribution of *trn*L-P6 compared to pollen (Figs. 4.2 and 4.3). Nevertheless, as discussed further below, relative changes between both proxies provided relevant insights into (a) the origin of the source material, (b) the landscape where the vegetation used to grow, and (c) the paleoenvironmental conditions that played a role in shaping these communities.

We first determined to what extent the paleovegetation communities differed significantly among the pollen- and chronozones. Canonical Analysis of Principal coordinates (CAP) analysis of the *trn*L-P6 dataset revealed three separate clusters with partial overlap between pollen zones: (a) LPAZ-1 and LPAZ-2; (b) LPAZ-3; and (c) LPAZ 4-6 (Fig. 4.4).
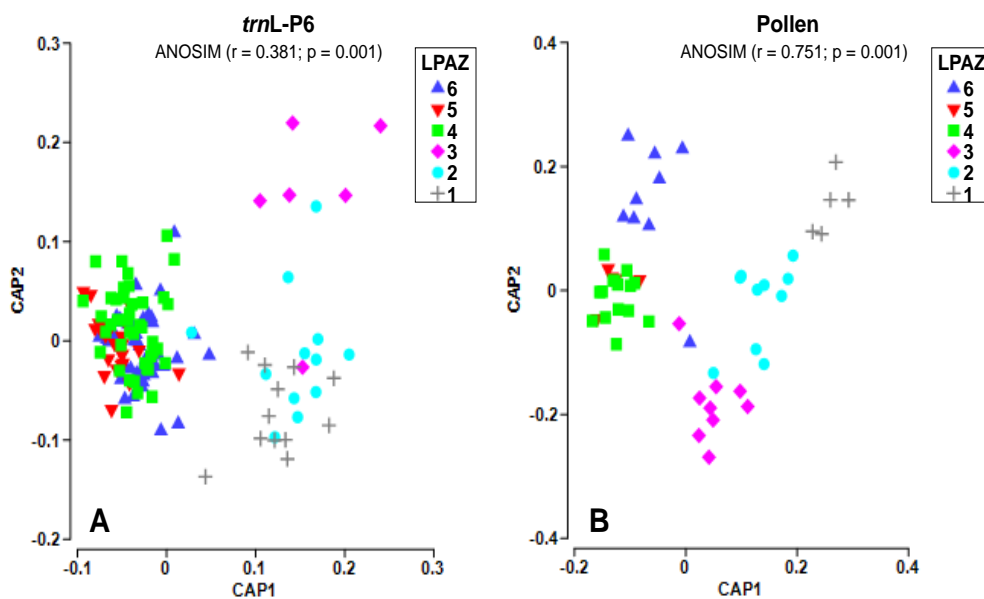
Figure 4.4 Canonical analysis of principal coordinates (CAP) showing the constrained ordination of paleovegetation assemblages identified in GGC18 using (A) pollen palynomorphs and (B) sedimentary *trn*L-P6 metabarcoding. The paleovegetation categories for both proxies are based on the six Local Pollen Assemblages Zones (LPAZ) previously defined from the pollen data of GGC18 by Filipova-Marinova et al. (2012). The global analyses of similarity (ANOSIM) results are displayed above the figures. According to ANOSIM, both proxies revealed that the overall community composition differed significantly among all sample categories. (See Table 4.1 for pairwise ANOSIM results).

Constrained ordination analysis using the pollen dataset revealed separate clusters for all pollen zones except for the overlap observed between samples from LPAZ-5 and 6 (Fig. 4.4). Subsequent analysis of similarity constructed on Bray-Curtis dissimilarity matrices of square root transformed abundance data revealed that the paleovegetation communities differed significantly among the pollen zones using both proxies ($p = 0.001$), albeit that the global r-value was higher for pollen ($r = 0.751$) than for *trn*L-P6 ($r = 0.365$) (Table 4.1). The global and pairwise ANOSIM test results did not differ substantially between pollen- and chronozones despite the differences between the timing of the LPAZ-4/LPAZ-5 (Atlantic/Preboreal) transition (Figs. 4.2 and 4.3). For simplicity, we will, from now on, describe downcore changes in pollen vs. *trn*L-P6 paleovegetation assemblages according to their association with chronozones. Pairwise ANOSIM tests showed that pollen vegetation assemblages did not differ significantly between the warm and humid Atlantic and the Subboreal. In contrast, the marginally significant difference observed for the *trn*L-P6 vegetation between these chronozones cannot be considered biologically relevant because of the low corresponding r-value of 0.08 (Table 4.1).

Table 4.1 Global and pairwise analysis of similarities (ANOSIM) tests to identify significant dissimilarities ($p < 0.05$) in *trn*L-P6- vs pollen paleovegetation between sample groups: (i) LPAZ (1 to 6) and the closely overlapping (ii) chronozones: Younger Dryas (YD), Boreal, Preboreal (PB), Atlantic/Holocene Climate Optimum (HCO), Subboreal (SB), and Subatlantic (SA), respectively). ANOSIM tests were based on Bray-Curtis dissimilarities of normalised and square root-transformed datasets. Significance levels: 0 '***' 0.001 '**' 0.01 '*' 0.05 and not significant (NS).

trnL-P6

LPAZ	r-value	p-value	Sign. Level	Chronozones	r-value	p-value	Sign. Level
Global test	0.365	0.001	***	Global test	0.391	0.001	***
LPAZ-6 x LPAZ-5	-0.029	0.764	NS	SA x SB	0.013	0.204	NS
LPAZ-6 x LPAZ-4	0.068	0.006	**	SA x HCO	0.101	0.009	**
LPAZ-6 x LPAZ-3	0.938	0.001	***	SA x Boreal	0.938	0.001	***
LPAZ-6 x LPAZ-2	0.778	0.001	***	SA x PB	0.777	0.001	***
LPAZ-6 x LPAZ-1	0.681	0.001	***	SA x PB	0.645	0.001	***
LPAZ-5 x LPAZ-4	-0.025	0.754	NS	SB x HCO	0.08	0.01	*
LPAZ-5 x LPAZ-3	0.929	0.001	***	SB x Boreal	0.947	0.001	***
LPAZ-5 x LPAZ-2	0.774	0.001	***	SB x PB	0.792	0.001	***
LPAZ-5 x LPAZ-1	0.791	0.001	***	SB x YD	0.78	0.001	***
LPAZ-4 x LPAZ-3	0.88	0.001	***	HCO x Boreal	0.849	0.001	***
LPAZ-4 x LPAZ-2	0.77	0.001	***	HCO x PB	0.718	0.001	***
LPAZ-4 x LPAZ-1	0.767	0.001	***	HCO x YD	0.785	0.001	***
LPAZ-3 x LPAZ-2	0.111	0.146	NS	Boreal x PB	0.114	0.127	NS
LPAZ-3 x LPAZ-1	0.489	0.003	**	Boreal x YD	0.54	0.004	**
LPAZ-2 x LPAZ-1	0.031	0.24	NS	PB x YD	-0.022	0.59	NS

Pollen

LPAZ	r-value	p-value	Sign. Level	Chronozones	r-value	p-value	Sign. Level
Global test	0.751	0.001	***	Global test	0.739	0.001	***
LPAZ-6 x LPAZ-5	0.337	0.016	*	SA x SB	0.502	0.001	***
LPAZ-6 x LPAZ-4	0.419	0.001	***	SA x HCO	0.466	0.001	***
LPAZ-6 x LPAZ-3	0.841	0.001	***	SA x Boreal	0.833	0.001	***
LPAZ-6 x LPAZ-2	0.961	0.001	***	SA x PB	0.945	0.001	***
LPAZ-6 x LPAZ-1	1	0.001	***	SA x PB	1	0.005	**
LPAZ-5 x LPAZ-4	-0.129	0.796	NS	SB x HCO	0.077	0.114	NS
LPAZ-5 x LPAZ-3	0.988	0.001	***	SB x Boreal	0.951	0.001	***
LPAZ-5 x LPAZ-2	0.999	0.002	**	SB x PB	0.988	0.001	***
LPAZ-5 x LPAZ-1	1	0.008	**	SB x YD	1	0.005	**
LPAZ-4 x LPAZ-3	0.865	0.001	***	HCO x Boreal	0.883	0.001	***
LPAZ-4 x LPAZ-2	0.985	0.001	***	HCO x PB	0.98	0.001	***
LPAZ-4 x LPAZ-1	1	0.001	***	HCO x YD	1	0.003	**
LPAZ-3 x LPAZ-2	0.674	0.001	***	Boreal x PB	0.569	0.001	***
LPAZ-3 x LPAZ-1	0.99	0.002	**	Boreal x YD	0.975	0.003	**
LPAZ-2 x LPAZ-1	0.6	0.001	***	PB x YD	0.449	0.016	*

This lack of a significant difference between the overall paleovegetation assemblages was initially unexpected, given that the Subboreal is generally considered relatively dry (Fulton et al., 2012). However, highly accurate dD isotopic analysis on long-chain alkenones (i.e., specific biomarkers of haptophyte algae) from core GGC18

recently showed that the surface water salinity (SSS) of the Black Sea dropped substantially between 3.6 and 1.6 ka cal. BP (Huang et al., 2021). The reduced SSS implied that the second half of the Subboreal period was probably the wettest period during the Holocene in the region (Huang et al., 2021).

The *trn*L-P6 paleovegetation assemblages did not differ significantly between the Subatlantic & Subboreal, Boreal & Peboreal, and Preboreal & Younger Dryas. The association of low abundant aquatic species with the Subatlantic (Table 4.2) was the driving force behind the weak significant difference in *trn*L-P6 paleovegetation assemblages between Subatlantic and Atlantic chronozones.

Table 4.2 Significant indicator taxa for LPAZ and chronozones identified using *trn*L-P6 metabarcoding vs pollen palynomorphs. The best indicator species are those found only in sites belonging to one group (A=1.000) and are present in all samples within that group (B=1.000). Only taxa with a significance level (p-value) of less than 0.05 are shown in the table. Significance levels: 0 '***' 0.001 '**' 0.01 '*' 0.05. Taxonomic levels: o_(order); f_(family); cl_(clade), sf_(subfamily); tr_(tribe); g_(genus); s_(species). HCO (Holocene Climate Optimum). Chronozones are considered to overlap with the GGC18 pollen zones, according to Filipova-Marinova et al. (2012). Note that the significant indicator taxa are ordered alphabetically.

A — *trn*L-P6

Significant indicator taxa	Vegetation type	GGC18-LPAZ	A	B	r-value	p-value	sign. Level	Chronozone	A	B	r-value	p-value	sign. Level
o_Alismatales;f_Zosteraceae;g_Zostera	Aquatics	LPAZ-6	0.8498	0.1818	0.393	0.047	*	Suabtlantic	-	-	-	-	-
o_Asterales;f_Asteraceae;tr_Anthemideae; g_Artemisia & Achillea	Herbs & Shrubs	LPAZ-5	0.3464	1	0.589	0.001	***	Subboreal	0.3248	1	0.57	0.001	***
o_Cupressales;f_Taxaceae;g_Taxus	Conifers	LPAZ-4	0.6824	0.4146	0.532	0.02	*	Atlantic/HCO	0.6639	0.3871	0.507	0.026	*
o_Fabales;f_Fabaceae;sf_Faboideae;tr_Phaseoleae	Herbs	LPAZ-2	0.6735	0.3333	0.474	0.041	*	Preboreal	0.6741	0.3333	0.474	0.047	*
o_Fagales;f_Betulaceae;g_Alnus	Deciduous trees	LPAZ-1	0.4258	0.8333	0.596	0.014	*	Younger Dryas	0.4291	0.8333	0.598	0.014	*
o_Fagales;f_Betulaceae;g_Carpinus & Corylus	Deciduous trees	-	-	-	-	-	-	Boreal	0.9282	0.125	0.341	0.023	*
o_Fagales;f_Fagaceae;g_Quercus	Deciduous trees	LPAZ-3	0.989	0.125	0.352	0.046	*	Boreal	0.9872	0.125	0.351	0.043	*
o_Fagales;f_Juglandaceae	Deciduous trees	LPAZ-3	0.764	0.3333	0.505	0.004	**	Boreal	0.9755	0.25	0.494	0.005	**
o_Malpighiales;f_Salicaceae;g_Populus	Deciduous trees	LPAZ-1	0.5752	0.6667	0.619	0.003	**	Younger Dryas	0.5791	0.6667	0.621	0.003	**
o_Malpighiales;f_Salicaceae;g_Salix	Deciduous trees	LPAZ-1	0.8721	0.4	0.591	0.001	***	Younger Dryas	0.8802	0.3846	0.582	0.001	***
o_Malvales;f_Malvaceae;g_Tilia	Deciduous trees	LPAZ-4	0.549	0.4651	0.505	0.009	**	Atlantic	0.84	0.25	0.458	0.011	*
o_Poales;f_Poaceae;cl_BOP;sf_Pooideae	C3 grasses	LPAZ-1	0.9278	0.3333	0.556	0.001	***	Younger Dryas	0.9278	0.3333	0.556	0.001	***
o_Poales;f_Poaceae;Cl_BOP;sf_Pooideae;tr_Tritiaceae;g_Secale & Elymus	C3 grasses (Anthropophytes?)	LPAZ-1	0.5958	0.75	0.668	0.001	***	Younger Dryas	0.5862	0.75	0.663	0.002	**
o_Poales;f_Poaceae;cl_PACMAD;sf_Arundinoideae;g_Phragmites ;s_P.australis	C3 grasses (Aquatics)	LPAZ-1	0.9261	0.1333	0.351	0.018	*	-	-	-	-	-	-
o_Poales;f_Poaceae;cl_PACMAD;sf_Panicoideae	C4 grasses	-	-	-	-	-	-	Preboreal	0.5834	0.2222	0.36	0.05	*
o_Rosales;f_Rosaceae;g_Pyrus	Deciduous trees	LPAZ-1	1	0.1333	0.365	0.017	*	-	-	-	-	-	-
o_Polypodiales; f_Athyriaceae; g_Athyrium	Ferns	LPAZ-5	0.3678	1	0.606	0.001	***	Subboreal	0.3753	1	0.613	0.001	***
o_Sapindales;f_Sapindaceae;g_Acer	Deciduous trees	LPAZ-3	0.4945	0.6667	0.574	0.01	**	Boreal	0.4799	0.6667	0.566	0.01	**

B — Pollen

Significant indicator taxa	Vegetation type	GGC18-LPAZ	A	B	r-value	p-value	sign. Level	Chronozone	A	B	r-value	p-value	sign. Level
o_Apiales; f_Araliaceae; g_Hedera	Shrubs	LPAZ-5	0.4236	0.8	0.582	0.008	**	-	-	-	-	-	-
o_Asterales;f_Asteraceae;tr_Anthemideae; g_Artemisia & Achillea	Herbs & Shrubs	LPAZ-1	0.2202	1	0.469	0.001	***	Preboreal	0.2026	1	0.45	0.048	*
o_Caryophyllales; ; f_Chenopodiaceae	Herbs & Shrubs	LPAZ-1	0.295	1	0.543	0.001	***	Younger Dryas	0.3202	1	0.566	0.001	***
o_Caryophyllales; f_Polypodiaceae	Herbs	LPAZ-1	0.2471	1	0.497	0.013	*	-	-	-	-	-	-
o_Cupressales; f_Cupressaceae; g_Juniperus	Conifers	LPAZ-2	0.4943	0.9	0.667	0.002	**	Preboreal	0.4908	0.9091	0.668	0.011	*
o_Ephedrales; f_Ephedraceae; g_Ephedra	Shrubs	-	-	-	-	-	-	Preboreal	0.4676	0.6364	0.546	0.02	*
o_Ericales; f_Ericaceae; g_Rhododendron	Shrubs	LPAZ-6	0.5929	0.7778	0.679	0.003	**	Subatlantic	0.6279	0.7778	0.699	0.008	**
o_Fagales; f_Betulaceae; g_Alnus	Deciduous trees	LPAZ-6	0.3551	1	0.596	0.001	***	Subatlantic	0.3617	1	0.601	0.001	***
o_Fagales; f_Betulaceae; g_Carpinus ; s_C. betulus	Deciduous trees	LPAZ-5	0.3241	1	0.569	0.001	***	Subboreal	0.3395	1	0.583	0.001	***
o_Fagales; f_Betulaceae; g_Carpinus ; s_C. orientalis	Deciduous trees	LPAZ-5	0.414	1	0.643	0.001	***	Subboreal	0.4473	1	0.669	0.001	***
o_Fagales; f_Betulaceae; g_Corylus	Deciduous trees	LPAZ-4	0.271	1	0.521	0.002	**	Atlantic/HCO	0.2889	1	0.537	0.003	**
o_Fagales; f_Fagaceae; g_Fagus	Deciduous trees	LPAZ-5	0.3205	1	0.566	0.001	***	Subboreal	0.3172	1	0.563	0.001	***
o_Fagales; f_Fagaceae; g_Quercus	Deciduous trees	LPAZ-3	0.2221	1	0.471	0.001	***	Boreal	0.2224	1	0.472	0.001	***
o_Fagales; f_Juglandaceae; g_Juglans	Deciduous trees	LPAZ-5	0.5581	0.8	0.668	0.003	**	-	-	-	-	-	-
o_Lamiales; f_Lamiaceae	Herbs	LPAZ-2	0.3297	0.9	0.545	0.03	*	-	-	-	-	-	-
o_Lamiales; f_Oleaceae; g_Fraxinus ; s_F. excelsior _type	Deciduous trees	LPAZ-6	0.2505	1	0.501	0.019	*	Subatlantic	0.2457	1	0.496	0.039	*
o_Lamiales; f_Plantagiaceae; g_Plantago ; s_P. lanceolata	Herbs (Anthropophytes)	LPAZ-6	0.4337	0.8889	0.621	0.005	**	Subatlantic	0.4742	0.8889	0.649	0.005	**
o_Malpighiales; f_Malvaceae; g_Tilia	Deciduous trees	-	-	-	-	-	-	Subboreal	0.2398	1	0.49	0.035	*
o_Pinales; f_Pinaceae; g_Pinus ; s_P. diploxylon _type	Conifers	LPAZ-1	0.2236	1	0.473	0.005	**	Younger Dryas	0.2307	1	0.48	0.005	**
o_Poales; f_Poaceae; g_Cerealia_type	C3 grasses (Anthropophytes)	LPAZ-6	0.5292	0.8889	0.686	0.002	**	Subatlantic	0.5337	0.8889	0.689	0.005	**
o_Poales; f_Poaceae; g_Triticum	C3 grasses (Anthropophytes?)	LPAZ-6	0.7468	0.5556	0.644	0.007	**	Subatlantic	0.6838	0.5556	0.616	0.026	*
o_Poales; f_Typhaceae; g_Typha	Aquatics	LPAZ-6	0.5397	0.6667	0.6	0.013	*	Subatlantic	0.559	0.6667	0.61	0.019	*
o_Rosales; f_Ulmaceae; g_Ulmus	Deciduous trees	LPAZ-4	0.2345	1	0.484	0.001	***	Atlantic/HCO	0.2372	1	0.487	0.002	**

However, higher significant dissimilarities could be observed between the Boreal and Younger Dryas and before and after the Boreal/Atlantic transition (~8 ka cal. BP) (Table 4.2). Based on the ANOSIM results, we will separate our discussion concerning the overlap vs. discrepancies between both paleovegetation proxies for the (a) Younger Dryas and Preboreal combined, (b) Boreal, (c) Atlantic, Subboreal, and Subatlantic combined.

4.4.3 Paleovegetation associated with the Younger Dryas and Preboreal (GGC18-LPAZ 1 & 2)

During the Younger Dryas, the pollen grain approach revealed a predominance of xerophytic steppe, most notably *Artemisia* (Asteraceae) and Chenopodiaceae (Filipova-Marinova et al., 2012; Fig. 4.3). While *Artemisia* and Chenopodiaceae pollen were recovered throughout the record, indicator species analysis (ISA; this study) confirmed that both xerophytes were significantly associated with the Younger Dryas (Table 4.2). Ephedraceae (*Ephedra distachya*), Carophyllaceae, Apiaceae and other Asteraceae (*Aster*-type, *Achillea*-type, *Centaurea*) may also have represented constituents of the arid steppe herbs, according to Filipova-Marinova et al. (2012) (Fig. 4.3). However, of those herbs, only unclassified Carophyllaceae were identified as additional pollen indicator species for the Younger Dryas (Table 4.2). In contrast, *trn*L-P6 sequences related to Chenopodiaceae, Ephedraceae, and Carophyllaceae were not identified anywhere throughout the record. They were classified as Athemideae, a tribe within the Asteraceae that includes *Artemisia*, which were only sparsely recovered from sediment intervals deposited during the Younger Dryas and Preboreal. (Fig. 4.3). Previous pollen studies suggested that most of the xerophytic steppe vegetation was growing on the part of the modern shelf after the withdrawal of the sea during the Neoeuxinic regression (e.g., Atanassova, 2005; Filipova-Marinova et al., 2012). *Artemisia* and other dominant steppe vegetation are wind-pollinated and produce abundant pollen and may, therefore, be overrepresented in sedimentary records (Magyari et al., 2012). The high pollen over *trn*L-P6 ratio (Parducci et al., 2015) suggests that the herbal steppe vegetation was not growing near the Black Sea's shoreline. Namely, reduced precipitation and riverine/continental runoff under arid glacial conditions would have prevented efficient drainage of chloroplast-rich litter from xerophytic steppe vegetation growing further away from the catchment areas.

During the Younger Dryas, conifers (*Pinus*) and deciduous trees such as *Corylus*, *Tilia* and *Betula* were likely distributed at mid-altitude locations in the Stara Planina Mountains of the Eastern Balkan Range, where precipitation would have been higher than on the plains (van der Hammen et al., 1971; Beug, 1975). A remote location, notably that of *Corylus* and *Pinus*, which produce large amounts of wind-dispersed pollen (Rojo et al., 2020), would explain the relatively low pollen content of this refuge vegetation (Filipova-Marinova et al., 2012; Fig. 4.3). Unlike most angiosperms, gymnosperm produces pollen that contains chloroplasts (Lubna et al., 2021). The concurrent low relative read abundance of *trn*L-P6 from remote *Pinus* stands throughout the record shows that contamination with airborne pollen was negatable and that vegetation that used to grow in areas where their chloroplast-rich biomass could have efficiently drained into the Black Sea at times of increased precipitation and runoff was the predominant source of the plant barcoding gene instead.

According to Filipova-Marinova (2012), true grasses (Poaceae) were also part of the xerophytic steppe vegetation. However, unclassified Poaceae were also relatively abundant pollen taxa throughout the Holocene interval of GGC18 (Fig. 4.3) and did not represent significant pollen indicator taxa for the Younger Dryas (Table 4.2). Most native grasses can only be identified from pollen at the family level (i.e., Poaceae). In contrast, sequencing analysis of preserved plant marker genes has the potential to distinguish between dry climate C_4 grasses indicative of a steppe/open landscape environment vs. wet- and cool climate C_3 grasses, which could also have been growing in wetlands, lake catchment, and along riverbanks and are therefore not per definition indicative of steppe-like open landscape conditions. Whereas all grasses in the BOP clade exclusively use the C_3 carbon fixation pathway, taxonomic resolution at subfamily or lower ranks is required to distinguish between the C_4 and C_3 grass lineages in the PACMAD clade. Using the *trn*L-P6 metabarcoding approach, we identified Panicoideae (PACMAD clade) as the relatively most abundant Poaceae (Burke et al., 2016). While some lineages in this subfamily use the C_3 carbon fixation pathway, the highest relative read abundance of this PACMAD subfamily in the Younger Dryas and the Preboreal chronozones (Klink & Joly, 1989) suggests that they represented C_4 grasses. However, since dominant pollen steppe vegetation was not well represented in the pool of recovered *trn*L-P6 (Liu et al., 2020), the Panicoideae

154

identified from the chloroplast marker gene may have been growing in proximity to the Black Sea's catchment rather than in the dry steppe open landscape. The *trn*L-P6 approach also identified the sporadic presence of common reed grass (*Phragmites australis*) as a significant indicator taxon for the Younger Dryas (Pagter et al., 2005). Pollen analysis failed to identify *P. australis* because of the region's overlapping morphology with other grass pollen palynomorphs (Rossignol et al., 2012). Nowadays, this C_4 grass belonging to the PACMAD clade covers large marsh-wetland areas, mainly around the Danube Delta's coastal lakes and along the Bulgaria Danube River (Lazarova & Boziolova, 2001).

Sedimentary *trn*L-P6 metabarcoding also identified pooid grasses (BOP clade) within the wheat tribe Triticeae with 98-100% sequence similarity to a wide range of species within the genera *Secale*, *Triticum*, *Hordeum*, *Aegilops*, or *Elymus*. These genera include native wild grasses that are closely related to cultivated cereals such as rye (*Secale cerale*), wheat (*Triticum eastivum*), and Barley (*Hordeum vulgare*). Triticeae were recovered from Younger Dryas intervals using *trn*L-P6 metabarcoding as old as 12.1 ka cal. BP and represented significant indicator taxa for this chronozone (Table 4.2). In contrast, *Triticum*-type and Cerealia-type pollen first appeared with the onset of the Atlantic (Fig. 4.3) when agricultural activities and land use started in south-eastern Europe (Eastwood et al., 2018). Since the first appearance of sedimentary chloroplast DNA from these grasses preceded the earliest agricultural activities in south-eastern Europe by several millennia, we most likely identified native members of the wheat tribe. The relative read abundance of the identical sequences, as well as *Triticum*- and Cerealia-type pollen, increased again during the Subatlantic chronozone (Filipova-Marinova et al., 2012) when increased riverine and terrestrial runoff contributed to the vast expansion of the Danube Delta (e.g., Giosan et al., 2012). However, it is essential to note that all genera listed above are native to Bulgaria, including wild relatives of *Triticum*, *Elymus*, and *Aegilops* distributed along the Black Sea coastline today (Spetsov et al., 2006). Other metabarcoding genes need to be developed that offer the taxonomic resolution required to differentiate between native and cultivated varieties of Triticeae. At the same time, these metabarcoding genes need to be suitable for *sed*aDNA analysis and ideally not exceed ~200

nucleotides in length (Coissac et al., 2012). Even more promising would be the use of baits hybridisation capture using probes designed to target all members of the Triticeae. This approach, which is vastly growing in popularity in *sed*aDNA research (e.g., Armbrecht et al., 2022), eliminates PCR bias, and baits can be designed using multiple metabarcoding genes to improve the taxonomic resolution of past vegetation (e.g., Foster et al., 2022).

Furthermore, deciduous trees *Alnus* (alders) and *Populus* (poplar) represented significant indicator taxa for the Younger Dryas. At the same time, leguminous herbs of the tribe Phaeoleae (Fabaceae) and the above-described PACMAD clade grasses (Panicoideae) were significant indicator taxa for the warmer but still relatively dry Preboreal. *Alnus* continued to be relatively abundant during the Preboreal. At the same time, *trn*L-P6 reads assigned to *Acer* (maples), which comprised only a small proportion of the pollen spectrum throughout GGC18, started to increase in relatively abundant during this early Holocene chronozone. Besides Fabaceae, non-leguminous *Alnus*, *Populus*, and *Acer* are known to form root nodules with nitrogen-fixing bacteria (Santi et al., 2013). N-fixing pioneer vegetation plays an important role in soil fertilisation (Sifton et al., 2022) and may have promoted the development of more nutrient-demanding secondary forest vegetation. In agreement with earlier studies (Atanassova, 2005; Connor et al., 2013; Mudie et al., 2007; Shumilovskikh et al., 2012), pollen grains from *Ulmus* (elms) were covered in at least 11.8 kyr-old sediment intervals of GGC-18 (Filipova-Marinova et al., 2012; Fig. 4.3), and *Ulmus* is therefore thought to have been early postglacial counterparts of the low land forest vegetation. The spreading of *Ulmus* to lower elevations near the Black Sea coastal catchment occurred possibly one kyr after the onset of the Preboreal, as evident from the initial recovery of their chloroplast marker gene at ~10.4 ka cal. BP (Fig. 4.2).

4.4.4 Paleovegetation associated with the Boreal (GGC18-LPAZ-3)

The *trn*L-P6 metabarcoding approach (Fig. 4.2) confirmed that the warmer and more humid Boreal chronozone was associated with an increase in the relative read abundance of arboreal pollen grains (Fig. 4.3) indicative of denser forest communities (e.g., Atanassova, 2005; Filipova-Marinova et al., 2012). Despite the few samples from the Boreal that were available for DNA analysis, both approaches showed partial

overlap in (indicator) species composition during the Boreal. Both approaches revealed a maximum extension of *Quercus* (oak) forests (Figs. 4.2, 4.3) and identified *Quercus* to be a significant indicator taxon for the Boreal (Table 4.2). The two independent biomarkers also revealed an increase in the relative read abundance of *Corylus* (hazel), *Tilia* (linden) and *Fagus* (beech), which are significant components of oak forest in the region today Bondev (1991). Although both proxies disagreed in their significant association with the chronozones (Table 4.2), the deposition of chloroplast DNA at the coring location implies that the oak forest vegetation was growing near the Black Sea catchment during the Boreal.

By way of another notable example, Juglandaceae, which includes native *Juglans* (walnut), also represented a significant *trn*L-P6 indicator taxon for the Boreal (Fig. 4.2., Table 4.1). Juglandaceae comprised a large relative read abundance of the total *trn*L-P6 pool towards the end of the Boreal at 8.3 ka cal. BP only represented more than 0.5% of the total *trn*L-P6 pool at 10.1 ka cal. BP (Fig. 4.2). In contrast, *Juglans* pollen grains first appeared 7.1 ka cal. BP and comprised less than 0.5% of the total pollen count throughout the Atlantic stage (Filipova-Marinova et al., 2012; Fig. 4.3). However, in an earlier study, single pollen grains of *Juglans* along the southern Bulgarian Sea coast were also identified as early as 10 ka cal. BP, concomitant with the timing of the oldest relatively high abundance of Juglandaceae *trn*L-P6 in our record (Filipova-Marinova, 2003). The relatively high quantity of chloroplast DNA from Juglandaceae at 10.1 ka cal. BP likely preceded human settlement, which contradicts the debated alternative possibility that man-made changes in the natural vegetation caused the spread of *Juglans* in the region (Filipova-Marinova et al., 2012). Instead, the locally sourced chloroplast marker gene and the finding of single pollen grains in early Holocene sediments of the Black Sea (Filipova-Marinova, 2003) agrees with a possibly relict origin of *Juglans* in the Balkan Peninsula (Bottema, 1980). Moreover, the high relative read abundance of Juglandaceae *trn*L-P6 at 8.3 ka cal. BP (Filipova-Marinova et al., 2012) overlaps with the widespread 8.2 ka BP cold event (e.g., Bahr et al., 2005), also reported from the Balkan region (Panagiotopoulos et al., 2013). The short-term cold event possibly forced Juglandaceae to migrate more closely to the Black Sea coastal catchment area. In addition, *Acer* (maple) was only observed to be relatively abundant during the Boreal using *trn*L-P6 metabarcoding.

4.4.5 Paleovegetation since 8 ka cal. BP spanning the Atlantic, Subboreal, and Subatlantic (GGC18-LPAZ 4-6)

As discussed in detail below, throughout the last 8 Ka BP (i.e., since the Boreal/Atlantic transition), the *trn*L-P6 approach revealed an increase in the relative read abundances of (a) coastal marshland and (b) riparian floodplain forest vegetation that are subject to periodic flooding and cycles of erosion and deposition of nutrient-rich alluvial sediments (Kosir et al., 2013). This implies that during increased precipitation, sedimentary *trn*L-P6 at the coring location was mainly sourced from chloroplast-rich decaying plant biomass in seasonally flooded marshland or periodically flooded riverine catchment areas.

4.4.5.1 Paleovegetation associated with marshland expansion as sources of sedimentary trnL-P6

Saltmarshes are usually dominated by a small number of plant species, notably halophytes. These communities are typically spatially segregated into vegetation zones. Taxa that have adapted to or can tolerate frequent or long-term exposure to flooding and inundation are zoned more closely to the shoreline. In contrast, more drought and salinity-tolerant taxa are zoned slightly more elevated and further away from the coastline (Watson & Byrne, 2009). The inundation regime and salinity are the main drivers shaping the community structure in salt marshes (Baldwin et al., 1996). For example, across a 150-m-long transect near the Black Sea coast (Turkey), *Artemisia santonicum* formed a monospecific stand ~ 4 m.a.s.l. and was mainly inundated during the rainy winter months (Apaydin et al., 2009). In our record, the substantial increase in the relative read abundance of *Artemisia trn*L-P6 after ~8 ka BP implies that postglacial sea-level rise and the reconnection of the Black Sea with the world's oceans resulted in large areas of the coastal plains being transformed into saline marshland and that *Artemisia* represented prominent members of this newly formed landscape. A comparable scenario was suggested from a Holocene pollen grain record from the Liaohe Delta in NE China, where an increase in *Artemisia* pollen coincided with a warmer, more humid early Holocene climate, elevated regional sea level, and an expansion of coastal marshland (Yang et al., 2022). Efficient drainage of both plant biomarkers from flooded marshland would explain why *Artemisia* pollen

continued to be relatively abundant throughout the Holocene (Fig. 4.3). Although species-level identification was not possible, the single most abundant ASV showed 100% sequence similarity with *A. maritima*, which is a widely distributed and abundant salt marsh inhabitant and native to Bulgaria (Pigott et al., 2000; Velasco et al., 2016).

Furthermore, Apaydin et al. (2009) showed that *Carex* (Cyperaceae) formed mono stands within the 150-m-long transect closest to the coastline (~3 m.a.s.l.), which was inundated during most of the year. *Carex* and other dominant obligate partially submerged wetland vegetation growing along the modern-day brackish Black Sea coastline, such as common reed grass (*Phragmites australis*) and *Typha*, spread through aerenchymous rhizomes (Chun & Choi, 2009). Oxygen transport to their root systems enables them to inhabit waterlogged anoxic sediments. Being less prone to de-rooting and die-off during periodic flooding events would have resulted in less litter from this wetland vegetation being drained and deposited at the relatively remote coring location, explaining the sporadic distribution of the chloroplast marker gene in the GGC18 record. While *Phragmites* pollen cannot be differentiated from other grass pollen due to overlap in morphology (Filipova-Marinova et al., 2012), both biomarkers showed that *Typha* and Cyperaceae were most consistently present during the Subatlantic (Figs. 4.2 and 4.3) when sea surface salinity reached modern levels (Coolen et al., 2013; Giosan et al., 2012; Huang et al., 2021; van der Meer et al., 2008). *Typha* pollen grains were identified as *T. angustifolia*, representing a marginally significant pollen indicator taxon (p=0.038) for this Subatlantic chronozone (Table 4.2).

In addition, native seagrasses (*Zostera* and *Zanichella*), which also spread via rhizomes (Milchakova, 1999), were identified using the *trn*L-P6 metabarcoding approach (Berov et al., 2020). *Zostera* represented a significant indicator taxon for the Subatlantic chronozone. Although species-level classification was not possible, the most abundant ASV classified at the genus level showed 100% sequence similarity with *Zostera marina* (eelgrass) (Foster et al., 2022), which nowadays forms extensive completely submerged meadows in shallow bays, bights, and estuaries, especially in the northwestern part of the Black Sea (Milchakova, 1999). The presence of

sedimentary chloroplast DNA from *Z. marina* DNA is not surprising given the estimated 50 kilotons of wet-weight litter from this species that is lost following storm events (e.g., Lukina, 1986). The surface water salinity where *Z. marina* and associated macroalgal communities are found in these Black Sea localities ranges between 11 and 19 ppt (Milchakova, 1999). Interestingly this lower end of the salinity range is also the minimum salinity requirement of the calcifying marine haptophyte *Emiliania huxleyi*, which started to form extensive blooms in the Black Sea and deposit the coccolith-bearing Unit I interval with the onset of the Subatlantic (Fig. 4.1; Hay, 1988). The amount of coastal surface areas covered by seagrasses is in decline globally due to their sensitivity to turbidity and eutrophication caused by intensified terrestrial runoff of sediments and nutrients linked to the rapid increase in urban colonisation and agricultural land use (Erftemeijer & Robin, 2006). We previously presented sedimentary and paleoenvironmental evidence that wetter conditions and deforestation during the Subatlantic resulted in a substantial increase in sediment loads delivered by the Danube River, the main tributary of the Black Sea (Giosan et al., 2012). However, *Zostera* cpDNA was detected in a subset of Subatlantic sediment intervals as young as 600 y cal. BP (Fig. 4.3), suggesting that these paleoenvironmental perturbations did not lead to a complete loss of *Zostera* colonies or that these seagrasses could re-establish after flooding events.

4.4.5.2 Seasonally flooded riparian forest vegetation as putative sources of sedimentary trnL-P6

The optimal climate conditions (high temperature and humidity) associated with the onset of the Atlantic resulted in an expansion of arboreal vegetation (Filipova et al., 2012; Fig. 4.3). *Quercus* was identified as a specific indicator taxon for the Boreal (Table 4.2) and remained a significant constituent of the mixed oak forest. The pollen data showed a notable increase in the relative read abundance of broad-leaved deciduous *Corylus* with the onset of the Atlantic (Fig. 4.3). Judged from the concomitant presence of single pollen grains from putative anthropophytes (Cerelia-type, *Triticum*, and ruderals such as *Plantago lanceolata*), the increase in *Corylus* was previously suggested to be associated with clearance of mixed oak forests for enlargement of cultivated areas along the coast (Filipova-Marinova, 2006).

Alternatively, *Corylus* could have formed abundant mono stands in more remote open landscape areas (Filipova-Marinova et al., 2012) since this broadleaved deciduous tree produces large amounts of pollen that could have travelled long distances (Damialis et al., 2006)). The second scenario is supported by a presumed absence of *Corylus* *trn*L-P6 throughout the record. Unfortunately, the *trn*L-P6 metabarcoding approach failed to distinguish between *Corylus* and *Carpinus* (both Betulaceae). However, *Carpinus* (*C. betulus*) was the more likely source of the chloroplast marker gene. In addition to being a constituent of mixed forest vegetation, *C. betulus* is thought to have been growing along river valleys draining into the Black Sea (Filipova-Marinova et al., 2012). The timing in the increase in the relative read abundance of *trn*L-P6 of this deciduous tree (~ one Kyr into the Atlantic) roughly coincided with the rise in *Carpinus betulus* pollen (Figs. 4.2, 4.3).

Carpinus likely continued to grow near rivers, draining their chloroplast-rich litter and pollen into the Black Sea throughout the remainder of the wetter Holocene. According to pollen grain analysis, *Fagus* (*F. orientalis*) became a consistent arboreal member of the coastal oak forest vegetation with the arrival of the moist and warm Atlantic, as well as throughout the remainder of the Holocene (Fig. 4.3). The simultaneous presence of its *trn*L-P6 in a subset of sediment intervals spanning the last eight kyr of deposition confirmed that the optimal climate conditions allowed this deciduous tree to spread to lower elevations in proximity of the coastal catchment. *Alnus* pollen also became more abundant with the onset of the Atlantic. In addition to being part of the mixed oak forest, the maximum relative read abundance of its pollen during the cooler and wetter Atlantic was thought to be associated with the formation of the "longoz" forest (Filipova-Marinova et al., 2006). These periodically flooded forests can be found along the river valleys, and in south-eastern Europe, they are found to be widespread close to large rivers, including the Danube. Both soft- and hardwood forests can be identified in flooded forests (Douda et al., 2016). Softwood-flooded forests throughout Europe are typically inhabited by light-demanding tree species of the genera *Alnus*, *Salix*, *Populus*, and *Tilia,* which usually occupy the area closest to the rivers that are often inundated and when groundwater is high (Kosir et al., 2013). Notably, along the Mura River in NE Slovenia (the largest tributary of the Drava River, which drains into the Danube), *Salix* and *Populus* were identified as

diagnostic members of the part of the riparian forest that was often inundated with high groundwater levels and the presence of alluvium deposits (Kosir et al., 2013). In our record, the relative read abundance of *trn*L-P6 from *Salix* wildly succeeded that of its pollen, whereas *Populus* was only identified using *trn*L-P6 amplicon sequencing (Filipova-Marinova et al., 2012). *Salix* is usually absent or a minor component in an *Alnus*-dominated inundated riparian forest (Van Pelt et al., 2006). Non-riverine *Alnus* forest is nowadays typical for the coast of the brackish Baltic Sea (Deptuła et al., 2020). Therefore, the inverse relationship between downcore changes in the relative read abundances of *Salix* and *Populus* vs. *Alnus* may reflect changes in the extent of inundation, paleo precipitation, and fluctuations in the water balance of the Black Sea.

Moreover, *Athyrium filix-femina* (lady fern) became a relatively abundant source of sedimentary *trn*L-P6 since the onset of the Atlantic (Fig. 4.2). This fern has a global distribution in temperate regions. It can be an abundant ground cover of nutrient-rich moist soils of periodically flooded riverbanks, including areas where *Alnus* and/or *Salix* are relatively abundant (Fagerstrom, 1999). The perennial herb *Filipendula ulmaria* (meadowsweet) is abundant ground cover vegetation along riverbanks, native to the Stara Planina Mountain range (THE BULGARIAN FLORA ONLINE, 2008). Both approaches revealed a relative increase or a most consistent presence of *Filipendula* during the Subatlantic (Figs. 4.2, 4.3). In Holocene pollen records, *Filipendula* is generally considered an anthropophyte, indicative of past agricultural activities (e.g., Filipova-Marinova, 2012). Although a native member of *Filipendula* is more likely in this situation, we could not conclusively identify *F. ulmaria* as the (sole) source of the sedimentary chloroplast marker gene due to sequence overlap with other species of this genus. However, once more, the *trn*L-P6 approach mainly identified local catchment vegetation and showed that riparian forest vegetation already developed in the region no later than with the onset of the Atlantic.

In contrast, a predominance of pollen over *trn*L-P6 was observed for long-lived hardwood species, including *Ulmus, Carpinus betulus, Quercus*, and *Acer* (Novak et al., 2023). This vegetation benefits from interrupted inundation of long habitat continuity (Glaeser & Wulf, 2009) and is, therefore, usually zoned further away from the rivers (Kosir et al., 2013). Despite the less even distribution of *trn*L-P6 inferred

paleovegetation assemblages compared to pollen, the relative read abundance of the chloroplast marker gene of these hardwood taxa has declined with the onset of the Subatlantic. In agreement with Filipova-Marinova et al. (2006), this indicates that increased precipitation during this cooler and wetter chronozone resulted in the most significant expansion of periodically flooded surface areas in riparian forests occupied by softwood forest taxa (Fig. 4.2).

4.5 Conclusions

Pollen grain analysis revealed mostly xerophytic herb vegetation (*Artemisia* and *Chenopodiaceae*), which dominated the steppe landscape of the coastal plains surrounding the Black Sea during the cold and dry Younger Dryas. These xerophytic steppe herbs were also identified as significant indicator taxa for the Younger Dryas but remained relatively abundant throughout the wetter and warmer Holocene. According to the pollen analysis, the warm and wet conditions with the onset of the Atlantic (~ 8 ka cal. BP) resulted in an expansion of arboreal oak forest vegetation by hardwood species (*Quercus*, *Corylus*, *Carpinus betulus*, *Fraxinus*, *Fagus*, and *Ulmus*). Alnus and Tilia were the predominant pollen-producing softwood trees. Furthermore, putative anthropophytes such as cultivated cereals (*Triticum* and cereale-type pollen) and ruderals (e.g., *Filipendula* and *Plantago lanceolata*) indicative of early farming practices were found as early as the Neolithic. They were most consistently present during the Bronze Age, overlapping with the most recent Subatlantic chronozone.

The community composition of the paleovegetation identified through amplicon sequencing of sedimentary *trn*L-P6 partly overlapped with the taxa identified through pollen, with the best overlap observed for trees. However, differences in relative read abundances and significant associations with the various chronozones resulted in different interpretations of the origin of the source plants and the landscape this vegetation occupied. High pollen-producing xerophytic steppe vegetation identified with pollen (*Artemisia*) were minor contributors to the *trn*L-P6 pool during the Younger Dryas and Preboreal. Instead, the *trn*L-P6 approach identified different types of vegetation presumable from the coastal plains and beaches in the catchment area of the then freshwater or oligohaline Black Sea. This vegetation included C_4 grasses (Panicoideae) of the PACMAD clade. Moreover, *trn*L-P6 metabarcoding showed that native C_3 Pooid grasses within the wheat tribe Triticeae were significant indicator taxa

for the Younger Dryas and may have been used for cultivation of cereal crops by early farmers as suggested from the increase in cereal-type pollen grains and other anthropophytes since the Neolithic. Moreover, nitrogen-fixing pioneer vegetation (Fabaceae, Alnus, and Populus) were relatively abundant sources of the cpDNA marker gene during the Younger Dryas and the Preboreal and may have occupied the coastal freshwater catchment before the reconnection with the Mediterranean Sea ~9 ka cal. BP. Here, this vegetation may have contributed to soil fertilisation, paving the way for the succession of secondary forest vegetation. With the onset of the Atlantic, increased precipitation likely resulted in an increased discharge of chloroplast-rich plant litter from halophytic marshland vegetation and vegetation typically lining periodically inundated riparian forests. Most notably, the onset of the Atlantic saw a drastic increase in the relative read abundance of the common and native marshland inhabiting halophyte *Artemisia maritima* as the possible source of *Artemisia* pollen, which would explain why *Artemisia* remained a relatively abundant pollen source throughout the wetter Holocene.

Softwood arboreal taxa (*Alnus*, *Salix*, *Populus*, and *Tilia*), which usually occupy nutrient-rich alluvial sediments closest to the rivers that are often inundated, predominated the *trn*L-P6 pool over hardwood taxa (*Ulmus, Carpinus betulus, Quercus*, and *Acer*), which benefit from interrupted inundation of long habitat continuity and are, therefore, usually zoned further away from the rivers. Lastly, sedimentary *trn*L-P6 metabarcoding identified native *Athyrium filix-femina* (lady fern) and *Filipendula ulmaria* (meadowsweet). These taxa can be abundant members of the low diversity ground cover vegetation in moist riparian forests, arguing against *Filipendula* being an anthropophyte used as a ruderal during prehistoric agricultural activities.

This study shows that marine basins can provide valuable long-term archives of cpDNA marker genes and can complement fossil pollen for the reconstruction of paleovegetation assemblages of the hinterland and to refine the pollen-inferred interpretation of climatic vs anthropogenically induced changes to the regional landscape.

4.6 References

Alsos, I. G., Lammers, Y., Yoccoz, N. G., Jorgensen, T., Sjogren, P., Gielly, L., & Edwards, M. E. (2018). Plant DNA metabarcoding of lake sediments: How does it represent the contemporary vegetation. *Plos One, 13*(4).

Alsos, I. G., Lammers, Y., Kjellman, S. E., Merkel, M. K. F., Bender, E. M., Rouillard, A., Erlendsson, E., Guðmundsdóttir, E. R., Benediktsson, Í. Ö., Farnsworth, W. R., Brynjólfsson, S., Gísladóttir, G., Eddudóttir, S. D., & Schomacker, A. (2021). Ancient sedimentary DNA shows rapid post-glacial colonisation of Iceland followed by relatively stable vegetation until the Norse settlement (Landnám) AD 870. *Quaternary science reviews*, *259*, 106903.

Anshari, G., Kershaw, P., van der Kaars, S., & Jacobsen, G. (2004). Environmental change and peatland forest dynamics in the Lake Sentarum area, West Kalimantan, Indonesia. *Journal of Quaternary Science, 19*, 637-655.

Apaydin, Z., Kutbay, H. G., Ozbucak, T., Yalcin, E., & Bilgin, A. (2009). Relationships between vegetation zonation and edaphic factors in a salt-marsh community (Black Sea Coast). *Polish Journal of Ecology, 57*(1), 99-112.

Armbrecht, L., Weber, M. E., Raymo, M. E., Peck, V. L., Williams, T., Warnock, J., Kato, Y., Hernandez-Almeida, I., Hoem, F., Reilly, B., Hemming, S., Bailey, I., Martos, Y. M., Gutjahr, M., Percuoco, V., Allen, C., Brachfeld, S., Cardillo, F. G., Du, Z., . . . Zheng, X. (2022). Ancient marine sediment DNA reveals diatom transition in Antarctica. *Nature communications, 13*(5787), 5787-5787.

Atanassova, J. (2005). Palaeoecological setting of the western Black Sea area during the last 15 000 years. *Holocene, 15*(4), 576-584.

Bahr, A., Lamy, F., Arz, H., Kuhlmann, H., & Wefer, G. (2005). Late glacial to Holocene climate and sedimentation history in the NW Black Sea. *Marine Geology, 214*, 309-322.

Baldwin, A. H. (1996). *The role of seed banks, disturbance, and sea level rise in determining the plant community structure of oligohaline coastal marshes* [Doctoral dissertation, Louisiana State University].

Berglund, M., Eriksson, J. A., & Fernlund, J. M. (1994). The late Weichselian in Halland, Southwestern Sweden: A pollen-analytical study. *GFF, 116*(4), 215-230.

Berov, D., Klayn, S., Deyanova, D., & Karamfilov, V. (2022). Current distribution of Zostera seagrass meadows along the Bulgarian Black Sea coast (SW Black Sea, Bulgaria) (2010-2020). Biodiversity data journal, 10, 78942.

Boere, A. C., Sinninghe Damsté, J. S., Rijpstra, W. I. C., Volkman, J. K., & Coolen, M. J. L. (2011). Source-specific variability in post-depositional DNA preservation with potential implications for DNA based paleoecological records. *Organic geochemistry, 42*(10), 1216-1225.

Bondev, I. (1991). *Vegetation of Bulgaria: 1:600,000 Map with Explanatory Text.* ["St. Kliment Ohrdski" University Press, Sofia (in Bulgarian)].

Bottema, S. (1980). On the history of the walnut (Juglans regia L.) in southeastern Europe. *Acta Botanica Neerlandica, 29*(5-6), 343-349.

Boyer, F., Mercier, C., Bonin, A., Le Bras, Y., Taberlet, P., & Coissac, E. (2016). Obitools: a unix-inspired software package for DNA metabarcoding. *Molecular Ecology Resources, 16*(1), 176-182.

Burke, S. V., Wysocki, W. P., Zuloaga, F. O., Craine, J. M., Pires, J. C., Edger, P. P., Mayfield-Jones, D., Clark, L. G., Kelchner, S. A., & Duvall, M. R. (2016). Evolutionary relationships in Panicoid grasses based on plastome phylogenomics (Panicoideae; Poaceae). BMC Plant Biol, *16*(1), 140.

Capo, E., Giguet-Covex, C., Rouillard, A., Nota, K., Heintzman, P. D., Vuillemin, A., Ariztegui, D., Arnaud, F., Belle, S., Bertilsson, S., Bigler, C., Bindler, R., Brown, A. G., Clarke, C. L., Crump, S. E., Debroas, D., Englund, G., Ficetola, G. F., Garner, R. E., Gauthier, J., Gregory-Eaves, I., Heinecke, L., Herzschuh, U., Ibrahim, A., Kisand, V., Kjaer, K. H., Lammers, Y., Littlefair, J., Messager, E., Monchamp, M. E., Olajos, F., Orsi, W., Pedersen, M. W., Rijal, D. P., Rydberg, J., Spanbauer, T., Stoof-Leichsenring, K. R., Taberlet, P., Talas, L., Thomas, C., Walsh, D. A., Wang, Y. C., Willerslev, E., van Woerkom, A., Zimmermann, H. H., Coolen, M. J. L., Epp, L. S., Domaizon, I., Alsos, I. G.,

& Parducci, L. (2021). Lake Sedimentary DNA Research on Past Terrestrial and Aquatic Biodiversity. Overview and Recommendations. *Quaternary, 4*(1).

Chun, Y.-M., & Choi, Y. D. (2009). Expansion of Phragmites australis (Cav.) Trin. ex Steud. (Common Reed) into Typha spp. (Cattail) Wetlands in Northwestern Indiana, USA. *Journal of Plant Biology, 52*(3), 220-228.

Clarke, K. R., & Gorley, R. N. (2015). PRIMER v7: User Manual/Tutorial. PRIMER-E Ltd.

Cleal, C., Pardoe, H. S., Berry, C. M., Cascales-Minana, B., Davis, B. A. S., Diez, J. B., Filipova-Marinova, M. V., Giesecke, T., Hilton, J., Ivanov, D., Kustatscher, E., Leroy, S. A. G., McElwain, J. C., Oplustil, S., Popa, M. E., Seyfullah, L. J., Stolle, E., Thomas, B. A., & Uhl, D. (2021). Palaeobotanical experiences of plant diversity in deep time; 1, How well can we identify past plant diversity in the fossil record? *Palaeogeography, palaeoclimatology, palaeoecology, 576,* 110481.

Coissac, E., Riaz, T., & Puillandre, N. (2012). Bioinformatic challenges for DNA metabarcoding of plants and animals. *Molecular Ecology, 21,* 1834–1847.

Connor, S. E., Ross, S. A., Sobotkova, A., Herries, A. I. R., Mooney, S. D., Longford, C., & Iliev, I. (2013). Environmental conditions in the SE Balkans since the Last Glacial Maximum and their influence on the spread of agriculture into Europe. *Quaternary Science Reviews, 68*, 200-215.

Connor, S. E., Ross, S. A., Sobotkova, A., Herries, A. I. R., Mooney, S. D., Longford, C., & Iliev, I. (2013). Environmental conditions in the SE Balkans since the Last Glacial Maximum and their influence on the spread of agriculture into Europe. *Quaternary Science Reviews*, *68*, 200-215.

Connor, S. E., Thomas, I., & Kvavadze, E. V. (2007). A 5600-yr history of changing vegetation, sea levels and human impacts from the Black Sea coast of Georgia. *Holocene, 17*(1), 25-36.

Coolen, M. J. L. (2011). 7000 years of Emiliania huxleyi viruses in the Black Sea. *Science, 333*(6041), 451-452.

Coolen, M. J. L., Boere, A., Abbas, B., Baas, M., Wakeham, S. G., & Sinninghe Damste, J. S. (2006). Ancient DNA derived from alkenone-biosynthesizing haptophytes and other algae in Holocene sediments from the Black Sea. *Paleoceanography, 21*(1), 1005.

Coolen, M. J. L., Orsi, W. D., Balkema, C., Quince, C. H., Keith, Sylva, S. P., Filipova-Marinova, M., & Giosan, L. (2013). Evolution of the plankton paleome in the Black Sea from the Deglacial to Anthropocene. *Proceedings of the National Academy of Sciences of the United States of America, 110*(21), 8609-8614.

Coolen, M. J. L., Saenz, J. P., Giosan, L., Trowbridge, N. Y., Dimitrov, P., Dimitrov, D., & Eglinton, T. I. (2009). DNA and lipid molecular stratigraphic records of haptophyte succession in the Black Sea during the Holocene. *Earth and Planetary Science Letters, 284*(3-4), 610-621.

Cordova, C. E., Harrison, S. P., Mudie, P. J., Riehl, S., Leroy, S. A. G., & Ortiz, N. (2009). Pollen, plant macrofossil and charcoal records for palaeovegetation reconstruction in the Mediterranean-Black Sea Corridor since the Last Glacial Maximum. *Quaternary International, 197*, 12-26.

Corinaldesi, C., Barucca, M., Luna, G. M., & Dell'Anno, A. (2011). Preservation, origin and genetic imprint of extracellular DNA in permanently anoxic deep-sea sediments. *Molecular Ecology, 20*(3), 642-654.

Courtin, J., Andreev, A. A., Raschke, E., Bala, S., Biskaborn, B. K., Liu, S. S., Zimmermann, H., Diekmann, B., Stoof-Leichsenring, K. R., Pestryakova, L. A., & Herzschuh, U. (2021). Vegetation Changes in Southeastern Siberia During the Late Pleistocene and the Holocene. *Frontiers in Ecology and Evolution, 09*.

Dalén, L., Heintzman, P. D., Kapp, J. D., & Shapiro, B. (2023). Deep-time paleogenomics and the limits of DNA survival. Science, 382(6666), 48-53.

Damialis, A., Syropoulou, E., Gioulekas, D., & Vokou, D. (2006, June 10). Long-distance transport of hazel (Corylus avellana) airborne pollen into the city of Thessaloniki, north Greece: Randomness or a systematic atmospheric circulation pattern? : XXV Congress of the European Academy of Allergology and Clinical Immunology, Vienna, Austria.

De Caceres, M., & Legendre, P. (2009). Associations between species and groups of sites: indices and statistical inference. *Ecology, 90*(12), 3566-3574.

Deptuła, M., Piernik, A., Nienartowicz, A., Hulisz, P., & Kamiński, D. (2020). Alnus glutinosa L. Gaertn. as potential tree for brackish and saline habitats. *Global ecology and conservation, 22*, 977.

Dong, W., Liu, J., Yu, J., Wang, L., & Zhou, S. (2012). Highly Variable Chloroplast Markers for Evaluating Plant Phylogeny at Low Taxonomic Levels and for DNA Barcoding. *PLOS ONE, 7*(4), 35071.

Douda, J., Boublík, K., Slezák, M., Biurrun, I., Nociar, J., Havrdová, A., Doudová, J., Aćić, S., Brisse, H., Brunet, J., Chytrý, M., Claessens, H., Csiky, J., Didukh, Y., Dimopoulos, P., Dullinger, S., FitzPatrick, Ú., Guisan, A., Horchler, P. J., . . . Schwabe-Kratochwil, A. (2016). Vegetation classification and biogeography of European floodplain forests and alder carrs. *Applied vegetation science, 19*(1), 147-163.

Dufrene, M., & Legendre, P. (1997). Species assemblages and indicator species: The need for a flexible asymmetrical approach. *Ecological Monographs, 67*(3), 345-366.

Eastwood, W. J., Fairbairn, A., Stroud, E., Roberts, N., Lamb, H., Yigitbasioglu, H., Senkul, C., Moss, A., Turner, R., & Boyer, P. (2018). Comparing pollen and archaeobotanical data for Chalcolithic cereal agriculture at Catalhoyuk, Turkey. *Quaternary science reviews, 202,* 4-18.

Epp, L. S., Gussarova, C., Boessenkool, S., Olsen, J., Haile, J., Schroder-Nielsen, A., Ludikova, A., Hassel, K., Stenoien, H. K., Funder, S., Willerslev, E., Kjaer,

K., & Brochmann, C. (2015). Lake sediment multi-taxon DNA from North Greenland records early post-glacial appearance of vascular plants and accurately tracks environmental changes. *Quaternary Science Reviews, 117*, 152-163.

Erftemeijer, P. L. A., & Robin, L. R. R. (2006). Environmental impacts of dredging on seagrasses: A review. *Marine pollution bulletin, 52*(12), 1553-1572.

Fagerstrom., M. (1999). *Athyrium filix-femina - lady fern.* Portland State University.

Filipova-Marinova, M. (2003). Palaeoenvironmental changes in the Southern Bulgarian Black Sea area during the last 29,000 years. *Phytologia Balcanica, 9*, 275-292.

Filipova-Marinova, M. (2006). Palynostratigraphy of Pleistocene and Holocene sediments from the western Black Sea area. *Comptes Rendus De L Academie Bulgare Des Sciences, 60*(3), 279-290.

Filipova-Marinova, M., Pavlov, D., Coolen, M. J. L., & Giosan, L. (2012). First high-resolution marinopalynological stratigraphy of Late Quaternary sediments from the central part of the Bulgarian Black Sea area. *Quaternary International, 293*, 170-183.

Foster, N. R., Dijk, K. j., Biffin, E., Young, J. M., Thomson, V. A., Gillanders, B. M., Jones, A. R., & Waycott, M. (2022). A targeted capture approach to generating reference sequence databases for chloroplast gene regions. *Ecology and evolution, 12*(4), 8816.

Fulton, J. M., Arthur, M. A., & Freeman, K. H. (2012). Subboreal aridity and scytonemin in the Holocene Black Sea. *Organic geochemistry, 49,* 47-55.

Gielly, L., & Taberlet, P. (1994). The use of chloroplast DNA to resolve plant phylogenies - noncoding versus RBCL sequences. *Molecular Biology and Evolution, 11*(5), 769-777.

Giesecke, T., Davis, B., Brewer, S., Finsinger, W., Wolters, S., Blaauw, M., de Beaulieu, J.-L., Binney, H., Fyfe, R. M., Gaillard, M.-J., Gil-Romera, G., van der Knaap, W. O., Kuneš, P., Kühl, N., van Leeuwen, J. F. N., Leydet, M.,

Lotter, A. F., Ortu, E., Semmler, M., & Bradshaw, R. H. W. (2014). Towards mapping the late Quaternary vegetation change of Europe. *Vegetation history and archaeobotany*, *23*(1), 75-86.

Giosan, L., Coolen, M. J. L., Kaplan, J. O., Constantinescu, S., Filip, F., Filipova-Marinova, M., Kettner, A. J., & Thom, N. (2012). Early anthropogenic transformation of the danube-black sea system. *Scientific reports, 2*(1), 582-582.

Glaser, J., & Wulf, M. (2009). Effects of water regime and habitat continuity on the plant species composition of floodplain forests. *Journal of Vegetation Science, 20*, 37–48.

Golovnina, K. A., Glushkov, S. A., Blinov, A. G., Mayorov, V. I., Adkison, L. R., & Goncharov, N. P. (2007). Molecular phylogeny of the genus Triticum L. *Plant Systematics and Evolution, 264*(3-4), 195-216.

Hay, B. J. (1988). Sediment accumulation in the central western Black Sea over the past 5100 years. *Paleoceanography, 3*(4), 491-508.

Hope, G. (2001). Environmental change in the Late Pleistocene and later Holocene at Wanda site, Soroako, South Sulawesi, Indonesia. *Palaeogeography Palaeoclimatology Palaeoecology, 171*(3-4), 129-145.

Hoyle, T. M., Bista, D., Flecker, R., Krijgsman, W., & Sangiorgi, F. (2021). Climate-driven connectivity changes of the Black Sea since 430 ka; testing a dual palynological and geochemical approach. *Palaeogeography, palaeoclimatology, palaeoecology*, *561*, 110069.

Huang, Y., Zheng, Y., Heng, P., Giosan, L., & Coolen, M. J. L. (2021). Black Sea paleosalinity evolution since the last deglaciation reconstructed from alkenone-inferred Isochrysidales diversity. *Earth and planetary science letters, 564,* 116881.

Klink, C. A., & Joly, C. A. (1989). Identification and Distribution of C3 and C4 Grasses in Open and Shaded Habitats in Sao Paulo State, Brazil. Biotropica, *21*(1), 30–34.

Kosir, P., Carni, A., Marinsek, A., & Silc, U. (2013). Floodplain forest communities along the Mura River (NE Slovenia). *Acta Botanica Croatica, 72*(1), 71-95.

Lazarova, M., & Bozilova, E. (2001). Studies on the Holocene history of vegetation in the region of lake Srebarna (northeast Bulgaria). *Vegetation history and archaeobotany, 10*(2), 87-95.

Leroy, S. A. G., & Roiron, P. (1996). Latest Pliocene pollen and leaf floras from Bernasso palaeolake (Escandorgue Massif, Herault, France). *Review of palaeobotany and palynology, 94*(3-4), 295-328.

Li, K., Stoof-Leichsenring, K. R., Liu, S. S., Jia, W. H., Liao, M. N., Liu, X. Q., Ni, J., & Herzschuh, U. (2021). Plant sedimentary DNA as a proxy for vegetation reconstruction in eastern and northern Asia. *Ecological Indicators, 132*.

Liu, S. S., Stoof-Leichsenring, K. R., Kruse, S., Pestryakova, L. A., & Herzschuh, U. (2020). Holocene vegetation and plant diversity changes in the Northeastern Siberian treeline region from pollen and sedimentary ancient DNA. *Frontiers in Ecology and Evolution, 8*.

Lubna, Asaf, S., Khan, A. L., Jan, R., Khan, A., Khan, A., Kim, K. M., & Lee, I. J. (2021). The dynamic history of gymnosperm plastomes: Insights from structural characterization, comparative analysis, phylogenomics, and time divergence. *The plant genome, 14*(3), 20130.

Lukina, G.D. (1986). *Polysaccharide seagrasses of the Black Sea: the chemical composition, structure, propertiesand practical use.* [Doctoral dissertation, Odessa Russia].

Magyari, E. K., Chapman, J., Fairbairn, A. S., Francis, M., & de Guzman, M. (2012). Neolithic human impact on the landscapes of North-East Hungary inferred from pollen and settlement records. *Vegetation history and archaeobotany, 21*(4/5), 279-302.

Major, C., Ryan, W., Lericolais, G., & Hajdas, I. (2002). Constraints on Black Sea outflow to the Sea of Marmara during the last glacial-interglacial transition. *Marine Geology, 190*(1-2), 19-34.

Mander, L., & Punyasena, S. W. (2014). On the taxonomic resolution of pollen and spore records of earth's vegetation. *International Journal of Plant Sciences, 175*(8), 931-945.

Manske, A. K., Henssge, U., Glaeser, J., & Overmann, J. (2008). Subfossil 16S rRNA gene sequences of green sulfur bacteria in the Black Sea and their implications for past photic zone anoxia. *Applied and Environmental Microbiology, 74*, 624-632.

Milchakova, N. A. (1999). On the status of seagrass communities in the Black Sea. *Aquatic botany, 65*(1), 21-31.

Mudie, P. J., Marret, F., Aksu, A. E., Hiscott, R. N., & Gillespie, H. (2007). Palynological evidence for climatic change, anthropogenic activity and outflow of Black Sea water during late Pleistocene and Holocene: Centennial-to decadal-scale records from the Black and Marmara Seas. *Quaternary International, 167*, 73-90.

Mudie, P. J., Rochon, A., & Aksu, A. E. (2002). Pollen stratigraphy of Late Quaternary cores from Marmara Sea: land-sea correlation and paleoclimatic history. *Marine Geology, 190*(1-2), 233-260.

Murray, J. W., Jannasch, H. W., Honjo, S., Anderson, R. F., Reeburgh, W. S., Top, Z., Friederich, G. E., Codispoti, L. A., & Izdar, E. (1989). Unexpected changes in the oxic/anoxic interface in the Black Sea. *Nature*, *338*(6214), 411-413.

Niemeyer, B., Epp, L. S., Stoof-Leichsenring, K. R., Pestryakova, L. A., & Herzschuh, U. (2017). A comparison of sedimentary DNA and pollen from lake sediments in recording vegetation composition at the Siberian treeline. *Molecular Ecology Resources, 17*(6), 46-62.

Novák, P., Willner, W., Biurrun, I., Gholizadeh, H., Heinken, T., Jandt, U., Kollar, J., Kozhevnikova, M., Naqinezhad, A., Onyshchenko, V., Pielech, R., Rašomavičius, V., Shirokikh, P., Vassilev, K., Wohlgemuth, T., Večeřa, M., & Chytrý, M. (2023). Classification of European oak-hornbeam forests and related vegetation types. *Applied Vegetation Science*, *26*, 12712.

Pagter, M., Bragato, C., & Brix, H. (2005). Tolerance and physiological responses of Phragmites australis to water deficit. Aquatic Botany, *81*(4), 285-299.

Palmer, J. D., Jansen, R. K., Michaels, H. J., Chase, M. W., & Manhart, J. R. (1988). Chloroplast DNA variation and plant phylogeny. *Annals of the Missouri Botanical Garden, 75*(4), 1180-1206.

Panagiotopoulos, K. (2013). *Late Quaternary ecosystem and climate interactions in SW Balkans inferred from Lake Prespa sediments* [Doctoral dissertation, Universität zu Köln].

Parducci, L., Bennett, K. D., Ficetola, G. F., Alsos, I. G., Suyama, Y., Wood, J. R., & Pedersen, M. W. (2017). *Ancient plant DNA in lake sediments. New Phytologist, 214*(3), 924-942.

Parducci, L., Matetovici, I., Fontana, S. L., Bennett, K. D., Suyama, Y., Haile, J., Kjaer, K. H., Larsen, N. K., Drouzas, A. D., & Willerslev, E. (2013). Molecular- and pollen-based vegetation analysis in lake sediments from central Scandinavia. *Molecular Ecology, 22*(13), 3511-3524.

Parducci, L., Suyama, Y., Lascoux, M., & Bennett, K. D. (2005). Ancient DNA from pollen: a genetic record of population history in Scots pine. *Molecular Ecology, 14*(9), 2873-2882.

Parducci, L., Valiranta, M., Salonen, J. S., Ronkainen, T., Matetovici, I., Fontana, S. L., Eskola, T., Sarala, P., & Suyama, Y. (2015). Proxy comparison in ancient peat sediments: pollen, macrofossil, and plant DNA. *Philosophical transactions of the Royal Society of London Series B, Biological sciences, 370*(1660), 20130382.

Paus, A., Boessenkool, S., Brochmann, C., Epp, L. S., Fabel, D., Haflidason, H., & Linge, H. (2015). Lake Store Finnsjoen - a key for understanding Lateglacial/early Holocene vegetation and ice sheet dynamics in the central Scandes Mountains. *Quaternary Science Reviews, 121*, 36-51.

Pedersen, M. W., Ginolhac, A., Orlando, L., Olsen, J., Andersen, K., Holm, J., Funder, S., Willerslev, E., & Kjaer, K. H. (2013). A comparative study of ancient environmental DNA to pollen and macrofossils from lake sediments reveals

taxonomic overlap and additional plant taxa. *Quaternary Science Reviews, 75*, 161-168.

Pigott, C., Ratcliffe, D., Malloch, A., Birks, H., & Proctor, M. (2000). SM17: Artemisia maritima salt-marsh community: *Artemisietum maritimae* Hocquette 1927. In J. Rodwell (Ed.), British Plant Communities (British Plant Communities, pp. 84-85). Cambridge: Cambridge University Press.

POWO (2023). *Plants of the World Online.* Royal Botanic Gardens, Kew.

Reitalu, T., Bjune, A. E., Blaus, A., Giesecke, T., Helm, A., Matthias, I., Peglar, S. M., Salonen, J. S., Seppä, H., Väli, V., Birks, H. J. B., Palaeo, e., Coastal dynamics, F. s., & Global, c. (2019). Patterns of modern pollen and plant richness across northern Europe. *The Journal of ecology, 107*(4), 1662-1677.

Rojo, J., Oteros, J., Picornell, A., Ruëff, F., Werchan, B., Werchan, M., Bergmann, K.-C., Schmidt-Weber, C. B., & Buters, J. (2020). Land-Use and Height of Pollen Sampling Affect Pollen Exposure in Munich, Germany. *Atmosphere, 11*(2), 145.

Rossignol, I., Kaniewski, D., Van Campo, E., Petrescu, M., & Baralis, A. (2012). A modern pollen rain study from the Black Sea coast of Romania. *Review of palaeobotany and palynology, 174*, 39-47.

Santi, C., Bogusz, D., & Franche, C. (2013). Biological nitrogen fixation in non-legume plants. *Ann Bot, 111*(5), 743-767.

Shumilovskikh, L. S., Tarasov, P., Arz, H. W., Fleitmann, D., Marret, F., Nowaczyk, N., Plessen, B., Schluetz, F., & Behling, H. (2012). Vegetation and environmental dynamics in the southern Black Sea region since 18 kyr BP derived from the marine core 22-GC3. *Palaeogeography Palaeoclimatology Palaeoecology, 337*, 177-193.

Sifton, M. A., Lim, P., Smith, S. M., & Thomas, S. C. (2022). Interactive effects of biochar and N-fixing companion plants on growth and physiology of *Acer saccharinum. Urban Forestry & Urban Greening, 74,* 127652.

Sonstebo, J. H., Gielly, L., Brysting, A. K., Elven, R., Edwards, M., Haile, J., Willerslev, E., Coissac, E., Rioux, D., Sannier, J., Taberlet, P., & Brochmann, C. (2010). Using next-generation sequencing for molecular reconstruction of past Arctic vegetation and climate. *Molecular Ecology Resources, 10*(6), 1009-1018.

Spetsov, P., Plamenov, D., & Kiryakova, V. (2006). Distribution and characterization of *Aegilops* and *Triticum* species from the Bulgarian Black Sea coast. *Central European journal of biology, 1*(3), 399-411.

Stevenson, J. (2018). Vegetation and climate of the Last Glacial Maximum in Sulawesi. In S. O. orcid, D. B. orcid, J. Meyer (Eds.), *The Archaeology of Sulawesi. Current Research on the Pleistocene to the Historic Period* (pp. 17-29). ANU Press.

Taberlet, P., Coissac, E., Pompanon, F., Gielly, L., Miquel, C., Valentini, A., Vermat, T., Corthier, G., Brochmann, C., & Willerslev, E. (2007). Power and limitations of the chloroplast trnL (UAA) intron for plant DNA barcoding. *Nucleic Acids Research, 35*(3), 14.

THE BULGARIAN FLORA ONLINE (2008). *Filipendula ulmaria.* (https://bgflora.net/families/rosaceae/filipendula/filipendula_ulmaria/filipendula_ulmaria_en.html).

Tonkov, S., & Bozilova, E., (1995). Palaeoecological data about the end of the Holocene climatic optimum in Bulgaria e IV millennium BC. *Annual of Sofia University, Biology 87*(2), 5-17.

van der Hammen, T., Wijmstra, A., & Zagwijn, W., (1971). The floral record of the Late Cenozoic of Europe. In K. K. Turekian (Ed.), *The Late Cenozoic Glacial Ages.* Yale University Press, New Heaven.

van der Meer, M. T. J., Sangiorgi, F., Baas, M., Brinkhuis, H., Sinninghe Damste, J. S., & Schouten, S. (2008). Molecular isotopic and dinoflagellate evidence for late Holocene freshening of the Black Sea. *Earth and planetary science letters, 267*(3-4), 426-434.

Van Pelt, R., O'Keefe, T. C., Latterell, J. J., & Naiman, R. J. (2006). Riparian forest stand development along the Queets River in Olympic National Park, Washington. *Ecological monographs, 76*(2), 277-298.

Velasco, L., Pérez-Vich, B., & Fernández-Martínez, J. M. (2016). Research on resistance to sunflower broomrape: An integrated vision. *Oléagineux corps gras lipides, 23*(2), D203.

Voldstad, L. H., Alsos, I. G., Farnsworth, W. R., Heintzman, P. D., Hakansson, L., Kjellman, S. E., Rouillard, A., Schomacker, A., & Eidesen, P. B. (2020). A complete Holocene lake sediment ancient DNA record reveals long-standing high Arctic plant diversity hotspot in northern Svalbard. *Quaternary Science Reviews, 234*.

Wanner, H., Beer, J., Buetikofer, J., Crowley, T. J., Cubasch, U., Flueckiger, J., Goosse, H., Grosjean, M., Joos, F., Kaplan, J. O., Kuettel, M., Mueller, S. A., Prentice, I. C., Solomina, O., Stocker, T. F., Tarasov, P., Wagner, M., & Widmann, M. (2008). Mid- to Late Holocene climate change: an overview. *Quaternary Science Reviews, 27*(19-20), 1791-1828.

Watson, E. B., & Byrne, R. (2009). Abundance and diversity of tidal marsh plants along the salinity gradient of the San Francisco Estuary: implications for global change ecology. *Plant Ecology, 205*(1), 113-128.

Wick, L., Lemcke, G., & Sturm, M. (2003). Evidence of Lateglacial and Holocene climatic change and human impact in eastern Anatolia: high-resolution pollen, charcoal, isotopic and geochemical records from the laminated sediments of Lake Van, Turkey. *The Holocene, 13*(5), 665-675.

Willerslev, E., & Cooper, A. (2005). Ancient DNA. *Proceedings of the Royal Society of London Series B-Biological Sciences, 272*(1558), 3-16.

Yang, S., Gu, F., Song, B., Ye, S., Yuan, Y., He, L., Li, J., Zhao, G., Ding, X., Pei, S., Laws, E. A., & Sangiorgi, F. (2022). Holocene vegetation history and responses to climate and sea-level change in the Liaohe Delta, northeast China. *Catena (Giessen), 217*, 106438.

Zimmermann, H. H., Raschke, E., Epp, L. S., Stoof-Leichsenring, K. R., Schwamborn, G., Schirrmeister, L., Overduin, P. P., & Herzschuh, U. (2017). Sedimentary ancient DNA and pollen reveal the composition of plant organic matter in Late Quaternary permafrost sediments of the Buor Khaya Peninsula (northeastern Siberia). *Biogeosciences, 14*(3), 575-596.

4.7 Supplementary materials
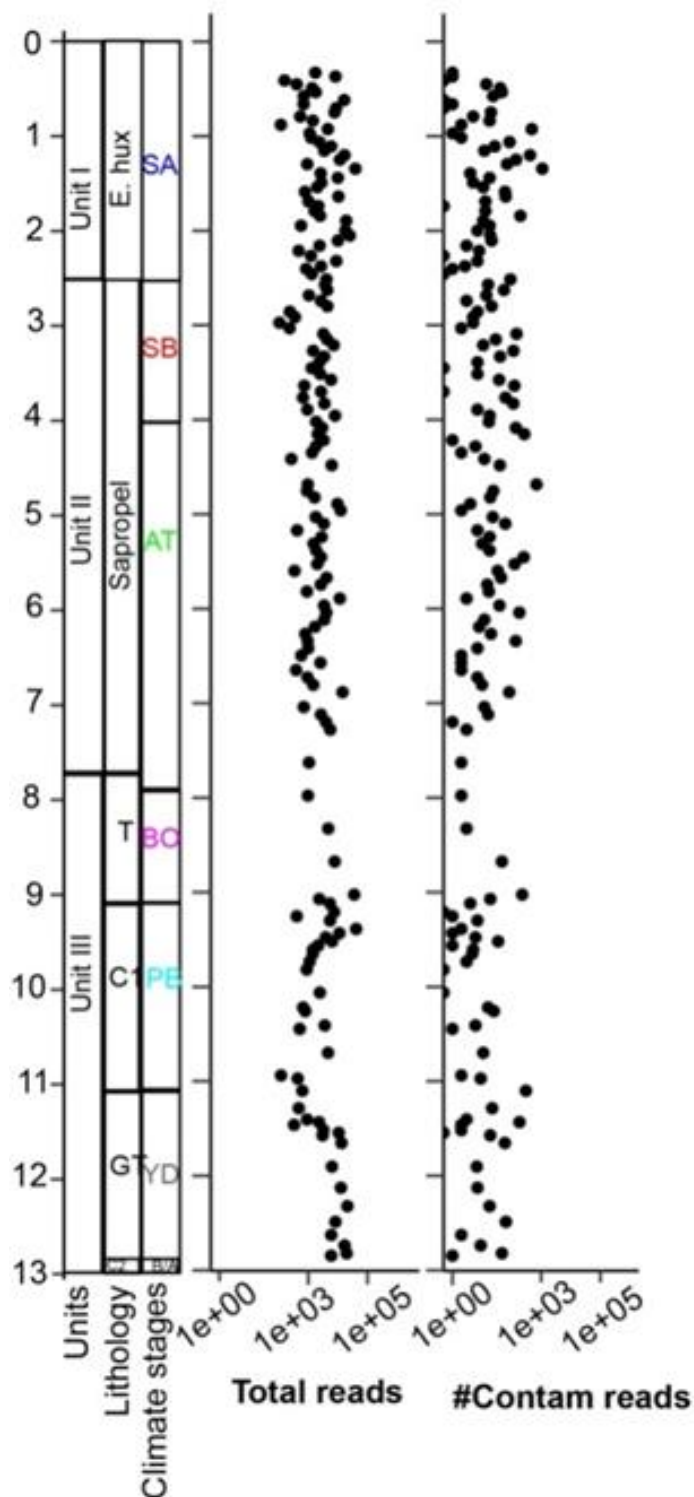
Figure S4.1 The dot plots show the down core distribution of the *trn*LP-6 recovered total reads and contamination reads. The age model, lithology, and climate stages of MC19 and GGC18 are also plotted. For more about the factors please see the legend of Fig. 4.1 and the text inside the corresponding chapter.

Table S4.1 The *trn*LP-6 identified vegetation at order, family, subfamily, class, genus, and species level.

Vegetation Type	Taxa (trnL-P6)
Aquatics	o_Alismatales;f_Potamogetonaceae;g_*Zannichellia*
Aquatics	o_Alismatales;f_Zosteraceae;g_*Zostera*
Aquatics	o_Poales;f_Typhaceae;g_*Typha*
Aquatics	o_Saxifragales;f_Haloragaceae;g_*Myriophyllum*
Sedges	o_Poales;f_Cyperaceae;g_*Carex*
Ferns	o_Polypodiales;_f_Athyriaceae;_g_*Athyrium*
C3_grasses	o_Poales;f_Poaceae;Cl_BOP;sf_Pooideae
C3_grasses	o_Poales;f_Poaceae;Cl_BOP;sf_Pooideae;tr_Barchypodieae;g_*Brachypodium*;s_*distachyon*
C3_grasses	o_Poales;f_Poaceae;Cl_BOP;sf_Pooideae;tr_Poeae_Chloroplast_Groupl_Aveneae_Type
C3_grasses	o_Poales;f_Poaceae;cl_PACMAD;sf_Arundinoideae;g_*Phragmites*;s_*P.australis*
C3_grasses	o_Poales;f_Poaceae;cl_PACMAD;sf_Danthonioideae
C3_grasses_cultivars	o_Poales;f_Poaceae;Cl_BOP;sf_Pooideae;tr_Tritiaceae;g_*Secale__Elymus*
C3C4_grasses	o_Poales;f_Poaceae;cl_PACMAD;sf_Panicoideae
C4_grasses	o_Poales;f_Poaceae;cl_PACMAD;sf_Chloridoideae;tr_Eragroistideae
C4_grasses	o_Poales;f_Poaceae;cl_PACMAD;sf_Chlorodoideae
Herbs	o_Apiales;f_Apiaceae;g_*Sison*;s_*S. amomum*
Herbs	o_Asparagales;f_Amaryllidaceae;g_*Allium*
Herbs	o_Asterales;f_Asteraceae;sf_Asteroideae
Herbs	o_Asterales;f_Asteraceae;sf_Asteroideae;tr_Anthemideae
Herbs	o_Asterales;f_Asteraceae;sf_Chichorieae
Herbs	o_Fabales;f_Fabaceae;sf_Faboideae;tr_Cicereae;g_*Cicer*
Herbs	o_Fabales;f_Fabaceae;sf_Faboideae;tr_Phaseoleae
Herbs	o_Fabales;f_Fabaceae;sf_Faboideae;tr_Trifoliaceae;g_*Trifolium*
Herbs	o_Gentianales;f_Rubiaceae
Herbs	o_Lamiales;f_Lamiaceae
Herbs	o_Malpighiales;f_Euphorbiaceae;g_*Euphorbia*
Herbs	o_Rosales;f_Cannabaceae;g_*Humulus*
Herbs	o_Rosales;f_Rosaceae;g_*Filipendula*
TRSH	o_Cornales;f_Cornaceae;g_*Cornus*
TRSH	o_Crossosomatales;f_Staphyleaceae;g_*Staphylea*
TRSH	o_Fagales;f_Betulaceae;g_*Alnus*
TRSH	o_Fagales;f_Betulaceae;g_*Betula*
TRSH	o_Fagales;f_Betulaceae;g_*Carpinus_Corylus*
TRSH	o_Fagales;f_Fagaceae;g_*Castanea*
TRSH	o_Fagales;f_Fagaceae;g_*Fagus*
TRSH	o_Fagales;f_Fagaceae;g_*Quercus*
TRSH	o_Fagales;f_Juglandaceae
TRSH	o_Malpighiales;f_Salicaceae;g_*Populus*
TRSH	o_Malpighiales;f_Salicaceae;g_*Salix*
TRSH	o_Malvales;f_Malvaceae;g_*Tilia*
TRSH	o_Rosales;f_Moraceae
TRSH	o_Rosales;f_Rhamnaceae
TRSH	o_Rosales;f_Rosaceae;g_*Pyrus*
TRSH	o_Rosales;f_Ulmaceae;g_*Ulmus*
TRSH	o_Sapindales;f_Sapindaceae;g_*Acer*
Conifers	o_Cupressales;f_Cupressaceae;g_*Juniperus*
Conifers	o_Cupressales;f_Taxaceae;g_*Taxus*
Conifers	o_Pinales;f_Pinaceae;g_*Abies*
Conifers	o_Pinales;f_Pinaceae;g_*Cedrus*
Conifers	o_Pinales;f_Pinaceae;g_*Picea*
Conifers	o_Pinales;f_Pinaceae;g_*Pinus*

Chapter 5

Conclusion and Future Prospective

5.1 Ancient DNA archives in Lake and Marine sediments

Chapter 2 of this PhD dissertation investigated the preservation potential of the plant chloroplast metabarcoding gene *trn*L-P6 in Late-Pleistocene sediments of tropical Lake Towuti. Despite long-term exposure to unfavourable high *in situ* temperatures, substantial amounts of the chloroplast marker gene could be recovered and sequenced from >1 Ma-old sediments of the lake and complement geochemical datasets in reconstructing local paleovegetation assemblages and concomitant paleoenvironmental conditions spanning several glacial-interglacial cycles.

In Chapter 3, the same DNA extracts from the Lake Towuti record served as the template for 18SV9 amplicon sequencing and to generate a parallel record of fungal community changes. Integration of this 18SV9-inferred fungal community composition dataset with the *trn*L-P6 paleovegetation record of Chapter 2 and previously analysed geochemical paleoenvironmental parameters showed that tropical lakes can also form long-term genomic archives of direct- (phytopathogenic, mycorrhizal) and indirect- (soil-, wood-, and sedimentary organic matter decomposing) fungal-plant-soil (paleo)associations.

In Chapter 4, the *trn*L-P6 amplicon sequencing approach was employed on Late-Glacial and Holocene sediments from the southwestern Black Sea to investigate (a) if remote marine basins with much more extensive and complicated catchment areas compared to inland lakes represent suitable *sed*aDNA archives of terrestrial and marine paleovegetation communities and (b) if the metabarcoding approach could complement, refine, or overturn pollen-inferred interpretations concerning the climatic or anthropogenic perturbations that may have contributed to changes in the regional paleo floristic landscape. A more detailed overview of the findings for each research chapter is outlined below.

5.2 (Chapter 2): A 1 Ma sedimentary ancient DNA (*sed*aDNA) record of catchment vegetation changes and the developmental history of tropical Lake Towuti (Sulawesi, Indonesia)

For this Chapter, we successfully amplified and sequenced sedimentary *trn*L-P6 from more than 1-Ma-old tropical Lake Towuti sediments. At least 45 native taxa were identified at family or lower taxonomic ranks. Downcore changes in the relative read abundance of these paleovegetation assemblages reflected changes in the paleodepositional environment as inferred from Pearson correlations with previously analysed organic and inorganic parameters during the lakes' more than 1 Myr history. Nitrogen-fixing pioneer vegetation and shallow wetland herbs were most strongly associated with more than one Ma-old peat and felsic silt intervals deposited in a tectonically active landscape of active river channels, shallow lakes, and peat swamps. A statistically significant shift in the paleovegetation was observed ~200 ka after the transition into a permanent lake (i.e., ~800 ka ago), which coincided with a decrease in tectonic activity and catchment adjustments. Most notably, the newly emerged shoreline vegetation comprised putative peatland forest trees and partially submerged C_3 grasses (Oryzaceae). Positive Pearson correlations between relative changes in their *trn*L-P6 content with %TOC and the TLE/TOC ratio suggest that this vegetation grew and rooted in muddy organic-rich shoreline sediments. Stratified and anoxic conditions likely contributed to preserving the labile sedimentary OM, and bioavailable Fe(II) would have been readily available. An increase in nutrient availability from frequent turnover of the water column combined with the slow release of tephra-bound phosphorus could have contributed to the expansion of Java water dropwort, which coincided with the formation of diatom blooms, as evident from the correlation between changes in the relative read abundance of sedimentary *trn*L-P6 of this aquatic herb with silica content. In contrast herbs (Brassicaceae, Fabaceae), trees/shrubs (Theaceae), and C_3 grasses (Pooideae) showed the highest positive Pearson correlations with sediments of an ultramafic signature (e.g., rich in Fe, Ni and Cr). These plant families include the highest number of taxa with highly efficient strategies to extract bioavailable Fe(II) from iron-rich rocks and are capable of hyperaccumulating phytotoxic metals, including Ni and Cr. Therefore, this vegetation was likely adapted to grow on the ultramafic rocks within the lake's catchment, and their chloroplast-rich biomass drained into Lake Towuti mixed with

eroded ultramafic substrates during drier periods. Rainforest trees (e.g., *Toona*), shady ground cover herbs (Zingiberaceae), and tree orchids (*Luisia*), showed the highest Pearson correlations with inorganic parameters indicating increased drainage of felsic substrates from the Loeha River to the east of Lake Towuti during periods of increased precipitation. However, the co-presence of sedimentary *trn*L-P6 from dry climate-adapted vegetation (i.e., C_4 grasses and *Castanopsis*/*Lithocarpus*) implies that more seasonal climates also resulted in a predominance of felsic drainage, not just wetter conditions. In conclusion, this study showed that despite unfavourable high *in situ* temperatures, tropical lake *sed*aDNA records could complement morphological and geochemical proxies in reconstructing temporal changes in local terrestrial and aquatic paleovegetation assemblages and concomitant paleoenvironmental conditions spanning several glacial-interglacial cycles.

5.3 (Chapter 3): A 1 Ma sedimentary ancient DNA (*sed*aDNA) record of tropical paleovegetation assemblages and their associations with parasitic, endophytic, and saprophytic fungi

Fungi have a global distribution and exhibit diverse functional traits that are pivotal in driving terrestrial ecosystem dynamics. Short-term time series experiments have shown that the diversity and composition of soil fungi are subject to change in a global warming scenario, with potentially significant implications for the resilience of forest functioning, plant diversity, and soil processes. However, the analysis of geobiological archives (e.g., lake sediments) is required to cover climate-induced compositional changes of vegetation and associated fungal communities that take place at decadal to millennial timescales. Unfortunately, unlike pollen palynomorphs, diagnostic morphological features of fungi are rarely present. Sedimentary ancient DNA (*sed*aDNA) metabarcoding offers the opportunity to reconstruct past ecosystems, including taxa that lack morphological remains. This approach was recently used to reconstruct Quaternary fungal associations with Arctic tundra vegetation. However, similar studies have yet to be performed from tropical lake records where high *in situ* temperatures are expected to be unsuitable for the long-term preservation of *sed*aDNA.

For this chapter, we used 18S rRNA gene metabarcoding to study the eukaryotic community composition at millennium-scale resolution in the same 1 Ma-year-old sediments from tropical Lake Towuti (Sulawesi, Indonesia) that were

analysed for paleovegetation using *trn*L-P6 metabarcoding (Chapter 2 of this thesis). Fungi comprised >96% of the eukaryotic reads in all 82 sediment intervals. All identified fungal taxa belonged to Ascomycota (mainly Dothiodeomycetes, Eurotiomycetes, and Leotiomycetes) and Basidiomycota (dominated by Agaricomycetes). Most taxa were related to soil OM and wood decaying saprotrophs and, to a lesser extent, with ectomycorrhizal or necrotrophic phytopathogens. Pearson correlation analysis between relative changes in fungi and geochemical parameters vs. *trn*L-P6 paleovegetation communities showed that the downcore distribution of the fungal community composition was mainly shaped by soil mineral composition, the amount and maturity of sedimentary OM, and paleovegetation categories that differ in their lignocellulosic fibre content. Didymellaceae (Dothideomycetes) and Basidiomycota most strongly correlated with TRSH and were most likely involved in lignocellulosic wood decay. Ascomycota belonging to the soil clade GS35, Eurotiomycetes (Aspergillaceae and Herpotrichiellaceae) and Leotiomycetes (Pseudeurotiaceae and Gelatiodiscaceae) most strongly correlated with grasses and may have been part of the rhizosphere or as free-living saprotrophic soil OM degraders. Leptospheriaceae and Phaeosphaeriaceae (Dothideomycetes) most likely formed a close association with herbs as necrotrophic phytopathogens, and their combined biomass was mixed in with felsic substrates, which drained into Lake Towuti from the Loeha River catchment during prolonged periods of elevated precipitation and seasonality. The strongest Pearson correlation was observed between *Exophiala* (Herpotrichiellaceae) and organic-rich diatom ooze intervals, where these putative anaerobic fermenters may continue to form a syntrophic partnership with hydrogenotrophic methanogens. Altogether, our data show that tropical lakes can form long-term genomic archives of direct- (phytopathogenic, mycorrhizal) and indirect- (soil-, wood-, and sedimentary OM decomposing) fungal-plant-soil (paleo)associations.

5.4 (Chapter 4): A combined pollen and *sed*aDNA record of late-Glacial and Holocene vegetation changes in the Black Sea region

Several studies have shown that lake sediments represent valuable archives of ancient plant DNA that can be extracted and sequenced to complement palynological studies in reconstructing past vegetation assemblages and their responses to paleoenvironmental and more recent anthropogenic perturbations. However, similar studies have yet to be

performed in detail from marine basins. This research chapter used amplicon sequencing analysis of the chloroplast marker gene *trn*L-P6 to reconstruct late-Glacial and Holocene vegetation changes in the southwestern Black Sea region.

Parallel pollen grain analysis revealed mostly xerophytic herb vegetation (*Artemisia* and *Chenopodiaceae*), which dominated the steppe landscape of the coastal plains surrounding the Black Sea during the cold and dry Younger Dryas. These xerophytic steppe herbs were also identified as significant indicator taxa for the Younger Dryas but remained relatively abundant throughout the wetter and warmer Holocene. According to the pollen analysis, the warm and wet conditions with the onset of the Atlantic (~ 8 ka cal. BP) resulted in an expansion of arboreal oak forest vegetation by hardwood species (*Quercus*, *Corylus*, *Carpinus betulus*, *Fraxinus*, *Fagus*, and *Ulmus*). *Alnus* and *Tilia* were the predominant pollen-producing softwood trees. Furthermore, putative anthropophytes such as cultivated cereals (*Triticum* and cereale-type pollen) and ruderals (e.g., *Filipendula* and *Plantago lanceolata*) indicative of early farming practices were found as early as the Neolithic. They were most consistently present during the Bronze Age, overlapping with the most recent Subatlantic chronozone.

The community composition of the paleovegetation identified through amplicon sequencing of sedimentary *trn*L-P6 partly overlapped with the taxa identified through pollen, with the best overlap observed for trees. However, differences in relative read abundances and significant associations with the various chronozones resulted in different interpretations of the origin of the source plants and the landscape this vegetation occupied. High pollen-producing xerophytic steppe vegetation identified with pollen (*Artemisia*) were minor contributors to the *trn*L-P6 pool during the Younger Dryas and Preboreal. Instead, the *trn*L-P6 approach identified different types of vegetation presumably from the coastal plains and beaches in the catchment area of the then freshwater or oligohaline Black Sea. This vegetation included C_4 grasses (Panicoideae) of the PACMAD clade. Moreover, *trn*L-P6 metabarcoding showed that native C_3 Pooid grasses within the wheat tribe Triticeae were significant indicator taxa for the Younger Dryas and may have been used for cultivation of cereal crops by early farmers as suggested from the increase in cereal-type pollen grains and other

anthropophytes since the Neolithic. In addition, nitrogen-fixing pioneer vegetation (Fabaceae, *Alnus*, and *Populus*) were relatively abundant sources of the cpDNA marker gene during the Younger Dryas and the Preboreal and may have occupied the coastal freshwater catchment before the reconnection with the Mediterranean Sea ~9 ka cal. BP. Here, this vegetation may have contributed to soil fertilisation, paving the way for the succession of secondary forest vegetation. With the onset of the Atlantic, increased precipitation likely resulted in an increased discharge of chloroplast-rich plant litter from halophytic marshland vegetation and vegetation typically lining periodically inundated riparian forests. Most notably, the onset of the Atlantic saw a drastic increase in the relative read abundance of the common and native marshland inhabiting halophyte *Artemisia maritima* as the possible source of *Artemisia* pollen, which would explain why *Artemisia* remained a relatively abundant pollen source throughout the wetter Holocene.

Softwood arboreal taxa (*Alnus*, *Salix*, *Populus*, and *Tilia*), which usually occupy nutrient-rich alluvial sediments closest to the rivers that are often inundated, predominated the *trn*L-P6 pool over hardwood taxa (*Ulmus, Carpinus betulus, Quercus*, and *Acer*), which benefit from interrupted inundation of long habitat continuity and are, therefore, usually zoned further away from the rivers Lastly, sedimentary *trn*L-P6 metabarcoding identified native *Athyrium filix-femina* (lady fern) and *Filipendula ulmaria* (meadowsweet). These taxa can be abundant members of the low diversity ground cover vegetation in moist riparian forests, arguing against *Filipendula* being an anthropophyte used as a ruderal during prehistoric agricultural activities.

This study showed that marine basins can provide valuable long-term archives of cpDNA marker genes and can complement fossil pollen for the reconstruction of paleovegetation assemblages of the hinterland and to refine the pollen-inferred interpretation of climatic vs. anthropogenically induced changes to the regional landscape.

5.5 Limitations and Future Perspectives

There is a critical need to increase the collection of sequence data from plants in the world's floristically diverse tropical provinces. The limited availability of reference sequences of metabarcoding genes from tropical forest vegetation in public databases, notably from this tropical biodiversity hotspot, could in part, explain why a vast number of the *trn*L-P6 reads from the Lake Towuti record could not be assigned.

Moreover, amplicon sequencing usually targets a single gene locus from environmental samples and may fail to capture a substantial fraction of the community diversity in environmental samples. Many taxa could be overlooked due to PCR bias caused by, for example, inefficient primer annealing. Instead, targeting multiple metabarcoding genes using the hybridisation capture approach (Armbrecht et al., 2022; Foster et al., 2022) avoids PCR bias and enhances the probability of identifying more species, particularly from fragmented *sed*aDNA. Therefore, hybridisation capture targeting multiple metabarcoding genes would drastically improve the overall taxonomic resolution of past tropical vegetation. However, this approach would only have merit once a vastly extended database of metabarcoding gene sequencing from tropical plants becomes available.
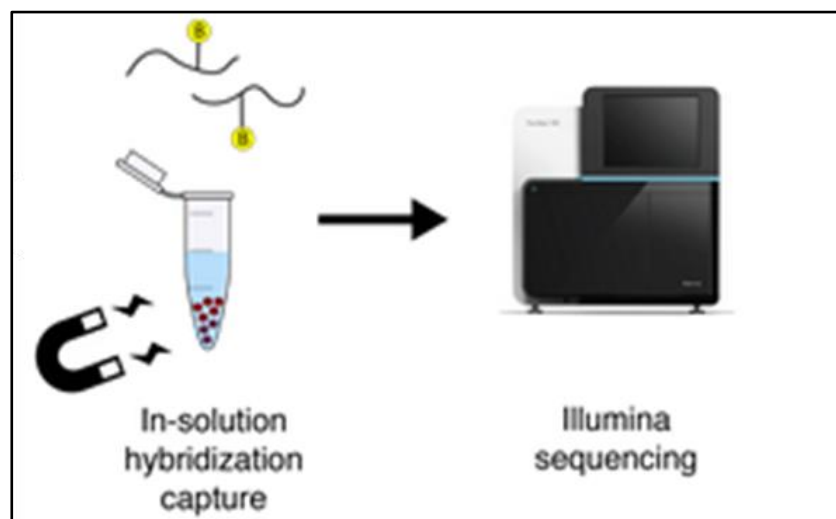
Figure 5.1 Simplified overview of the Hybridisation Capture approach
(http://www.mauranolab.org/SARSCoV2_pipeline.html).

Bibliography

Aldrian, E. & Susanto, R.D. (2003). Identification of three dominant rainfall regions within Indonesia and their relationship to sea surface temperature. *International Journal of Climate, 23,*1435–1452.

Aliscioni, S., Bell, H. L., Besnard, G., Christin, P. A., Columbus, J. T., Duvall, M. R., Edwards, E. J., Giussani, L., Hasenstab-Lehman, K., Hilu, K. W., Hodkinson, T. R., Ingram, A. L., Kellogg, E. A., Mashayekhi, S., Morrone, O., Osborne, C. P., Salamin, N., Schaefer, H., Spriggs, E., Smith, S. A., Zuloaga, F., & Grass Phylogeny Working, G., II. (2012). New grass phylogeny resolves deep evolutionary relationships and discovers C4 origins. *New Phytologist, 193*(2), 304-312.

Alsos, I. G., Lammers, Y., Kjellman, S. E., Merkel, M. K. F., Bender, E. M., Rouillard, A., Erlendsson, E., Guðmundsdóttir, E. R., Benediktsson, Í. Ö., Farnsworth, W. R., Brynjólfsson, S., Gísladóttir, G., Eddudóttir, S. D., & Schomacker, A. (2021). Ancient sedimentary DNA shows rapid post-glacial colonisation of Iceland followed by relatively stable vegetation until the Norse settlement (Landnám) AD 870. *Quaternary science reviews*, *259*, 106903.

Alsos, I. G., Lammers, Y., Yoccoz, N. G., Jorgensen, T., Sjogren, P., Gielly, L., & Edwards, M. E. (2018). Plant DNA metabarcoding of lake sediments: How does it represent the contemporary vegetation. *Plos One, 13*(4).

Alsos, I. G., Sjögren, P., Edwards, M. E., Landvik, J. Y., Gielly, L., Forwick, M., Coissac, E., Brown, A. G., Jakobsen, L. V., Føreid, M. K., & Pedersen, M. W. (2016). Sedimentary ancient DNA from Lake Skartjørna, Svalbard: Assessing the resilience of arctic flora to Holocene climate change. *The Holocene, 26*(4), 627-642.

Amaral-Zettler, L. A., McCliment, E. A., Ducklow, H. W., & Huse, S. M. (2009). A Method for Studying Protistan Diversity Using Massively Parallel Sequencing of V9 Hypervariable Regions of Small-Subunit Ribosomal RNA Genes. *PLOS ONE, 4*(7), 6372.

An, X., & Xie, B. (2022). Phytoliths from Woody Plants: A Review. *Diversity (Basel), 14*(5), 339.

Anshari, G., Kershaw, P., van der Kaars, S., & Jacobsen, G. (2004). Environmental change and peatland forest dynamics in the Lake Sentarum area, West Kalimantan, Indonesia. *Journal of Quaternary Science, 19*, 637-655.

Apaydin, Z., Kutbay, H. G., Ozbucak, T., Yalcin, E., & Bilgin, A. (2009). Relationships between vegetation zonation and edaphic factors in a salt-marsh community (Black Sea Coast). *Polish Journal of Ecology, 57*(1), 99-112.

Armbrecht, L., Weber, M. E., Raymo, M. E., Peck, V. L., Williams, T., Warnock, J., Kato, Y., Hernandez-Almeida, I., Hoem, F., Reilly, B., Hemming, S., Bailey, I., Martos, Y. M., Gutjahr, M., Percuoco, V., Allen, C., Brachfeld, S., Cardillo, F. G., Du, Z., . Zheng, X. (2022). Ancient marine sediment DNA reveals diatom transition in Antarctica. *Nature communications, 13*(5787), 5787-5787.

Atanassova, J. (2005). Palaeoecological setting of the western Black Sea area during the last 15 000 years. *Holocene, 15*(4), 576-584.

Bahr, A., Lamy, F., Arz, H., Kuhlmann, H., & Wefer, G. (2005). Late glacial to Holocene climate and sedimentation history in the NW Black Sea. *Marine Geology, 214*, 309-322.

Bajard, M., Poulenard, J., Sabatier, P., Develle, A.-L., Giguet-Covex, C., Jacob, J., Crouzet, C., David, F., Pignol, C., Arnaud, F. (2017). Progressive and Regressive Soil Evolution Phases in the Anthropocene. *Catena, 150*, 39–52.

Baldwin, A. H. (1996). *The role of seed banks, disturbance, and sea level rise in determining the plant community structure of oligohaline coastal marshes* [Doctoral dissertation, Louisiana State University].

Baldwin, A. H., McKee, K. L., & Mendelssohn, I. A. (1996). The influence of vegetation, salinity, and inundation on seed banks of oligohaline coastal marshes. *American Journal of Botany, 83*, 470-479.Bellemain, E., Davey, M. L., Kauserud, H., Epp, L. S., Boessenkool, S., Coissac, E., Geml, J., Edwards, M., Willerslev, E., Gussarova, G., Taberlet, P., Haile, J., & Brochmann, C. (2013). Fungal palaeodiversity revealed using high-throughput metabarcoding of ancient DNA from arctic permafrost. *Environ Microbiol*, *15*(4), 1176-1189.

Berglund, M., Eriksson, J. A., & Fernlund, J. M. (1994). The late Weichselian in Halland, Southwestern Sweden: A pollen-analytical study. *GFF, 116*(4), 215-230.

Berov, D., Klayn, S., Deyanova, D., & Karamfilov, V. (2022). Current distribution of Zostera seagrass meadows along the Bulgarian Black Sea coast (SW Black Sea, Bulgaria) (2010-2020). Biodiversity data journal, 10, 78942.

Bi, X., Sheng, G., Liu, X., Li, C., & Fu, J. (2005). Molecular and carbon and hydrogen isotopic composition of n-alkanes in plant leaf waxes. *Organic Geochemistry, 36*(10), 1405–1417.

Biagioni, S., Wundsch, M., Haberzettl, T., & Behling, H. (2015). Assessing resilience/sensitivity of tropical mountain rainforests towards climate variability of the last 1500 years: The long-term perspective at Lake Kalimpaa (Sulawesi, Indonesia). *Review of Palaeobotany and Palynology, 213,* 42-53.

Birks, H. H. (2001). Plant Macrofossils. In J. P. Smol, H. J. B. Birks, W. M. Last, R. S. Bradley, & K. Alverson (Eds.), *Tracking Environmental Change Using Lake Sediments: Terrestrial, Algal, and Siliceous Indicators* (pp. 49-74). Springer Netherlands.

Birks, H. H. (2003). The importance of plant macrofossils in the reconstruction of lateglacial vegetation and climate; examples from Scotland, western Norway, and Minnesota, USA. *Quaternary science reviews*, *22*(5-7), 453-473.

Boere, A. C., Sinninghe Damsté, J. S., Rijpstra, W. I. C., Volkman, J. K., & Coolen, M. J. L. (2011). Source-specific variability in post-depositional DNA preservation with potential implications for DNA based paleoecological records. *Organic geochemistry, 42*(10), 1216-1225.

Boessenkool, S., McGlynn, G., Epp, L. S., Taylor, D., Pimentel, M., Gizaw, A., Nemomissa, S., Brochmann, C., & Popp, M. (2014). Use of Ancient Sedimentary DNA as a Novel Conservation Tool for High-Altitude Tropical Biodiversity. *Conservation Biology, 28*(2), 446-455.

Bolyen, E., Rideout, J. R., Dillon, M. R., Bokulich, N. A., Abnet, C. C., Al-Ghalith, G. A., Alexander, H., Alm, E. J., Arumugam, M., Asnicar, F., Bai, Y., Bisanz, J. E., Bittinger, K., Brejnrod, A., Brislawn, C. J., Brown, C. T., Callahan, B. J., Caraballo-Rodríguez, A. M., Chase, J., . . . Caporaso, J. G. (2019). Reproducible, interactive, scalable and extensible microbiome data science using QIIME 2. *Nature Biotechnology*, *37*(8), 852-857.

Bondev, I. (1991). *Vegetation of Bulgaria: 1:600,000 Map with Explanatory Text.* ["St. Kliment Ohrdski" University Press, Sofia (in Bulgarian)].

Bottema, S. (1980). On the history of the walnut (Juglans regia L.) in southeastern Europe. *Acta Botanica Neerlandica, 29*(5-6), 343-349.

Boyer, F., Mercier, C., Bonin, A., Le Bras, Y., Taberlet, P., & Coissac, E. (2016). Obitools: a unix-inspired software package for DNA metabarcoding. *Molecular Ecology Resources, 16*(1), 176-182.

Braga, R. M., Padilla, G., & Araújo, W. L. (2018). The biotechnological potential of Epicoccum spp.: diversity of secondary metabolites. *Critical Reviews in Microbiology*, *44*(6), 759-778.

Bramburger, A.J., Hamilton, P.B., Hehanussa, P.E., Haffner, G.D. (2008). Processes regulating the community composition and relative abundance of taxa in the diatom communities of the Malili Lakes, Sulawesi Island, Indonesia. *Hydrobiologia, 615,* 215–224.

Bremond, L., Favier, C., Ficetola, G. F., Tossou, M. G., Akouegninou, A., Gielly, L., Giguet-Covex, C., Oslisly, R., & Salzmann, U. (2017). Five thousand years of tropical lake sediment DNA records from Benin. *Quaternary Science Reviews, 170,* 203-211.

Burke, S. V., Wysocki, W. P., Zuloaga, F. O., Craine, J. M., Pires, J. C., Edger, P. P., Mayfield-Jones, D., Clark, L. G., Kelchner, S. A., & Duvall, M. R. (2016). Evolutionary relationships in Panicoid grasses based on plastome phylogenomics (Panicoideae; Poaceae). BMC Plant Biol, *16*(1), 140.

Calabon, M., Hyde, K., Jones, E., Bao, D.-F., Bhunjun, C. S., Phukhamsakda, C., Shen, H.-W., Gentekaki, E., Al Sharie, A., Barros, J., Chandrasiri, S., Hu, D.-M., Hurdeal, V., Rossi, W., Guardia Valle, L., Zhang, H., Figueroa, M., Raja, H., Sahadevan, S., & Balasuriya, A. (2023). *Freshwater fungal biology, 14*, 195–413.

Callahan, B. J., McMurdie, P. J., Rosen, M. J., Han, A. W., Johnson, A. J. A., & Holmes, S. P. (2016). DADA2: High-resolution sample inference from Illumina amplicon data. *Nature Methods*, *13*(7), 581-583.

Cannon, C.H., Morley, R.J., & Bush, A.B. (2009). The current refugial rainforests of Sundaland are unrepresentative of their biogeographic past and highly vulnerable to disturbance. *Proceedings of the National Academy of Sciences, 106*(27), 11188–11193.

Capo, E., Debroas, D., Arnaud, F., Guillemot, T., Bichet, V., Millet, L., Gauthier, E., Massa, C., Develle, A. L., Pignol, C., Lejzerowicz, F., & Domaizon, I. (2016). Long-term dynamics in microbial eukaryotes communities: a palaeolimnological view based on sedimentary DNA. *Mol Ecol, 25*(23), 5925-5943.

Capo, E., Giguet-Covex, C., Rouillard, A., Nota, K., Heintzman, P. D., Vuillemin, A., Ariztegui, D., Arnaud, F., Belle, S., Bertilsson, S., Bigler, C., Bindler, R., Brown, A. G., Clarke, C. L., Crump, S. E., Debroas, D., Englund, G., Ficetola, G. F., Garner, R. E., . . . Parducci, L. (2021). Lake Sedimentary DNA Research on Past Terrestrial and Aquatic Biodiversity: Overview and Recommendations. *Quaternary*, *4*(1), 6.

Capo, E., Monchamp, M.-E., Coolen, M., Domaizon, I., Armbrecht, L., & Bertilsson, S. (2022). Environmental paleomicrobiology: using DNA preserved in aquatic sediments to its full potential. *Environmental Microbiology*, *24*.

Caporaso, J. G., Lauber, C. L., Walters, W. A., Berg-Lyons, D., Huntley, J., Fierer, N., Owens, S. M., Betley, J., Fraser, L., Bauer, M., Gormley, N., Gilbert, J. A., Smith, G., & Knight, R. (2012). Ultra-high-throughput microbial community analysis on the Illumina HiSeq and MiSeq platforms. *Isme Journal, 6*(8), 1621-1624.

Caraco, N. F., Cole, J. J., & Likens, G. E. (1989). Evidence for sulfate-controlled phosphorus release from sediments of aquatic systems. *Nature, 341*(6240), 316-318.

Chang, Y. M., Chang, C. L., Li, W. H., & Shih, A. C. C. (2013). Historical profiling of maize duplicate genes shed light on the evolution of C4 photosynthesis in grasses. *Molecular Phylogenetics and Evolution, 66*(2), 453-462.

Chaturvedi, V., DeFiglio, H., & Chaturvedi, S. (2018). Phenotype profiling of white-nose syndrome pathogen Pseudogymnoascus destructans and closely-related Pseudogymnoascus pannorum reveals metabolic differences underlying fungal lifestyles. *F1000Res*, *7*, 665.

Chikaraishi, Y. & Naraoka, H, (2003). Compound-specific δD–δ13C analyses of n-alkanes extracted from terrestrial and aquatic plants. *Phytochemistry, 63*(3), 361–371.

Christen-Zaech, S., Patel, S., & Mancini, A. J. (2008). Recurrent cutaneous Geomyces pannorum infection in three brothers with ichthyosis. *J Am Acad Dermatol*, *58*(5), 112-113.

Chun, Y.-M., & Choi, Y. D. (2009). Expansion of Phragmites australis (Cav.) Trin. ex Steud. (Common Reed) into Typha spp. (Cattail) Wetlands in Northwestern Indiana, USA. *Journal of Plant Biology, 52*(3), 220-228.

Clarke, C. L., Alsos, I. G., Edwards, M. E., Paus, A., Gielly, L., Haflidason, H., Mangerud, J., Regnéll, C., Hughes, P. D. M., Svendsen, J. I., & Bjune, A. E. (2020). A 24,000-year ancient DNA and pollen record from the Polar Urals reveals temporal dynamics of arctic and boreal plant communities. *Quaternary science reviews, 247,* 106564.

Clarke, K. R., Gorley, R. N. (2015). PRIMER v7: User Manual/Tutorial. PRIMER-E Ltd.

Cleal, C., Pardoe, H. S., Berry, C. M., Cascales-Minana, B., Davis, B. A. S., Diez, J. B., Filipova-Marinova, M. V., Giesecke, T., Hilton, J., Ivanov, D., Kustatscher, E., Leroy, S. A. G., McElwain, J. C., Oplustil, S., Popa, M. E., Seyfullah, L. J., Stolle, E., Thomas, B. A., & Uhl, D. (2021). Palaeobotanical experiences of plant diversity in deep time; 1, How well can we identify past plant diversity in the fossil record? *Palaeogeography, palaeoclimatology, palaeoecology, 576,* 110481.

Cockell, C. S., Schaefer, B., Wuchter, C., Coolen, M. J. L., Grice, K., Schnieders, L., Morgan, J. V., Gulick, S. P. S., Wittmann, A., Lofi, J., Christeson, G. L., Kring, D. A., Whalen, M. T., Bralower, T. J., Osinski, G. R., Claeys, P., Kaskes, P., de Graaff, S. J., Déhais, T. (2021). Shaping of the Present-Day Deep Biosphere at Chicxulub by the Impact Catastrophe That Ended the Cretaceous. Frontiers in Microbiology, 12Coissac, E., Riaz, T., & Puillandre, N. (2012). Bioinformatic challenges for DNA metabarcoding of plants and animals. *Molecular Ecology, 21,* 1834–1847.

Connor, S. E., Ross, S. A., Sobotkova, A., Herries, A. I. R., Mooney, S. D., Longford, C., & Iliev, I. (2013). Environmental conditions in the SE Balkans since the Last Glacial Maximum and their influence on the spread of agriculture into Europe. *Quaternary Science Reviews*, *68*, 200-215.

Connor, S. E., Thomas, I., & Kvavadze, E. V. (2007). A 5600-yr history of changing vegetation, sea levels and human impacts from the Black Sea coast of Georgia. *Holocene, 17*(1), 25-36.

Coolen, M. J. L. (2011). 7000 years of Emiliania huxleyi viruses in the Black Sea. *Science, 333*(6041), 451-452.

Coolen, M. J. L., & Overmann, J. (2007). 217 000-year-old DNA sequences of green sulfur bacteria in Mediterranean sapropels and their implications for the paleoenvironment reconstruction. *Environmental Microbiology, 9*(1), 238-249.

Coolen, M. J. L., Boere, A., Abbas, B., Baas, M., Wakeham, S. G., & Sinninghe Damste, J. S. (2006). Ancient DNA derived from alkenone-biosynthesizing

haptophytes and other algae in Holocene sediments from the Black Sea. *Paleoceanography, 21*(1), 1005.

Coolen, M. J. L., Hopmans, E. C., Rijpstra, W. I. C., Muyzer, G., Schouten, S., Volkman, J. K., & Sinninghe Damsté, J. S. (2004). Evolution of the methane cycle in Ace Lake (Antarctica) during the Holocene: response of methanogens and methanotrophs to environmental change. *Organic geochemistry*, *35*(10), 1151-1167.

Coolen, M. J. L., Muyzer, G., Rijpstra, W. I. C., Schouten, S., Volkman, J. K., & Damste, J. S. S. (2004). Combined DNA and lipid analyses of sediments reveal changes in Holocene haptophyte and diatom populations in an Antarctic lake. *Earth and Planetary Science Letters, 223*(1-2), 225-239.

Coolen, M. J. L., Orsi, W. D., Balkema, C., Quince, C. H., Keith, Sylva, S. P., Filipova-Marinova, M., & Giosan, L. (2013). Evolution of the plankton paleome in the Black Sea from the Deglacial to Anthropocene. *Proceedings of the National Academy of Sciences of the United States of America, 110*(21), 8609-8614.

Coolen, M. J. L., & Overmann, J. (2007). 217 000-year-old DNA sequences of green sulfur bacteria in Mediterranean sapropels and their implications for the paleoenvironment reconstruction. Environmental *Microbiology, 9*(1), 238-249.

Coolen, M. J. L., Saenz, J. P., Giosan, L., Trowbridge, N. Y., Dimitrov, P., Dimitrov, D., & Eglinton, T. I. (2009). DNA and lipid molecular stratigraphic records of haptophyte succession in the Black Sea during the Holocene. *Earth and Planetary Science Letters, 284*(3-4), 610-621.

Cordova, C. E., Harrison, S. P., Mudie, P. J., Riehl, S., Leroy, S. A. G., & Ortiz, N. (2009). Pollen, plant macrofossil and charcoal records for palaeovegetation reconstruction in the Mediterranean-Black Sea Corridor since the Last Glacial Maximum. *Quaternary International, 197*, 12-26.

Corinaldesi, C., Barucca, M., Luna, G. M., & Dell'Anno, A. (2011). Preservation, origin and genetic imprint of extracellular DNA in permanently anoxic deep-sea sediments. *Molecular Ecology, 20*(3), 642-654.

Costa, K. M., Russell, J. M., Vogel, H., & Bijaksana, S. (2015). Hydrological connectivity and mixing of Lake Towuti, Indonesia in response to paleoclimatic changes over the last 60,000 years. *Palaeogeography Palaeoclimatology Palaeoecology, 417,* 467-475.

Courtin, J., Andreev, A. A., Raschke, E., Bala, S., Biskaborn, B. K., Liu, S. S., Zimmermann, H., Diekmann, B., Stoof-Leichsenring, K. R., Pestryakova, L. A., & Herzschuh, U. (2021). Vegetation Changes in Southeastern Siberia During the Late Pleistocene and the Holocene. *Frontiers in Ecology and Evolution, 09*.

Crowe, S. A., O'Neill, A. H., Katsev, S., Hehanussa, P., Haffner, G. D., Sundby, B., Mucci, A., & Fowle, D. A. (2008). The biogeochemistry of tropical lakes: A case study from Lake Matano, Indonesia. *Limnology and Oceanography, 53*(1), 319-331.

Culmsee, H., Leuschner, C., Moser, G., & Pitopang, R. (2010). Forest aboveground biomass along an elevational transect in Sulawesi, Indonesia, and the role of Fagaceae in tropical montane rain forests. *Journal of Biogeography, 37*(5), 960-974.

Dalén, L., Heintzman, P. D., Kapp, J. D., & Shapiro, B. (2023). Deep-time paleogenomics and the limits of DNA survival. *Science, 382*(6666), 48-53.

Damialis, A., Syropoulou, E., Gioulekas, D., & Vokou, D. (2006, June 10). Long-distance transport of hazel (Corylus avellana) airborne pollen into the city of Thessaloniki, north Greece: Randomness or a systematic atmospheric circulation pattern?: XXV Congress of the European Academy of Allergology and Clinical Immunology, Vienna, Austria.

De Caceres, M., and Legendre, P. (2009). Associations between species and groups of sites: indices and statistical inference. *Ecology, 90*(12), 3566-3574.

De Schepper, S., Ray, J. L., Skaar, K. S., Sadatzki, H., Ijaz, U. Z., Stein, R., & Larsen, A. (2019). The potential of sedimentary ancient DNA for reconstructing past sea ice evolution. *The ISME Journal*, *13*(10), 2566-2577.

Dean, W. E., & Arthur, M. A. (2010). *Geochemical characteristics of Holocene laminated sapropel (Unit II) and underlying lacustrine Unit III in the Black Sea*. US Department of the Interior, Geological Survey.

Demaneche, S., Jocteur-Monrozier, L., Quiquampoix, H., & Simonet, P. (2001). Evaluation of biological and physical protection against nuclease degradation of clay-bound plasmid DNA. *Applied and Environmental Microbiology, 67*(1), 293-299.

Deptuła, M., Piernik, A., Nienartowicz, A., Hulisz, P., & Kamiński, D. (2020). Alnus glutinosa L. Gaertn. as potential tree for brackish and saline habitats. *Global ecology and conservation, 22*, 977.

Dighton, J. (2016). *Fungi in Ecosystem Processes, 2nd Edition*.

Direito, S. O. L., Marees, A., & Roling, W. F. M. (2012). Sensitive life-detection strategies for low-biomass environments: optimizing the extraction of nucleic acids adsorbing to terrestrial and Mars analogue minerals. *FEMS Microbiology Ecology, 81*(1), 111-123.

Dommain, R., Andama, M., McDonough, M. M., Prado, N. A., Goldhammer, T., Potts, R., Maldonado, J. E., Nkurunungi, J. B., & Campana, M. G. (2020). The challenges of reconstructing tropical biodiversity with sedimentary ancient DNA: A 2200-year-long metagenomic record from Bwindi Impenetrable Forest, Uganda. *Frontiers in Ecology and Evolution, 8.*

Dong, W., Liu, J., Yu, J., Wang, L., & Zhou, S. (2012). Highly Variable Chloroplast Markers for Evaluating Plant Phylogeny at Low Taxonomic Levels and for DNA Barcoding. *PLOS ONE, 7*(4), 35071.

Douda, J., Boublík, K., Slezák, M., Biurrun, I., Nociar, J., Havrdová, A., Doudová, J., Aćić, S., Brisse, H., Brunet, J., Chytrý, M., Claessens, H., Csiky, J., Didukh,

Y., Dimopoulos, P., Dullinger, S., FitzPatrick, Ú., Guisan, A., Horchler, P. J., . . . Schwabe-Kratochwil, A. (2016). Vegetation classification and biogeography of European floodplain forests and alder carrs. *Applied vegetation science, 19*(1), 147-163.

Doughty, C. E. (2013). Preindustrial Human Impacts on Global and Regional Environment. *Annual Review of Environment and Resources*, *38*(1), 503-527.

Dufrene, M., & Legendre, P. (1997). Species assemblages and indicator species: The need for a flexible asymmetrical approach. *Ecological Monographs, 67*(3), 345-366.

Eastwood, W. J., Fairbairn, A., Stroud, E., Roberts, N., Lamb, H., Yigitbasioglu, H., Senkul, C., Moss, A., Turner, R., & Boyer, P. (2018). Comparing pollen and archaeobotanical data for Chalcolithic cereal agriculture at Catalhoyuk, Turkey. *Quaternary science reviews, 202,* 4-18.

El-Elimat, T., Raja, H. A., Figueroa, M., Falkinham III, J. O., & Oberlies, N. H. (2014). Isochromenones, isobenzofuranone, and tetrahydronaphthalenes produced by Paraphoma radicina, a fungus isolated from a freshwater habitat. *Phytochemistry*, *104*, 114-120.

Epp, L. S., Gussarova, C., Boessenkool, S., Olsen, J., Haile, J., Schroder-Nielsen, A., Ludikova, A., Hassel, K., Stenoien, H. K., Funder, S., Willerslev, E., Kjaer, K., & Brochmann, C. (2015). Lake sediment multi-taxon DNA from North Greenland records early post-glacial appearance of vascular plants and accurately tracks environmental changes. *Quaternary Science Reviews, 117*, 152-163.

Epure, L., Meleg, I. N., Munteanu, C.-M., Roban, R. D., & Moldovan, O. T. (2014). Bacterial and Fungal Diversity of Quaternary Cave Sediment Deposits. *Geomicrobiology Journal*, *31*(2), 116-127.

Erftemeijer, P. L. A., & Robin, L. R. R. (2006). Environmental impacts of dredging on seagrasses: A review. *Marine pollution bulletin, 52*(12), 1553-1572.

Fagerstrom., M. (1999). *Athyrium filix-femina - lady fern.* Portland State University.

Ferrari, R., Gautier, V., & Silar, P. (2021). Chapter Three - Lignin degradation by ascomycetes. In M. Morel-Rouhier & R. Sormani (Eds.), *Advances in Botanical Research* (Vol. 99, pp. 77-113). Academic Press.

Feurdean, A., & Bennike, O. (2008). Plant macrofossils analysis from Steregoiu NW Romania: taphonomy, representation, and comparison with pollen analysis. *Studia Universitatis Babeş-Bolyai. Geologia*, *53*(1), 5-10.

Filipova-Marinova, M. (2003). Palaeoenvironmental changes in the Southern Bulgarian Black Sea area during the last 29,000 years. *Phytologia Balcanica, 9*, 275-292.

Filipova-Marinova, M. (2006). Palynostratigraphy of Pleistocene and Holocene sediments from the western Black Sea area. *Comptes Rendus De L Academie Bulgare Des Sciences, 60*(3), 279-290.

Filipova-Marinova, M., Pavlov, D., Coolen, M. J. L., & Giosan, L. (2012). First high-resolution marinopalynological stratigraphy of Late Quaternary sediments from the central part of the Bulgarian Black Sea area. *Quaternary International, 293*, 170-183.

Finlay, R. D. (2008). Ecological aspects of mycorrhizal symbiosis: with special emphasis on the functional diversity of interactions involving the extraradical mycelium. *Journal of Experimental Botany*, *59*(5), 1115-1126.

Foster, N. R., Dijk, K. j., Biffin, E., Young, J. M., Thomson, V. A., Gillanders, B. M., Jones, A. R., & Waycott, M. (2022). A targeted capture approach to generating reference sequence databases for chloroplast gene regions. *Ecology and evolution, 12*(4), 8816.

Friese, A., Kallmeyer, J., Kitte, J., Montaño Martinez, I., Bijaksana, S., & Wagner, D. (2017). A simple and inexpensive technique for assessing contamination during drilling operations. *Limnology and Oceanography: Methods, 15*.

Friese, A., Bauer, K., Glombitza, C., Ordoñez, L., Ariztegui, D., Heuer, V. B., Vuillemin, A., Henny, C., Nomosatryo, S., & Simister, R. (2021). Organic

matter mineralization in modern and ancient ferruginous sediments. *Nature communications*, *12*(1), 2216.

Freeman, C. L., Dieudonné, L., Agbaje, O. B. A., Žure, M., Sanz, J. Q., Collins, M., & Sand, K. K. (2023). Survival of environmental DNA in sediments: Mineralogic control on DNA taphonomy. *Environmental DNA, 00*, 1–15.

Fulton, J. M., Arthur, M. A., & Freeman, K. H. (2012). Subboreal aridity and scytonemin in the Holocene Black Sea. *Organic geochemistry, 49*, 47-55.

Gancedo, J. M. (1998). Yeast carbon catabolite repression. *Microbiology and molecular biology reviews, 62*(2), 334-361.

Garnier, J., Quantin, C., Raous, S., Guimaraes, E., & Becquer, T. (2021). Field availability and mobility of metals in Ferralsols developed on ultramafic rock of Niquelandia, Brazil. *Brazilian Journal of Geology, 51*(1).

Gastaldo, R. A., & Demko, T. M. (2010). The Relationship Between Continental Landscape Evolution and the Plant-Fossil Record: Long Term Hydrologic Controls on Preservation. In (pp. 249-285). Springer Netherlands.

Geel, B. (2006). Non-Pollen Palynomorphs. In (Vol. 3, pp. 99-119).

Geml, J., Morgado, L. N., Semenova, T. A., Welker, J. M., Walker, M. D., & Smets, E. (2015). Long-term warming alters richness and composition of taxonomic and functional groups of arctic fungi. *FEMS Microbiology Ecology*, *91*(8), 095.

Gielly, L., & Taberlet, P. (1994). The use of chloroplast DNA to resolve plant phylogenies - noncoding versus RBCL sequences. *Molecular Biology and Evolution, 11*(5), 769-777.

Giesecke, T., Davis, B., Brewer, S., Finsinger, W., Wolters, S., Blaauw, M., de Beaulieu, J.-L., Binney, H., Fyfe, R. M., Gaillard, M.-J., Gil-Romera, G., van der Knaap, W. O., Kuneš, P., Kühl, N., van Leeuwen, J. F. N., Leydet, M., Lotter, A. F., Ortu, E., Semmler, M., & Bradshaw, R. H. W. (2014). Towards mapping the late Quaternary vegetation change of Europe. *Vegetation history and archaeobotany*, *23*(1), 75-86.

Giosan, L., Coolen, M. J. L., Kaplan, J. O., Constantinescu, S., Filip, F., Filipova-Marinova, M., Kettner, A. J., & Thom, N. (2012). Early anthropogenic transformation of the danube-black sea system. *Scientific reports, 2*(1), 582-582.

Glaser, J., & Wulf, M. (2009). Effects of water regime and habitat continuity on the plant species composition of floodplain forests. *Journal of Vegetation Science, 20*, 37–48.

Gobet, E., Tinner, W., Bigler, C., Hochuli, P. A., & Ammann, B. (2005). Early-Holocene afforestation processes in the lower subalpine belt of the Central Swiss Alps as inferred from macrofossil and pollen records. *The Holocene, 15*(5), 672-686.

Golovnina, K. A., Glushkov, S. A., Blinov, A. G., Mayorov, V. I., Adkison, L. R., & Goncharov, N. P. (2007). Molecular phylogeny of the genus Triticum L. *Plant Systematics and Evolution, 264*(3-4), 195-216.

Goudge, T. A., Russell, J. M., Mustard, J. F., Head, J. W., & Bijaksana, S. (2017). A 40,000 yr record of clay mineralogy at Lake Towuti, Indonesia: Paleoclimate reconstruction from reflectance spectroscopy and perspectives on paleolakes on Mars. *Bulletin, 129*(7-8), 806-819.

Gregory, P. H. (1978). Distribution of airborne pollen and spores and their long-distance transport. *Pure and Applied Geophysics PAGEOPH, 116*(2-3), 309-315.

Greif, M. D., & Currah, R. S. (2007). Patterns in the occurrence of saprophytic fungi carried by arthropods caught in traps baited with rotted wood and dung. *Mycologia, 99*(1), 7-19.

Haberle, S. G., Tibby, J., Dimitriadis, S., & Heijnis, H. (2006). The impact of European occupation on terrestrial and aquatic ecosystem dynamics in an Australian tropical rain forest. *Journal of Ecology, 94*(5), 987-1002.

Hadziavdic, K., Lekang, K., Lanzen, A., Jonassen, I., Thompson, E. M., & Troedsson, C. (2014). Characterization of the 18S rRNA gene for designing universal eukaryote specific primers. *PLoS One, 9*(2), 87624.

Haitjema, C. H., Solomon, K. V., Henske, J. K., Theodorou, M. K., & O'Malley, M. A. (2014). Anaerobic gut fungi: Advances in isolation, culture, and cellulolytic enzyme discovery for biofuel production. *Biotechnol Bioeng*, *111*(8), 1471-1482.

Hamilton, R., Hall, T., Stevenson, J., & Penny, D. (2019b). Distinguishing the pollen of Dipterocarpaceae from the seasonally dry and moist tropics of south-east Asia using light microscopy. *Review of Palaeobotany and Palynology, 263,*117-133.

Hamilton, R., Stevenson, J., Li, B., & Bijaksana, S. (2019a). A 16,000-year record of climate, vegetation and fire from Wallacean lowland tropical forests. *Quaternary Science Reviews, 224,* 105929.

Hasberg, A. K. M., Bijaksana, S., Held, P., Just, J., Melles, M., Morlock, M. A., Opitz, S., Russell, J. M., Vogel, H., & Wennrich, V. (2019). Modern sedimentation processes in Lake Towuti, Indonesia, revealed by the composition of surface sediments. *Sedimentology, 66*(2), 675-698.

Hay, B. J. (1988). Sediment accumulation in the central western Black Sea over the past 5100 years. *Paleoceanography, 3*(4), 491-508.

Hendon, H.H. (2003). Indonesian rainfall variability: impacts of ENSO and local air-sea interaction. *Journal of Climate, 16,* 1775–1790.

Hess, M., Paul, S. S., Puniya, A. K., van der Giezen, M., Shaw, C., Edwards, J. E., & Fliegerová, K. (2020). Anaerobic Fungi: Past, Present, and Future. *Front Microbiol*, *11*, 584893.

Hippel, V. B., Stoof-Leichsenring, K. R., Schulte, L., Seeber, P., Epp, L. S., Biskaborn, B. K., Diekmann, B., Melles, M., Pestryakova, L., & Herzschuh, U. (2022). Long-term fungus–plant covariation from multi-site sedimentary ancient DNA metabarcoding. *Quaternary science reviews, 295,* 107758.

Hirayama, H., Abe, M., Miyazaki, J., Sakai, S., & Takai, K. (2015). Data report: cultivation of microorganisms from basaltic rock and sediment cores from the

North Pond on the western flank of the Mid-Atlantic Ridge, IODP Expedition 336. *Sci Technol (JAMSTEC)*, *2*, 15.

Hope, G. (2001). Environmental change in the Late Pleistocene and later Holocene at Wanda site, Soroako, South Sulawesi, Indonesia. *Palaeogeography Palaeoclimatology Palaeoecology, 171*(3-4), 129-145.

Hopkins, H.C.F. (1994). The Indo-Pacific Species of Parkia (Leguminosae: Mimosoideae). *Kew Bulletin, 49*(2), 181-234.

Horrocks, M. (2020). Recovering Plant Microfossils from Archaeological and other Palaeoenvironmental Deposits: A Practical Guide Developed from Pacific Region Experience. *Asian perspectives (Honolulu)*, *59*(1), 186-207.

Hoyle, T. M., Bista, D., Flecker, R., Krijgsman, W., & Sangiorgi, F. (2021). Climate-driven connectivity changes of the Black Sea since 430 ka; testing a dual palynological and geochemical approach. *Palaeogeography, palaeoclimatology, palaeoecology*, *561*, 110069.

Huang, Y., Zheng, Y., Heng, P., Giosan, L., & Coolen, M. J. L. (2021). Black Sea paleosalinity evolution since the last deglaciation reconstructed from alkenone-inferred Isochrysidales diversity. *Earth and planetary science letters, 564,* 116881.

Inagaki, F., Hinrichs, K.-U., Kubo, Y., Bowles, M., Heuer, V., Hong, W.-L., Hoshino, T., Ijiri, A., Imachi, H., Ito, M., Kaneko, M., Lever, M., Lin, Y.-S., Methé, B., Morita, S., Morono, Y., Tanikawa, W., Bihan, M., Bowden, S., & Yamada, Y. (2015). Exploring deep microbial life in coal-bearing sediment down to ~2.5 km below the ocean floor. *Science, 349*, 420-424.

Isola, D., Scano, A., Orrù, G., Prenafeta-Boldú, F. X., & Zucconi, L. (2021). Hydrocarbon-contaminated sites: Is there something more than Exophiala xenobiotica? New insights into black fungal diversity using the long cold incubation method. *Journal of Fungi, 7*(10), 817.

IUCN. (2019). International Union for Conservation of Nature annual report 2019.

Ivarsson, M., Bengtson, S., & Neubeck, A. (2016). The igneous oceanic crust – Earth's largest fungal habitat? *Fungal ecology*, *20*, 249-255.

Jia, W., Liu, X., Kathleen R. Stoof-Leichsenring, Liu, S., Li, K., & Herzschuh, U. (2022). Preservation of sedimentary plant DNA is related to lake water chemistry. *Environmental DNA, 4*(2), 425-439.

Jogaiah, S., Kumar, T., Niranjana, S., & Shetty, S. (2004). First report of gummy stem blight caused by Didymella bryoniae on muskmelon (Cucumis melo) in India. *Plant Pathology*, *53*, 364-369.

Jorgensen, T., Haile, J., MÖLler, P. E. R., Andreev, A., Boessenkool, S., Rasmussen, M., Kienast, F., Coissac, E., Taberlet, P., Brochmann, C., Bigelow, N. H., Andersen, K., Orlando, L., Gilbert, M. T. P., & Willerslev, E. (2012). A comparative study of ancient sedimentary DNA, pollen and macrofossils from permafrost sediments of northern Siberia reveals long-term vegetational stability: Comparative Study of Ancient Sedimentary DNA, Pollen AND Macrofossil. *Molecular ecology*, *21*(8), 1989-2003.

Kanbar, H., Olajos, F., Englund, G., & Holmboe, M. (2020). Geochemical identification of potential DNA-hotspots and DNA-infrared fingerprints in lake sediments. *Applied Geochemistry, 122*, 104728.

Kazakou, E., Dimitrakopoulos, P. G., Baker, A. J. M., Reeves, R. D., & Troumbis, A. Y. (2008). Hypotheses, mechanisms, and trade-offs of tolerance and adaptation to serpentine soils from species to ecosystem level. *Biological Reviews, 83*(4), 495-508.

Kessler, P. J. A., Bos, M., Sierra+Daza, S. E. C., Kop, A., Willemse, L., Pitopang, R., & Gradstein, S. (2002). Checklist of woody plants of Sulawesi, Indonesia. *Blumea journal of plant taxonomy and plant geography, 14,* 1-160.

Khejornsart, P., & Wanapat, M. (2010). Diversity of Rumen Anaerobic Fungi and Methanogenic Archaea in Swamp Buffalo Influenced by Various Diets. *Journal of Animal and Veterinary Advances*, *9*, 3062-3069.

Kiko, R., & Hauss, H. (2019). On the Estimation of Zooplankton-Mediated Active Fluxes in Oxygen Minimum Zone Regions. *Frontiers in Marine Science*, *6*.

Kirk, P., Cannon, P., Minter, D., & Stalpers, J. (2008). *Ainsworth and Bisby's Dictionary of the Fungi*. Cabi.

Kirkpatrick, J. B., Walsh, E. A., & D'Hondt, S. (2016). Fossil DNA persistence and decay in marine sediment over hundred-thousand-year to million-year time scales. *Geology, 44*(8), 615-618.

Klink, C. A., & Joly, C. A. (1989). Identification and Distribution of C3 and C4 Grasses in Open and Shaded Habitats in Sao Paulo State, Brazil. Biotropica, *21*(1), 30–34.

Koop-Jakobsen, K., Meier, R.J., Mueller, P. (2021). Plant-mediated rhizosphere oxygenation in the native invasive salt marsh grass Elymus athericus. *Frontiers in Plant Sciences, 10*(12), 66975.

Kosir, P., Carni, A., Marinsek, A., & Silc, U. (2013). Floodplain forest communities along the Mura River (NE Slovenia). *Acta Botanica Croatica, 72*(1), 71-95.

Krehenwinkel, H., Wolf, M., & Lim, J.Y. (2017). Estimating and mitigating amplification bias in qualitative and quantitative arthropod metabarcoding. *Scientific Reports, 7*, 17668.

Kurakov, A. V., Lavrent'ev, R. B., Nechitailo, T. Y., Golyshin, P. N., & Zvyagintsev, D. G. (2008). Diversity of facultatively anaerobic microscopic mycelial fungi in soils. Microbiology, 77(1), 90-98.

Kwaśna, H., Szewczyk, W., Baranowska, M., Gallas, E., Wiśniewska, M., & Behnke-Borowczyk, J. (2021). Mycobiota Associated with the Vascular Wilt of Poplar. *Plants*, *10*(5), 892.

Lancelotti, C., & Madella, M. (2018). Phytoliths and the Human Past: Archaeology, Ethnoarchaeology and Palaeoenvironmental Studies.

Lasut, M. T. (2009). The floristic study of herbaceous grasses in Sulawesi. http://repository.ipb.ac.id/handle/123456789/22507

Lazarova, M., & Bozilova, E. (2001). Studies on the Holocene history of vegetation in the region of lake Srebarna (northeast Bulgaria). *Vegetation history and archaeobotany, 10*(2), 87-95.

Lê Cao, K.-A., Costello, M.-E., Lakis, V. A., Bartolo, F., Chua, X.-Y., Brazeilles, R., & Rondeau, P. (2016). MixMC: A Multivariate Statistical Framework to Gain Insight into Microbial Communities. *PLOS ONE, 11*(8), 0160169.

Lee, C., Lee, S., & Park, T. (2017). Statistical methods for metagenomics data analysis. *International Journal of Data Mining and Bioinformatics, 19*(4), 366-385.

Leroy, S. A. G., & Roiron, P. (1996). Latest Pliocene pollen and leaf floras from Bernasso palaeolake (Escandorgue Massif, Herault, France). *Review of palaeobotany and palynology, 94*(3-4), 295-328.

Li, K., Stoof-Leichsenring, K. R., Liu, S. S., Jia, W. H., Liao, M. N., Liu, X. Q., Ni, J., & Herzschuh, U. (2021). Plant sedimentary DNA as a proxy for vegetation reconstruction in eastern and northern Asia. *Ecological Indicators, 132*.

Lisztes-Szabó, Z., Braun, M., Csík, A., & Pető, Á. (2019). Phytoliths of six woody species important in the Carpathians: characteristic phytoliths in Norway spruce needles. *Vegetation history and archaeobotany, 28*(6), 649-662.

Liu, S. S., Stoof-Leichsenring, K. R., Kruse, S., Pestryakova, L. A., & Herzschuh, U. (2020). Holocene vegetation and plant diversity changes in the Northeastern Siberian treeline region from pollen and sedimentary ancient DNA. *Frontiers in Ecology and Evolution, 8*.

Loughlin, N., Gosling, W., & Montoya, E. (2017). Identifying environmental drivers of fungal non-pollen palynomorphs in the montane forest of the eastern Andean flank, Ecuador. *Quaternary Research, 89*, 1-15.

Lubna, Asaf, S., Khan, A. L., Jan, R., Khan, A., Khan, A., Kim, K. M., & Lee, I. J. (2021). The dynamic history of gymnosperm plastomes: Insights from structural characterization, comparative analysis, phylogenomics, and time divergence. *The plant genome, 14*(3), 20130.

Lukina, G.D. (1986). *Polysaccharide seagrasses of the Black Sea: the chemical composition, structure, propertiesand practical use.* [Doctoral dissertation, Odessa Russia].

Lydolph, M. C., Jacobsen, J., Arctander, P., Gilbert, M. T., Gilichinsky, D. A., Hansen, A. J., Willerslev, E., & Lange, L. (2005). Beringian paleoecology inferred from permafrost-preserved fungal DNA. *Appl Environ Microbiol*, *71*(2), 1012-1017.

Magyari, E. K., Chapman, J., Fairbairn, A. S., Francis, M., & de Guzman, M. (2012). Neolithic human impact on the landscapes of North-East Hungary inferred from pollen and settlement records. *Vegetation history and archaeobotany, 21*(4/5), 279-302.

Major, C., Ryan, W., Lericolais, G., & Hajdas, I. (2002). Constraints on Black Sea outflow to the Sea of Marmara during the last glacial-interglacial transition. *Marine Geology, 190*(1-2), 19-34.

Mander, L., & Punyasena, S. W. (2014). On the taxonomic resolution of pollen and spore records of earth's vegetation. *International Journal of Plant Sciences, 175*(8), 931-945.

Manske, A. K., Henssge, U., Glaeser, J., & Overmann, J. (2008). Subfossil 16S rRNA gene sequences of green sulfur bacteria in the Black Sea and their implications for past photic zone anoxia. *Applied and Environmental Microbiology, 74*, 624-632.

Markesteijn, L., Poorter, L., & Bongers, F. (2007). Light-dependent leaf trait variation in 43 tropical dry forest tree species. *American Journal of Botany, 94*(4), 515-525.

McDonald, J. E., Houghton, J. N., Rooks, D. J., Allison, H. E., & McCarthy, A. J. (2012). The microbial ecology of anaerobic cellulose degradation in municipal waste landfill sites: evidence of a role for fibrobacters. *Environ Microbiol, 14*(4), 1077-1087.

Melinda, P. (2018). Characteristics of Collapsing Ecosystems and Main Factors of Collapses. In H. Levente (Ed.), *Ecosystem Services and Global Ecology* (pp. Ch. 2). IntechOpen.

Milchakova, N. A. (1999). On the status of seagrass communities in the Black Sea. *Aquatic botany, 65*(1), 21-31.

More, K. D., Orsi, W. D., Galy, V., Giosan, L., He, L. J., Grice, K., & Coolen, M. J. L. (2018). A 43 kyr record of protist communities and their response to oxygen minimum zone variability in the Northeastern Arabian Sea. *Earth and Planetary Science Letters, 496,* 248-256.

Morlock, M. A., Vogel, H., Nigg, V., Ordonez, L., Hasberg, A. K. M., Melles, M., Russell, J. M., Bijaksana, S., & Team, T. D. P. S. (2019). Climatic and tectonic controls on source-to-sink processes in the tropical, ultramafic catchment of Lake Towuti, Indonesia. *Journal of Paleolimnology, 61*(3), 279-295.

Morlock, M.A., Vogel, H., Russell, J.M., Anselmetti, F.S., & Bijaksana, S. (2021). Quaternary environmental changes in tropical Lake Towuti, Indonesia, inferred from end-member modelling of X-ray fluorescence core-scanning data. *Journal of Quaternary Science, 36,* 1040–1051.

Morrissey, J., & Guerinot, M. L. (2009). Iron uptake and transport in plants: The good, the bad, and the ionome. *Chemical Reviews, 109*(10), 4553-4567.

Moslemi, A., Ades, P. K., Groom, T., Crous, P. W., Nicolas, M. E., & Taylor, P. W. (2016). Paraphoma crown rot of pyrethrum (Tanacetum cinerariifolium). *Plant Disease, 100*(12), 2363-2369.

Mudie, P. J., Marret, F., Aksu, A. E., Hiscott, R. N., & Gillespie, H. (2007). Palynological evidence for climatic change, anthropogenic activity and outflow of Black Sea water during late Pleistocene and Holocene: Centennial-to decadal-scale records from the Black and Marmara Seas. *Quaternary International, 167*, 73-90.

Mudie, P. J., Rochon, A., & Aksu, A. E. (2002). Pollen stratigraphy of Late Quaternary cores from Marmara Sea: land-sea correlation and paleoclimatic history. *Marine Geology, 190*(1-2), 233-260.

Mundra, S., Bahram, M., & Eidesen, P. B. (2016). Alpine bistort (Bistorta vivipara) in edge habitat associates with fewer but distinct ectomycorrhizal fungal species: a comparative study of three contrasting soil environments in Svalbard. *Mycorrhiza*, *26*(8), 809-818.

Murray, J. W., Jannasch, H. W., Honjo, S., Anderson, R. F., Reeburgh, W. S., Top, Z., Friederich, G. E., Codispoti, L. A., & Izdar, E. (1989). Unexpected changes in the oxic/anoxic interface in the Black Sea. *Nature*, *338*(6214), 411-413.

Myers, N., Mittermeier, R. A., Mittermeier, C. G., da Fonseca, G. A. B., & Kent, J. (2000). Biodiversity hotspots for conservation priorities. *Nature, 403*(6772), 853-858.

Nagano, Y., Nagahama, T., Hatada, Y., Nunoura, T., Takami, H., Miyazaki, J., Takai, K., & Horikoshi, K. (2010). Fungal diversity in deep-sea sediments – the presence of novel fungal groups. *Fungal Ecol.*, *3*, 316-325.

Naranjo-Ortiz, M. A., & Gabaldón, T. (2019). Fungal evolution: diversity, taxonomy and phylogeny of the Fungi. *Biol Rev Camb Philos Soc*, *94*(6), 2101-2137.

Niemeyer, B., Epp, L. S., Stoof-Leichsenring, K. R., Pestryakova, L. A., & Herzschuh, U. (2017). A comparison of sedimentary DNA and pollen from lake sediments in recording vegetation composition at the Siberian treeline. *Molecular Ecology Resources, 17*(6), 46-62.

Nijburg, J.W., Coolen, M.J.L., Gerards, S., Gunnewiek, P.J.A.K., & Laanbroek, H.J. (1997). Effects of nitrate availability and the presence of *Glyceria maxima* on the composition and activity of the dissimilatory nitrate-reducing bacterial community. *Applied and Environmental Microbiology, 63*(3), 931-937.

Nottingham, A., Scott, J. J., Saltonstall, K., Broders, K., Montero-Sanchez, M., Püspök, J., Bååth, E., & Meir, P. (2022). Microbial diversity decline and community response are decoupled from increased respiration in warmed tropical forest soil. *Nature Microbiology*, *7*, 1650-1660.

Novák, P., Willner, W., Biurrun, I., Gholizadeh, H., Heinken, T., Jandt, U., Kollar, J., Kozhevnikova, M., Naqinezhad, A., Onyshchenko, V., Pielech, R., Rašomavičius, V., Shirokikh, P., Vassilev, K., Wohlgemuth, T., Večeřa, M., & Chytry, M. (2023). Classification of European oak-hornbeam forests and related vegetation types. *Applied Vegetation Science*, *26*, 12712.

Ollerton, J., Winfree, R., & Tarrant, S. (2011). How many flowering plants are pollinated by animals? *Oikos, 120*(3), 321-326.

Orsi, W. D., Coolen, M. J. L., Wuchter, C., He, L., More, K. D., Irigoien, X., Chust, G., Johnson, C., Hemingway, J. D., Lee, M., Galy, V., & Giosan, L. (2017). Climate oscillations reflected within the microbiome of Arabian Sea sediments. *Scientific Reports*, *7*(1), 6040.

Osono, T. (2019). Functional diversity of ligninolytic fungi associated with leaf litter decomposition. *Ecological Research*, *35*.

Pagter, M., Bragato, C., & Brix, H. (2005). Tolerance and physiological responses of Phragmites australis to water deficit. Aquatic Botany, *81*(4), 285-299.

Palazzesi, L., Gottschling, M., Barreda, V., & Weigend, M. (2012). First Miocene fossils of Vivianiaceae shed new light on phylogeny, divergence times, and historical biogeography of Geraniales. *Biological Journal of the Linnean Society*, *107*(1), 67-85.

Palmer, J. D., Jansen, R. K., Michaels, H. J., Chase, M. W., & Manhart, J. R. (1988). Chloroplast DNA variation and plant phylogeny. *Annals of the Missouri Botanical Garden, 75*(4), 1180-1206.

Panagiotopoulos, K. (2013). *Late Quaternary ecosystem and climate interactions in SW Balkans inferred from Lake Prespa sediments* [Doctoral dissertation, Universität zu Köln].

Pansu, J., Giguet-Covex, C., Ficetola, G.F., Gielly, L., Boyer, F., Zinger, L., Arnaud, F., Poulenard, J., Taberlet, P., Choler, P. (2015). Reconstructing Long-Term Human Impacts on Plant Communities: An Ecological Approach Based on Lake Sediment DNA. *Molecular Ecology, 24*, 1485–1498.

Parducci, L., Bennett, K. D., Ficetola, G. F., Alsos, I. G., Suyama, Y., Wood, J. R., & Pedersen, M. W. (2017). *Ancient plant DNA in lake sediments. New Phytologist, 214*(3), 924-942.

Parducci, L., Matetovici, I., Fontana, S. L., Bennett, K. D., Suyama, Y., Haile, J., Kjaer, K. H., Larsen, N. K., Drouzas, A. D., & Willerslev, E. (2013). Molecular- and pollen-based vegetation analysis in lake sediments from central Scandinavia. *Molecular Ecology, 22*(13), 3511-3524.

Parducci, L., Suyama, Y., Lascoux, M., & Bennett, K. D. (2005). Ancient DNA from pollen: a genetic record of population history in Scots pine. *Molecular Ecology, 14*(9), 2873-2882.

Parducci, L., Valiranta, M., Salonen, J. S., Ronkainen, T., Matetovici, I., Fontana, S. L., Eskola, T., Sarala, P., & Suyama, Y. (2015). Proxy comparison in ancient peat sediments: pollen, macrofossil, and plant DNA. *Philosophical transactions of the Royal Society of London Series B, Biological sciences, 370*(1660), 20130382.

Pastré, D., Hamon, L., Landousy, F., Sorel, I., David, M.-O., Zozime, A., Le Cam, E., & Piétrement, O. (2006). Anionic polyelectrolyte adsorption on mica mediated by multivalent cations: A solution to DNA imaging by atomic force microscopy under high ionic strengths. *Langmuir, 22*(15), 6651–6660.

Paus, A., Boessenkool, S., Brochmann, C., Epp, L. S., Fabel, D., Haflidason, H., & Linge, H. (2015). Lake Store Finnsjoen - a key for understanding Lateglacial/early Holocene vegetation and ice sheet dynamics in the central Scandes Mountains. *Quaternary Science Reviews, 121*, 36-51.

Pedersen, M. W., Ginolhac, A., Orlando, L., Olsen, J., Andersen, K., Holm, J., Funder, S., Willerslev, E., & Kjaeer, K. H. (2013). A comparative study of ancient environmental DNA to pollen and macrofossils from lake sediments reveals taxonomic overlap and additional plant taxa. *Quaternary Science Reviews, 75*, 161-168.

Pedregosa, F., Varoquaux, G., Gramfort, A., Michel, V., Thirion, B., Grisel, O., Blondel, M., Prettenhofer, P., Weiss, R., Dubourg, V., Vanderplas, J., Passos, A., Cournapeau, D., Brucher, M., Perrot, M., & Duchesnay, É. (2011). Scikit-learn: Machine Learning in Python. *J. Mach. Learn. Res., 12*, 2825–2830.

Phookamsak, R., Liu, J.-K., McKenzie, E. H. C., Manamgoda, D. S., Ariyawansa, H., Thambugala, K. M., Dai, D.-Q., Camporesi, E., Chukeatirote, E., Wijayawardene, N. N., Bahkali, A. H., Mortimer, P. E., Xu, J.-C., & Hyde, K. D. (2014). Revision of Phaeosphaeriaceae. *Fungal Diversity*, *68*(1), 159-238.

Pietramellara, G., Ascher, J., Borgogni, F., Ceccherini, M. T., Guerri, G., & Nannipieri, P. (2009). Extracellular DNA in soil and sediment: fate and ecological relevance. *Biology and Fertility of Soils, 45*(3), 219-235.

Pigott, C., Ratcliffe, D., Malloch, A., Birks, H., & Proctor, M. (2000). SM17: Artemisia maritima salt-marsh community: Artemisietum maritimae Hocquette 1927. In J. Rodwell (Ed.), British Plant Communities (British Plant Communities, pp. 84-85). Cambridge: Cambridge University Press.

Piperno, D. R. (2006). *Phytoliths: a comprehensive guide for archaeologists and paleoecologists*. Rowman Altamira.

POWO (2023). *Plants of the World Online*. Royal Botanic Gardens, Kew.

Prasad, M. N. V., & Freitas, H. M. D. (2003). Metal hyperaccumulation in plants - Biodiversity prospecting for phytoremediation technology. *Electronic Journal of Biotechnology, 6*(3), 285-321.

Prenafeta-Boldú, F. X., Summerbell, R., & Sybren de Hoog, G. (2006). Fungi growing on aromatic hydrocarbons: biotechnology's unexpected encounter with biohazard? *FEMS Microbiol Rev*, *30*(1), 109-130.

Quamar, M. F., & Stivrins, N. (2021). Modern pollen and non-pollen palynomorphs along an altitudinal transect in Jammu and Kashmir (Western Himalaya), India. *Palynology*, *45*(4), 669-684.

Randlett, M. E., Coolen, M. J. L., Stockhecke, M., Pickarski, N., Litt, T., Balkema, C., Kwiecien, O., Tomonaga, Y., Wehrli, B., & Schubert, C. J. (2014). Alkenone distribution in Lake Van sediment over the last 270 ka: influence of temperature and haptophyte species composition. *Quaternary Science Reviews, 104,* 53-62.

Reitalu, T., Bjune, A. E., Blaus, A., Giesecke, T., Helm, A., Matthias, I., Peglar, S. M., Salonen, J. S., Seppä, H., Väli, V., Birks, H. J. B., Palaeo, e., Coastal

dynamics, F. s., & Global, c. (2019). Patterns of modern pollen and plant richness across northern Europe. *The Journal of ecology, 107*(4), 1662-1677.

Riaz, T., Shehzad, W., Viari, A., Pompanon, F., Taberlet, P., & Coissac, E. (2011). ecoPrimers: inference of new DNA barcode markers from whole-genome sequence analysis. *Nucleic acids research, 39*(21), 145-145.

Rodriguez-Martinez, S., Klaminder, J., Morlock, M. A., Dalén, L., & Yu-Tuan Huang, D. (2023). The topological nature of tag jumping in environmental DNA metabarcoding studies. *Molecular Ecology Resources, 23*(3), 621-631.

Rohart, F., Gautier, B., Singh, A., & Le Cao, K. A. (2017). mixOmics: An R package for 'omics feature selection and multiple data integration. *Plos Computational Biology, 13*(11).

Rojo, J., Oteros, J., Picornell, A., Ruëff, F., Werchan, B., Werchan, M., Bergmann, K.-C., Schmidt-Weber, C. B., & Buters, J. (2020). Land-Use and Height of Pollen Sampling Affect Pollen Exposure in Munich, Germany. *Atmosphere, 11*(2), 145.

Ross, DA.& Degens, ET. (1974). Recent sediments of Black Sea. *AAPG Bull, 20*, 183–199.

Rossignol, I., Kaniewski, D., Van Campo, E., Petrescu, M., & Baralis, A. (2012). A modern pollen rain study from the Black Sea coast of Romania. *Review of palaeobotany and palynology, 174*, 39-47.

Rull, V. (2022). Biodiversity crisis or sixth mass extinction? Does the current anthropogenic biodiversity crisis really qualify as a mass extinction? *EMBO reports*, *23*(1), 54193.

Russell, J. M., Bijaksana, S., Vogel, H., Melles, M., Kallmeyer, J., Ariztegui, D., Crowe, S., Fajar, S., Hafidz, A., Haffner, D., Hasberg, A., Ivory, S., Kelly, C., King, J., Kirana, K., Morlock, M., Noren, A., O'Grady, R., Ordonez, L., Stevenson, J., von Rintelen, T., Vuillemin, A., Watkinson, I., Wattrus, N., Wicaksono, S., Wonik, T., Bauer, K., Deino, A., Friese, A., Henny, C., Imran, Marwoto, R., Ngkoimani, L., Nomosatryo, S., Safiuddin, L., Simister, R., &

Tamuntuan, G. (2016). The Towuti Drilling Project: paleoenvironments, biological evolution, and geomicrobiology of a tropical Pacific lake. *Scientific Drilling, 21,* 29-40.

Russell, J. M., Vogel, H., Bijaksana, S., Melles, M., Deino, A., Hafidz, A., Haffner, D., Hasberg, A. K. M., Morlock, M., von Rintelen, T., Sheppard, R., Stelbrink, B., & Stevenson, J. (2020). The late quaternary tectonic, biogeochemical, and environmental evolution of ferruginous Lake Towuti, Indonesia. *Palaeogeography Palaeoclimatology Palaeoecology, 556.*

Russell, J. M., Vogel, H., Konecky, B. L., Bijaksana, S., Huang, Y. S., Melles, M., Wattrus, N., Costa, K., & King, J. W. (2014). Glacial forcing of central Indonesian hydroclimate since 60,000 y BP. *Proceedings of the National Academy of Sciences of the United States of America, 111*(14), 5100-5105.

Rustler, S., Chmura, A., Sheldon, R. A., & Stolz, A. (2008). Characterisation of the substrate specificity of the nitrile hydrolyzing system of the acidotolerant black yeast Exophiala oligosperma R1. *Stud Mycol, 61*, 165-174.

Ryan, W. B. F., & Pitman, W. C. (1998). *Noah's Flood: The New Scientific Discoveries about the Event that Changed History*. Simon & Schuster.

Ryberg, M., & Matheny, P. B. (2011). Asynchronous origins of ectomycorrhizal clades of Agaricales. *Proceedings of the Royal Society B: Biological Sciences*, *279*, 2003 - 2011.

Ryves, D. B., Juggins, S., Fritz, S. C., & Battarbee, R. W. (2001). Experimental diatom dissolution and the quantification of microfossil preservation in sediments. *Palaeogeography, palaeoclimatology, palaeoecology*, *172*(1-2), 99-113.

Santi, C., Bogusz, D., & Franche, C. (2013). Biological nitrogen fixation in non-legume plants. *Ann Bot, 111*(5), 743-767.

Sheppard, R. Y., Milliken, R. E., Russell, J. M., Dyar, M. D., Sklute, E. C., Vogel, H., Melles, M., Bijaksana, S., Morlock, M. A., & Hasberg, A. K. M. (2019). Characterization of Iron in Lake Towuti sediment. *Chemical Geology, 512,* 11-30.

Sheppard, R. Y., Milliken, R. E., Russell, J. M., Sklute, E. C., Dyar, M. D., Vogel, H., Melles, M., Bijaksana, S., Hasberg, A. K. M., & Morlock, M. A. (2021). Iron Mineralogy and Sediment Colour in a 100 m Drill Core from Lake Towuti, Indonesia Reflect Catchment and Diagenetic Conditions. *Geochemistry Geophysics Geosystems, 22*(8).

Shillito, L.-M. (2013). Grains of truth or transparent blindfolds? A review of current debates in archaeological phytolith analysis. *Vegetation history and archaeobotany*, *22*(1), 71-82.

Shoun, H., & Tanimoto, T. (1991). Denitrification by the fungus Fusarium oxysporum and involvement of cytochrome P-450 in the respiratory nitrite reduction. *J Biol Chem, 266*(17), 11078-11082.

Shumilovskikh, L. S., Tarasov, P., Arz, H. W., Fleitmann, D., Marret, F., Nowaczyk, N., Plessen, B., Schluetz, F., & Behling, H. (2012). Vegetation and environmental dynamics in the southern Black Sea region since 18 kyr BP derived from the marine core 22-GC3. *Palaeogeography Palaeoclimatology Palaeoecology, 337*, 177-193.

Sifton, M. A., Lim, P., Smith, S. M., & Thomas, S. C. (2022). Interactive effects of biochar and N-fixing companion plants on growth and physiology of Acer saccharinum. *Urban Forestry & Urban Greening, 74,* 127652.

Sisk-Hackworth, L., & Kelley, S. T. (2020). An application of compositional data analysis to multiomic time-series data. *Nar Genomics and Bioinformatics, 2*(4).

Slon, V., Hopfe, C., Weiss, C. L., Mafessoni, F., de la Rasilla, M., Lalueza-Fox, C., & Meyer, M. (2017). Neandertal and denisovan DNA from Pleistocene sediments. *Science, 356*(6338), 605–608.

Solaiman, Z. M., Abbott, L. K., & Varma, A. (2015). Role of Mycorrhizal Fungi in the Alleviation of Heavy Metal Toxicity in Plants. In (Vol. 41, pp. 241-258). Springer Berlin / Heidelberg.

Sonstebo, J. H., Gielly, L., Brysting, A. K., Elven, R., Edwards, M., Haile, J., Willerslev, E., Coissac, E., Rioux, D., Sannier, J., Taberlet, P., & Brochmann, C. (2010). Using next-generation sequencing for molecular reconstruction of past Arctic vegetation and climate. *Molecular ecology resources*, *10*(6), 1009-1018.

Souto, M., Castro, D., García-Rodeja, E., & Pontevedra-Pombal, X. (2019). The Use of Plant Macrofossils for Paleoenvironmental Reconstructions in Southern European Peatlands. *Quaternary*, *2*(4), 34.

Spetsov, P., Plamenov, D., & Kiryakova, V. (2006). Distribution and characterization of Aegilops and Triticum species from the Bulgarian Black Sea coast. *Central European journal of biology, 1*(3), 399-411.

Steffen, W., Grinevald, J., Crutzen, P., & McNeill, J. (2011). The Anthropocene; conceptual and historical perspectives. *Philosophical transactions of the Royal Society of London. Series A: Mathematical, physical, and engineering sciences*, *369*(1938), 842-867.

Stevenson, J. (2018). Vegetation and climate of the Last Glacial Maximum in Sulawesi. In S. O. orcid, D. B. orcid, J. Meyer (Eds.), *The Archaeology of Sulawesi. Current Research on the Pleistocene to the Historic Period* (pp. 17-29). ANU Press.

Strömberg, C. A., Dunn, R. E., Madden, R. H., Kohn, M. J., & Carlini, A. A. (2013). Decoupling the spread of grasslands from the evolution of grazer-type herbivores in South America. *Nature communications*, *4*(1), 1478.

Taberlet, P., Coissac, E., Pompanon, F., Gielly, L., Miquel, C., Valentini, A., Vermat, T., Corthier, G., Brochmann, C., & Willerslev, E. (2007). Power and limitations of the chloroplast trnL (UAA) intron for plant DNA barcoding. *Nucleic Acids Research, 35*(3), 14.

Talas, L., Stivrins, N., Veski, S., Tedersoo, L., & Kisand, V. (2021). Sedimentary Ancient DNA (sedaDNA) Reveals Fungal Diversity and Environmental

Drivers of Community Changes throughout the Holocene in the Present Boreal Lake Lielais Svētiņu (Eastern Latvia). *Microorganisms*, *9*(4).

Tedersoo, L., Bahram, M., Puusepp, R., Nilsson, R. H., & James, T. (2017). Novel soil-inhabiting clades fill gaps in the fungal tree of life. *Microbiome*, *5*.

Teunissen, M., Kets, E., Op den Camp, H., Huis in't Veld, J., & Vogels, G. (1992). Effect of coculture of anaerobic fungi isolated from ruminants and non-ruminants with methanogenic bacteria on cellulolytic and xylanolytic enzyme activities. *Archives of microbiology, 157*, 176-182.

THE BULGARIAN FLORA ONLINE (2008). *Filipendula ulmaria.* (families/rosaceae/ filipendula/filipendula_ulmaria/filipendula_ulmaria_en.html).

Tonkov, S., & Bozilova, E., (1995). Palaeoecological data about the end of the Holocene climatic optimum in Bulgaria e IV millennium BC. *Annual of Sofia University, Biology 87*(2), 5-17.

Tournier, N., Fabbri, S.C., Anselmetti, F.S., Cahyarini, S.Y., Bijaksana, S., Wattrus, N., Russell, J.M., & Vogel, H. (2023). Climate-controlled sensitivity of lake sediments to record earthquake-related mass wasting in tropical Lake Towuti during the past 40 kyr. *Quaternary Science Reviews, 305,* 108015.

Turney, C. S. M., & Brown, H. (2007). Catastrophic early Holocene sea level rise, human migration and the Neolithic transition in Europe. *Quaternary science reviews*, *26*(17), 2036-2041.

Ulfers, A., Hesse, K., Zeeden, C., Russell, J. M., Vogel, H., Bijaksana, S., & Wonik, T. (2021). Cyclostratigraphy and paleoenvironmental inference from downhole logging of sediments in tropical Lake Towuti, Indonesia. *Journal of paleolimnology*, *65*, 377-392.

van der Hammen, T., Wijmstra, A., & Zagwijn, W., (1971). The floral record of the Late Cenozoic of Europe. In K. K. Turekian (Ed.), *The Late Cenozoic Glacial Ages*. Yale University Press, New Heaven.

van der Meer, M. T. J., Sangiorgi, F., Baas, M., Brinkhuis, H., Sinninghe Damste, J. S., & Schouten, S. (2008). Molecular isotopic and dinoflagellate evidence for late Holocene freshening of the Black Sea. *Earth and planetary science letters, 267*(3-4), 426-434.

Van Pelt, R., O'Keefe, T. C., Latterell, J. J., & Naiman, R. J. (2006). Riparian forest stand development along the Queets River in Olympic National Park, Washington. *Ecological monographs, 76*(2), 277-298.

Velasco, L., Pérez-Vich, B., & Fernández-Martínez, J. M. (2016). Research on resistance to sunflower broomrape: An integrated vision. *Oléagineux corps gras lipides, 23*(2), D203.

Vogel, H., Russell, J., Cahyarini, S., Bijaksana, S., Wattrus, N., Rethemeyer, J., & Melles, M. (2015). Depositional modes and lake-level variability at Lake Towuti, Indonesia, during the past similar to 29 kyr BP. *Journal of Paleolimnology, 54*(4), 359-377.

Voldstad, L. H., Alsos, I. G., Farnsworth, W. R., Heintzman, P. D., Hakansson, L., Kjellman, S. E., Rouillard, A., Schomacker, A., & Eidesen, P. B. (2020). A complete Holocene lake sediment ancient DNA record reveals long-standing high Arctic plant diversity hotspot in northern Svalbard. *Quaternary Science Reviews, 234*.

Volkov, I., & L.N, N. (2007). Hydrogen Sulfide in the Black Sea. In (Vol. 5, pp. 309-331).

Vuillemin, A., Friese, A., Alawi, M., Henny, C., Nomosatryo, S., Wagner, D., Crowe, S. A., & Kallmeyer, J. (2016). Geomicrobiological Features of Ferruginous Sediments from Lake Towuti, Indonesia. *Front Microbiol, 7*, 1007.

Vuillemin, A., Horn, F., Alawi, M., Henny, C., Wagner, D., Crowe, S. A., & Kallmeyer, J. (2017). Preservation and Significance of Extracellular DNA in Ferruginous Sediments from Lake Towuti, Indonesia. *Frontiers in Microbiology, 8.*

Vuillemin, A., Horn, F., Friese, A., Winkel, M., Alawi, M., Wagner, D., Henny, C., Orsi, W. D., Crowe, S. A., & Kallmeyer, J. (2018). Metabolic potential of

microbial communities from ferruginous sediments. *Environmental Microbiology*, *20*(12), 4297-4313.

Vuillemin, A., Wirth, R., Kemnitz, H., Schleicher, A. M., Friese, A., Bauer, K. W., Simister, R., Nomosatryo, S., Ordonez, L., Ariztegui, D., Henny, C., Crowe, S. A., Benning, L. G., Kallmeyer, J., Russell, J. M., Bijaksana, S., Vogel, H., & Towuti Drilling Project Sci, T. (2019). Formation of diagenetic siderite in modern ferruginous sediments. *Geology, 47*(6), 540-544.

Wang, S. N., Fan, Y. G., & Yan, J. Q. (2022). Iugisporipsathyrareticulopilea gen. et sp. nov. (Agaricales, Psathyrellaceae) from tropical China produces unique ridge-ornamented spores with an obvious suprahilar plage. *MycoKeys*, *90*, 147-162.

Wang, Z., Wang, C., & Liu, H. (2022). Higher dissolved oxygen levels promote downward migration of phosphorus in the sediment profile: Implications for lake restoration. *Chemosphere, 301,*134705.

Wanner, H., Beer, J., Buetikofer, J., Crowley, T. J., Cubasch, U., Flueckiger, J., Goosse, H., Grosjean, M., Joos, F., Kaplan, J. O., Kuettel, M., Mueller, S. A., Prentice, I. C., Solomina, O., Stocker, T. F., Tarasov, P., Wagner, M., & Widmann, M. (2008). Mid- to Late Holocene climate change: an overview. *Quaternary Science Reviews, 27*(19-20), 1791-1828.

Watson, E. B., & Byrne, R. (2009). Abundance and diversity of tidal marsh plants along the salinity gradient of the San Francisco Estuary: implications for global change ecology. *Plant Ecology, 205*(1), 113-128.

Whitten, A.J., Mustafa, M., & Henderson, G.S. (1988). *The Ecology of Sulawesi.* Gadjah Mada University Press, Indonesia.

Wick, L., Lemcke, G., & Sturm, M. (2003). Evidence of Lateglacial and Holocene climatic change and human impact in eastern Anatolia: high-resolution pollen, charcoal, isotopic and geochemical records from the laminated sediments of Lake Van, Turkey. *The Holocene, 13*(5), 665-675.

Wickham, H. (2016). *Ggplot2: Elegant graphics for data analysis* (2nd ed.). Springer-Verlag New York.

Willerslev, E., & Cooper, A. (2005). Ancient DNA. *Proceedings of the Royal Society of London Series B-Biological Sciences, 272*(1558), 3-16.

Yanchilina, A. G., Ryan, W. B., McManus, J. F., Dimitrov, P., Dimitrov, D., Slavova, K., & Filipova-Marinova, M. (2017). Compilation of geophysical, geochronological, and geochemical evidence indicates a rapid Mediterranean-derived submergence of the Black Sea's shelf and subsequent substantial salinification in the early Holocene. *Marine Geology*, *383*, 14-34.

Yang, S., Gu, F., Song, B., Ye, S., Yuan, Y., He, L., Li, J., Zhao, G., Ding, X., Pei, S., Laws, E. A., & Sangiorgi, F. (2022). Holocene vegetation history and responses to climate and sea-level change in the Liaohe Delta, northeast China. *Catena (Giessen), 217*, 106438.

Zhang, N., & Wang, Z. (2015). 3 Pezizomycotina: Sordariomycetes and Leotiomycetes. In (pp. 57-88).

Zimmermann, H. H., Raschke, E., Epp, L. S., Stoof-Leichsenring, K. R., Schwamborn, G., Schirrmeister, L., Overduin, P. P., & Herzschuh, U. (2017). Sedimentary ancient DNA and pollen reveal the composition of plant organic matter in Late Quaternary permafrost sediments of the Buor Khaya Peninsula (northeastern Siberia). *Biogeosciences, 14*(3), 575-596.
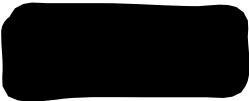
Appendix

Statement of contributions:

Chapter 2: Md Akhtar-E Ekram, Matthew Campbell, Chloe Plet, Rebecca Hamilton, Satria Bijaksana, Kliti Grice, James Russell, Janelle Stevenson, and Marco JL Coolen. **A 1Ma sedimentary ancient DNA (*sed*aDNA) record of catchment vegetation changes and the developmental history of tropical Lake Towuti (Sulawesi, Indonesia). Published in *Geobiology (DOI:10.1111/gbi.12599).***

To whom It May Concern,

I, Matthew Campbell, contributed to the chapter 2 entitled:

"A 1Ma sedimentary ancient DNA (*sed*aDNA) record of catchment vegetation changes and the developmental history of tropical Lake Towuti (Sulawesi, Indonesia)."

Signature:

Date: 29/092023

To whom It May Concern,

I, Chloe Plet, contributed to the chapter 2 entitled:

"A 1Ma sedimentary ancient DNA (sedaDNA) record of catchment vegetation changes and the developmental history of tropical Lake Towuti (Sulawesi, Indonesia)." Submitted in Geobiology (Under review).

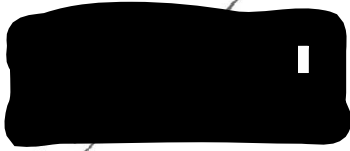Signature:

Date: 03/10/2023.

To whom It May Concern,

I, Rebecca Hamilton, contributed to the chapter 2 entitled:

"A 1Ma sedimentary ancient DNA (*sed*aDNA) record of catchment vegetation changes and the developmental history of tropical Lake Towuti (Sulawesi, Indonesia)."

Signature:

Date: 28/09/2023

To whom It May Concern,

I, Satria Bijaksana, contributed to the chapter 2 entitled:

"A 1Ma sedimentary ancient DNA (*sed*aDNA) record of catchment vegetation changes and the developmental history of tropical Lake Towuti (Sulawesi, Indonesia)."

Signature:
Date: September 26, 2023

To whom It May Concern,

I, Kliti Grice, contributed to the chapter 2 entitled:

"A 1Ma sedimentary ancient DNA (*sed*aDNA) record of catchment vegetation changes and the developmental history of tropical Lake Towuti (Sulawesi, Indonesia)."

Signature:

Date: 2/10/2023

To whom It may concern,

I, James Russell, contributed to the chapter 2 entitled:

"A 1Ma sedimentary ancient DNA (*sed*aDNA) record of catchment vegetation changes and the developmental history of tropical Lake Towuti (Sulawesi, Indonesia)."

Signature

James M Russell   Date 25/09/2023

To whom It May Concern,

I, Janelle Stevenson, contributed to the chapter 2 entitled:

"A 1Ma sedimentary ancient DNA (*sed*aDNA) record of catchment vegetation changes and the developmental history of tropical Lake Towuti (Sulawesi, Indonesia)." Submitted in Geobiology (Under review).

Signature:

Date: 28/09/23

To whom It May Concern,

I, Marco Coolen, contributed to the chapter 2 entitled:

"A 1Ma sedimentary ancient DNA (*sed*aDNA) record of catchment vegetation changes and the developmental history of tropical Lake Towuti (Sulawesi, Indonesia)." Submitted in Geobiology (Under review).

Signature:

Date: 03/11/2023

Chapter 3:

Md Akhtar-E Ekram, Cornelia Wuchter, Kliti Grice, James Russell, and Marco JL Coolen. **A 1 Ma *sed*aDNA record of tropical paleovegetation assemblages and their associations with parasitic, endophytic, and saprophytic fungi.** *Earth and Planetary Science Letters*, in Preparation.

To whom It May Concern,

I, Cornelia Wuchter, contributed to the chapter 3 entitled:

"A 1 Ma sedimentary ancient DNA (sedaDNA)record of tropical paleovegetation assemblages and their associations with parasitic, endophytic, and saprophytic fungi."

Signature:

Date: 16/10/2023

To whom It May Concern,

I, Kliti Grice, contributed to the chapter 3 entitled:

"A 1 Ma *sed*aDNA record of tropical paleovegetation assemblages and their associations with parasitic, endophytic, and saprophytic fungi."

Signature:

Date: 2/10/2023

Statement of contributions:

To whom I may concern,

I, James Russell, contributed to chapter 3 entitled:

"A 1 Ma sedimentary ancient DNA (*sed*aDNA) record of tropical paleovegetation assemblages and their associations with parasitic, endophytic, and saprophytic fungi."

Signature

James M Russell   Date 25/09/2023

To whom It May Concern,

I, Marco Coolen, contributed to the chapter 3 entitled:

"A 1 Ma *sed*aDNA record of tropical paleovegetation assemblages and their associations with parasitic, endophytic, and saprophytic fungi.''

Signature:

Date:03/11/2023

Chapter 4: Md Akhtar-E Ekram, Cornelia Wuchter, Liviu Giosan, Kliti Grice, and Marco JL Coolen. **A combined pollen and *sed*aDNA record of late-Glacial and Holocene coastal marshland and riparian vegetation assemblages in the Black Sea region.** *Geobiology*, in Preparation.

To whom It May Concern,

I, Cornelia Wuchter, contributed to the chapter 4 entitled:

"A combined pollen and *sed*aDNA record of late-Glacial and Holocene coastal marshland and riparian vegetation assemblages in the Black Sea region.''

Signature:

Date: 02 / 10 / 2023

To whom It May Concern,

I, Liviu Giosan, contributed to the chapter 4 entitled:

"A combined pollen and *sed*aDNA record of late-Glacial and Holocene coastal marshland and riparian vegetation assemblages in the Black Sea region.''

Signature:

Date: Oct 9, 2023

To whom It May Concern,

I, Kliti Grice, contributed to the chapter 4 entitled:

"A combined pollen and *sed*aDNA record of late-Glacial and Holocene coastal marshland and riparian vegetation assemblages in the Black Sea region.''

Signature:

Date:2/10/2023

To whom It May Concern,

I, Marco Coolen, contributed to the chapter 4 entitled:

"A combined pollen and *sed*aDNA record of late-Glacial and Holocene coastal marshland and riparian vegetation assemblages in the Black Sea region.''

Signature:

Date:03/11/2023